

AWARD NUMBER: W81XWH-16-1-0691

TITLE: Selective AAK1 and GAK inhibitors for combating dengue and other emerging viral infections

PRINCIPAL INVESTIGATOR: Shirit Einav

CONTRACTING ORGANIZATION: Stanford University

REPORT DATE: Oct 2019

TYPE OF REPORT: Annual

PREPARED FOR: U.S. Army Medical Research and Materiel Command
Fort Detrick, Maryland 21702-5012

DISTRIBUTION STATEMENT: Approved for Public Release;
Distribution Unlimited

The views, opinions and/or findings contained in this report are those of the author(s) and should not be construed as an official Department of the Army position, policy or decision unless so designated by other documentation.

REPORT DOCUMENTATION PAGE

Form Approved
OMB No. 0704-0188

Public reporting burden for this collection of information is estimated to average 1 hour per response, including the time for reviewing instructions, searching existing data sources, gathering and maintaining the data needed, and completing and reviewing this collection of information. Send comments regarding this burden estimate or any other aspect of this collection of information, including suggestions for reducing this burden to Department of Defense, Washington Headquarters Services, Directorate for Information Operations and Reports (0704-0188), 1215 Jefferson Davis Highway, Suite 1204, Arlington, VA 22202-4302. Respondents should be aware that notwithstanding any other provision of law, no person shall be subject to any penalty for failing to comply with a collection of information if it does not display a currently valid OMB control number. **PLEASE DO NOT RETURN YOUR FORM TO THE ABOVE ADDRESS.**

1. REPORT DATE Oct 2019		2. REPORT TYPE Annual		3. DATES COVERED 15 Sept2018 - 15 Sept2019	
4. TITLE AND SUBTITLE Selective AAK1 and GAK inhibitors for combating dengue and other emerging viral infections				5a. CONTRACT NUMBER W81XWH-16-1-0691	
				5b. GRANT NUMBER PR151090	
				5c. PROGRAM ELEMENT NUMBER	
6. AUTHOR(S) Shirit Einav, Steven De Jonghe, Jennifer Brannan, Raul Andino E-Mail: seinav@stanford.edu				5d. PROJECT NUMBER	
				5e. TASK NUMBER	
				5f. WORK UNIT NUMBER	
7. PERFORMING ORGANIZATION NAME(S) AND ADDRESS(ES) Stanford University School of Medicine, Stanford CA 94305 KU Leuven, 3000 Leuven, Belgium USAMRIID, Frederick, MD 21702 University of California San Francisco, San Francisco, CA 94143				8. PERFORMING ORGANIZATION REPORT	
9. SPONSORING / MONITORING AGENCY NAME(S) AND ADDRESS(ES) U.S. Army Medical Research and Materiel Command Fort Detrick, Maryland 21702-5012				10. SPONSOR/MONITOR'S ACRONYM(S)	
				11. SPONSOR/MONITOR'S REPORT NUMBER(S)	
12. DISTRIBUTION / AVAILABILITY STATEMENT Approved for Public Release; Distribution Unlimited					
13. SUPPLEMENTARY NOTES					
14. ABSTRACT Emerging viruses, such as dengue (DENV) and Ebola (EBOV), pose threats to military and global health. There are no approved drugs or vaccines available against these viruses. Our goal is to develop broad-spectrum antivirals with a high genetic barrier to resistance by targeting host proteins that are critical to the life cycle of multiple viruses. The goals of this project are to optimize selective inhibitors of AAK1 and GAK, host kinases we discovered as targets for broad-spectrum antivirals, and advance their development to a pre-IND stage. This approach would also protect against multiple other biothreat agents. During the past year we have continued to optimize our inhibitors. Our promising AAK1 and GAK inhibitors have broad spectrum activity (DENV, EBOV and CHIKV). Effort to enhance their PK and advance them to in vivo experiments are ongoing. We have generated a series of derivatives of AAK1 inhibitors based on the Azaindole series with several hits showing promising antiviral activity. We have also demonstrated synergy between AAK1 and GAK inhibitors and a high barrier to resistance in mice.					
15. SUBJECT TERMS Antivirals, kinase inhibitors, dengue virus, Ebola virus, broad-spectrum antivirals, host-targeted antivirals					
16. SECURITY CLASSIFICATION OF:			17. LIMITATION OF ABSTRACT	18. NUMBER OF PAGES	19a. NAME OF RESPONSIBLE PERSON
a. REPORT	b. ABSTRACT	c. THIS PAGE			USAMRMC
Unclassified	Unclassified	Unclassified	Unclassified	15	19b. TELEPHONE NUMBER (include area code)

Table of Contents

	<u>Page</u>
1. Introduction.....	4
2. Keywords.....	4
3. Accomplishments.....	4-15
4. Impact.....	15
5. Changes/Problems.....	16
6. Products.....	16
7. Participants & Other Collaborating Organizations.....	17-20
8. Special Reporting Requirements.....	20
9. Appendices.....	21-68

1. INTRODUCTION:

Emerging viruses, such as dengue (DENV), chikungunya (CHIKV), and Ebola (EBOV), pose major threats to military and global health. There are no approved drugs or vaccines available against these viruses. The current “one drug, one threat” approach to drug development is slow and expensive and is therefore not easily scalable to meet the large unmet clinical need. Our overall goal is to develop broad-spectrum antiviral drugs with a high genetic barrier to resistance by targeting host proteins that are critical to the life cycle of multiple viruses. We discovered an Achilles' heel of multiple unrelated viruses: a requirement for AP2-associated protein kinase 1 (AAK1) and cyclin G-associated kinase (GAK), host kinases that regulate clathrin adaptor proteins-mediated pathways. Our data point to AAK1 and GAK as "master regulators" of viral infection and attractive targets for broad-spectrum antivirals. We discovered that approved anticancer drugs that target these kinases; sunitinib and erlotinib, potently inhibit replication of multiple viruses *in vitro* and reduce mortality in mice infected with DENV and EBOV. This approach is being advanced into clinical trials for both of these indications. Nevertheless, potential toxicity resulting from inhibition of other host cell kinases by these non-selective inhibitors may limit their use. The goals of this project are to optimize novel, chemically distinct, selective lead AAK1 and GAK inhibitors, already demonstrating great promise against DENV, and advance their development to a pre-IND stage. This approach would also protect against biothreat agents from multiple other viral families, including EBOV and CHIKV.

2. KEYWORDS:

Antivirals, kinase inhibitors, dengue virus, Ebola virus, broad-spectrum antivirals, host-targeted antivirals

3. ACCOMPLISHMENTS:

The major goals of the project and the accomplishments under these goals

Specific Aim 1: Optimize lead inhibitors of AAK1 and/or GAK and maximize their therapeutic index.

Proposed tasks and milestones (approved SOW)

	Time-line (months)	Site 1	Site 2	Site 3	Site 4
Major Task 1: Optimize the metabolic stability and pharmacokinetic (PK) properties of the current leads.					
Subtask 1: Synthesize focused sets of analogs.	1-28	Einav		Herdewijn	
Subtask 2: Measure their affinity of binding to AAK1 and GAK or kinase activity.	1-30	Einav *			
Subtask 3: Determine their <i>in vitro</i> metabolic stability, aqueous solubility, absorption, and stability in mouse and human plasma.	3-30	Einav *			
Subtask 4: Determine their selectivity and mode of binding to AAK1 and/or GAK.	6-30	Einav *			

Major Task 1 achievements

GAK inhibitors

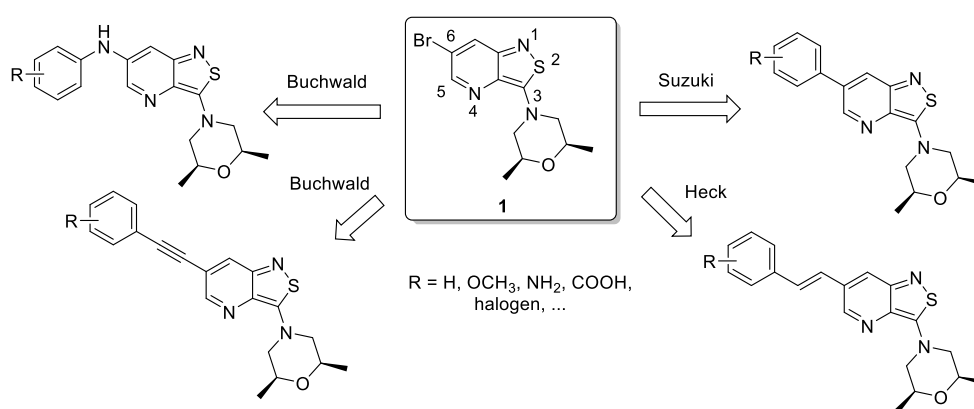
Previous research revealed that 3,6-disubstituted isothiazolo[4,3-*b*]pyridines are potent and selective GAK inhibitors with broad spectrum antiviral activity. Although a broad structural variety has been introduced at position 3 of the isothiazolo[4,3-*b*]pyridine scaffold, and a wide range of different scaffolds have been prepared, the structure-activity relationship (SAR) study of the pyridine moiety has not been previously studied in detail. Therefore, we embarked on a synthesis program with a focus on the introduction of structural variety on the pyridine moiety.

Two different positions of the scaffold were explored.

a) SAR at position 6

For the synthesis of the 6-substituted isothiazolo[4,3-*b*]pyridines, 6-bromo-3-(*cis*-2,6-dimethylmorpholino)isothiazolo[4,3-*b*]pyridine **1** was selected as the key intermediate (Figure 1). Several (hetero)aryl groups were conveniently introduced by Suzuki cross-couplings using classical reaction circumstances. The insertion of an ethenyl linker between the central core structure and the phenyl ring was performed by a palladium-catalyzed cross-coupling using styrene applying Heck reaction conditions. Coupling of different anilines at position 6 of the isothiazolo[4,3-*b*]pyridine scaffold was achieved via a Buchwald reaction. The same Buchwald conditions were also used for the coupling of phenylacetylene. Overall, these efforts led to the synthesis of a library of 21 isothiazolo[4,3-*b*]pyridines that were evaluated for their GAK binding affinity. The most potent GAK inhibitors ($IC_{50} < 100$ nM), with their antiviral data against DENV, are shown in Table 1.

Figure 1

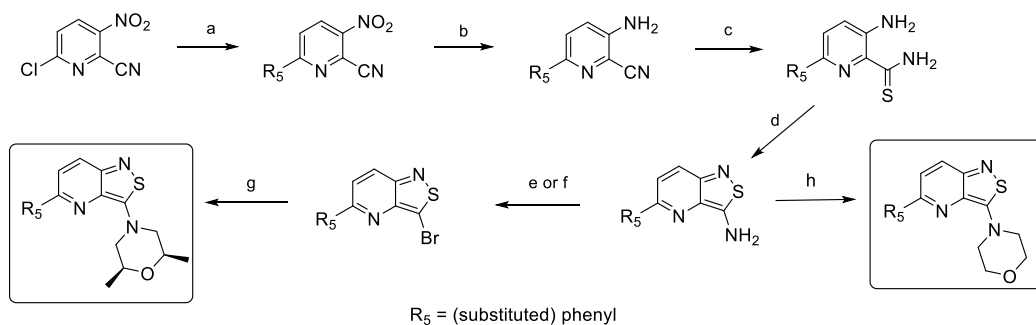


b) SAR at position 5

The synthesis of 3,5-disubstituted isothiazolo[4,3-*b*]pyridines was not reported in the literature before and a new synthetic scheme was established (Scheme 1). The appropriate aryl group was inserted on commercially available 6-chloro-2-cyano-3-nitropyridine via a Suzuki cross-coupling reaction in the first step of the synthesis. Reduction of the nitro group by treatment with iron under acidic conditions affording 3-amino-6-aryl-picolinonitriles. Thionation of the nitrile functionality using phosphorus pentasulfide yielded thioamides. The isothiazole moiety was then constructed by an oxidative ring closure using hydrogen peroxide in methanol, yielding 5-aryl-3-amino-isothiazolo[4,3-*b*]pyridines. The conversion of the amino group to a bromine was achieved via a Sandmeyer reaction, either using classical reaction conditions (NaNO₂, HBr, CuBr, water) or alternatively, to minimize aromatic bromination side reactions, milder conditions (tBuONO, CuBr₂ and dry acetonitrile) were applied. Finally, *cis*-2,6-dimethylmorpholine was introduced at position 3 of the isothiazolo[4,3-*b*]pyridine scaffold.

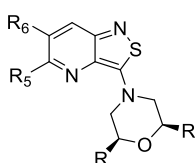
The Sandmeyer reaction was very often problematic, and therefore, a 3-*N*-morpholinyl moiety was directly synthesized from the corresponding 3-amino congeners, by reaction with 2-bromoethyl ether. Based on this synthetic protocol, nine 3,5-disubstituted isothiazolo[4,3-*b*]pyridines were prepared and evaluated for GAK affinity and antiviral activity against DENV. The most promising congeners from this family are mentioned in Table 1.

Scheme 1



Reagents and conditions. a) R₅B(OH)₂, Pd(PPh₃)₄, K₂CO₃, toluene or dioxane/H₂O, 95 °C; b) Fe, CH₃COOH, 60 °C; c) P₂S₅, EtOH, 75 °C; d) 35% aq. H₂O₂, MeOH, rt; e) NaNO₂, HBr, CuBr, H₂O, 0 °C to rt; f) *t*BuONO, CuBr₂, dry CH₃CN, -10 °C to rt; g) 2,6-dimethylmorpholine, EtOH, reflux; h) 2-bromoethyl ether, K₂CO₃, DMF, 100 °C.

Table 1



Cmpd	R	R ₅	R ₆	GAK IC ₅₀ (μM)	DENV EC ₅₀ (μM)	DENV CC ₅₀ (μM)
RMC-118	CH ₃	H		0.071	2.79	>10
RMC-122	CH ₃	H		0.042	>10	>10
RMC-146	CH ₃	H		0.022	10.05	>10
RMC-167	CH ₃	H		0.083	8.85	>10
RMC-178	CH ₃	H		0.073	5.83	>10
RMC-203	CH ₃		H	0.099	>10	>10
RMC-217	CH ₃		H	0.024	1.049	>10

The results of this research were recently published in *Bioorg. Med. Chem* and in *Eur J Med Chem* (See both papers attached).

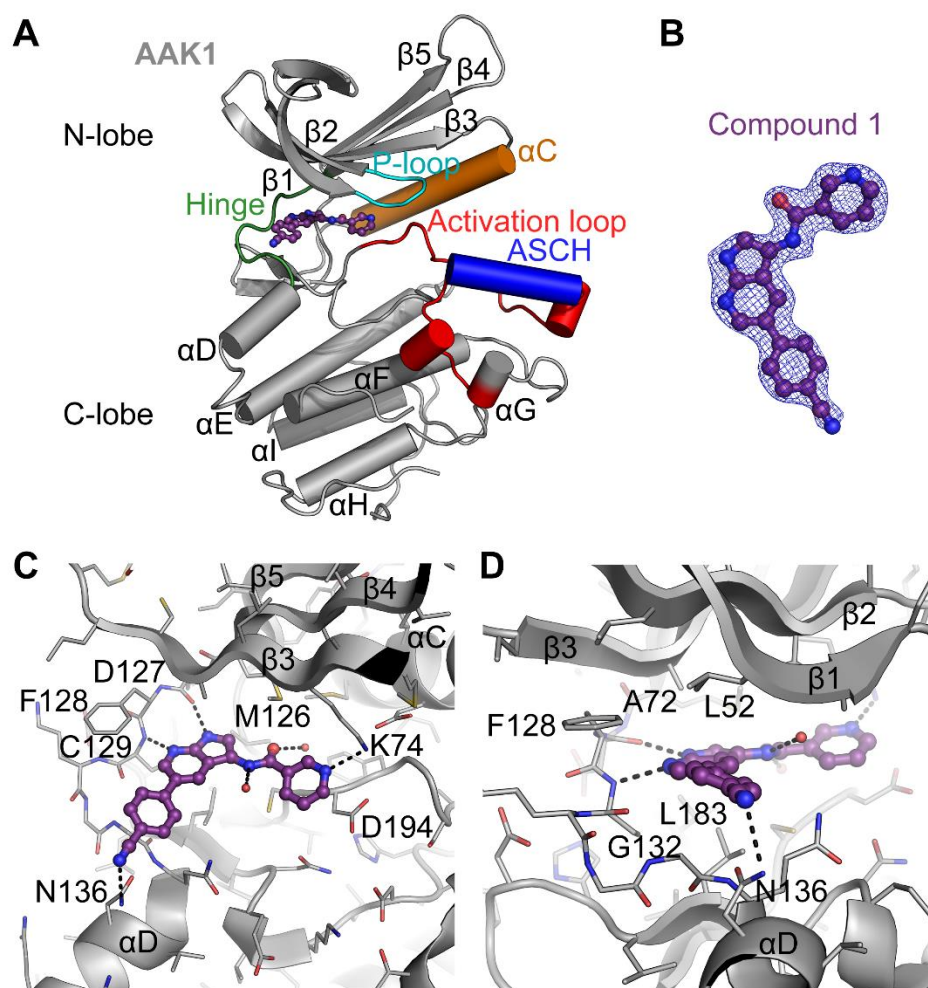
AAK1 inhibitors

No further chemistry was done on the pyrrolo[2,3-*b*]pyridine series as low nM AAK1 binding affinity was already achieved by the synthesis of 8g (RMC-34) and 21b (RMC-76), as explained in previous report. Therefore, the focus this year was on further biological profiling of both compounds.

Antiviral activity of the most potent AAK1 inhibitors was studied in first in Huh7 cells (see Task 2 below).

To assess the kinase selectivity of the optimized AAK1 inhibitors, 21b was screened against 468 kinases via the KINOMEScan assay (DiscoverX) at a single concentration of 10 μ M. This screening revealed that 21b cannot be considered as a selective AAK1 inhibitor.

To analyse the binding mode of compound **1** (the parental Azaindole-based AAK1 inhibitor), the crystal structure of compound **1** bound to AAK1 to 2.0 \AA resolution was determined in collaboration with the Knapp lab (**Figure 2**). Data collection and refinement statistics are provided in Supplemental Table 1 (see Supporting Information) and PDB coordinates are deposited under PDB ID 5L4Q. Compound **1** binds in the ATP-binding site of AAK1 in a relatively planar manner (Figure 5), with the pyrrolo[2,3-*b*]pyridine moiety bound directly between the side-chains of two highly conserved residues: Ala72 from β 2 in the kinase N-lobe and Leu183 of the C-lobe, the location where the adenine ring of ATP would bind. The nitrogen atoms of the pyrrolo[2,3-*b*]pyridine moiety form two hydrogen bonds to the peptide backbone of residues Asp127 and Cys129 at the kinase hinge region (Figure 5). The 4-cyanophenyl moiety is oriented towards the solvent with the phenyl ring directly sandwiched between the backbone of Gly132 of the hinge and Leu52 of β 1 in the N-lobe, and the nitrogen of the cyano moiety forming a polar interaction with the side-chain of Asn136. The nicotinamide moiety is bound against the “gatekeeper” residue Met126, and forms a hydrogen bond to the side chain of Lys74, another highly conserved residue that normally links the phosphate of ATP to the α C-helix and required for correct positioning of the N-lobe for efficient catalysis. Compound **1** also interacts with two water molecules, one situated at the back of the ATP pocket that bridges between the oxygen of the amide moiety and the backbone nitrogen of Asp194, and a second at the front of the adenosine binding site directly below Val60 in the β 1 strand that interacts with the amide nitrogen and surrounding solvent. The DFG motif (Asp194) is in the conformation expected of active AAK1 (Figure 5), with the activation loop of AAK1 in the same conformation as seen in previous AAK1 and BMP2K crystal structures, including the activation-segment C-terminal helix (ASCH), a structural element that is rare amongst other protein kinases, but conserved across the NAK family.³⁹



1)

Figure 2. Crystal structure of AAK1 (grey) in complex with compound **1** (purple), PDB ID 5L4Q.

A: Overview of the crystal structure of AAK1. Highlighted are areas that are important for kinase function. Compound **1** bound at the hinge is shown. ASCH = Activation Segment C-terminal Helix, a feature unique to kinases of the NAK family. **B:** $2F_o-F_c$ Electron density map contoured at 1σ around compound **1**, showing the fit of the model to the map. **C and D:** Detailed views of the interactions of compound **1** in the ATP-binding site from two orientations. Black dotted lines indicate polar interactions, red spheres indicate water molecules. Note that residues 48-63 from $\beta 1$ and $\beta 2$ are removed from **C** for clarity.

These data (i.e. synthesis, biochemical AAK1 affinity data, kinase selectivity and antiviral evaluation) were recently published in *J. Med. Chem.*

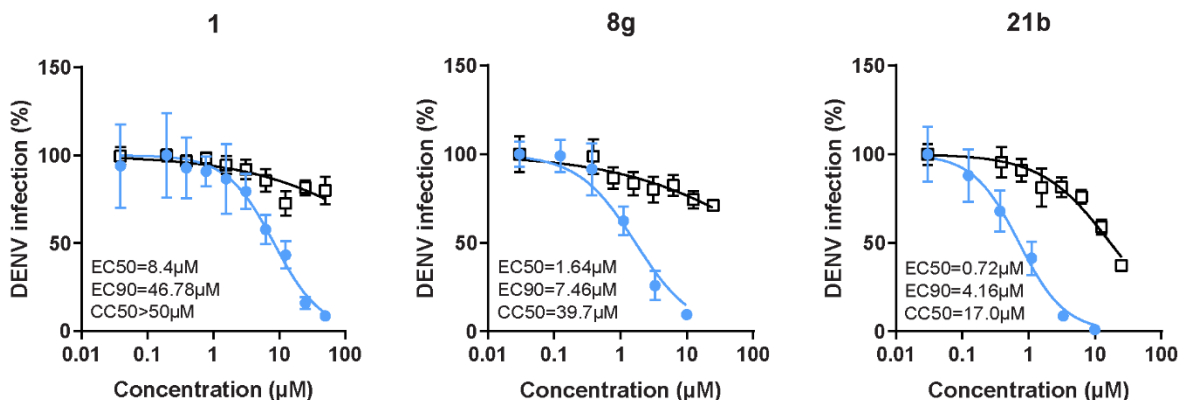
Milestone achieved:

- Several GAK inhibitors with comparable antiviral activity combined with good kinase activity and selectivity identified.
- Novel azaindole-based AAK1 inhibitors with improved antiviral activity identified.

Major Task 2: Determine antiviral activity of the optimized compounds alone and in combinations.				
Subtask 1: Determine the efficacy of the optimized leads' against DENV <i>in vitro</i> .	3-30	Einav		
Subtask 2: Establish expanded broad-spectrum potential against at least 1 viral threat that is unrelated to DENV by evaluating efficacy against EBOV and CHIKV <i>in vitro</i> .	3-30		Dye, Brannan	
Subtask 3: Determine the compounds' EC ₅₀ when used in combination with each other or other antivirals against DENV <i>in vitro</i> .	12-30	Einav		

We have studied all the compounds synthesized in Task 1 for their *in vitro* anti-DENV activity and cellular toxicity, as proposed. Huh7 cells were infected with a DENV-luciferase reporter virus for 4 hours followed by treatment with increasing concentrations of the compounds for 3 days. DENV infection was measured by luciferase assays and cellular viability by alamarBlue-based assays in the same cells. EC₅₀, EC₉₀ and CC₅₀ values were calculated.

Figure 3. Compounds **8g and **21b** suppress DENV infection more effectively than compound **1**.** Dose response of DENV infection (blue) and cell viability (black) to compounds **1**, **8g**, and **21b** measured by luciferase and alamarBlue assays, respectively, 48 hours after infection. Data are plotted relative to vehicle control. Shown are representative experiments from at least two conducted, each with 5 biological replicates; shown are means \pm SD.



As discussed above, 8g and 21b are improved AAK1 inhibitors. The kinetics of antiviral activity of these compounds is much faster than the parental compounds (i.e. their EC50 and EC90 are quite close to each other).

Excitingly, in collaboration with the Dye lab (USAMRIID) and the Narayanan lab (George Mason University) most of these compounds have already been tested and demonstrated activity with no apparent toxicity against unrelated viruses including EBOV, CHIKV and/or VEEV in vitro, attesting to their broad-spectrum potential.

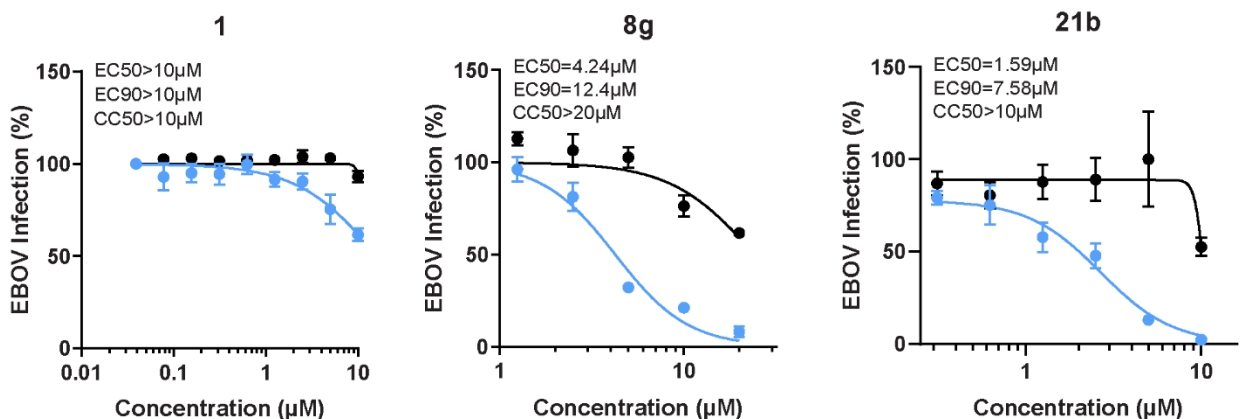
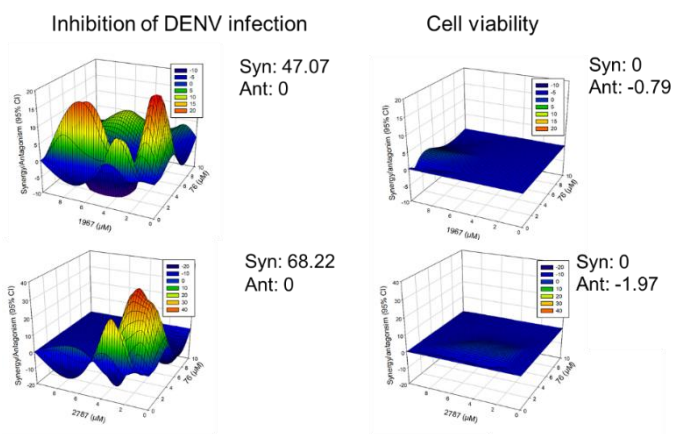


Figure 4. Compounds 1, 8g and 21b suppress EBOV infection. Dose response of EBOV infection (blue) and cell viability (black) to compounds 1, 8g and 21b measured by plaque assay (for compound 1) or immunofluorescence assays (for compounds 8g and 21b) and CellTiter-Glo luminescent cell viability assay in Huh7 cells 48 hours after infection. Data are plotted relative to vehicle control. Shown are representative experiments from at least two conducted, each with 3 biological replicates; shown are means \pm SD.

Additionally, to test our hypothesis that AAK1 and GAK inhibitors display synergistic antiviral effect, we started studying combination drug treatment with these compounds. Our data indicate that the combination of either 1966 or next generation GAK inhibitor, 2787, with the Azaindole-based AAK1 inhibitor (21b) is synergistic (Figure 2). These combinations did not have a synergistic effect on cellular toxicity (Figure 2).

Figure 5. MacSynergy plots demonstrating that AAK1 and GAK inhibitors exhibit synergistic anti-DENV activity. Top panels: 1966 (a GAK inhibitor) with 21b (Azaindole-based AAK1 inhibitor). Bottom panels: 2787 (a GAK inhibitor) with 21b (Azaindole-based AAK1 inhibitor). Left panels: Effect of the combination treatment on antiviral activity by luciferase-based assays in Huh7 cells 72 hours postinfection. Right panels: Effect of the combination treatment on cellular toxicity by alamarBlue assays in the same cells. Peaks above the plane of additivity indicate synergy. Synergy and antagonism volumes at the 95% CI are indicated.



Milestone achieved:

- ii. Two AAK1 inhibitors with improved broad-spectrum antiviral activity was identified.
- ii. AAK1 and GAK inhibitors demonstrate synergistic antiviral effect with no synergistic toxicity.

Aim 2: Determine the *in vivo* metabolism, activity, and relative barrier to resistance of the AAK1 and GAK inhibitors.

Proposed tasks and milestones (approved SOW)

	Time-line (months)	Site 1	Site 2	Site 3	Site 4
Major task 3: Determine PK and demonstrate efficacy with no toxicity in best available murine models of emerging viruses.					
Subtask 1: Determine the PK of optimized inhibitors leads and PK-enhanced compounds and their major metabolites.			9-30		

While we haven't shown *in vivo* activity due to the limited PK, to further determine the therapeutic potential of compounds 8g and 21b as anti-DENV compounds, we studied their antiviral effect in human primary monocyte-derived dendritic cells (MDDCs); an established *ex vivo* model system for DENV. We measured a dose-dependent inhibition of DENV infection with minimal cytotoxicity following a 3-day compound treatment by plaque assays and alamarBlue assays, respectively (**Figure 6**). Dendritic cells represent the primary target of DENV in humans. Moreover, primary cells model human physiology and disease better than immortalized cell lines. Our finding that treatment exhibits antiviral efficacy in MDDCs may therefore more accurately reflect the dependence of DENV on AAK1 during human infection and support the biological relevance of this approach.

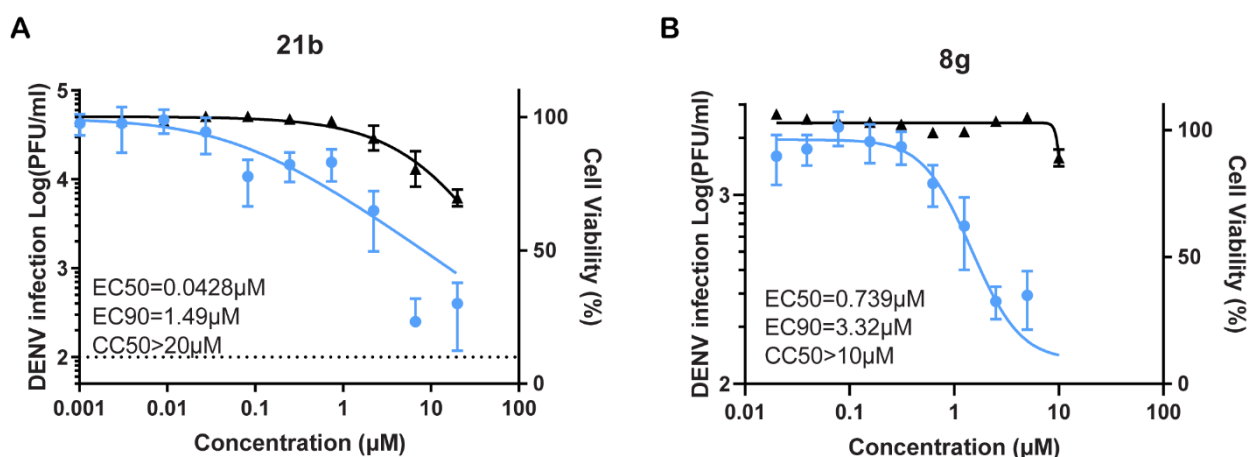


Figure 6. *Ex vivo* antiviral activity of 21b and 8g in human primary dendritic cells. Dose response of DENV infection (blue) and cell viability (black) to compounds **21b** (A) and **8g** (B) measured by plaque assays and alamarBlue assays, respectively, 72 hours after infection of primary human monocyte-derived dendritic cells (MDDCs). Shown is a representative experiment with cells from a single donor, out of 2 independent experiments conducted with cells derived from 2 donors, each with 6 biological replicates; shown are means \pm SD.

	Time-line (months)	Site 1	Site 2	Site 3	Site 4
Major task 4: Determine the potential for emergence of drug resistance compared to direct acting antiviral (DAAs).					
Subtask 1: Identify phenotypic and/or genotypic resistance in DENV infected cells by infectivity assays and circular sequencing of viral genome, respectively.	6-30	Einav			Andino, Rouzine
Subtask 2: Identify phenotypic and/or genotypic resistance in DENV infected AG129 mice by infectivity assays and next generation sequencing of viral genome, respectively.	20-36	Einav			Andino, Rouzine

In collaboration with the Andino lab (UCSF) we have conducted both in vitro and in vivo analysis to determine the genetic barrier to resistance of representative AAK1 and GAK inhibitors alone and in combination.

No phenotypic resistance is detected with AAK1 and/or GAK inhibitors in DENV-infected cultured cells.

To select for viral resistant variants in cultured cells, we serially passaged (N=9 passages) DENV in the presence of the sunitinib (AAK1 inhibitor) and/or erlotinib (GAK inhibitor) at concentrations between their EC₅₀ and EC₉₀. Virus was titered between each passage. No phenotypic resistance was detected (**Figure 7**).

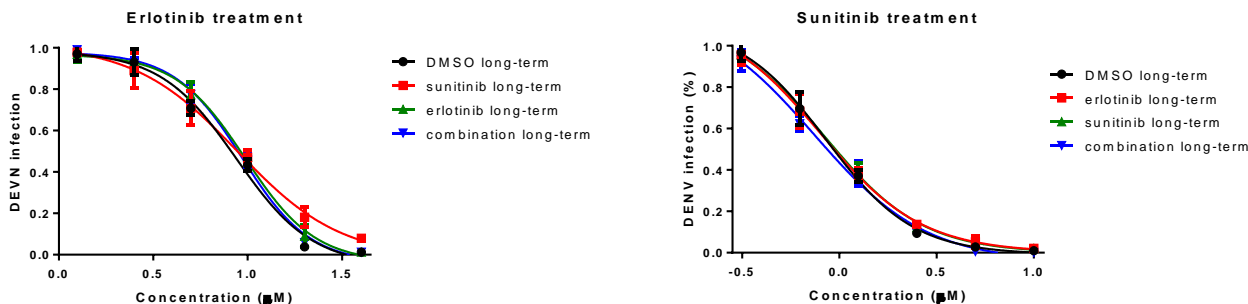


Figure 7. Dose response curves demonstrating the anti-DENV effect of erlotinib (left) and sunitinib (right) in Huh7 cells infected with DENV that was previously passaged for 9 passages in DMSO, sunitinib and/or erlotinib via plaque assays. No shifts in the EC₅₀ or EC₉₀ are shown, indicating absence of phenotypic resistance.

No genotypic resistance is detected with AAK1 and/or GAK inhibitors following serial passaging of DENV in mice.

We analyzed amplicon sequencing data from 12 samples obtained from sunitinib- and erlotinib- or mock-treated mice infected with Dengue 2. Two mutations shown in **Figure 8** are of particular interest in terms of the potential drug resistance effect. Because samples collected here only from the passage 5, we set out to evaluate how frequencies of these two mutations change in previous passages.

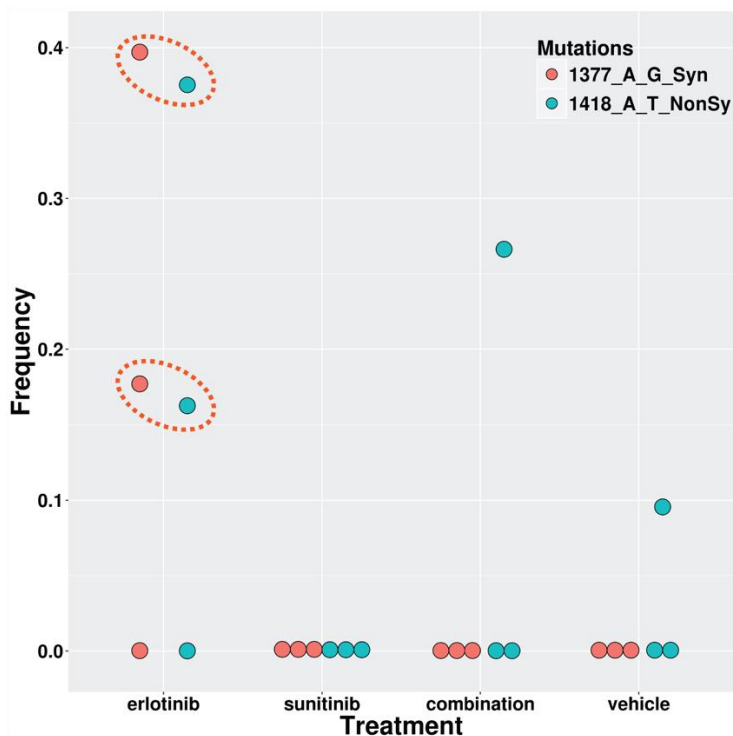


Figure 8. The frequencies of two potential drug resistant mutations. The A-to-G mutation at position 1377 is synonymous. The other A-to-T mutation at 1418 is nonsynonymous. Frequencies were calculated as the number of mutations divided by the coverage at corresponding loci.

In newly generated amplicon sequencing libraries. We focused on erlotinib (2R) treatment and two mice (190 and 191) which carry those two mutations of interest at passage 5. Details on the samples from which amplicon sequencing libraries were made are shown in Table 2.

SampleID	Sample
1	P1-190-2R
2	P1-191-2R
3	P2-190-2R
4	P2-191-2R
5	P3-190-2R
6	P3-191-2R
7	P4-190-2R

Table. 2 Samples used to make amplicon sequencing libraries.

Notes: P1-P4 denotes passage 1 to 4; 190, 191 represents each individual mouse; 2R refers to erlotinib treatment.

Data analyses

We firstly mapped reads to DENV2 virus genome (NCBI Accession Number: NC_001474.2) and kept reads that can be uniquely mapped to one locus of the genome. Afterwards, genetic mutations were called and corresponding frequencies were calculated from the sequencing coverage information.

Two goals of analyses are, 1) to evaluate the frequencies of 1377 and 1418 mutations in Passage 1 to 4; 2) to combine data from Passage 1 to 5 and check whether there are novel mutations with potential drug resistance effects.

Results

- 1) Although we observe relatively high frequencies of 1377 and 1418 mutations at Passage 5 (Fig.1), the mutation at locus 1377 is almost not detectable in previous passages while the mutation at locus 1418 can be detected in one mouse sample (Mouse190) (**Figure 9**).

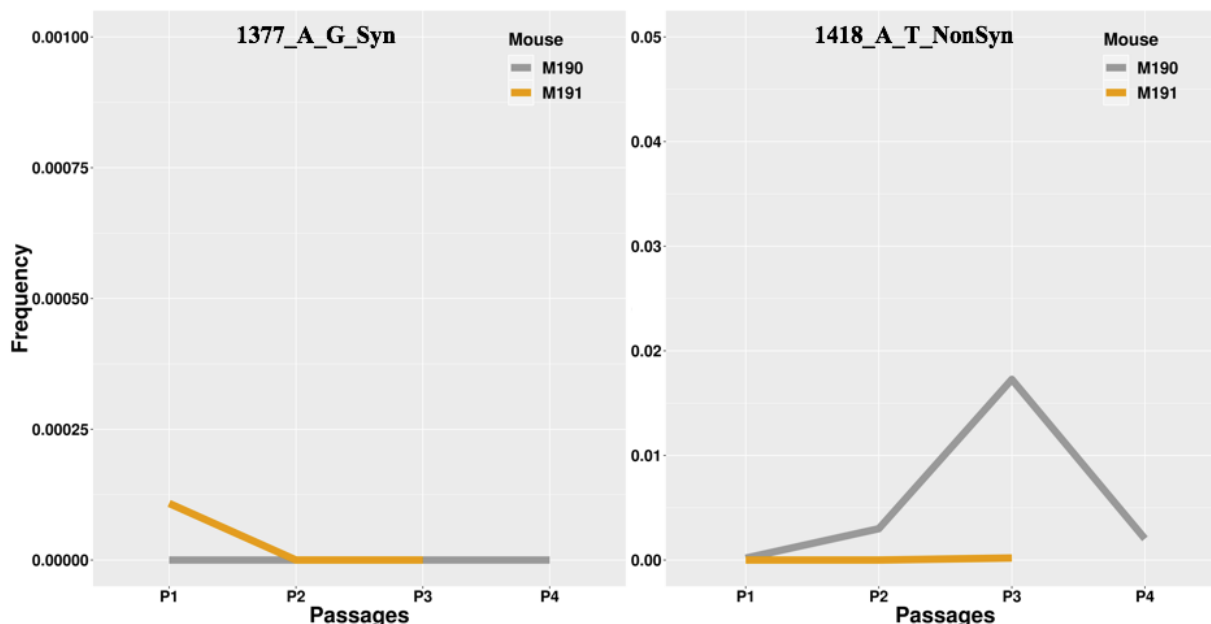


Figure 9. Trajectories of frequencies of 1377 and 1418 mutations in Passage 1 to 4.

- To exclude false positives from sequencing errors, we set a cutoff of base quality scores at Q20, checked mutations with a frequency higher than 0.01 and shared by Mouse190 and Mouse 191 (Table. 2). However, these mutations are not unique and can be detected in other treatments or controls.

Passage	Loci of shared mutations
1	123,248,6513
2	123,124
3	123, 3200

Table 3. Shared mutation at Passage 1 to 3 in erlotinib (2R) treatment groups.

Conclusion: There was no genotypic resistance detected upon passaging DENV2 in mice in the presence of AAK1/GAK inhibitors combination.

Milestones Achieved: i. No phenotypic resistance demonstrated *in vitro*. ii. No genotypic resistance shown *in vivo*.

Aim 3: Select AAK1 and GAK inhibitors as pre-IND candidates.

Proposed tasks and milestones (approved SOW)

Major Task 5: Conduct <i>in vitro</i> ADME-toxicity studies and initial preclinical animal safety testing on the optimized leads and their major metabolites.					
Subtask 1: Test compounds for cell permeability, drug-drug interactions, plasma protein binding, etc.	24-30	Einav *			

We have recently tested representative compounds from each series for key ADME parameter. 8g and 21b data is included in our recently published JMC paper (see attached). Testing included: mean aqueous solubility in PBS and in SIF (simulated intestine fluid) and SGF (simulated gastric fluid). Mean A-B permeability, mean B-A permeability, mean half-life and mean protein binding. We are now incorporating these results in our ongoing SAR.

Milestones Achieved: Key in vitro ADME-Tox parameters determined for representative compounds from each series.

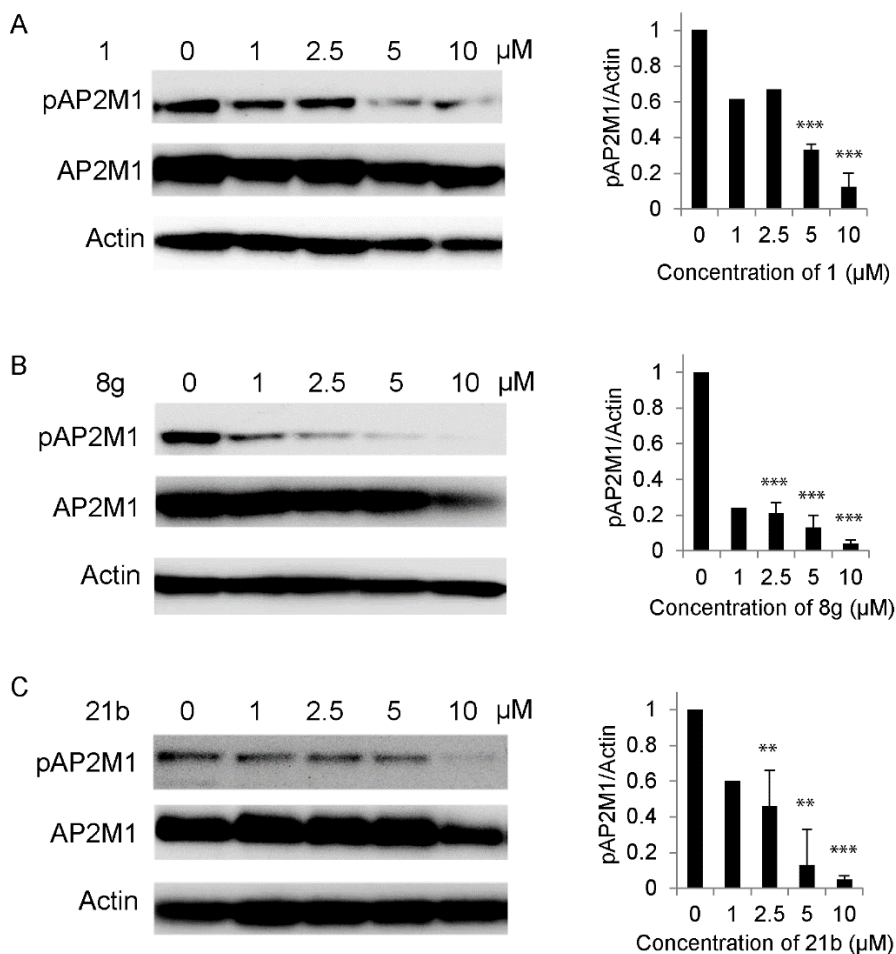
Specific Aim 4: Validate the mechanism of action (MOA) of selective AAK1 and GAK inhibitors in DENV infection

Major Task 6: Validate the molecular targets underlying the antiviral effect of AAK1 and GAK inhibitors and examine these compounds' binding to their predicted antiviral target and its modulation.					
Subtask 1: <i>In vitro</i> validate the molecular targets of AAK1 and GAK inhibitors and monitor functional substrate modulation.	18-30	Einav			

The antiviral effect of AAK1 and GAK inhibitors correlates with functional inhibition of these kinases.

Key AAK1 and GAK inhibitors were tested for their effect on AP2 phosphorylation. For example, to confirm that the observed antiviral activity 8g and 21b is correlated with functional inhibition of AAK1 activity, we measured levels of the phosphorylated form of the μ subunit of the AP-2 complex, AP2M1, upon treatment with these compounds. Since AP2M1 phosphorylation is transient (due to phosphatase PP2A activity)²⁷, to allow capturing of the phosphorylated state, Huh7 cells were incubated for 30 minutes in the presence of the PP2A inhibitor calyculin A prior to lysis. Treatment with 8g or 21b reduced AP2M1 phosphorylation (**Figure 10**), indicating modulation of AP2M1 phosphorylation via AAK1 inhibition.

Figure 10. Antiviral effect of compounds 1, 8g and 21b correlate with functional inhibition of AAK1. Dose response of AP2M1 phosphorylation to treatment with 1 (A), 8g (B), and 21b (C) by Western analysis in lysates derived from Huh7 cells. Representative membranes (from two independent experiments) blotted with anti-phospho-AP2M1 (pAP2M1), anti-AP2M1 (AP2M1), and anti-Actin (Actin) antibodies and quantified data of pAP2M1/actin protein ratio normalized to DMSO controls are shown. ** p < 0.01, *** p < 0.001 by 2-tailed unpaired t test.



Milestones Achieved: Target modulation demonstrated.

Training opportunities that the project provided

- Students and postdoctoral fellows at the Einav, Herdewijn, Andino and Dye labs are being mentored by the respective PI and benefit from interdisciplinary training provided by this project. The PIs are actively involved in designing experiments, data analysis, overseeing the study strategies and participating in presentations and manuscripts preparation.

- The trainees at Stanford are enjoying the privilege of participating in the Stanford SPARK program; a Stanford-based initiative aimed at translating targets to drugs, directed by Dr. Mochly-Rosen. SPARK consultants have expertise in multiple aspects of the development process including medicinal-chemistry, PK/PD, formulation, toxicology, regulatory process, and successful early drug development. The trainees meet on a weekly basis with this talented group of consultants. In addition, they present their progress to the SPARK medicinal chemistry group every quarter.

- All the trainees on this project have also benefited from regular conference calls, which enrich their multidisciplinary training opportunities to students and research fellows.

- The Stanford trainees have attended the annual Bay Virology Symposium, the annual retreats of the Microbiology Department and the division of infectious diseases, as well as monthly seminars of the NIH U19 (to SE) which is focused on developing host-targeted broad-spectrum antiviral approaches.

Dissemination of the results to communities of interest

DTRA is funding a follow up project that is built on this award. The DTRA project is focused on developing countermeasures based on AAK1 and GAK inhibitors to combat the encephalitic alphaviruses (VEEV, EEEV and WEEV). This work is synergistic, yet non-overlapping with the current work. It expands the scope of work to other series of compounds and modifications as well as new disease models.

Plans for the next reporting period

1. Synthesizing covalent AAK1 and GAK inhibitors to enhance their activity and PK
2. PK studies with 8g and 21b.

4. IMPACT:

The impact on the development of the principal discipline(s) of the project

The identification of AAK1 and GAK inhibitors with improved broad-spectrum antiviral activity and metabolic stability is of high impact as these can be potentially advanced into mice experiments. The translational impact of this work is delivering a near-clinical stage product for use against DENV and multiple other currently untreatable biothreats to which our military service members are exposed. Our product is thus intended to fill a large gap in our biodefense and public health capabilities and meet the biodefense community's objective of "one drug, multiple threats". Moreover, our studies provide insight into virus-host interactions and virus evolution under a host-targeted approach. The long-term impact is that a safe broad-spectrum therapeutic could be administered even before a viral biothreat has been accurately diagnosed, thereby improving protection. Such a therapeutic can also be used to treat viral co-infections, such as DENV-CHIKV, and will position us to combat newly emerging pathogens. Lastly, since AAK1 and

GAK are implicated in other diseases, such as Parkinson's, our compounds may find additional clinical indications beyond viral infections.

The impact on other disciplines

Our DTRA grant expands the work to encephalitic alphaviruses; currently untreatable biothreat agents highly relevant to military personnel.

The impact on technology transfer

Nothing to Report.

The impact on society beyond science and technology

Nothing to Report.

5. CHANGES/PROBLEMS:

Changes in approach and reasons for change

There have been no changes in objectives or scope.

Actual or anticipated problems or delays and actions or plans to resolve them

There has been no delay. Nevertheless, as discussed above, we have encountered challenges with advancing former compounds to in vivo experiments. We hope that our additional SAR efforts will enhance the PK of these compounds and/or that 8g or 21b will demonstrate a good PK profile.

Changes that had a significant impact on expenditures

None

Significant changes in use or care of human subjects, vertebrate animals, biohazards, and/or select agents

None

Significant changes in use or care of human subjects

N/A

Significant changes in use or care of vertebrate animals.

None

Significant changes in use of biohazards and/or select agents

None

6. PRODUCTS:

Journal publications:

1. Verdonck S, Pu S, Sorrell FJ, Elkins JM, Froeyen M, Gao LJ, Prugar LI, Dorosky DE, Brannan JM, Barouch-Bentov R, Knapp S, Dye JM, Herdewijn P, Einav S,* De Jonghe S*. Synthesis and structure-activity relationships of 3,5-disubstituted-pyrrolo[2,3-b]pyridines as inhibitors of adaptor associated kinase 1 (AAK1) with antiviral activity. *Journal of Medicinal Chemistry*. 2019 Jun 27;62(12):5810-5831. doi: 10.1021/acs.jmedchem.9b00136. PMID: 31136173
2. Wouters R, Pu SY, Froeyen M, Lescrinier E, Einav S, Herdewijn P, De Jonghe S. Cyclin G-associated kinase (GAK) affinity and antiviral activity studies of a series of 3-C-substituted isothiazolo[4,3-b]pyridines. *Eur J Med Chem*. 2018 Nov 28;163:256-265. doi: 10.1016/j.ejmech.2018.11.065.PMID: 30529544
Link: <https://www.sciencedirect.com/science/article/pii/S0223523418310249?via%3Dihub>
3. Martinez-Gualda B, Pu SY, Froeyen M, Herdewijn P, Einav S, De Jonghe S. Structure-activity relationship study of the pyridine moiety of isothiazolo[4,3-b]pyridines as antiviral agents targeting cyclin G-associated kinase. *Bioorg Med Chem*. 2019 Nov 11:115188. doi: 10.1016/j.bmc.2019.115188. [Epub ahead of print] PMID: 31757682

Presentations:

1. “Broad-spectrum host-targeted approaches to combat emerging viral infections.”
Pharmaceutical & BioScience Society/SPARK conference. Foster City, California, March 2019
2. XVIII International Conference on Heterocycles in Bioorganic Chemistry (Bioheterocycles 2019)
June 17 to 20, 2019 ; Gent (Belgium)
Poster : Inhibitors of cyclin G associated kinase based on novel heterocyclic scaffolds
Steven De Jonghe, Randy Wouters, Junjun Tian, Piet Herdewijn
3. VIII EFMC International Symposium on Advances in Synthetic and Medicinal Chemistry (EFMC-ASMC'19)
Athens, Greece ; September 1-5, 2019
Poster : Synthesis and Structure–Activity Relationships of 3,5-Disubstituted-pyrrolo[2,3-b]pyridines as Inhibitors of Adaptor-Associated Kinase 1 with Antiviral Activity
Sven Verdonck, Szu-Yuan Pu, Fiona J. Sorrell, Jon M. Elkins, Mathy Froeyen, Ling-Jie Gao, Laura I. Prugar, Danielle E. Dorosky, Jennifer M. Brannan, Rina Barouch-Bentov, Stefan Knapp, John M. Dye, Piet Herdewijn, Shirit Einav, Steven De Jonghe

7. PARTICIPANTS & OTHER COLLABORATING ORGANIZATIONS

Individuals who have worked on the project:

Name:	Shirit Einav
Project Role:	PD/PI
Researcher Identifier (e.g. ORCID ID):	0000-0001-6441-4171
Nearest person month worked:	3.5
Contribution to Project:	In charge of coordinating between the teams on the project, designing experiments, ensuring research goals are met in a timely manner and within budget, training the student and postdocs on this project etc.
Funding Support:	DoD, Falk foundation, DTRA, emergent Biosolutions
Name:	Rina Barouch Bentov
Project Role:	Research Associate
Researcher Identifier (e.g. ORCID ID):	0000-0002-5964-2329
Nearest person month worked:	5.2
Contribution to Project:	Rina is involved in the mechanistic studies in this project – i.e. validation of target modulation, molecular target etc. She is also assisting with the resistance assays and antiviral assays.

Funding Support:	DoD, NIAID
Name:	Zhiyuan Yao
Project Role:	Postdoctoral fellow
Researcher Identifier (e.g. ORCID ID):	0000-0002-5759-9822
Nearest person month worked:	1.75
Contribution to Project:	Helped with mechanistic characterization of compounds
Funding Support:	DoD, Catalyst, DTRA
Name:	Stanford Schor
Project Role:	MD/PhD student
Researcher Identifier (e.g. ORCID ID):	0000-0001-6470-2130
Nearest person month worked:	0.5
Contribution to Project:	Has helped conducting AAK1 and GAK kinase assays.
Funding Support:	Stanford MSTP program
Name:	Szuyuan Pu
Project Role:	Postdoctoral fellow
Researcher Identifier (e.g. ORCID ID):	0000-0002-9805-6357
Nearest person month worked:	3
Contribution to Project:	Is involved in designing and executing the antiviral and viability studies, as well as PK, in vitro metabolic studies, and resistance assays.
Funding Support:	DoD, DTRA

Name:	Steven De Jonghe
Project Role:	Co-investigator
Researcher Identifier (e.g. ORCID ID):	0000-0002-3872-6558
Nearest person month worked:	4
Contribution to Project:	Supervising the medicinal chemistry efforts of this project
Funding Support:	DoD
Name:	Belén Martínez Gualda

Project Role:	Postdoctoral fellow
Researcher Identifier (e.g. ORCID ID):	0000-0002-9374-0715
Nearest person month worked:	12
Contribution to Project:	Dr. Martinez Gualda has been focusing on the synthesis of GAK inhibitors.
Funding Support:	DoD grant
Name:	Elisabetta Groaz
Project Role:	Postdoctoral fellow
Researcher Identifier (e.g. ORCID ID):	
Nearest person month worked:	1
Contribution to Project:	Dr. Groaz contributed to the hit-to-lead optimization campaign of GAK inhibitors
Name:	Colette Atdijan
Project Role:	Postdoctoral fellow
Researcher Identifier (e.g. ORCID ID):	0000-0003-3600-7848
Nearest person month worked:	10
Contribution to Project:	Dr. Atdijan contributed to the hit-to-lead optimization campaign of GAK inhibitors.
Funding Support:	DoD grant
Name:	Sven Verdonck
Project Role:	Doctoral student
Researcher Identifier (e.g. ORCID ID):	0000-0002-6017-2491
Nearest person month worked:	1
Contribution to Project:	Mr. Verdonck contributed to the hit-to-lead optimization campaign of AAK1 inhibitors.
Funding Support:	FWO (Fund for Scientific Research – Flanders - Belgium)
Funding Support:	<i>DoD, NIAID</i>

Name:	Raul Andino
Project Role:	Co-I
Researcher Identifier (e.g. ORCID ID):	5503-9349

Nearest person month worked:	4
Contribution to Project:	Dr. Andino is involved in the analysis of virus evolution. He and his group is determining whether Dengue virus develop resistance to AAK1 and GAK inhibitors.
Funding Support:	The Ford Foundation (Complete only if the funding support is provided from other than this award).
Name:	Yinghong Xiao, 10/1/18 – 12/31/18 Weiyi Li, 12/1/18 – 10/18/19
Project Role:	<i>Postdoctoral fellow</i>
Researcher Identifier (e.g. ORCID ID):	0000-0002-6850-6521/ Dr. Xiao 0000-0002-1168-7093/ Dr. Li
Nearest person month worked:	<i>6-Dr. Li</i>
Contribution to Project:	Is involved in the analysis of virus evolution under AAK1 and GAK inhibitors.
Funding Support:	<i>DoD, NIAID</i>

Changes in the active other support of the PD/PI(s) or senior/key personnel:

Einav:

Investigator-Initiated Research Award (GRANT12711429)

09/15/2019-09/14/2022

2.4 calendar

Department of Defense office of the Congressionally Directed Medical Research Programs (CDMRP), Peer Reviewed Medical Research Program (PRMRP)

PI: Einav (Co-Is: Khatri, Quake, Pinsky)

\$400,000 per year

“Towards better understanding and predicting severe dengue.”

The goals of this project are to: 1) monitor transcriptomic responses in multiple cell subtypes in natural dengue infection in adults to identify predictive biomarkers of severity; and 2) validate a 20-gene set to predict severe dengue in adults.

No overlap

Catalyst Award

12/31/2018 to 11/29/2020

Dr. Ralph & Marian Falk Medical Research Trust

1.2 calendar

PI: Einav (co-Is: Khatri, Quake, Pinsky)

\$300,000 total award

“Towards Predicting and Preventing the Development of Severe Dengue.”

The goals of this project are to monitor transcriptomic responses in multiple cell subtypes in natural dengue infection to identify biomarkers of severity in children.

Other organizations involved as partners:

We have been collaborating with USAMRIID, KU Leuven and UCSF as per the original proposal.

Otherwise there is nothing to report.

8. SPECIAL REPORTING REQUIREMENTS

Partnering PI AWARD: Dr. John Dye, our Partnering PI, has submitted a separate report describing the work conducted in his lab during this award period.

9. APPENDIX: Our 3 recently published papers are attached.

Synthesis and Structure–Activity Relationships of 3,5-Disubstituted-pyrrolo[2,3-*b*]pyridines as Inhibitors of Adaptor-Associated Kinase 1 with Antiviral Activity

Sven Verdonck,[†] Szu-Yuan Pu,[‡] Fiona J. Sorrell,[§] Jon M. Elkins,^{§,||} Mathy Froeyen,^{†,‡} Ling-Jie Gao,[†] Laura I. Prugar,[#] Danielle E. Dorosky,[#] Jennifer M. Brannan,[#] Rina Barouch-Bentov,[‡] Stefan Knapp,^{§,‡,‡} John M. Dye,[#] Piet Herdewijn,^{†,‡} Shirit Einav,^{*,‡,‡} and Steven De Jonghe^{*,†,‡}

[†]Medicinal Chemistry, Rega Institute for Medical Research, KU Leuven, Herestraat 49—bus 1041, 3000 Leuven, Belgium

[‡]Department of Medicine, Division of Infectious Diseases and Geographic Medicine, and Department of Microbiology and Immunology, Stanford University School of Medicine, Stanford, California 94305, United States

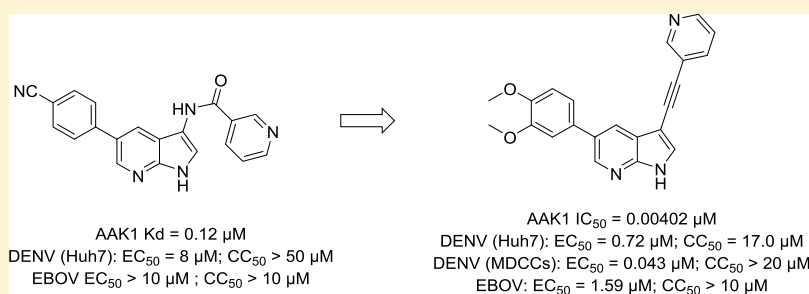
[§]Nuffield Department of Clinical Medicine, Target Discovery Institute (TDI) and Structural Genomics Consortium (SGC), University of Oxford, Old Road Campus, Roosevelt Drive, Oxford OX3 7DQ, U.K.

^{||}Structural Genomics Consortium, Universidade Estadual de Campinas, Cidade Universitária Zeferino Vaz, Av. Dr. André Tosello, 550, Barão Geraldo, Campinas, São Paulo 13083-886, Brazil

[‡]Institute for Pharmaceutical Chemistry, Buchmann Institute for Life Sciences Campus Riedberg, Goethe-University Frankfurt, 60438 Frankfurt am Main, Germany

[#]US Army Medical Research Institute of Infectious Diseases, Viral Immunology Branch, Fort Detrick, Maryland 21702, United States

Supporting Information



ABSTRACT: There are currently no approved drugs for the treatment of emerging viral infections, such as dengue and Ebola. Adaptor-associated kinase 1 (AAK1) is a cellular serine–threonine protein kinase that functions as a key regulator of the clathrin-associated host adaptor proteins and regulates the intracellular trafficking of multiple unrelated RNA viruses. Moreover, AAK1 is overexpressed specifically in dengue virus-infected but not bystander cells. Because AAK1 is a promising antiviral drug target, we have embarked on an optimization campaign of a previously identified 7-azaindole analogue, yielding novel pyrrolo[2,3-*b*]pyridines with high AAK1 affinity. The optimized compounds demonstrate improved activity against dengue virus both in vitro and in human primary dendritic cells and the unrelated Ebola virus. These findings demonstrate that targeting cellular AAK1 may represent a promising broad-spectrum antiviral strategy.

INTRODUCTION

Dengue virus (DENV) is an enveloped, positive-sense, single-stranded RNA virus belonging to the Flaviviridae family. DENV is transmitted by the mosquitoes *Aedes aegypti* and *Aedes albopictus*, which mainly reside in (sub)tropical climates. Hence, dengue outbreaks are mainly confined to equatorial areas, where more than 100 countries have been declared dengue-endemic.¹ The World Health Organization (WHO) estimates that up to 3.9 billion people are at risk of dengue infection at any given time.² In 2013, the WHO reported 3.2 million cases of severe dengue and more than 9000 dengue-

related deaths worldwide.³ Up to 80% of DENV-infected patients remain asymptomatic. Symptomatic patients usually experience an acute febrile illness, characterized by high fever, muscle and joint pain, and sometimes rash.¹ The likelihood of progression to severe dengue, manifesting by shock, hemorrhage, and organ failure, is greater upon secondary infection with a heterologous dengue serotype (of four that circulate) due to antibody-dependent enhancement.⁴

Received: January 23, 2019

Published: May 28, 2019

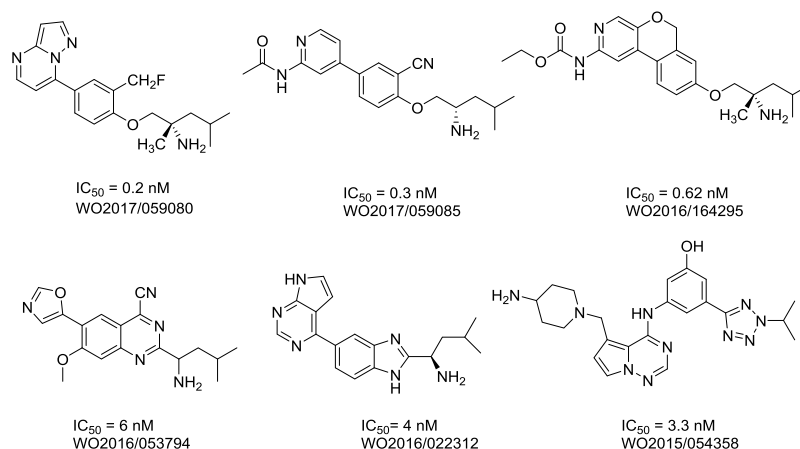


Figure 1. Known AAK1 inhibitors.

Ebola virus (EBOV) is a member of the Filoviridae family. Four of the five known EBOV species have been responsible for over 20 outbreaks and over 10,000 deaths since their identification in 1976.⁵

Current efforts in search for drugs active against DENV focus primarily on viral targets, such as the NS3 helicase, NS2B-NS3 protease, NS4B, NS5 methyltransferase, NS5 polymerase, and the viral envelope.⁶ In search for anti-EBOV drugs, the RNA-dependent RNA polymerase L, the viral surface glycoprotein GP, and viral proteins VP24 and VP35 have been explored as candidate targets.⁶ However, targeting viral functions is often associated with the rapid emergence of drug resistance and usually provides a “one drug, one bug” approach. DENV and EBOV rely extensively on host factors for their replication and survival. These cellular factors represent attractive candidate targets for antiviral agents, potentially with a higher barrier to resistance. In addition, when targeting a host function required for the replication of several unrelated viruses, such compounds are more likely to exhibit broad-spectrum antiviral activity.^{7,8}

Intracellular membrane trafficking is an example of a cellular process that is hijacked by various viruses.⁹ Intracellular membrane trafficking depends on the function of tyrosine- and dileucine-based signals in host cargo proteins, which are recognized by $\mu 1-5$ subunits of the clathrin adaptor protein (AP) complexes AP1-5. Adaptor complexes mediate the sorting of cargo proteins to specific membrane compartments within the cell. While AP2 sorts in the endocytic pathway, AP1 and AP4 sort in the secretory pathway.¹⁰

The activity of AP2M1 and AP1M1, the μ subunits of AP2 and AP1, respectively, is regulated by two host cell kinases, adaptor-associated kinase 1 (AAK1) and cyclin G-associated kinase (GAK). Phosphorylation of specific threonine residues in AP2M1 and AP1M1 by these kinases is known to stimulate their binding to tyrosine signals in cargo proteins and enhance vesicle assembly and internalization. Both AAK1 and GAK regulate clathrin-mediated endocytosis by recruiting clathrin and AP2 to the plasma membrane. AAK1 also regulates clathrin-mediated endocytosis of cellular receptors via alternative sorting adaptors that collaborate with AP-2, for example, by phosphorylation of NUMB.¹⁰ Additionally, AAK1 has been implicated in the regulation of epidermal growth factor receptor (EGFR) internalization and recycling to the plasma membrane via its effects on and interactions with alternate endocytic adaptors. We have demonstrated that

AAK1 and GAK regulate hepatitis C virus (HCV) entry and assembly by modulating AP2 activity^{10,11} and viral release and cell-to-cell spread via regulation of AP1.^{7,12} AAK1 and GAK are also required in the life cycles of DENV and EBOV.⁷

We have reported that the approved anticancer drugs sunitinib and erlotinib that potently inhibit AAK1 and GAK, respectively, demonstrate broad-spectrum in vitro antiviral activity against different members of the Flaviviridae family (HCV, DENV, Zika virus, West Nile virus), as well as against various unrelated families of RNA viruses.⁷ We have also demonstrated that the combination of these two drugs effectively reduces viral load, morbidity, and mortality in mice infected with DENV and EBOV.^{7,13} These data provide a proof of concept that small-molecule inhibition of AAK1 and GAK can yield broad-spectrum antiviral agents.^{7,13} Moreover, using single-cell transcriptomic analysis, AAK1 has been validated as a particularly attractive target because it is overexpressed specifically in DENV-infected and not bystander cells (uninfected cells from the same cell culture), and its expression level increases with cellular virus abundance.¹³

AAK1 has been studied primarily as a drug target for the treatment of neurological disorders, such as schizophrenia, Parkinson's disease, neuropathic pain,¹⁴ bipolar disorders, and Alzheimer's disease.^{15,16} Consequently, very potent AAK1 inhibitors based on different chemotypes have been disclosed in the patent literature. Figure 1 shows representative examples of these AAK1 inhibitors and their enzymatic inhibition data.

Despite the fact that AAK1 has emerged as a promising antiviral target, none of these compound classes have been evaluated and/or optimized for antiviral activity, the only exception being a series of imidazo[1,2-*b*]pyridazines, which were originally developed by Lexicon Pharmaceuticals (Figure 2).¹⁴ We have previously resynthesized these molecules, confirmed their potent AAK1 affinity, and demonstrated their antiviral activity against HCV and DENV.⁷

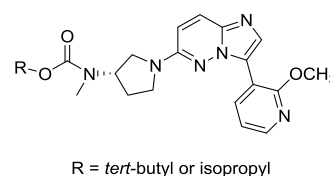


Figure 2. AAK1 inhibitors with documented antiviral activity.

Here, rather than starting from a potent AAK1 inhibitor, we started from a structurally simple compound with reasonable AAK1 activity from which easy structural variation could be introduced. A screening campaign of 577 structurally diverse compounds (representing kinase inhibitor chemical space) across a panel of 203 protein kinases using the DiscoverX binding assay format previously identified a pyrrolo[2,3-*b*]pyridine or 7-aza-indole derivative (compound **1**, Figure 3) as a potent AAK1 inhibitor ($K_D = 53$ nM).¹⁷ In this manuscript, we describe our efforts to optimize the AAK1 affinity and antiviral activity of compound **1**.

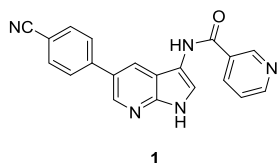


Figure 3. Pyrrolo[2,3-*b*]pyridine (7-aza-indole) based AAK1 inhibitor.

RESULTS AND DISCUSSION

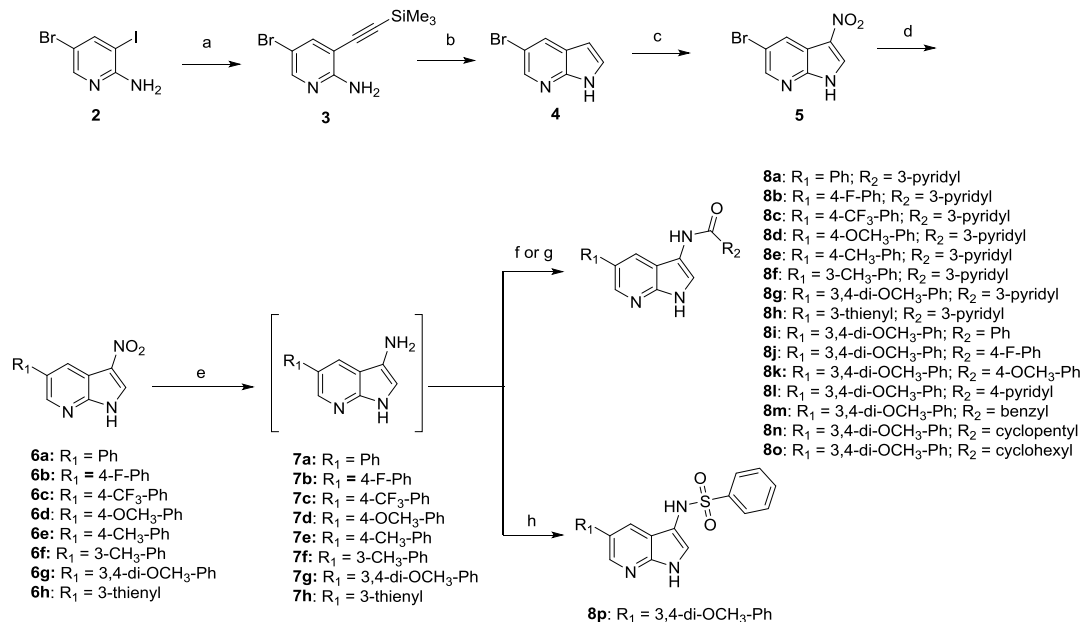
Chemistry. *Synthesis of 3-Substituted-5-aryl Pyrrolo[2,3-*b*]pyridines.* A regioselective Sonogashira coupling of trimethylsilylacetylene with commercially available 5-bromo-3-iodo-2-aminopyridine **2** afforded the alkynyl derivative **3** (Scheme 1).¹⁸ Compound **3** was then reductively ring-closed with a strong base yielding pyrrolo[2,3-*b*]pyridine **4**. Initially, NaH was used as base,¹⁸ but later on potassium *tert*-butoxide¹⁹ was applied as this gave a cleaner reaction outcome and an improved yield. Initial attempts to nitrate position 3 of the 7-azaindole scaffold employed a mixture of a 65% HNO₃ solution and sulfuric acid.²⁰ However, the desired product was difficult to isolate from this reaction mixture, and

therefore, the nitration was performed by treatment of compound **4** with fuming nitric acid.²¹ The 3-nitro derivative **5** precipitated from the reaction mixture and was conveniently isolated by filtration. Suzuki coupling of compound **5** with a number of arylboronic acids yielded the 3-nitro-5-aryl-pyrrolo[2,3-*b*]pyridines **6a–h** in yields ranging from 65 to 85%.²² Catalytic hydrogenation of the nitro moiety yielded the corresponding amino derivatives **7a–h**. Because of the instability of the 3-amino-pyrrolo[2,3-*b*]pyridines, these were not purified and used as such for further reaction. Coupling with an acid chloride in a mixture of pyridine and dichloromethane (DCM)²³ or alternatively, reaction with a carboxylic acid using (benzotriazol-1-yl)oxytris(dimethylamino)phosphonium hexafluorophosphate (BOP) as a coupling reagent²⁴ yielded a small library of pyrrolo[2,3-*b*]pyridines **8a–o**. A sulfonamide derivative **8p** was prepared via reaction of **7g** with phenylsulfonyl chloride in pyridine.

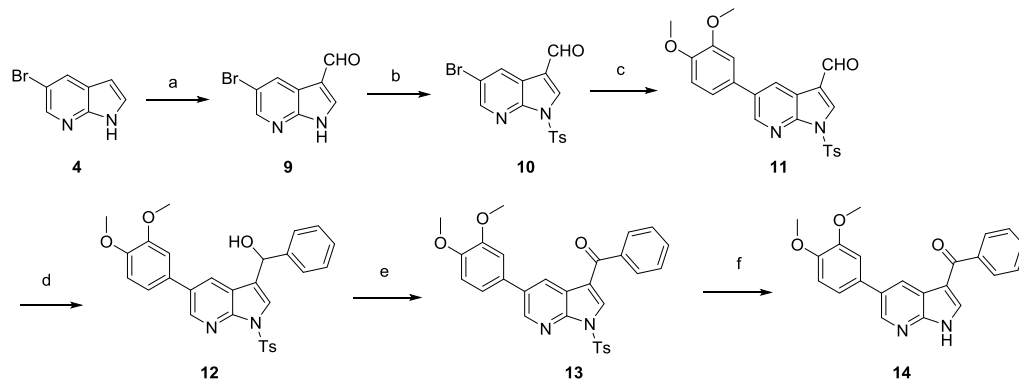
*Synthesis of 3-Benzoyl-5-(3,4-dimethoxyphenyl)-pyrrolo[2,3-*b*]pyridine.* Formylation of compound **4** by a Duff reaction²⁵ yielded 3-formyl-5-bromo-azaindole **9** (Scheme 2). The pyrrole nitrogen was protected²⁶ using NaH and tosylchloride yielding compound **10**. Suzuki coupling reaction with 3,4-dimethoxyphenylboronic acid furnished compound **11**. Nucleophilic addition²⁷ of phenylmagnesium bromide to the aldehyde furnished the secondary alcohol **12**. Oxidation²⁸ of the benzylic alcohol using MnO₂ afforded ketone **13**. Finally, alkaline deprotection²⁹ of the tosyl group yielded the desired compound **14**.

*Synthesis of 3-Phenyl-5-(3,4-dimethoxyphenyl)-pyrrolo[2,3-*b*]pyridine.* Iodination of compound **4** with *N*-iodosuccinimide³⁰ afforded compound **15** (Scheme 3). Reaction of compound **15** with phenylboronic acid led only to recovery of unreacted starting material. Therefore, the pyrrole nitrogen of the 7-azaindole scaffold was protected as a tosyl group,²⁶ affording compound **16**. A regioselective Suzuki coupling

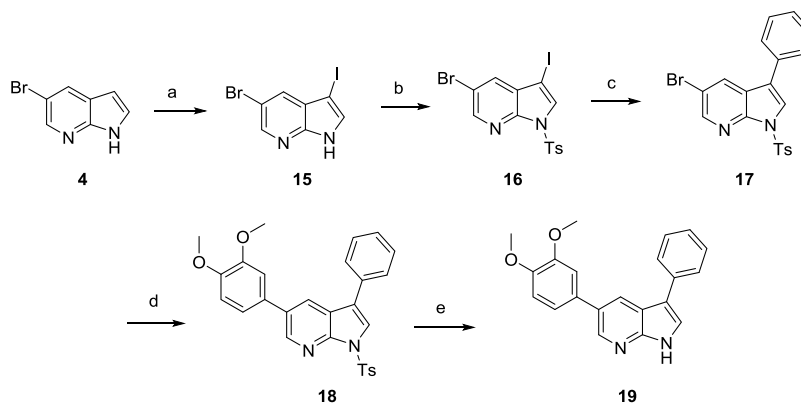
Scheme 1. Synthesis of 3-Substituted-5-aryl Pyrrolo[2,3-*b*]pyridines **8a–p**^a



^aReagents and conditions. (a) TMSA, Pd(PPh₃)₂Cl₂, CuI, Et₃N, THF, rt; (b) KO^tBu, NMP, 80 °C; (c) HNO₃, 0 °C to rt; (d) Pd(PPh₃)₄, K₂CO₃, ArB(OH)₂, H₂O, dioxane, 105 °C; (e) H₂, Pd/C, THF, rt; (f) RCOCl, pyridine, THF, 1 M NaOH, rt; (g) RCOOH, BOP, Et₃N, DMF, rt; (h) PhSO₂Cl, pyridine, rt.

Scheme 2. Synthesis of 3-Benzoyl-5-(3,4-dimethoxyphenyl)-pyrrolo[2,3-*b*]pyridine 14^a

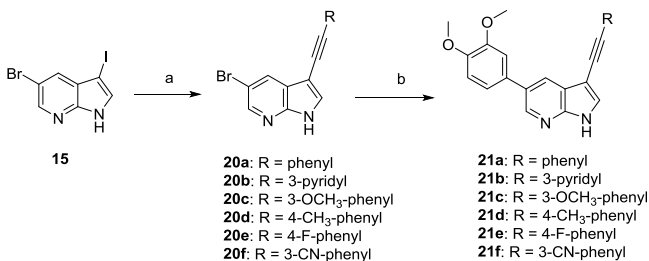
^aReagents and conditions. (a) Hexamine, H₂O, CH₃COOH, 120 °C; (b) NaH, TsCl, 0 °C to rt; (c) 3,4-dimethoxyphenylboronic acid, Pd(PPh₃)₄, 2 M K₂CO₃, toluene, EtOH, 105 °C; (d) 3 M PhMgBr, THF, rt; (e) MnO₂, THF, rt; (f) KOH, EtOH, 80 °C.

Scheme 3. Synthesis of 3-Phenyl-5-(3,4-dimethoxyphenyl)-pyrrolo[2,3-*b*]pyridine 19^a

^aReagents and conditions. (a) NIS, acetone, rt; (b) NaH, TsCl, THF, 0 °C to rt; (c) PhB(OH)₂, Pd(PPh₃)₄, K₂CO₃, toluene, EtOH, H₂O, 90 °C; (d) 3,4-dimethoxyphenylboronic acid, Pd(PPh₃)₄, K₂CO₃, toluene, EtOH, H₂O, 105 °C; (e) KOH, EtOH, 80 °C.

reaction using phenylboronic acid furnished the 3-phenylpyrrolo[2,3-*b*]pyridine analogue 17. A subsequent Suzuki reaction²² with 3,4-dimethoxyphenylboronic acid yielded compound 18. Finally, alkaline cleavage of the tosyl protecting group afforded the desired target compound 19.²⁹

Synthesis of 3-Alkynyl-5-(3,4-dimethoxyphenyl)-pyrrolo[2,3-*b*]pyridines. Sonogashira reaction of compound 15 with a number of (hetero)arylacetylenes yielded regioselectively compounds 20a–f in yields varying from 20 to 70% (Scheme 4).¹⁸ In contrast to Suzuki couplings (Scheme 3), protection of

Scheme 4. Synthesis of 3-Alkynyl-5-(3,4-dimethoxyphenyl)-pyrrolo[2,3-*b*]pyridines 21a–f^a

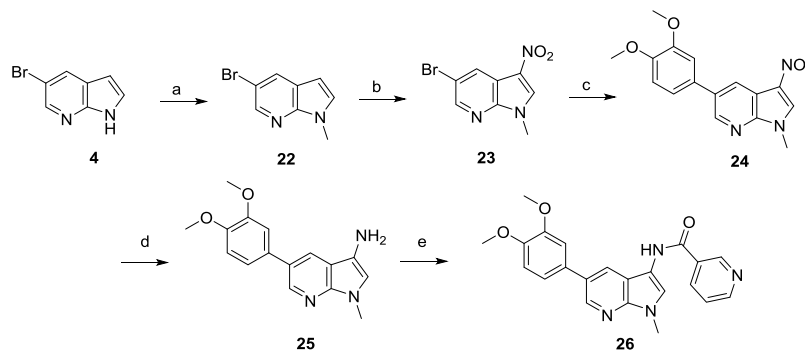
^aReagents and conditions. (a) RC≡CH, Pd(PPh₃)₂Cl₂, CuI, THF, Et₃N, rt; (b) 3,4-dimethoxyphenylboronic acid, Pd(PPh₃)₄, K₂CO₃, H₂O, dioxane, 105 °C.

the pyrrole nitrogen was not necessary. Subsequent Suzuki coupling²² with 3,4-dimethoxyphenylboronic acid gave access to final compounds 21a–f.

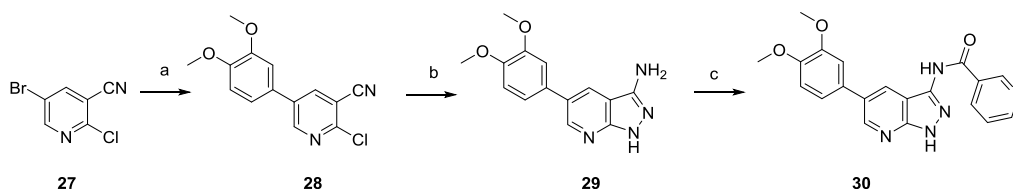
Synthesis of 1-Methyl-1H-pyrrolo[2,3-*b*]pyridine. Methylation³¹ of compound 4 using NaH and MeI furnished compound 22 (Scheme 5). Nitration,²¹ followed by Suzuki coupling,²² gave access to compound 24. Finally, catalytic reduction of the nitro group, followed by condensation²³ of the exocyclic amino group of compound 25 with nicotinoyl chloride, yielded target compound 26.

Synthesis of Pyrrolo[3,4-*b*]pyridine. Suzuki coupling²² between commercially available 5-bromo-2-chloronicotinonitrile 27 and 3,4-dimethoxyphenylboronic acid yielded regioselectively compound 28. Nucleophilic displacement of the chlorine by hydrazine, with a concomitant nucleophilic addition at the cyano group,³² allowed to construct the pyrazole moiety, yielding compound 29. Finally, amide formation³³ using nicotinoyl chloride yielded the final compound 30 (Scheme 6).

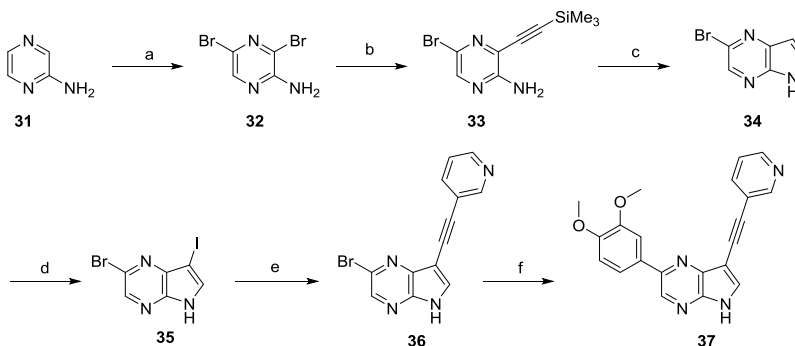
Synthesis of Pyrrolo[2,3-*b*]pyrazine. Treatment of 2-aminopyrazine 31 with *N*-bromosuccinimide yielded the 3,5-dibromopyrazine intermediate 32 (Scheme 7).³⁴ A regioselective Sonogashira coupling with trimethylsilylacetylene, followed by a reductive ring closure with potassium *tert*-butoxide, furnished pyrrolo[2,3-*b*]pyrazine 34.³⁵ Iodination³⁶ with *N*-iodosuccinimide yielded the dihalogenated intermedi-

Scheme 5. Synthesis of 1-Methyl-1*H*-pyrrolo[2,3-*b*]pyridine 26^a

^aReagents and conditions. (a) NaH, MeI, THF, 0 °C to rt; (b) HNO₃, 0 °C to rt; (c) 3,4-dimethoxyphenylboronic acid, Pd(PPh₃)₄, K₂CO₃, H₂O, dioxane, 105 °C; (d) H₂, THF, rt; (e) nicotinoyl chloride, pyridine, THF, 1 M NaOH, rt.

Scheme 6. Synthesis of Pyrazolo[3,4-*b*]pyridine 30^a

^aReagents and conditions (a) 3,4-dimethoxyphenylboronic acid, Pd(PPh₃)₄, K₂CO₃, H₂O, dioxane, 105 °C; (b) 35% hydrazine hydrate, EtOH, 80 °C; (c) nicotinoyl chloride, pyridine, rt.

Scheme 7. Synthesis of Pyrrolo[2,3-*b*]pyrazine 37^a

^aReagents and conditions (a) NBS, DMSO, rt; (b) Me₃SiC≡CH, Pd(PPh₃)₂Cl₂, CuI, THF, Et₃N, rt; (c) KO^tBu, NMP, 100 °C; (d) NIS, acetone, rt; (e) 3-ethynylpyridine, Pd(PPh₃)₂Cl₂, CuI, THF, Et₃N, rt; (f) 3,4-dimethoxyphenylboronic acid, Pd(PPh₃)₄, K₂CO₃, H₂O, dioxane, 105 °C.

ate 35 that was subsequently treated with 3-ethynylpyridine¹⁸ and 3,4-dimethoxyphenylboronic acid²² leading to the desired pyrrolo[2,3-*b*]pyrazine 37.

Kinase Profiling and X-ray Crystallography of Compound 1. AAK1 is a serine–threonine kinase that belongs to the family of NUMB-associated kinases (NAKs). Other members of this kinase family include BIKE/BMP2K (BMP-2 inducible kinase), GAK (cyclin G-associated kinase), and MPSK1 (myristoylated and palmitoylated serine–threonine kinase 1, also known as STK16). As part of an early profiling of hit compound 1, we assessed its selectivity by a binding-displacement assay against each of the four NAK family kinases (Figure 4). Conversion of the experimentally determined IC₅₀ values to K_i values to allow estimation of the selectivity showed that compound 1 was 3-fold more selective for AAK1 over GAK, and 8-fold and 22-fold more selective for AAK1 over BMP2K and STK16, respectively (Table 1).

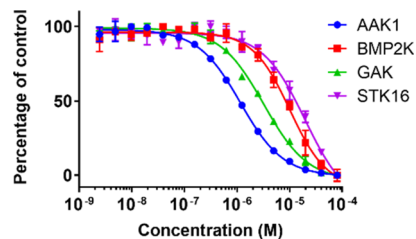


Figure 4. Binding displacement assay of compound 1 against the NAK family members.

To analyze the binding mode of compound 1, the crystal structure of compound 1 bound to AAK1 to 2.0 Å resolution was determined (Figure 5). Data collection and refinement statistics are provided in Table S1 (see Supporting Information), and PDB coordinates are deposited under PDB ID 5L4Q. Compound 1 binds in the ATP-binding site of AAK1 in a relatively planar manner (Figure 5), with the

Table 1. Selectivity of Compound 1 for AAK1 against the NAK Family Kinases

NAK	binding displacement assay		
	IC ₅₀ (μM)	K _i (μM)	K _i /K _i (AAK1)
AAK1	1.17	0.541	1.0
BMP2K	10.1	4.40	8.13
GAK	3.25	1.75	3.23
STK16	20.0	11.9	22.0

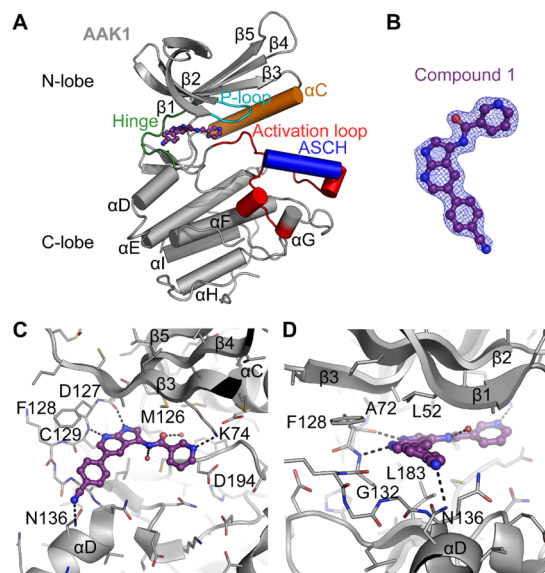


Figure 5. Crystal structure of AAK1 (gray) in complex with compound 1 (purple), PDB ID 5L4Q. (A) Overview of the crystal structure of AAK1. Highlighted are areas that are important for kinase function. Compound 1 bound at the hinge is shown. ASCH = activation segment C-terminal Helix, a feature unique to kinases of the NAK family. (B) $2F_o - F_c$ electron density map contoured at 1σ around compound 1, showing the fit of the model to the map. (C,D) Detailed views of the interactions of compound 1 in the ATP-binding site from two orientations. Black dotted lines indicate polar interactions, and red spheres indicate water molecules. Note that residues 48–63 from $\beta 1$ and $\beta 2$ are removed from (C) for clarity.

pyrrolo[2,3-*b*]pyridine moiety bound directly between the side chains of two highly conserved residues: Ala72 from $\beta 2$ in the kinase N-lobe and Leu183 of the C-lobe, the location where the adenine ring of ATP would bind. The nitrogen atoms of the pyrrolo[2,3-*b*]pyridine moiety form two hydrogen bonds to the peptide backbone of residues Asp127 and Cys129 at the kinase hinge region (Figure 5). The 4-cyanophenyl moiety is oriented toward the solvent, with the phenyl ring directly sandwiched between the backbone of Gly132 of the hinge and Leu52 of $\beta 1$ in the N-lobe, and the nitrogen of the cyano moiety forming a polar interaction with the side chain of Asn136. The nicotinamide moiety is bound against the “gatekeeper” residue Met126 and forms a hydrogen bond to the side chain of Lys74, another highly conserved residue that normally links the phosphate of ATP to the αC -helix and is required for correct positioning of the N-lobe for efficient catalysis. Compound 1 also interacts with two water molecules, one situated at the back of the ATP pocket that bridges between the oxygen of the amide moiety and the backbone nitrogen of Asp194, and a second at the front of the adenosine binding site directly below Val60 in the $\beta 1$ strand that interacts with the amide nitrogen and surrounding solvent. The DFG motif (Asp194) is in the conformation expected of active AAK1 (Figure 5), with the activation loop of AAK1 in the same conformation as seen in previous AAK1 and BMP2K crystal structures, including the activation-segment C-terminal helix (ASCH), a structural element that is rare among other protein kinases, but conserved across the NAK family.³⁷

Structure–Activity Relationship Study. All compounds synthesized in this study were evaluated for AAK1 affinity using two different, commercially available AAK1 binding assays. In the early stage of the program, the proprietary KINOMEScan screening platform of DiscoverX was used. In this assay, compounds that bind the kinase active site prevent kinase binding to an immobilized ligand and reduce the amount of kinase captured on the solid support. Hits are then identified by measuring the amount of kinase captured in test versus control samples via quantitative polymerase chain reaction (qPCR) that detects an associated DNA label.³⁸ Later on in the project, compounds were evaluated by the LanthaScreen Eu kinase binding assay (ThermoFisher Scientific), in which binding of an Alexa Fluor conjugate or

Table 2. SAR at Position 5 of the 7-Aza-indole Scaffold

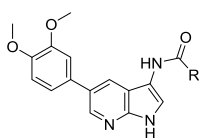
Cmpd#	R ₅	AAK1 enzymatic data		DENV antiviral activity		cytotoxicity CC ₅₀ (μM)
		AAK1 K _D (μM) (DiscoverX)	AAK1 IC ₅₀ (μM) LanthaScreen	EC ₅₀ (μM)	EC ₉₀ (μM)	
1	4-cyanophenyl	0.120	ND ^a	8.37	46.8	>50
8a	phenyl	0.0822	ND ^a	5.29	87.1	NE ^b
8b	4-F-phenyl	0.141	ND ^a	6.43	25.2	NE ^b
8c	4-CF ₃ -phenyl	ND ^a	0.23	2.94	12.0	57.0
8d	4-OCH ₃ -phenyl	0.0194	ND ^a	4.39	25.8	NE ^b
8e	4-Me-phenyl	0.0532	ND ^a	2.60	33.6	>100
8f	3-Me-phenyl	ND ^a	0.0186	4.86	10.8	16.0
8g	3,4-di-OCH ₃ -phenyl	0.00673	0.00432	1.64	7.46	39.7
8h	3-thienyl	0.0161	ND ^a	3.01	66.8	NE ^b
sunitinib		0.0110	0.0474	1.35	2.71	246

^aND: not determined. ^bNE: No effect (no apparent effect on cellular viability up to a concentration of 10 μM).

“tracer” to a kinase is detected by addition of a Eu-labeled anti-tag antibody. Binding of the tracer and antibody to a kinase results in a high degree of fluorescence resonance energy transfer (FRET), whereas displacement of the tracer with a kinase inhibitor results in loss of FRET.

The compounds were also assessed for antiviral activity in human hepatoma (Huh7) cells infected with DENV2. Their effect on overall infection was measured at 48 h postinfection with DENV2 via luciferase assays and the half-maximal effective concentration and the 90% effective concentrations (EC_{50} and EC_{90} values, respectively) were calculated. In parallel, the cytotoxicity of the compounds (expressed as the half-maximal cytotoxic concentration or CC_{50} value) was measured via an alamarBlue assay in the DENV-infected Huh7 cells (Tables 2–6).

Table 3. SAR of the N-Acyl Moiety

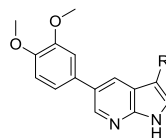


Cmpd#	R	AAK1 enzymatic data		DENV antiviral activity		Cytotoxicity
		AAK1 IC_{50} (μ M) LanthaScreen	EC_{50} (μ M)	EC_{90} (μ M)	CC_{50} (μ M)	
8g	3-pyridyl	0.00432	1.64	7.46	39.7	
8i	phenyl	0.108	4.07	50.5	17.3	
8j	4-F-phenyl	0.161	8.34	30.2	15.9	
8k	4-OCH ₃ -phenyl	0.0721	NE ^a	NE ^a	23.6	
8l	4-pyridyl	0.381	12.6	26.8	NE ^a	
8m	benzyl	0.612	142	NE ^a	NE ^a	
8n	cyclopentyl	0.398	3.42	8.34	15.2	
8o	cyclohexyl	0.319	4.27	10.8	14.7	

^aNE: no effect (no apparent antiviral effect or effect on cellular viability up to a concentration of 10 μ M).

In all these enzymatic and antiviral assays, sunitinib was included as a positive control (Table 2). Sunitinib has potent

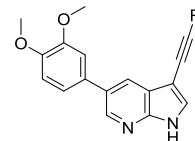
Table 4. SAR of the Linker Moiety at Position 3



Cmpd#	R	AAK1 enzymatic data		DENV antiviral activity		Cytotoxicity
		AAK1 IC_{50} (μ M) LanthaScreen	EC_{50} (μ M)	EC_{90} (μ M)	CC_{50} (μ M)	
8i		0.108	4.07	50.5	17.3	
19		0.0236	3.02	8.34	990	
14		0.184	1.07	3.73	35.3	
21a		0.209	5.64	10.58	20.1	
8p		4.44	8.14	106	NE ^a	

^aNE: no effect (no apparent effect on cellular viability up to a concentration of 10 μ M).

Table 5. SAR of Phenylacetylene Moiety



Cmpd#	R	AAK1 enzymatic data		DENV antiviral activity		cytotoxicity
		AAK1 IC_{50} (μ M) LanthaScreen	EC_{50} (μ M)	EC_{90} (μ M)	CC_{50} (μ M)	
21a	phenyl	0.209	5.64	10.58	20.1	
21b	3-pyridyl	0.00402	0.72	4.16	17.0	
21c	3-OCH ₃ -phenyl	0.149	NE ^a	NE ^a	19.6	
21d	4-CH ₃ -phenyl	0.420	7.45	20.5	NE ^a	
21e	4-F-phenyl	0.387	4.21	8.57	19.9	
21f	3-CN-phenyl	0.381	10.2	41.2	NE ^a	

^aNE: no effect (no apparent antiviral effect or effect on cellular viability up to a concentration of 10 μ M).

AAK1 affinity as measured by the KinomeScan format ($K_D = 11$ nM) and LanthaScreen assay ($IC_{50} = 47$ nM) and displayed potent activity against DENV with an EC_{50} value of 1.35 μ M.

Structure–Activity Relationship at Position 5 of the 7-Aza-indole Scaffold. We confirmed the AAK1 binding affinity of hit compound **1**, yet in our hands, a K_D value of 120 nM was measured (vs the reported $K_D = 53$ nM).¹⁷ This hit demonstrated antiviral activity, although it was rather weak ($EC_{50} = 8.37$ μ M). Substitution of the 5-(4-cyanophenyl) moiety of compound **1** by phenyl (compound **8a**), thienyl (compound **8h**), and substituted phenyl rings with electron-withdrawing groups (compound **8c**), electron-donating substituents (compounds **8d–g**), and a halogen (compound **8b**) gave rise to a series of analogues with structural variety that were at least equipotent to compound **1**, suggesting that structural modification at this position is tolerated for AAK1 binding (Table 2). The synthesis of this limited number of analogues allowed us to quickly identify the 5-(3,4-dimethoxyphenyl) congener (compound **8g**) with low nM AAK1

Table 6. Scaffold Modifications

Cmpd#	Structure	AAK1 enzymatic data	DENV antiviral activity		Cytotoxicity
		AAK1 IC ₅₀ (μM) LanthaScreen	EC ₅₀ (μM)	EC ₉₀ (μM)	CC ₅₀ (μM)
26		3.39	NE ^a	NE ^a	NE ^a
30		0.462	2.09	19.0	16.0
37		0.00927	3.28	7.68	4.81

^aNE: no effect (no apparent antiviral effect or effect on cellular viability up to a concentration of 10 μM).

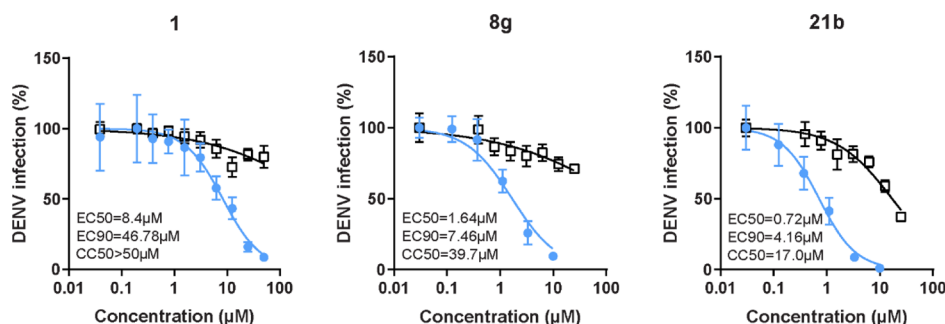


Figure 6. Compounds **8g** and **21b** suppress DENV infection more effectively than compound **1**. Dose response of DENV infection (blue) and cell viability (black) to compounds **1**, **8g**, and **21b** measured by luciferase and alamarBlue assays, respectively, 48 h after infection. Data are plotted relative to vehicle control. At least two representative experiments conducted are shown, each with 5 biological replicates, and the values are expressed as means ± SD.

binding affinity in both the KinomeScan and LanthaScreen assay, indicating an excellent correlation between the two assays. As compound **8g** showed stronger AAK1 affinity than the positive control sunitinib, no additional efforts were done to further explore the structure–activity relationship (SAR) at this position of the 7-aza-indole scaffold.

All analogues within this series had an improved antiviral activity against DENV, relative to the original hit **1**. The compound with the highest binding affinity for AAK1 (compound **8g**) also demonstrated the most effective anti-DENV activity, with EC₅₀ and EC₉₀ values of 1.64 and 7.46 μM, respectively (Figure 6).

SAR of the N-Acyl Moiety. Given the improved AAK1 affinity and antiviral activity of compound **8g**, the SAR of this compound was further examined through the replacement of the 3-pyridyl group by a number of (hetero)aromatics and cycloaliphatic groups, while the 3,4-dimethoxyphenyl residue was kept fixed (Table 3). Our findings indicate that the 3-pyridyl moiety is critical for AAK1 binding as all analogues showed a 100-fold decreased AAK1 affinity, when compared to compound **8g**, giving rise to AAK1 IC₅₀ values in the 0.1–0.6 μM range. Only the congener with a 4-methoxyphenyl residue (compound **8k**) was endowed with an enhanced AAK1 affinity with an IC₅₀ value of 0.072 μM. In correlation with their weaker affinity for AAK1, these compounds had a diminished antiviral activity relative to compound **8g**.

SAR of the Linker Moiety at Position 3. To evaluate the importance of the amide linker, a number of surrogates were prepared (Table 4). For synthetic feasibility reasons, compound **8i**, having a phenyl residue instead of a 3-pyridyl ring, and endowed with quite potent AAK1 affinity and moderate antiviral activity, was selected as a reference compound. Removing the amide linker furnished the 3-phenyl substituted analogue **19**, which was 4-fold more potent as AAK1 ligand than compound **8i**, and showed a slightly improved antiviral activity against DENV (EC₅₀ and EC₉₀ values of 3.02 and 8.34 μM, respectively). When the amide linker of compound **8i** was replaced by a ketone (compound **14**) or alkyne (compound **21a**) functionality, AAK1 affinity was retained. Compound **14** exhibited an improved antiviral activity in comparison with compound **8i**. Finally, replacement of the amide moiety by a sulfonamide linker was not well-tolerated, as compound **8p** showed close to 200-fold drop in AAK1 affinity.

SAR of Phenylacetylene. The data in Table 4 suggest that the amide moiety is not essential for AAK1 binding and can be replaced. Although the 3-phenyl derivative **19** displayed potent AAK1 affinity, 3,5-diaryl pyrrolo[2,3-*b*]pyridines are well known in the literature as kinase inhibitors. In contrast, 3-alkynyl-7-aza-indoles are studied to a much less extent. We, therefore, selected the acetylene derivate **21a** to decipher if it was possible to improve AAK1 affinity and antiviral activity by further modifying the substitution pattern. A number of

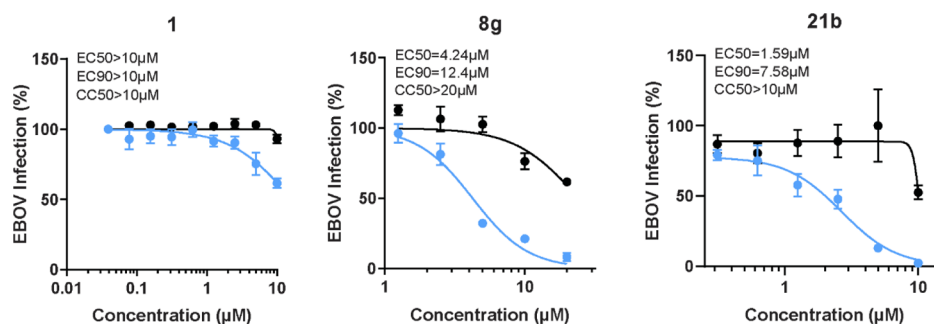


Figure 7. Compounds **1**, **8g**, and **21b** suppress EBOV infection. Dose response of EBOV infection (blue) and cell viability (black) to compounds **1**, **8g**, and **21b** measured by plaque assay (for compound **1**) or immunofluorescence assays (for compounds **8g** and **21b**) and CellTiter-Glo luminescent cell viability assay in Huh7 cells 48 h after infection. Data are plotted relative to vehicle control. A representative experiment, out of at least two conducted, is shown and the values are shown as means \pm SD.

substituted phenylacetylene derivatives were prepared (compounds **21b–f**). The SAR in this series was quite flat, as all compounds displayed very similar AAK1 affinity with IC_{50} values in the 0.1–0.4 μ M range (Table 5). In contrast, the introduction of a 3-pyridylacetylene (compound **21b**) led to a substantial improvement in AAK1 affinity ($IC_{50} = 0.0042 \mu$ M) with a concomitant improvement in antiviral activity ($EC_{50} = 0.72 \mu$ M) and only a moderate cytotoxic effect ($CC_{50} = 17 \mu$ M, Figure 6).

Scaffold Modifications. Lastly, our SAR exploration focused on the 7-aza-indole scaffold itself (Table 6). Methylation of the pyrrole nitrogen afforded compound **26**, displaying a greatly decreased AAK1 affinity (>800-fold loss in activity relative to compound **8g**) and antiviral activity ($EC_{50} > 10 \mu$ M). Insertion of an additional nitrogen atom in the pyrrole moiety yielded the pyrazolo[3,4-*b*]pyridine analogue **30** that is 100-fold less active as an AAK1 ligand relative to the parent compound **8g**. When the pyridine moiety of compound **21b** was replaced by a pyrazine ring, the pyrrolo[2,3-*b*]pyrazine analogue **37** was obtained. This compound was endowed with very potent AAK1 affinity ($IC_{50} = 0.00927 \mu$ M), comparable to its 7-aza-indole counterpart **21b**. Unfortunately, compound **37** demonstrated greater cytotoxicity than compound **21b** in Huh7 cells with CC_{50} 's of 4.81 versus 17.0 μ M, respectively.

Broad-Spectrum Antiviral Activity. AAK1 has been demonstrated to be important for the regulation of intracellular viral trafficking of multiple unrelated viruses.⁷ Sunitinib, an approved anticancer drug with potent anti-AAK1 activity, displayed antiviral activity against RNA viruses from six different families.⁷ To evaluate for potential broad-spectrum antiviral coverage of our molecules beyond DENV infection, hit compound **1** and the optimized congeners (compounds **8g** and **21b**) were tested for their activity against the unrelated EBOV. Huh7 cells were infected with EBOV and treated for 48 h with each compound (Figure 7). Whereas compound **1** did not show effective activity against EBOV, the more potent AAK1 inhibitors **8g** and **21b** displayed anti-EBOV activity with EC_{50} values in the low μ M range and $CC_{50} > 10$ – 20μ M.

Correlation of the Antiviral Effect of Compounds 1, 8g, and 21b with Functional AAK1 Inhibition. To confirm that the observed antiviral activity is correlated with functional inhibition of AAK1 activity, we measured levels of the phosphorylated form of the μ subunit of the AP2 complex, AP2M1, upon treatment with compounds **1**, **21b**, and **8g**. Because AP2M1 phosphorylation is transient (due to phosphatase PP2A activity),²⁷ to allow capturing of the phosphorylated state, Huh7 cells were incubated for 30 min

in the presence of the PP2A inhibitor calyculin A prior to lysis. Treatment with compounds **1**, **21b**, and **8g** reduced AP2M1 phosphorylation (Figure 8), indicating modulation of AP2M1 phosphorylation via AAK1 inhibition.

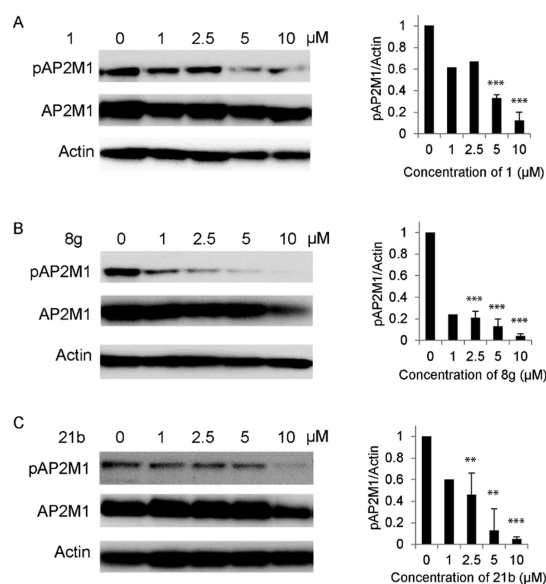


Figure 8. Antiviral effect of compounds **1**, **8g**, and **21b** correlates with functional inhibition of AAK1. Dose response of AP2M1 phosphorylation to treatment with **1** (A), **8g** (B), and **21b** (C) by western analysis in lysates derived from Huh7 cells. Representative membranes (from two independent experiments) blotted with anti-phospho-AP2M1 (pAP2M1), anti-AP2M1 (AP2M1), and anti-actin (actin) antibodies and quantified data of pAP2M1/actin protein ratio normalized to dimethyl sulfoxide (DMSO) controls are shown. ** $p < 0.01$, *** $p < 0.001$ by 2-tailed unpaired *t*-test.

Inhibition of DENV Infection in Human Primary Monocyte-Derived Dendritic Cells. To determine the therapeutic potential of the AAK1 inhibitors, their antiviral activity was studied in human primary dendritic cells. Primary cells are a physiologically more relevant model for DENV infection than immortalized cell lines and are considered an ex vivo model for DENV infection.³⁹ Compounds **21b** and **8g** showed a dose-dependent inhibition of DENV infection with EC_{50} and EC_{90} values of 0.0428 and 1.49 μ M and 0.739 and 3.32 μ M, respectively (Figure 9). This very potent activity in monocyte-derived dendritic cells (MDDCs) associated with minimal cytotoxicity ($CC_{50} > 20 \mu$ M), particularly of

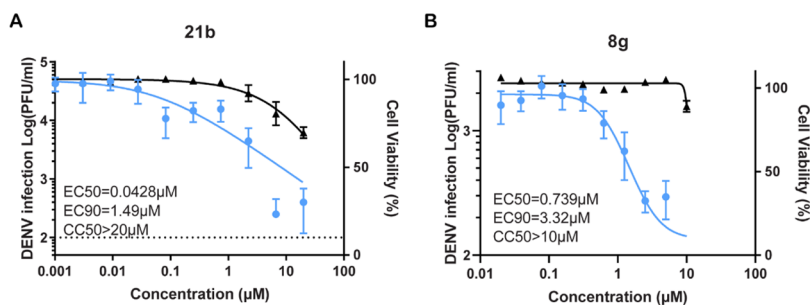


Figure 9. Ex vivo antiviral activity of **21b** and **8g** in human primary dendritic cells. Dose response of DENV infection (blue) and cell viability (black) to compounds **21b** (A) and **8g** (B) measured by plaque assays and alamarBlue assays, respectively, 72 h after infection of primary human MDDCs. A representative experiment with cells from a single donor is shown, out of 2 independent experiments conducted with cells derived from 2 donors, each with 6 biological replicates; the values are shown as means \pm SD.

compound **21b** demonstrates the potential of AAK1 inhibitors as antiviral agents.

Kinase Selectivity. To assess the kinase selectivity of the optimized AAK1 inhibitors, compound **21b** was screened against 468 kinases via the KINOMEScan assay (DiscoverX) at a single concentration of 10 μ M. As can be derived from the kinase interaction map (Figure 10), compound **21b** cannot be

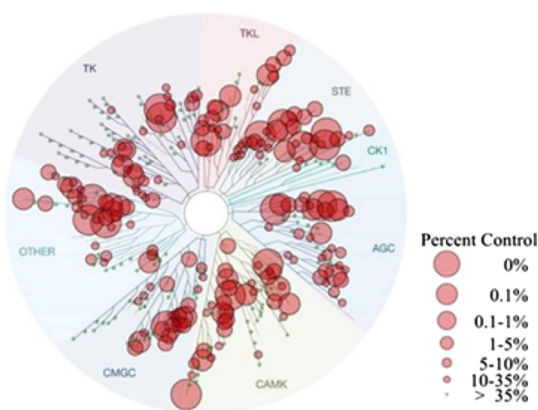


Figure 10. Kinome tree of compound **21b**. Kinases that bind compound **21b** are marked with red circles. The larger the circle, the stronger the binding affinity.

considered as a selective AAK1 inhibitor. Beyond AAK1, compound **21b** targets multiple other kinases (including the other members of the NAK family), which might contribute to its antiviral effect.

To quantitatively characterize the selectivity of compound **21b**, selectivity scores (*S*-scores) were calculated at a concentration of 10 μ M⁴⁰ (Table 7). The *S*(10) score of

Table 7. Selectivity Scores (*S* Scores) for Compound **21b at 10 μ M**

<i>S</i> -score type	number of hits	number of nonmutant kinases	selectivity score
<i>S</i> (35) ^a	212	403	0.526
<i>S</i> (10) ^b	138	403	0.342
<i>S</i> (1) ^c	49	403	0.122

^a*S*(35) = (number of nonmutant kinases with % ctrl <35)/(number of non-mutant kinases tested). ^b*S*(10) = (number of nonmutant kinases with % ctrl <10)/(number of non-mutant kinases tested). ^c*S*(1) = (number of nonmutant kinases with % ctrl <1)/(number of non-mutant kinases tested).

21b was calculated by dividing the number of kinases that showed binding at 10% of control or less upon drug treatment by the total number of kinases tested, excluding mutant variants and was found to be 0.342. In comparison, the *S*(3 μ M) score of sunitinib, which is the number of kinases found to bind with a dissociation constant of less than 3 μ M divided by the total number of non-mutant kinases tested, is 0.57.⁴⁰ Based on these data it can be deduced that, while **21b** is not a highly selective AAK1 inhibitor, its selectivity profile is improved relative to that of sunitinib, and it may therefore represent a better pharmacological tool to probe the role of AAK1 in viral infection.

Molecular Modeling. To rationalize the improved AAK1 affinity of compounds **8g** and **21b**, when compared to the original hit **1**, a docking study was performed using AutoDock Vina.⁴¹ A control docking experiment with the original inhibitor **1** (compound **1**), present in the 5L4Q PDB file, allowed to reproduce the original X-ray position very well. The best Vina docking scores are reported in Table 8. Despite the

Table 8. Vina Docking and MM/PBSA Results Calculated on Last 4 ns

compound	Vina score (kcal/mol)	MM ^a /GBSA ^b in kcal/mol (SD ^d)	MM ^a /PBSA ^c in kcal/mol (SD ^d)
1	-10.7	-31.5 (1.6)	-0.7 (2.3)
8g	-10.3	-38.6 (2.2)	-3.0 (2.9)
21b	-10.1	-40.6 (2.2)	-3.1 (2.8)

^aMM: molecular mechanics. ^bGB: generalized born surface area. ^cPBSA: Poisson-Boltzmann surface area. ^dSD: standard deviation.

higher AAK1 affinity of compounds **8g** and **21b**, their Vina docking scores are worse than reference compound **1**. This might be due to the fact that a rigid enzyme in the docking process that blocks induced-fit effects is used.

Therefore, for the three docked systems with the best Vina docking score, a molecular dynamics (MD) simulation using the Amber 18 software⁴² was performed. Figure 11 shows an overlap of representative structures of compounds **1**, **8g**, and **21b**, as extracted from the MD simulations. The three inhibitors form a hydrogen bond between the NH of the pyrrole ring and the backbone carbonyl group of D127. The nitrogen at position 3 of the pyridine ring seems to be essential for strong AAK1 affinity. In the X-ray of AAK1 with compound **1**, this nitrogen of the nicotinamide moiety makes a hydrogen bond with K74 side chain. However, this hydrogen/ionic bond is not maintained in the MD simulations of AAK1 with compound **1**, and neither with compounds **8g** and **21b**. On the

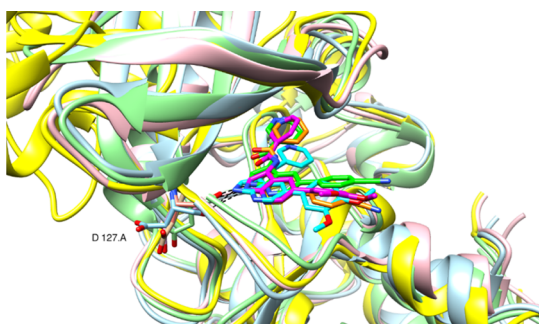


Figure 11. AAK1 snapshot structures with 3 ligands, compound **1** (green, lightgreen), compound **8g** (magenta, rose), and compound **21b** (cyan; lightblue), extracted from the last 4 ns of the MD trajectory as a representative structure from the biggest cluster using the average linkage clustering method available in cpptraj. The AAK1 and lkb X-ray structures are also shown (orange, yellow). Image made by the Chimera software.⁴⁴

other hand, for the three compounds, frequent van der Waals contacts between this nitrogen and the charged nitrogen in the side chain of K74 (distances < 4 Å) are observed.

For the last 4 ns of the trajectories, MM/GBSA and MM/PBSA (molecular mechanics energies with a generalized Born surface area continuum solvation model and molecular mechanics energies combined with the Poisson–Boltzmann surface area continuum solvation model, respectively)⁴³ binding affinity calculations were conducted. No entropy contributions were calculated (Table 8). From the data in Table 8, it is clear (more from the general born model than from the Poisson–Boltzmann model) that compounds **8g** and **21b** are stronger AAK1 binders than reference compound **1**. Both methoxy groups of compounds **8g** and **21b** contribute to the binding energy via van der Waals interactions with specific amino acids of AAK1. Residues L52, L62, F128, C129, R130, G131, G132, Q133, V135, and N136 are involved in binding to compound **21b**. The same residues plus E50 make contact with compound **8g**. On the other hand, the nitrile function of compound **1** shows clearly less van der Waals contacts with surrounding residues (L52, G132, Q133, and N136, Figure 12).

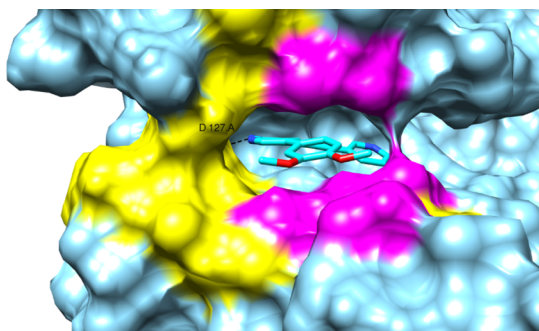


Figure 12. AAK1 enzyme with compound **21b** (same snapshot as in Figure 11). Amino acids making contact with the two methoxy groups (heavy atom distances < 4 Å) are colored in yellow and magenta. The magenta color represents also the residues having van der Waals contacts with the nitrile group of compound **1**. Image made by the Chimera software.⁴⁴

CONCLUSIONS

AAK1 is a promising host target for the development of broad-spectrum antiviral agents. In this article, the first systematic SAR study of AAK1 inhibitors as antiviral agents is presented. Starting from a known ligand with moderate AAK1 binding affinity and anti-DENV activity, a systematic SAR study was carried out. It led to the discovery of AAK1 ligands with low nM AAK1 binding affinity that display improved antiviral activity against DENV. Moreover, the optimized AAK1 inhibitors exhibit very potent activity in DENV-infected primary dendritic cells and anti-EBOV activity, supporting the potential to develop broad-spectrum antiviral agents based on AAK1 inhibition. Kinase profiling revealed that these compounds have an improved selectivity profile relative to sunitinib, yet further research is necessary to improve their kinase selectivity.

EXPERIMENTAL SECTION

All commercial reagents were obtained via Acros Organics, Sigma-Aldrich, AK Scientific and Fluorochem at least 99% purity unless indicated otherwise. Furthermore, all dry solvents were obtained via Acros Organics with an AcroSeal system, and regular solvents were obtained via Fisher Scientific at technical grade. Thin layer chromatography (TLC) of the reactions was performed on silica gel on aluminum foils (60 Å pore diameter) obtained from Sigma-Aldrich and visualized using ultraviolet light. Recording of the NMR spectra was performed using a Bruker 300, 500, or 600 MHz spectrometer. The chemical shifts are reported in ppm with Me₄Si as the reference and coupling constants (*J*) are reported in hertz. Mass spectra were acquired on a quadrupole orthogonal acceleration time-of-flight mass spectrometer (Synapt G2 HDMS, Waters, Milford, MA). Samples were infused at 3 μL/min and spectra were obtained in positive or negative ionization mode with a resolution of 15 000 (full width at half-maximum) using leucine enkephalin as lock mass. Purity of the compounds was analyzed on a Waters 600 HPLC system equipped with a Waters 2487 dual λ absorbance detector set at 256 nm using a 5 μm 4.6 × 150 mm XBridge reversed phase (C₁₈) column. The mobile phase was a gradient over 30 min starting from 95% A and 5% B and finishing at 5% A and 95% B with a flow rate of 1 mL per minute (solvent A: Milli-Q water; solvent B: acetonitrile). All synthesized final compounds had a purity of at least 95%. Compound **8o** was synthesized according to literature procedure.²²

5-Bromo-3-((trimethylsilyl)ethynyl)pyridin-2-amine (3). To a stirring suspension of 5-bromo-3-iodopyridin-2-amine **2** (520 mg, 1.74 mmol) in degassed triethylamine (10 mL) were added copper iodide (6.63 mg, 0.034 mmol) and Pd(PPh₃)₂Cl₂ (12 mg, 0.017 mmol). The system was flushed with nitrogen, and trimethylsilylacetylene (188 mg, 265 μL, 1.91 mmol) was added dropwise over 5 min. The reaction was allowed to stir for 3 h at room temperature. After reaction completion, the solvent was evaporated and water was added. The resulting suspension was extracted three times using ethyl acetate. The combined organic phases were washed with water and brine, dried over MgSO₄, and evaporated in vacuo. The crude residue was purified by silica gel flash column chromatography using a mixture of heptane and ethylacetate (in a ratio of 80:20) as a mobile phase, yielding the title compound as a yellow-beige solid (420 mg, 90%). ¹H NMR (300 MHz, DMSO-*d*₆): δ (ppm) 8.03 (s, 1H, ArH), 7.69 (s, 1H, ArH), 6.37 (s, 2H, NH₂), 0.24 (s, 9H, Si(CH₃)₃).

5-Bromo-1H-pyrrolo[2,3-*b*]pyridine (4). To a solution of 5-bromo-3-((trimethylsilyl)ethynyl)pyridin-2-amine **3** (200 mg, 0.743 mmol) in dry NMP (5 mL) was added portionwise KO^tBu (100 mg, 0.891 mmol). The reaction mixture was heated to 80 °C and stirred for 1 h. After reaction completion, the mixture was extracted with water and ethyl acetate three times. The combined organic phases were washed twice with water and once with brine, dried over MgSO₄, and evaporated in vacuo. The crude residue was then purified using silica gel flash column chromatography (using a mixture of heptane

and ethyl acetate in a ratio of 5:1 as mobile phase), yielding the title compound as a white solid (103 mg, 70%). ^1H NMR (300 MHz, DMSO- d_6): δ (ppm) 10.33 (br s, 1H, NH), 8.37 (d, $J = 2.1$ Hz, 1H, ArH), 8.09 (d, $J = 2.1$ Hz, 1H, ArH), 7.37 (m, 1H, ArH), 6.47 (m, 1H, ArH).

5-Bromo-3-nitro-1H-pyrrolo[2,3-*b*]pyridine (5). 5-Bromo-1H-pyrrolo[2,3-*b*]pyridine 4 (730 mg, 3.7 mmol) was added portionwise to a stirring solution of fuming nitric acid (2 mL) at 0 °C over 10 min. The reaction was allowed to stir for 30 min at 0 °C. The mixture was poured into ice water and the formed precipitate was collected via vacuum filtration. The filter cake was washed generously with water and heptane yielding the title compound as a yellow solid (853 mg, 95%). ^1H NMR (300 MHz, DMSO- d_6): δ (ppm) 13.48 (br s, 1H, NH), 8.87 (s, 1H, ArH), 8.51 (s, 2H, ArH). ^{13}C NMR (75 MHz, DMSO- d_6): δ (ppm) 145.98, 145.26, 132.13, 129.96, 126.32, 115.17, 114.32.

Synthesis of 3-Nitro-5-aryl-pyrrolo[2,3-*b*]pyridines (6a–h). *General Procedure.* To a solution of 5-bromo-3-nitro-1H-pyrrolo[2,3-*b*]pyridine 5 (1 equiv) in dioxane (8 mL) were added the appropriate boronic acid (1.2 equiv) and 2 mL of a K_2CO_3 (3 equiv) solution. The system was purged three times with argon and heated to 105 °C. After stirring for 10 min, $\text{Pd}(\text{PPh}_3)_4$ (0.1 equiv) was added and the reaction was purged once more with argon. The reaction mixture was stirred at 105 °C overnight. After completion, the reaction mixture was cooled to room temperature and filtered through Celite. The filtrate was extracted with water and ethyl acetate. The combined organic phases were washed with brine, dried over MgSO_4 , and evaporated in vacuo. Purification of the crude residue was achieved by silica gel flash column chromatography using the appropriate solvent mixture.

The following compounds were made according to this procedure.

3-Nitro-5-phenyl-1H-pyrrolo[2,3-*b*]pyridine (6a). The title compound was synthesized according to the general procedure using 5-bromo-3-nitro-1H-pyrrolo[2,3-*b*]pyridine 5 (100 mg, 0.413 mmol), phenylboronic acid (61 mg, 0.496 mmol), and K_2CO_3 (171 mg, 1.24 mmol). Purification by silica gel flash column chromatography using a mixture of DCM and ethyl acetate (in a ratio of 90:10) as the mobile phase, yielded the desired compound as a white solid (83 mg, 84%). ^1H NMR (300 MHz, DMSO- d_6): δ (ppm) 13.39 (br s, 1H, NH), 8.89 (s, 1H, HetH), 8.76 (d, $J = 2.1$ Hz, 1H, HetH), 8.60 (d, $J = 2.2$ Hz, 1H, HetH), 7.79 (d, $J = 7.2$ Hz, 2H, *o*-PhH), 7.54 (t, $J = 7.4$ Hz, 2H, *m*-PhH), 7.45 (t, $J = 7.3$ Hz, 1H, *p*-PhH).

5-(4-Fluorophenyl)-3-nitro-1H-pyrrolo[2,3-*b*]pyridine (6b). The title compound was synthesized according to the general procedure using 5-bromo-3-nitro-1H-pyrrolo[2,3-*b*]pyridine 5 (100 mg, 0.413 mmol), 4-fluorophenylboronic acid (69 mg, 0.496 mmol), and K_2CO_3 (171 mg, 1.24 mmol). Purification by silica gel flash column chromatography using a mixture of DCM and ethyl acetate (in a ratio of 90:10) as the mobile phase yielded the desired compound as a light brown solid (98 mg, 92%). ^1H NMR (300 MHz, DMSO- d_6): δ (ppm) 13.37 (br s, 1H, NH), 8.90 (s, 1H, HetH), 8.82 (d, $J = 2.9$ Hz, 1H, HetH), 8.68 (d, $J = 3.0$ Hz, 1H, HetH), 8.01 (m, 4H, PhH).

5-(4-(Trifluoromethyl)phenyl)-3-nitro-1H-pyrrolo[2,3-*b*]pyridine (6c). The title compound was synthesized according to the general procedure using 5-bromo-3-nitro-1H-pyrrolo[2,3-*b*]pyridine 5 (100 mg, 0.413 mmol), 4-trifluoromethylphenylboronic acid (94 mg, 0.496 mmol), and K_2CO_3 (171 mg, 1.24 mmol). Purification by silica gel flash column chromatography using a mixture of DCM and ethyl acetate (in a ratio of 90:10) as the mobile phase yielded the desired compound as a white solid (110 mg, 87%). ^1H NMR (300 MHz, DMSO- d_6): δ (ppm) 13.45 (br s, 1H, NH), 8.93 (s, 1H, HetH), 8.84 (d, $J = 3.2$ Hz, 1H, HetH), 8.70 (d, $J = 3.1$ Hz, 1H, HetH), 8.45 (m, 1H, PhH), 8.05 (d, $J = 8.8$ Hz, 2H, PhH), 7.89 (d, $J = 8.9$ Hz, 1H, PhH).

5-(4-Methoxyphenyl)-3-nitro-1H-pyrrolo[2,3-*b*]pyridine (6d). The title compound was synthesized according to the general procedure using 5-bromo-3-nitro-1H-pyrrolo[2,3-*b*]pyridine 5 (100 mg, 0.413 mmol), 4-methoxyphenylboronic acid (75 mg, 0.496 mmol), and K_2CO_3 (171 mg, 1.24 mmol). Purification by silica gel flash column chromatography using a mixture of DCM and ethyl

acetate (in a ratio of 90:10) as the mobile phase yielded the desired compound as a yellow solid (104 mg, 94%). ^1H NMR (300 MHz, DMSO- d_6): δ (ppm) 13.32 (br s, 1H, NH), 8.86 (s, 1H, HetH), 8.72 (d, $J = 2.8$ Hz, 1H, HetH), 8.55 (d, $J = 3.0$ Hz, 1H, HetH), 7.73 (d, $J = 8.5$ Hz, 2H, PhH), 7.10 (d, $J = 8.5$ Hz, 2H, PhH), 3.83 (s, 3H, OCH_3).

3-Nitro-5-(*p*-tolyl)-1H-pyrrolo[2,3-*b*]pyridine (6e). The title compound was synthesized according to the general procedure using 5-bromo-3-nitro-1H-pyrrolo[2,3-*b*]pyridine 5 (100 mg, 0.413 mmol), *p*-tolylboronic acid (67 mg, 0.496 mmol), and K_2CO_3 (171 mg, 1.24 mmol). Purification by silica gel flash column chromatography using a mixture of DCM and ethyl acetate (in a ratio of 90:10) as the mobile phase yielded the desired compound as a white solid (83 mg, 74%). ^1H NMR (300 MHz, DMSO- d_6): δ (ppm) 13.35 (br s, 1H, NH), 8.88 (s, 1H, HetH), 8.74 (d, $J = 3.2$ Hz, 1H, HetH), 8.58 (d, $J = 3.1$ Hz, 1H, HetH), 7.68 (d, $J = 7.8$ Hz, 2H, PhH), 7.35 (d, $J = 7.8$ Hz, 2H, PhH), 2.38 (s, 3H, CH_3).

3-Nitro-5-(*m*-tolyl)-1H-pyrrolo[2,3-*b*]pyridine (6f). The title compound was synthesized according to the general procedure using 5-bromo-3-nitro-1H-pyrrolo[2,3-*b*]pyridine 5 (100 mg, 0.413 mmol), *m*-tolylboronic acid (67 mg, 0.496 mmol), and K_2CO_3 (171 mg, 1.24 mmol). Purification by silica gel flash column chromatography using a mixture of DCM and ethyl acetate (in a ratio of 90:10) as the mobile phase yielded the desired compound as a white solid (83 mg, 74%). ^1H NMR (300 MHz, DMSO- d_6): δ (ppm) 13.35 (br s, 1H, NH), 8.88 (s, 1H, HetH), 8.74 (d, $J = 3.1$ Hz, 1H, HetH), 8.59 (d, $J = 3.1$ Hz, 1H, HetH), 7.58 (t, $J = 7.2$ Hz, 2H, PhH), 7.42 (t, $J = 7.3$ Hz, 1H, PhH), 7.26 (d, $J = 3.3$ Hz, 1H, PhH), 2.42 (s, 3H, CH_3).

5-(3,4-Dimethoxyphenyl)-3-nitro-1H-pyrrolo[2,3-*b*]pyridine (6g). The title compound was synthesized according to the general procedure using 5-bromo-3-nitro-1H-pyrrolo[2,3-*b*]pyridine 5 (100 mg, 0.413 mmol), 3,4-dimethoxyphenylboronic acid (63 mg, 0.496 mmol), and K_2CO_3 (171 mg, 1.24 mmol). The compound precipitated as a yellow solid that was washed twice with dioxane, followed by washing with water yielding the pure title compound (88 mg, 89%). ^1H NMR (300 MHz, DMSO- d_6): δ (ppm) 8.82 (s, 1H, HetH), 8.72 (d, $J = 2.1$ Hz, 1H, HetH), 8.54 (d, $J = 2.2$ Hz, 1H, HetH), 7.30 (m, 2H, PhH), 7.10 (d, $J = 8.3$ Hz, 1H, PhH), 3.88 (s, 3H, OCH_3), 3.82 (s, 3H, OCH_3).

3-Nitro-5-(3-thienyl)-1H-pyrrolo[2,3-*b*]pyridine (6h). The title compound was synthesized according to the general procedure using 5-bromo-3-nitro-1H-pyrrolo[2,3-*b*]pyridine 5 (100 mg, 0.413 mmol), 3-thienylboronic acid (69 mg, 0.496 mmol), and K_2CO_3 (171 mg, 1.24 mmol). Purification by silica gel flash column chromatography using a mixture of DCM and ethyl acetate (in a ratio of 90:10) as the mobile phase yielded the title compound as a brown solid (97 mg, 96%). ^1H NMR (300 MHz, DMSO- d_6): δ (ppm) 13.41 (br s, 1H, NH), 8.89 (d, $J = 3.0$ Hz, 1H, HetH), 8.83 (d, $J = 3.1$ Hz, 1H, HetH), 8.57 (d, $J = 3.0$ Hz, 1H, HetH), 7.69 (m, 2H, ThH) ppm, 7.22 (t, $J = 4.4$ Hz, 1H, ThH).

Synthesis of 5-Aryl-3-amino- and 5-Aryl-3-*N*-acetylamino Pyrrolo[2,3-*b*]pyridines (7a–f and 8a–o). *General Procedure.* To a solution of a 5-aryl-3-nitro-pyrrolo[2,3-*b*]pyridine 6a–h (100 mg) in tetrahydrofuran (THF) (5 mL) was added a slurry of Raney nickel in water in catalytic amounts. The reaction vessel was flushed three times with hydrogen gas and was stirred under a hydrogen atmosphere for 3–4 h. Upon completion of the reaction, the catalyst was removed and the solvent evaporated in vacuo. The crude residue was used in the next reaction without any purification because of the rapid decomposition of the 3-amino-pyrrolo[2,3-*b*]pyridine intermediates 7a–h. To a solution of compounds 7a–h (1 equiv) in dry pyridine (3 mL) was added a solution of nicotinoyl chloride hydrochloride (1.2 equiv) in CH_2Cl_2 (2 mL). The reaction was allowed to stir at room temperature for 3 h. The solvent was evaporated in vacuo. THF (5 mL) was added and the resulting solution was stirred for 5 min, followed by the addition of a 1 M NaOH solution in water (5 mL). The resulting suspension was stirred for an additional 10 min. The precipitate was collected via vacuum filtration and purified using flash column chromatography with the

appropriate solvent mixture as mobile phase. Compounds **8a–h** were synthesized according to this procedure.

N-[5-(Phenyl-1H-pyrrolo[2,3-b]pyridin-3-yl)nicotinamide (8a). The title compound was synthesized according to the general procedure using 3-nitro-5-phenyl-1H-pyrrolo[2,3-b]pyridine **6a** (84 mg, 0.351 mmol). Purification by silica gel flash column chromatography (eluting with a mixture of DCM and methanol in a gradient gradually ranging from 98:2 to 90:10) afforded the title compound as a dark brown solid (47 mg, 36%). Purity of 99%. ¹H NMR (300 MHz, DMSO-*d*₆): δ 11.62 (br s, 1H, NH), 10.58 (br s, 1H, NH), 9.19 (s, 1H, HetH), 8.79 (d, *J* = 3.0 Hz, 1H, HetH), 8.66 (s, 1H, ArH), 8.58 (s, 1H, ArH), 8.36 (d, *J* = 6.1 Hz, 1H, ArH), 7.98 (s, 1H, ArH), 7.75 (d, *J* = 8.8 Hz, 2H, ArH), 7.60 (t, *J* = 6.0 Hz, 1H, ArH), 7.51 (t, *J* = 7.3 Hz, 2H, ArH), 7.38 (t, *J* = 7.4 Hz, 1H, ArH) ppm. ¹³C NMR (75 MHz, DMSO-*d*₆): δ 163.46, 152.01, 148.87, 145.52, 142.23, 139.16, 135.60, 131.63, 130.52, 129.13, 127.06, 126.93, 125.49, 123.61, 117.52, 114.10, 113.45 ppm. HRMS *m/z*: [M + H]⁺ calcd for C₁₉H₁₄N₄O, 315.12403; found, 315.1237.

N-[5-(4-Fluorophenyl)-1H-pyrrolo[2,3-b]pyridin-3-yl]nicotinamide (8b). The title compound was synthesized according to the general procedure using 3-nitro-5-(4-fluorophenyl)-1H-pyrrolo[2,3-b]pyridine **6b** (98 mg, 0.381 mmol). Purification by silica gel flash column chromatography (using a mixture of DCM/methanol in a ratio gradually ranging from 98:2 to 90:10 as mobile phase) afforded the title compound as a brown solid (44 mg, 34%). Purity of 99%. ¹H NMR (300 MHz, DMSO-*d*₆): δ 11.63 (br s, 1H, NH), 10.57 (br s, 1H, NH), 9.17 (s, 1H, HetH), 8.78 (d, *J* = 5.8 Hz, 1H, ArH), 8.62 (s, 1H, HetH), 8.56 (s, 1H, ArH), 8.36 (d, *J* = 8.9 Hz, 1H, ArH), 7.98 (d, *J* = 3.2 Hz, 1H, ArH), 7.77 (t, *J* = 7.6 Hz, 2H, ArH), 7.61 (d, *J* = 9.0 Hz, 1H, ArH), 7.35 (t, *J* = 7.5 Hz, 2H, ArH) ppm. ¹³C NMR (75 MHz, DMSO-*d*₆): δ 162.24, 161.77 (d, *J*_{CF} = 242 Hz), 150.23, 148.62, 148.62, 145.58, 142.05, 138.10, 135.66, 128.86 (d, *J*_{CF} = 8.0 Hz), 126.77, 126.72, 125.74, 122.38, 117.74, 116.00, 115.85 (d, *J*_{CF} = 20.4), 113.75, 113.47 ppm. HRMS *m/z*: [M + H]⁺ calcd for C₁₉H₁₃N₄O_F, 333.11460; found, 333.1145. HRMS *m/z*: [M + Na]⁺ calcd for C₁₉H₁₃N₄O_F, 355.09658; found, 355.0950.

N-[5-(4-Trifluoromethylphenyl)-1H-pyrrolo[2,3-b]pyridin-3-yl]nicotinamide (8c). The title compound was synthesized according to the general procedure using 3-nitro-5-(4-trifluoromethylphenyl)-1H-pyrrolo[2,3-b]pyridine **6c** (116 mg, 377.56 μmol). Purification by silica gel flash column chromatography using a mixture of DCM and methanol (in a ratio gradually ranging from 98:2 to 90:10) as the mobile phase afforded the title compound as a white solid (49 mg, 36%). Purity of 99%. ¹H NMR (300 MHz, DMSO-*d*₆): δ 11.73 (br s, 1H, NH), 10.62 (br s, 1H, NH), 9.19 (d, *J* = 3.2 Hz, 1H, HetH), 8.78 (t, *J* = 6.1 Hz, 2H, ArH), 8.67 (d, *J* = 3.1 Hz, 1H, HetH), 8.36 (d, *J* = 3.0 Hz, 1H, ArH), 7.99 (d, *J* = 8.9 Hz, 3H, PhH), 7.87 (d, *J* = 9.0 Hz, 2H, PhH), 7.61 (q, *J* = 5.9 Hz, 1H, ArH) ppm. ¹³C NMR (75 MHz, DMSO-*d*₆): δ 163.52, 152.05, 148.85, 145.88, 143.25, 142.35, 135.58, 130.46, 127.48, 126.09, 123.61, 122.80, 117.84, 114.28, 113.52 ppm; missing peaks were observed in an APT spectrum. HRMS *m/z*: [M + H]⁺ calcd for C₂₀H₁₃N₄F₃O, 383.11141; found, 383.1114.

N-[5-(4-Methoxyphenyl)-1H-pyrrolo[2,3-b]pyridin-3-yl]nicotinamide (8d). The title compound was synthesized according to the general procedure using 3-nitro-5-(4-methoxyphenyl)-1H-pyrrolo[2,3-b]pyridine **6d** (105 mg, 0.390 mmol). Purification by silica gel flash column chromatography using a mixture of DCM and methanol (in a ratio gradually ranging from 98:2 to 90:10) as the mobile phase afforded the title compound as a pink solid (43 mg, 34%). Purity of 99%. ¹H NMR (300 MHz, DMSO-*d*₆): δ 11.56 (br s, 1H, NH), 10.56 (br s, 1H, NH), 9.18 (s, 1H, ArH), 8.78 (d, *J* = 6.1 Hz, 1H, ArH), 8.58 (s, 1H, ArH), 8.52 (s, 1H, ArH), 8.36 (d, *J* = 9.0 Hz, 1H, PhH), 7.96 (s, 1H, ArH), 7.62 (m, 3H, ArH), 7.08 (d, *J* = 8.9 Hz, 2H, PhH), 3.82 (s, 3H, OCH₃) ppm. ¹³C NMR (75 MHz, DMSO-*d*₆): δ 163.45, 158.74, 151.99, 148.85, 145.22, 141.99, 135.59, 131.54, 130.50, 128.00, 127.55, 124.87, 123.60, 117.43, 114.64, 113.94, 113.45, 55.34 ppm. HRMS *m/z*: [M + H]⁺ calcd for C₂₀H₁₆N₄O₂, 345.13459; found, 345.1343. HRMS *m/z*: [M + Na]⁺ calcd for C₂₀H₁₆N₄O₂, 367.11656; found, 367.1153.

N-(5-(*p*-Tolyl)-1H-pyrrolo[2,3-b]pyridin-3-yl)nicotinamide (8e).

The title compound was synthesized according to the general procedure using 3-nitro-5-(*p*-tolyl)-1H-pyrrolo[2,3-b]pyridine **6e** (96 mg, 0.379 mmol). Purification by silica gel flash column chromatography using a mixture of DCM and methanol (in a ratio gradually ranging from 98:2 to 90:10) as the mobile phase afforded the title compound as a beige solid (48 mg, 37%). Purity of 98%. ¹H NMR (300 MHz, DMSO-*d*₆): δ 11.60 (br s, 1H, NH), 10.59 (br s, 1H, NH), 9.19 (s, 1H, ArH), 8.78 (d, *J* = 2.9 Hz, 1H, ArH), 8.63 (s, 1H, ArH), 8.56 (s, 1H, ArH), 8.36 (d, *J* = 6.0 Hz, 1H, ArH), 7.99 (s, 1H, ArH), 7.59 (m, 3H, ArH), 7.31 (d, *J* = 9.3 Hz, 2H, ArH), 2.35 (s, 3H, CH₃) ppm. ¹³C NMR (75 MHz, DMSO-*d*₆): δ 163.49, 151.99, 148.85, 145.41, 142.10, 136.28, 136.22, 135.59, 130.51, 129.73, 127.68, 126.73, 125.12, 123.60, 117.50, 114.03, 113.47, 20.77 ppm. HRMS *m/z*: [M + H]⁺ calcd for C₂₀H₁₆N₄O, 329.13967; found, 329.1398.

N-[5-(*m*-Tolyl)-1H-pyrrolo[2,3-b]pyridin-3-yl]nicotinamide (8f).

The title compound was synthesized according to the general procedure using 3-nitro-5-(*m*-tolyl)-1H-pyrrolo[2,3-b]pyridine **6f** (97 mg, 0.304 mmol). Purification by silica gel flash column chromatography using a mixture of DCM and methanol (in a ratio gradually ranging from 98:2 to 90:10) as the mobile phase afforded the title compound as a beige solid (22 mg, 25% yield). Purity of 98%. ¹H NMR (300 MHz, DMSO-*d*₆): δ 11.61 (br s, 1H, NH), 10.59 (br s, 1H, NH), 9.19 (s, 1H, ArH), 8.79 (d, *J* = 2.8 Hz, 1H, ArH), 8.64 (s, 1H, ArH), 8.57 (s, 1H, ArH), 8.37 (d, *J* = 9.0 Hz, 1H, ArH), 7.99 (s, 1H, ArH), 7.59 (m, 3H, CH₃), 7.39 (t, *J* = 7.4 Hz, 1H), 7.19 (d, *J* = 6.1 Hz, 1H), 2.41 (s, 3H) ppm. ¹³C NMR (75 MHz, DMSO-*d*₆): δ 163.49, 151.99, 148.84, 145.47, 142.25, 139.08, 138.27, 135.59, 130.50, 129.02, 127.84, 127.71, 127.53, 125.39, 124.06, 123.60, 117.47, 114.07, 113.42, 21.28 ppm. HRMS *m/z*: [M + H]⁺ calcd for C₂₀H₁₆N₄O, 329.13967; found, 329.1397.

N-[5-(3,4-Dimethoxyphenyl)-1H-pyrrolo[2,3-b]pyridin-3-yl]nicotinamide (8g).

The title compound was synthesized according to the general procedure using 3-nitro-5-(3,4-dimethoxyphenyl)-1H-pyrrolo[2,3-b]pyridine **6g** (80 mg, 0.297 mmol). Purification by silica gel flash column chromatography using a mixture of DCM and methanol (in a ratio gradually ranging from 98:2 to 90:10) as the mobile phase afforded the title compound as a beige solid (56 mg, 50%). Purity of 97%. ¹H NMR (300 MHz, DMSO-*d*₆): δ 11.57 (br s, 1H, NH), 10.56 (br s, 1H, NH), 9.20 (s, 1H, ArH), 8.78 (d, *J* = 6.1 Hz, 1H, ArH), 8.58 (d, *J* = 3.2 Hz, 2H, ArH), 8.37 (d, *J* = 9.1 Hz, 1H, ArH), 7.97 (s, 1H, ArH), 7.60 (t, *J* = 6.0 Hz, 1H, ArH), 7.27 (t, *J* = 7.4 Hz, 2H, ArH), 7.09 (d, *J* = 9.0 Hz, 1H, ArH), 3.88 (s, 3H, OCH₃), 3.81 (s, 3H, OCH₃) ppm. ¹³C NMR (75 MHz, DMSO-*d*₆): δ 163.45, 152.00, 149.40, 148.88, 148.43, 145.28, 142.26, 135.61, 132.04, 130.51, 127.84, 124.96, 123.61, 119.23, 117.47, 113.93, 113.39, 112.70, 111.09, 55.92, 55.82 ppm. HRMS *m/z*: [M + H]⁺ calcd for C₂₁H₁₈N₄O₃, 375.14515; found, 375.1447. HRMS *m/z*: [M + Na]⁺ calcd for C₂₁H₁₈N₄O₃, 397.12713; found, 397.1264.

N-[5-(3-Thienyl)-1H-pyrrolo[2,3-b]pyridin-3-yl]nicotinamide (8h).

The title compound was synthesized according to the general procedure using 3-nitro-5-(3-thienyl)-1H-pyrrolo[2,3-b]pyridine **6h** (97 mg, 0.395 mmol). Purification by silica gel flash column chromatography using a mixture of DCM and methanol (in a ratio gradually ranging from 98:2 to 90:10) as the mobile phase, afforded the title compound as a brown solid (48 mg, 37%). Purity of 99%. ¹H NMR (300 MHz, DMSO-*d*₆): δ 11.58 (br s, 1H, NH), 10.54 (br s, 1H, NH), 9.20 (d, *J* = 2.8 Hz, 1H, ArH), 8.79 (d, *J* = 2.9 Hz, 1H, ArH), 8.67 (d, *J* = 2.9 Hz, 1H, ArH), 8.64 (d, *J* = 3.0 Hz, 1H, ArH), 8.36 (m, 1H, ArH), 7.93 (s, 1H, ArH), 7.84 (s, 1H, ArH), 7.71 (m, 1H, ArH), 7.60 (t, *J* = 5.9 Hz, 2H, ArH) ppm. ¹³C NMR (75 MHz, DMSO-*d*₆): δ 163.48, 152.02, 148.86, 145.30, 142.03, 140.21, 135.58, 130.49, 127.30, 126.37, 124.61, 123.60, 123.18, 119.78, 117.63, 113.94, 113.49 ppm. HRMS *m/z*: [M + H]⁺ calcd for C₁₇H₁₂N₄O_S, 321.08045; found, 321.0804.

N-(5-(3,4-Dimethoxyphenyl)-1H-pyrrolo[2,3-b]pyridin-3-yl)-benzamide (8i).

To a solution of 3-nitro-5-(3,4-dimethoxyphenyl)-1H-pyrrolo[2,3-b]pyridine **6g** (100 mg, 0.334 mmol) in THF (4 mL) was added a catalytic amount of a slurry of Raney nickel in water. The

vessel was flushed three times with hydrogen gas and kept under a hydrogen atmosphere for 4 h. After complete conversion, the catalyst was removed, and the solvent was evaporated in vacuo. The crude product was immediately used for further reaction without purification. To a solution of the crude residue from the previous reaction in pyridine (5 mL) was added a solution of benzoyl chloride (47 μ L, 0.401 mmol) in DCM (0.5 mL). The reaction was stirred overnight at room temperature. After reaction completion, the solvent was evaporated in vacuo, and the crude residue was extracted three times with water and ethyl acetate. The combined organic layers were dried over $MgSO_4$ and evaporated to dryness. Purification was achieved by silica gel flash column chromatography (using a mixture of DCM and methanol in a ratio of 97:3 as mobile phase), followed by precipitation of the residue from acetone. The precipitate was collected via filtration yielding the title compound as a white solid (27 mg, 22%). Purity of 98%. 1H NMR (300 MHz, $DMSO-d_6$): δ 11.52 (br s, 1H, NH), 10.37 (br s, 1H, NH), 8.56 (d, J = 6.52, 2H, ArH), 8.00 (m, 3H, ArH), 7.56 (d, J = 7.6 Hz, 3H, ArH), 7.25 (m, 2H, ArH), 7.08 (d, J = 8.2 Hz, 1H, ArH), 3.87 (s, 3H, OCH_3), 3.80 (s, 3H, OCH_3) ppm. ^{13}C NMR (75 MHz, $DMSO-d_6$): δ 165.07, 149.30, 148.30, 145.25, 142.12, 134.88, 132.01, 131.42, 128.48, 127.87, 127.70, 125.04, 119.14, 117.27, 114.22, 113.44, 112.52, 110.87, 55.83, 55.74 ppm. HRMS m/z : $[M + H]^+$ calcd for $C_{22}H_{19}N_3O_3$, 374.14990; found, 374.1493.

Synthesis of 5-(3,4-Dimethoxyphenyl)-3-N-acylamino Pyrrolo[2,3-b]pyridines. General Procedure. 3-Nitro-5-(3,4-dimethoxyphenyl)-1H-pyrrolo[2,3-b]pyridine **6g** (100 mg, 0.334 mmol) was hydrogenated with a catalytic amount of Raney nickel as a slurry in water (slurry in water? x mg/mL) in THF (5 mL) for 3 h. The solvents were evaporated in vacuo yielding crude 3-amino-5-(3,4-dimethoxyphenyl)-1H-pyrrolo[2,3-b]pyridine which was used in the next reaction without further purification (90 mg, 99%). To a solution of 3-amino-5-(3,4-dimethoxyphenyl)-1H-pyrrolo[2,3-b]pyridine (90 mg, 0.334 mmol) in dimethylformamide (DMF) (3 mL) was added the appropriate carboxylic acid (1 equiv), BOP (177 mg, 0.401 mmol), and triethylamine (140 μ L, 1 mmol). The mixture was stirred overnight. When the reaction reached completion, water was added and the mixture was extracted three times with ethyl acetate. The combined organic layers were washed with brine, dried over Na_2SO_4 , and evaporated in vacuo. The crude residue was purified by silica gel flash chromatography using an appropriate solvent system as the mobile phase. An additional purification was performed by preparative TLC using a mixture of DCM and acetone (in a ratio of 8:2) as eluent. The following compounds were prepared according to this procedure.

***N*-(5-(3,4-Dimethoxyphenyl)-1H-pyrrolo[2,3-b]pyridin-3-yl)-4-fluorobenzamide (8j).** The title compound was synthesized according to the general procedure using 4-fluorobenzoic acid (47 mg, 0.334 mmol). Purification by silica gel flash column chromatography (using a mixture of DCM and methanol as mobile phase in a ratio of 99:1) yielded the desired compound as a white solid (56 mg, 43%). Purity of 99%. 1H NMR (300 MHz, $DMSO-d_6$): δ 11.53 (br s, 1H, NH), 10.39 (br s, 1H, NH), 8.56 (d, J = 8.5 Hz, 2H, ArH), 8.12 (m, 2H, ArH), 7.93 (s, 1H, ArH), 7.38 (t, J = 8.7 Hz, 2H, ArH), 7.26 (m, 2H, ArH), 7.08 (d, J = 8.3 Hz, 1H, ArH), 3.87 (s, 3H, OCH_3), 3.81 (s, 3H, OCH_3) ppm. ^{13}C NMR (75 MHz, $DMSO-d_6$): δ 164.07 (J_{CF} = 245 Hz), 163.93, 149.30, 148.30, 145.25, 142.12, 131.99, 131.27, 130.57 (J_{CF} = 8.97 Hz), 127.69, 125.05, 119.12, 117.35, 115.39 (J_{CF} = 22 Hz), 114.11, 113.46, 112.53, 110.88, 55.84, 55.75 ppm. HRMS m/z : $[M + H]^+$ calcd for $C_{22}H_{18}FN_3O_3$, 392.14048; found, 392.1399.

***N*-(5-(3,4-Dimethoxyphenyl)-1H-pyrrolo[2,3-b]pyridin-3-yl)-4-methoxybenzamide (8k).** The title compound was synthesized according to the general procedure using 4-methoxybenzoic acid (51 mg, 0.334 mmol). Purification by silica gel flash column chromatography (using a mixture of DCM and methanol as mobile phase in a ratio of 99:1) yielded the desired compound as a white solid (64 mg, 47%). Purity of 97%. 1H NMR (600 MHz, $DMSO-d_6$): δ 11.46 (s, 1H, NH), 10.16 (s, 1H, NH), 8.55 (d, J = 1.92 Hz, 1H, ArH), 8.53 (d, J = 2.22 Hz, 1H, ArH), 8.01 (m, 2H, ArH), 7.90 (d, J = 2.46 Hz, 1H, ArH), 7.28 (d, J = 2.16 Hz, 1H, ArH), 7.22 (dd, J = 8.22,

2.16 Hz, ArH), 7.08 (m, 3H, ArH), 3.87 (s, 3H, OCH_3), 3.85 (s, 3H, OCH_3), 3.80 (s, 3H, OCH_3) ppm. ^{13}C NMR (150 MHz, $DMSO-d_6$): δ 164.43, 161.77, 149.25, 148.24, 145.21, 142.00, 131.99, 129.69, 127.58, 126.92, 124.98, 119.08, 117.14, 114.27, 113.65, 113.48, 112.48, 110.82, 55.78, 55.70, 55.50 ppm. HRMS m/z : $[M + H]^+$ calcd for $C_{23}H_{21}N_3O_4$, 404.16047; found, 404.1603.

***N*-(5-(3,4-Dimethoxyphenyl)-1H-pyrrolo[2,3-b]pyridin-3-yl)-2-phenylacetamide (8m).** The title compound was synthesized according to the general procedure using phenylacetic acid (45 mg, 0.334 mmol). Purification by silica gel flash column chromatography (using a mixture of DCM and methanol as mobile phase in a ratio of 99:1) yielded the desired compound as a white solid (49 mg, 54%). Purity of 99%. 1H NMR (300 MHz, $DMSO-d_6$): δ 11.36 (s, 1H, NH), 10.45 (s, 1H, NH), 8.53 (m, 2H, ArH), 7.79 (d, J = 2.3 Hz, 1H, ArH), 7.31 (m, 7H, ArH), 7.09 (d, J = 8.4 Hz, 1H, ArH), 3.88 (s, 3H, OCH_3), 3.81 (s, 3H, OCH_3), 3.76 (s, 2H, CH_2) ppm. ^{13}C NMR (75 MHz, $DMSO-d_6$): δ 168.21, 157.37, 149.33, 148.30, 145.01, 142.09, 136.54, 131.94, 129.28, 128.38, 127.55, 126.56, 124.40, 119.00, 115.78, 114.37, 112.78, 112.55, 110.80, 55.83, 55.76, 42.41 ppm. HRMS m/z : $[M + H]^+$ calcd for $C_{23}H_{21}N_3O_3$, 388.16555; found, 388.1660.

***N*-(5-(3,4-Dimethoxyphenyl)-1H-pyrrolo[2,3-b]pyridin-3-yl)-cyclopentanecarboxamide (8n).** To a solution of 3-nitro-5-(3,4-dimethoxyphenyl)-1H-pyrrolo[2,3-b]pyridine **6g** (100 mg, 0.334 mmol) in THF (5 mL) was added a catalytic amount of a slurry of Raney nickel in water. The vessel was flushed three times with hydrogen gas and kept under a hydrogen atmosphere for 4 h. After complete conversion, the catalyst was removed, and the solvent was evaporated in vacuo. The crude product was immediately used for further reaction without purification. To a solution of the crude residue in pyridine (5 mL) was added a solution of cyclopentylcarbonyl chloride (46 μ L, 0.401 mmol) in DCM (2 mL). The reaction was stirred overnight at room temperature. After reaction completion, the solvent was evaporated in vacuo, and the crude residue was extracted three times with water and ethyl acetate. The combined organic layers were dried over $MgSO_4$ and evaporated to dryness. Purification by silica gel flash column chromatography (using a mixture of DCM and methanol in a ratio of 97:3 as mobile phase) yielded the title compound as a white solid (39 mg, 32%). Purity of 99%. 1H NMR (300 MHz, $DMSO-d_6$): δ 11.33 (br s, 1H, NH), 9.96 (br s, 1H, NH), 8.51 (s, 1H, ArH), 8.44 (s, 1H, ArH), 7.82 (d, J = 2.2 Hz, 1H, ArH), 7.23 (m, 2H, ArH), 7.08 (d, J = 8.3 Hz, 1H, ArH), 3.88 (s, 3H, OCH_3), 3.81 (s, 3H, OCH_3), 2.90 (m, 1H, CH_2), 1.77 (m, 8H, CH_2) ppm. ^{13}C NMR (75 MHz, $DMSO-d_6$): δ 173.48, 149.31, 148.30, 145.00, 142.05, 132.01, 127.51, 124.19, 119.05, 115.69, 114.50, 112.71, 112.55, 110.80, 55.82, 55.75, 44.55, 30.46, 25.85. HRMS m/z : $[M + H]^+$ calcd for $C_{21}H_{23}N_3O_3$, 366.18120; found, 366.1808.

***N*-(5-(3,4-Dimethoxyphenyl)-1H-pyrrolo[2,3-b]pyridin-3-yl)-benzenesulfonamide (8p).** To a solution of 3-nitro-5-(3,4-dimethoxyphenyl)-1H-pyrrolo[2,3-b]pyridine (100 mg, 0.334 mmol) in THF (5 mL) was added a catalytic amount of a slurry of Raney nickel in water. The vessel was flushed with hydrogen gas three times and kept under a hydrogen atmosphere for 4 h. After complete conversion, the catalyst was removed and the solvent was evaporated. The crude was immediately used in the next reaction without further purification because of the rapid decomposition of the amine. To a solution of the crude from the previous reaction in pyridine (5 mL) was added a solution of benzenesulfonyl chloride (47 μ L, 0.368 mmol) in DCM (1 mL). The reaction was stirred overnight at room temperature. After reaction completion, the solvent was evaporated and the crude was extracted with water and ethyl acetate three times. The collected organics were dried with $MgSO_4$ and evaporated to dryness. Flash column chromatography (using a mixture of DCM and methanol as mobile phase in a ratio of 97:3) yielded the desired compound as an off-white solid (34 mg, 25%). Purity of 98%. 1H NMR (600 MHz, $DMSO-d_6$): δ 11.64 (br s, 1H, NH), 9.87 (br s, 1H, NH), 8.42 (d, J = 1.92 Hz, 1H, ArH), 7.73 (s, 1H, ArH), 7.72 (s, 2H, ArH), 7.55 (t, J = 7.5 Hz, 1H, ArH), 7.51 (t, J = 7.74 Hz, 2H, ArH), 7.20 (d, J = 2.52 Hz, 1H, ArH), 7.05 (m, 2H, ArH), 6.99 (d, J = 1.74 Hz, 1H, ArH),

3.85 (s, 3H, OCH₃), 3.80 (s, 3H, OCH₃) ppm. ¹³C NMR (150 MHz, DMSO-*d*₆): δ 149.18, 148.27, 145.66, 142.15, 140.05, 132.66, 131.55, 129.03, 128.23, 126.96, 123.76, 121.94, 118.96, 115.65, 113.91, 112.46, 111.06, 110.50, 55.70, 55.68 ppm. HRMS *m/z*: [M + H]⁺ calcd for C₂₁H₁₉N₃O₄S, 408.10234; found, 408.1024.

5-Bromo-1*H*-pyrrolo[2,3-*b*]pyridine-3-carbaldehyde (9). To a solution of 5-bromo-1*H*-pyrrolo[2,3-*b*]pyridine 4 (500 mg, 2.54 mmol) in a mixture of water and acetic acid (in a ratio of 3:1, 10 mL) was added hexamine (712 mg, 5.08 mmol). The reaction was heated to 120 °C and refluxed overnight. The formed precipitate was filtered off, affording the title compound (380 mg, 67%). ¹H NMR (300 MHz, DMSO-*d*₆): δ 12.93 (br s, 1H, NH), 9.93 (s, 1H, CHO), 8.55 (s, 1H, HetH), 8.53 (d, *J* = 2.3 Hz, 1H, HetH), 8.46 (d, *J* = 2.3 Hz, 1H, HetH) ppm. ¹³C NMR (75 MHz, DMSO-*d*₆): δ 185.58, 147.92, 145.09, 139.90, 131.01, 118.32, 116.04, 113.86 ppm.

5-Bromo-1-tosyl-pyrrolo[2,3-*b*]pyridine-3-carbaldehyde (10). To a suspension of 60% NaH on mineral oil (80 mg, 2 mmol) in dry THF (6 mL) was added 5-bromo-1*H*-pyrrolo[2,3-*b*]pyridine-3-carbaldehyde 9 (300 mg, 1.33 mmol) at 0 °C. After stirring for 20 min at room temperature, tosyl chloride (381 mg, 2 mmol) was added and the resulting solution was stirred for another 3 h at room temperature. After reaction completion, the solvent was evaporated in vacuo and the crude residue was extracted with water and DCM. The combined organic layers were dried over MgSO₄ and evaporated in vacuo, affording the title compound (460 mg, 91%). ¹H NMR (300 MHz, DMSO-*d*₆): δ 10.03 (s, 1H, CHO), 9.02 (s, 1H, HetH), 8.59 (d, *J* = 2.2 Hz, 1H, HetH), 8.55 (d, *J* = 2.2 Hz, 1H, HetH), 8.07 (d, *J* = 8.4 Hz, 2H, TsH), 7.48 (d, *J* = 8.2 Hz, 2H, TsH), 2.37 (s, 3H, CH₃) ppm.

5-(3,4-Dimethoxyphenyl)-1-tosyl-1*H*-pyrrolo[2,3-*b*]pyridine-3-carbaldehyde (11). To a solution of 5-bromo-1-tosyl-pyrrolo[2,3-*b*]pyridine-3-carbaldehyde 10 (240 mg, 0.633 mmol) in a mixture of toluene and ethanol (in a ratio of 3:1, 4 mL) was added 3,4-dimethoxyphenylboronic acid (138 mg, 0.759 mmol) and a 2 M solution of K₂CO₃ (950 μL, 1.90 mmol). The system was purged with argon and Pd(PPh₃)₄ (2 mol %) was added. The reaction was heated to 105 °C and was stirred for 4 h. After completion, the solvent was evaporated in vacuo and the residue was extracted with water and ethyl acetate. Purification by silica gel flash chromatography using a mixture of heptane and ethyl acetate (in a ratio of 7:3) as the mobile phase afforded the title compound (160 mg, 58%). ¹H NMR (300 MHz, DMSO-*d*₆): δ 10.09 (s, 1H, CHO), 9.00 (s, 1H, HetH), 8.76 (s, 1H, HetH), 8.55 (s, 1H, HetH), 8.11 (d, *J* = 7.7 Hz, 2H, TsH), 7.49 (d, *J* = 7.4 Hz, 2H, TsH), 7.24 (m, 2H, PhH), 7.07 (d, *J* = 8.2 Hz, 1H, PhH), 3.85 (s, 3H, OCH₃), 3.79 (s, 3H, OCH₃), 2.37 (s, 3H, CH₃) ppm.

5-(3,4-Dimethoxyphenyl)-1-tosyl-pyrrolo[2,3-*b*]pyridin-3-yl(phenyl)methanone (12). To a solution of 5-(3,4-dimethoxyphenyl)-1-tosyl-1*H*-pyrrolo[2,3-*b*]pyridine-3-carbaldehyde 11 (160 mg, 0.367 mmol) in dry THF (5 mL) at 0 °C was added a 3 M solution of phenylmagnesium bromide in diethylether (159 μL, 0.477 mmol). The reaction mixture was stirred for 1 h at 0 °C. After reaction completion, the mixture was quenched with a saturated NH₄Cl solution and extracted with water and ethyl acetate. The combined organic layers were dried over Na₂SO₄ and evaporated to dryness yielding the title compound (130 mg, 69%). ¹H NMR (300 MHz, DMSO-*d*₆): δ 8.62 (s, 1H, ArH), 7.99 (d, *J* = 8.8 Hz, 3H, ArH), 7.70 (s, 1H, ArH), 7.59–6.99 (m, 10H, ArH), 6.13 (d, *J* = 4.4 Hz, 1H, ArH), 6.02 (s, 1H, ArH), 3.82 (s, 3H, OCH₃), 3.78 (s, 3H, OCH₃), 2.34 (s, 3H, CH₃) ppm.

5-(3,4-Dimethoxyphenyl)-1-tosyl-pyrrolo[2,3-*b*]pyridin-3-yl(phenyl)methanone (13). To a solution of (5-(3,4-dimethoxyphenyl)-1-tosyl-pyrrolo[2,3-*b*]pyridin-3-yl) (phenyl)methanol 12 (130 mg, 0.253 mmol) in DCM (8 mL) was added manganese dioxide (220 mg, 2.53 mmol), and the reaction was stirred overnight at room temperature. After completion, the mixture was filtered through Celite, and the filtrate was evaporated to dryness. The crude residue was purified by silica gel flash column chromatography using a mixture of heptane and ethyl acetate (in a ratio of 6:4) as the mobile phase yielding the title compound (64 mg, 49%). ¹H NMR (300 MHz, DMSO-*d*₆): δ 8.78 (d, *J* = 2.1 Hz, 1H, HetH), 8.64 (d, *J* = 2.1

Hz, 1H, HetH), 8.33 (s, 1H), 8.16 (d, *J* = 8.3 Hz, 2H, ArH), 7.96 (d, *J* = 7.2 Hz, 2H, ArH), 7.70 (m, 3H, ArH), 7.47 (d, *J* = 8.2 Hz, 2H, ArH), 7.25 (m, 2H, ArH), 7.08 (d, *J* = 8.4 Hz, 1H, ArH), 3.86 (s, 3H, OCH₃), 3.81 (s, 3H, OCH₃), 2.37 (s, 3H, CH₃) ppm.

5-(3,4-Dimethoxyphenyl)-1*H*-pyrrolo[2,3-*b*]pyridin-3-yl(phenyl)methanone (14). To a solution of (5-(3,4-dimethoxyphenyl)-1-tosyl-pyrrolo[2,3-*b*]pyridin-3-yl) (phenyl)methanone 13 (64 mg, 0.124 mmol) in ethanol (10 mL) was added KOH (35 mg, 0.624 mmol), and the mixture was heated to 80 °C. The reaction was stirred for 3 h. After reaction completion, the solvent was evaporated in vacuo and the crude residue was partitioned between water and ethyl acetate. The combined organic layers were dried over MgSO₄ and evaporated to dryness, yielding the title compound as a white solid (34 mg, 76%). Purity of 95%. ¹H NMR (300 MHz, DMSO-*d*₆): δ 12.74 (br s, 1H, NH), 8.67 (s, 2H, ArH), 8.12 (s, 1H, ArH), 7.84 (d, *J* = 6.8 Hz, 2H, ArH), 7.61 (m, 3H, ArH), 7.25 (m, 2H, ArH), 7.10 (d, *J* = 8.3 Hz, 1H, ArH), 3.88 (s, 3H, OCH₃), 3.82 (s, 3H, OCH₃) ppm. ¹³C NMR (75 MHz, DMSO-*d*₆): δ 190.00, 149.38, 148.64, 148.45, 143.66, 139.77, 136.58, 131.13, 127.30, 119.42, 118.86, 113.88, 112.59, 110.91, 55.77, 55.75 ppm. HRMS *m/z*: [M + H]⁺ calcd for C₂₂H₁₈N₂O₃, 359.1390; found, 359.1393.

5-Bromo-3-iodo-1*H*-pyrrolo[2,3-*b*]pyridine (15). To a solution of 5-bromo-1*H*-pyrrolo[2,3-*b*]pyridine 4 (1.00 g, 5.08 mmol) in acetone (16 mL) was added portionwise *N*-iodosuccinimide (1.26 g, 5.58 mmol). The reaction mixture was stirred for 2 h at room temperature. The formed precipitate was collected via filtration, yielding the title compound as an off-white solid (1.50 g, 92%). ¹H NMR (300 MHz, DMSO-*d*₆): δ 12.36 (s, 1H, NH), 8.32 (d, *J* = 2.0 Hz, 1H, HetH), 7.87 (d, *J* = 1.7 Hz, 1H, HetH), 7.81 (d, *J* = 2.4 Hz, 1H, HetH) ppm.

5-Bromo-3-iodo-1-tosyl-1*H*-pyrrolo[2,3-*b*]pyridine (16). To a solution of 5-bromo-3-iodo-1*H*-pyrrolo[2,3-*b*]pyridine 15 (300 mg, 0.929 mmol) in dry THF (10 mL) was added portionwise NaH (41 mg, 1.02 mmol) at 0 °C. After stirring for 20 min at room temperature, tosyl chloride (230 mg, 1.21 mmol) was added, and the reaction was allowed to stir for another 2 h at room temperature. After reaction completion, the reaction was quenched with water and partitioned between water and ethyl acetate. The combined organic phases were dried over MgSO₄ and concentrated in vacuo, yielding the title compound as a white solid (420 mg, 95%). ¹H NMR (300 MHz, DMSO-*d*₆): δ 8.51 (d, *J* = 2.1 Hz, 1H, HetH), 8.22 (s, 1H, HetH), 8.00 (m, 3H, HetH/TsH), 7.43 (d, *J* = 8.5 Hz, 2H, TsH), 2.34 (s, 3H, CH₃) ppm.

5-Bromo-3-phenyl-1-tosyl-1*H*-pyrrolo[2,3-*b*]pyridine (17). To a solution of 5-bromo-3-iodo-1-tosyl-1*H*-pyrrolo[2,3-*b*]pyridine 16 (200 mg, 0.419 mmol) in a mixture of toluene and ethanol (in a ratio of 3:1) were added phenylboronic acid (51 mg, 0.419 mmol) and a 2 M solution of K₂CO₃ (420 μL, 0.838 mmol). The reaction was flushed with argon three times, followed by the addition of Pd(PPh₃)₄ (10 mg, 0.008 mmol). The reaction was stirred at 90 °C for 3 h. After reaction completion, the reaction was filtered through Celite and the filtrate was washed with water and ethyl acetate. The combined organic phases were dried over MgSO₄ and evaporated in vacuo. Purification by silica gel flash column chromatography using a mixture of heptane and ethyl acetate (in a ratio of 8:2) as the mobile phase yielded the title compound as a white solid (150 mg, 84%). ¹H NMR (300 MHz, DMSO-*d*₆): δ 8.54 (d, *J* = 2.1 Hz, 1H, HetH), 8.50 (d, *J* = 2.1 Hz, 1H, HetH), 8.29 (s, 1H, HetH), 8.04 (d, *J* = 8.4 Hz, 2H, TsH), 7.79 (d, *J* = 7.2 Hz, 2H, TsH), 7.45 (m, 5H, PhH), 2.35 (s, 3H, CH₃) ppm.

5-(3,4-Dimethoxyphenyl)-3-phenyl-1-tosyl-1*H*-pyrrolo[2,3-*b*]pyridine (18). To a solution of 5-bromo-3-phenyl-1-tosyl-1*H*-pyrrolo[2,3-*b*]pyridine (150 mg, 0.351 mmol) in a mixture of toluene and ethanol (in a ratio of 3:1) was added 3,4-dimethoxyphenylboronic acid (77 mg, 0.421 mmol) and a 2 M solution of K₂CO₃ in water (351 μL, 0.702 mmol). The system was flushed with argon and Pd(PPh₃)₄ (2 mol %) was added. The reaction was stirred for 4 h at 105 °C. Upon reaction completion, the solvents were evaporated in vacuo, and the crude residue was extracted with water and ethyl acetate. Purification by silica gel flash chromatography using a mixture

of heptane and ethyl acetate (in a ratio of 8:2) as the mobile phase yielded the desired compound (100 mg, 59%). ^1H NMR (300 MHz, $\text{DMSO-}d_6$): δ 8.71 (d, $J = 2.0$ Hz, 1H, HetH), 8.37 (d, $J = 2.0$ Hz, 1H, HetH), 8.23 (s, 1H, HetH), 8.08 (d, $J = 8.4$ Hz, 2H, ArH), 7.85 (d, $J = 7.2$ Hz, 2H, ArH), 7.46 (m, 5H, ArH), 7.29 (m, 2H, ArH), 7.06 (d, $J = 8.3$ Hz, 1H, ArH), 3.84 (s, 3H, OCH_3), 3.80 (s, 3H, OCH_3), 2.35 (s, 3H, CH_3) ppm.

5-(3,4-Dimethoxyphenyl)-3-phenyl-1H-pyrrolo[2,3-b]pyridine (19). To a solution of 5-(3,4-dimethoxyphenyl)-3-phenyl-1-tosyl-1H-pyrrolo[2,3-b]pyridine **18** (100 mg, 0.309 mmol) in ethanol (5 mL) was added KOH (87 mg, 1.55 mmol). The reaction was allowed to stir for 2 h at 80 °C. After completion, the solvent was evaporated in vacuo and the crude residue was purified by silica gel flash chromatography using a mixture of heptane and ethyl acetate (in a ratio of 7:3) as the mobile phase, affording the title compound (49 mg, 72%). Purity of 97% ^1H NMR (300 MHz, $\text{DMSO-}d_6$): δ 11.98 (s, 1H, NH), 8.56 (s, 1H, ArH), 8.39 (s, 1H, ArH), 7.90 (d, $J = 2.3$ Hz, 1H, ArH), 7.79 (d, $J = 7.5$ Hz, 2H, ArH), 7.45 (t, $J = 7.6$ Hz, 2H, ArH), 7.28 (m, 3H, ArH), 7.06 (d, $J = 8.3$ Hz, 1H, ArH), 3.87 (s, 3H, OCH_3), 3.80 (s, 3H, OCH_3) ppm. ^{13}C NMR (75 MHz, $\text{DMSO-}d_6$): δ 149.32, 148.56, 148.37, 142.16, 135.18, 132.07, 129.15, 129.06, 126.57, 125.83, 124.63, 119.50, 117.37, 114.73, 112.54, 111.27, 55.84, 55.76 ppm. HRMS m/z : $[\text{M} + \text{H}]^+$ calcd for $\text{C}_{21}\text{H}_{18}\text{N}_2\text{O}_2$, 331.1440; found, 331.1437.

Synthesis of 3-Alkynyl-5-bromo-pyrrolo[2,3-b]pyridines (20a–f). *General Procedure.* To a degassed solution of 5-bromo-3-iodo-1H-pyrrolo[2,3-b]pyridine **15** (1 equiv) in THF and triethylamine (3 equiv) were added CuI (0.02 equiv) and Pd(PPh₃)₂Cl₂ (0.01 equiv). The resulting mixture was stirred under an inert atmosphere for 10 min at room temperature. A solution of the appropriate alkyne (0.95 equiv) in THF was added to the mixture. The reaction mixture was stirred for an additional 4 h at room temperature. After completion, the reaction was filtered through Celite. The filtrate was extracted with water and ethyl acetate, washed with brine, and dried over MgSO₄. The crude residue was purified by silica gel flash column chromatography with an appropriate mobile phase. Compounds **20a–f** were made according to this procedure.

5-Bromo-3-(phenylethynyl)-1H-pyrrolo[2,3-b]pyridine (20a). The title compound was synthesized according to the general procedure using 5-bromo-3-iodo-1H-pyrrolo[2,3-b]pyridine **15** (200 mg, 0.619 mmol) and phenylacetylene (60 mg, 0.588 mmol). The crude residue was purified by silica gel flash column chromatography using a mixture of heptane and ethyl acetate (in a ratio of 8:2) as the mobile phase yielding the title compound as a white solid (85 mg, 51%). ^1H NMR (300 MHz, $\text{DMSO-}d_6$): δ 12.40 (br s, 1H, NH), 8.39 (d, $J = 2.2$ Hz, 1H, HetH), 8.32 (d, $J = 2.1$ Hz, 1H, HetH), 8.01 (s, 1H, HetH), 7.60 (m, 2H, PhH), 7.42 (m, 3H, PhH) ppm.

5-Bromo-3-(pyridin-3-ylethynyl)-1H-pyrrolo[2,3-b]pyridine (20b). The title compound was synthesized according to the general procedure using 5-bromo-3-iodo-1H-pyrrolo[2,3-b]pyridine **15** (200 mg, 0.619 mmol) and 3-ethynylpyridine (61 mg, 0.588 mmol). The crude residue was purified by silica gel flash column chromatography using a mixture of heptane and ethyl acetate (in a ratio of 7:3) as the mobile phase yielding the title compound as a white solid (140 mg, 75%). ^1H NMR (300 MHz, $\text{DMSO-}d_6$): δ 12.49 (br s, 1H, NH), 8.81 (s, 1H, ArH), 8.56 (d, $J = 4.8$ Hz, 1H, ArH), 8.40 (s, 2H, ArH), 8.04 (m, 2H, ArH), 7.46 (m, 1H, ArH) ppm.

5-Bromo-3-((3-methoxyphenyl)ethynyl)-1H-pyrrolo[2,3-b]pyridine (20c). The title compound was synthesized according to the general procedure using 5-bromo-3-iodo-1H-pyrrolo[2,3-b]pyridine **15** (200 mg, 0.619 mmol) and 3-methoxyphenylacetylene (60 mg, 0.588 mmol). The crude residue was purified by silica gel flash column chromatography using a mixture of heptane and ethyl acetate (in a ratio of 7:3) as the mobile phase, yielding the title compound as a white solid (105 mg, 51%). ^1H NMR (300 MHz, $\text{DMSO-}d_6$): δ 12.41 (br s, 1H, NH), 8.39 (d, $J = 2.2$ Hz, 1H, HetH), 8.34 (d, $J = 2.1$ Hz, 1H, HetH), 8.00 (s, 1H, HetH), 7.33 (t, $J = 8.1$ Hz, 1H, PhH), 7.16 (m, 2H, PhH), 6.96 (m, 1H, PhH), 3.81 (s, 3H, OCH_3) ppm.

5-Bromo-3-(p-tolylethynyl)-1H-pyrrolo[2,3-b]pyridine (20d). The title compound was synthesized according to the general procedure

using 5-bromo-3-iodo-1H-pyrrolo[2,3-b]pyridine **15** (200 mg, 0.619 mmol) and *p*-tolylacetylene (68 mg, 0.588 mmol). The crude residue was purified by silica gel flash column chromatography using a mixture of heptane and ethyl acetate (in a ratio of 7:3) as the mobile phase, yielding the title compound as a white solid (130 mg, 67%). ^1H NMR (300 MHz, $\text{DMSO-}d_6$): δ 12.36 (br s, 1H, NH), 8.38 (d, $J = 2.2$ Hz, 1H, HetH), 8.30 (d, $J = 2.2$ Hz, 1H, HetH), 7.98 (s, 1H, HetH), 7.48 (d, $J = 8.1$ Hz, 2H, PhH), 7.23 (d, $J = 7.9$ Hz, 2H, PhH), 2.34 (s, 3H, CH_3).

5-Bromo-3-((4-fluorophenyl)ethynyl)-1H-pyrrolo[2,3-b]pyridine (20e). The title compound was synthesized according to the general procedure using 5-bromo-3-iodo-1H-pyrrolo[2,3-b]pyridine **15** (200 mg, 0.619 mmol) and 4-fluorophenylacetylene (60 mg, 0.588 mmol). The crude residue was purified by silica gel flash column chromatography using a mixture of heptane and ethyl acetate (in a ratio of 8:2) as the mobile phase yielding the title compound as a white solid (110 mg, 56%). ^1H NMR (300 MHz, $\text{DMSO-}d_6$): δ 12.41 (br s, 1H, NH), 8.38 (d, $J = 2.1$ Hz, 1H, HetH), 8.34 (d, $J = 2.1$ Hz, 1H, HetH), 8.00 (s, 1H, HetH), 7.66 (dd, $J = 8.7, 5.6$ Hz, 2H, PhH), 7.27 (t, $J = 8.9$ Hz, 2H, PhH) ppm.

3-((5-Bromo-1H-pyrrolo[2,3-b]pyridin-3-yl)ethynyl)benzonitrile (20f). The title compound was synthesized according to the general procedure using 5-bromo-3-iodo-1H-pyrrolo[2,3-b]pyridine **15** (200 mg, 0.619 mmol) and 3-cyanophenylacetylene (75 mg, 0.588 mmol). The crude residue was purified by silica gel flash column chromatography using a mixture of heptane and ethyl acetate (in a ratio of 7:3) as the mobile phase, yielding the title compound as a white solid (90 mg, 45%). ^1H NMR (300 MHz, $\text{DMSO-}d_6$): δ 8.45 (d, $J = 2.2$ Hz, 1H, HetH), 8.40 (d, $J = 2.1$ Hz, 1H, HetH), 8.14 (s, 1H, HetH), 8.05 (s, 1H, PhH), 7.91 (d, $J = 8.0$ Hz, 1H, PhH), 7.84 (d, $J = 7.5$ Hz, 1H, PhH), 7.63 (t, $J = 7.9$ Hz, 1H, PhH) ppm.

Synthesis of 3-Alkynyl-5-(3,4-dimethoxyphenyl)-pyrrolo[2,3-b]pyridines (21a–f). *General Procedure.* To a solution of a 5-bromo-3-arylethynyl-1H-pyrrolo[2,3-b]pyridine derivative (1 equiv) in dioxane (4 mL) were added 3,4-dimethoxyphenylboronic acid (1.2 equiv) and 1 mL of a K₂CO₃ (3 equiv) solution. The system was purged three times with argon and heated to 105 °C. After stirring for 10 min, Pd(PPh₃)₄ (0.1 equiv) was added and the reaction was purged once more with argon. The reaction mixture was stirred at 105 °C for 3 h. After completion, the reaction mixture was cooled to room temperature and filtered through Celite. The filtrate was extracted with water and ethyl acetate. The combined organic layers were washed with brine, dried over MgSO₄, and evaporated in vacuo. The crude residue was purified by silica gel flash column chromatography with an appropriate mobile phase. Compounds **21a–f** were made according to this procedure.

5-(3,4-Dimethoxyphenyl)-3-(phenylethynyl)-1H-pyrrolo[2,3-b]pyridine (21a). The title compound was synthesized according to the general procedure using 3-(phenylethynyl)-1H-pyrrolo[2,3-b]pyridine **20a** (80 mg, 0.269 mmol). The crude residue was purified by silica gel flash column chromatography using a mixture of DCM and ethyl acetate (in a ratio of 9:1) as the mobile phase yielding the title compound as a brown solid (36 mg, 38%). Purity of 99%. ^1H NMR (300 MHz, $\text{DMSO-}d_6$): δ 12.21 (br s, 1H, NH), 8.61 (s, 1H, ArH), 8.25 (s, 1H, ArH), 7.96 (d, $J = 2.2$ Hz, 1H, ArH), 7.60 (d, $J = 6.5$ Hz, 1H, ArH), 8.01 (m, 2H, ArH), 7.35 (m, 6H, ArH), 7.06 (d, $J = 8.3$ Hz, 1H, ArH), 3.88 (s, 3H, OCH_3), 3.81 (s, 3H, OCH_3) ppm. ^{13}C NMR (75 MHz, $\text{DMSO-}d_6$): δ 149.33, 148.49, 147.24, 143.12, 131.42, 131.27, 131.17, 129.60, 128.80, 128.13, 124.93, 123.48, 120.29, 119.44, 112.48, 111.11, 95.31, 90.75, 83.53, 55.82, 55.73 ppm. HRMS m/z : $[\text{M} + \text{H}]^+$ calcd for $\text{C}_{23}\text{H}_{18}\text{N}_2\text{O}_2$, 355.14409; found, 355.1435.

5-(3,4-Dimethoxyphenyl)-3-(pyridin-3-ylethynyl)-1H-pyrrolo[2,3-b]pyridine (21b). The title compound was synthesized according to the general procedure using 5-bromo-3-(pyridin-3-ylethynyl)-1H-pyrrolo[2,3-b]pyridine **20b** (140 mg, 0.470 mmol). The crude residue was purified by silica gel flash column chromatography using a mixture of DCM and ethyl acetate (in a ratio of 9:1) as the mobile phase, yielding the title compound as a white solid (75 mg, 44%). Purity of 98% ^1H NMR (300 MHz, $\text{DMSO-}d_6$): δ 12.30 (s, 1H,

NH), 8.81 (s, 1H, ArH), 8.63 (d, $J = 2.0$ Hz, 1H, ArH), 8.55 (d, $J = 4.9$ Hz, 1H, ArH), 8.30 (d, $J = 1.9$ Hz, 1H, ArH), 8.01 (m, 2H, ArH), 7.46 (m, 1H, ArH), 7.31 (m, 2H, ArH), 7.07 (d, $J = 8.3$ Hz, 1H), 3.89 (s, 3H, OCH₃), 3.81 (s, 3H, OCH₃) ppm. ¹³C NMR (75 MHz, DMSO-*d*₆): δ 151.46, 149.33, 148.52, 148.34, 147.24, 143.24, 138.19, 131.78, 131.33, 129.73, 125.03, 123.68, 120.59, 120.28, 119.46, 112.47, 111.13, 94.77, 87.69, 86.87, 55.83, 55.74 ppm. HRMS m/z : [M + H]⁺ calcd for C₂₂H₁₇N₃O₂, 356.13934; found, 356.1393.

5-(3,4-Dimethoxyphenyl)-3-(3-methoxyphenylethynyl)-1H-pyrrolo[2,3-*b*]pyridine (21c). The title compound was synthesized according to the general procedure using 3-(3-methoxyphenylethynyl)-1H-pyrrolo[2,3-*b*]pyridine **20c** (110 mg, 0.353 mmol). The crude residue was purified by silica gel flash column chromatography using a mixture of DCM and ethyl acetate (in a ratio of 9:1). Further purification by preparative TLC (the mobile phase being a mixture of nitromethane/toluene in a ratio of 6:4) yielded the title compound as a white solid (25 mg, 20%). Purity of 97%. ¹H NMR (300 MHz, DMSO-*d*₆): δ 12.21 (s, 1H, NH), 8.61 (d, $J = 1.9$ Hz, 1H, ArH), 8.25 (d, $J = 1.9$ Hz, 1H, ArH), 7.96 (d, $J = 2.6$ Hz, 1H, ArH), 7.32 (m, 3H, ArH), 7.16 (m, 2H, ArH), 7.07 (d, $J = 8.3$ Hz, 1H, ArH), 6.96 (m, 1H, ArH), 3.89 (s, 3H, OCH₃), 3.81 (s, 3H, OCH₃), 3.80 (s, 3H, OCH₃) ppm. ¹³C NMR (75 MHz, DMSO-*d*₆): δ 159.33, 149.33, 148.50, 147.24, 143.12, 131.41, 131.34, 129.91, 129.60, 124.97, 124.56, 123.61, 120.28, 119.44, 115.95, 114.58, 112.49, 111.12, 95.24, 90.74, 83.43, 55.82, 55.75, 55.34 ppm. HRMS m/z : [M + H]⁺ calcd for C₂₄H₂₀N₂O₃, 385.15465; found, 385.1541.

5-(3,4-Dimethoxyphenyl)-3-(*p*-tolylethynyl)-1H-pyrrolo[2,3-*b*]pyridine (21d). The title compound was synthesized according to the general procedure using 3-(*p*-tolylethynyl)-1H-pyrrolo[2,3-*b*]pyridine **20d** (110 mg, 0.353 mmol). The crude residue was purified by silica gel flash column chromatography using a mixture of DCM and ethyl acetate (in a ratio of 9:1) as the mobile phase, yielding the title compound as a white solid (25 mg, 20%). Purity of 95%. ¹H NMR (300 MHz, DMSO-*d*₆): δ 12.18 (br s, 1H, NH), 8.60 (d, $J = 2.0$ Hz, 1H, ArH), 8.22 (d, $J = 1.8$ Hz, 1H, ArH), 7.93 (d, $J = 2.6$ Hz, 1H, ArH), 7.49 (d, $J = 8.0$ Hz, 2H, ArH), 7.27 (m, 4H, ArH), 7.03 (m, 2H, ArH), 3.88 (s, 3H, OCH₃), 3.81 (s, 3H, OCH₃), 2.34 (s, 3H, CH₃). ¹³C NMR (75 MHz, DMSO-*d*₆): δ 149.33, 148.48, 147.23, 143.07, 137.78, 131.45, 131.11, 131.04, 129.54, 129.42, 124.91, 120.46, 120.27, 119.43, 112.49, 111.11, 95.49, 90.81, 82.77, 55.83, 55.74, 21.14. HRMS m/z : [M + H]⁺ calcd for C₂₄H₂₀N₂O₂, 369.15974; found, 369.1593.

5-(3,4-Dimethoxyphenyl)-3-(4-fluorophenylethynyl)-1H-pyrrolo[2,3-*b*]pyridine (21e). The title compound was synthesized according to the general procedure using 3-(4-fluorophenylethynyl)-1H-pyrrolo[2,3-*b*]pyridine **20e** (80 mg, 0.269 mmol). The crude residue was purified by silica gel flash column chromatography using a mixture of DCM and ethyl acetate (in a ratio of 9:1), yielding the desired compound as a brown solid (34 mg, 36%). Purity of 98%. ¹H NMR (300 MHz, DMSO-*d*₆): δ 12.21 (br s, 1H, NH), 8.61 (s, 1H, ArH), 8.25 (s, 1H, ArH), 7.95 (d, $J = 2.4$ Hz, 1H, ArH), 7.65 (m, 2H, ArH), 7.28 (m, 4H, ArH), 7.06 (d, $J = 8.5$ Hz, 1H, ArH), 3.88 (s, 3H), 3.81 (s, 3H, OCH₃) ppm. ¹³C NMR (150 MHz, DMSO-*d*₆): δ 161.68 (d, $J_{CF} = 247$ Hz) 149.27, 148.44, 147.17, 143.07, 133.36 (d, $J_{CF} = 8.3$ Hz), 131.35, 131.20, 129.54, 124.91, 120.23, 119.90, 119.89, 119.38, 115.95 (d, $J_{CF} = 22$ Hz), 112.42, 111.05, 95.11, 89.60, 83.20, 55.76, 55.68 ppm. HRMS m/z : [M + H]⁺ calcd for C₂₃H₁₇FN₂O₂, 373.13467; found, 373.1333.

3-((5-(3,4-Dimethoxyphenyl)-1H-pyrrolo[2,3-*b*]pyridin-3-yl)-ethynyl)benzotrile (21f). The title compound was synthesized according to the general procedure using 3-(3-cyanophenylethynyl)-1H-pyrrolo[2,3-*b*]pyridine **20f** (100 mg, 0.310 mmol). The crude residue was purified by silica gel flash column chromatography using a mixture of DCM and ethyl acetate (in a ratio of 9:1) as the mobile phase, yielding the title compound as a brown solid (44 mg, 37%). Purity of 98%. ¹H NMR (300 MHz, DMSO-*d*₆): δ 12.31 (br s, 1H, NH), 8.62 (d, $J = 2.0$ Hz, 1H, ArH), 8.32 (d, $J = 1.9$ Hz, 1H, ArH), 8.11 (s, 1H, ArH), 8.00 (d, $J = 2.5$ Hz, 1H, ArH), 7.91 (d, $J = 7.9$ Hz, 1H, ArH), 7.82 (d, $J = 7.9$ Hz, 1H, ArH), 7.62 (t, $J = 7.9$ Hz, 2H, ArH), 7.31 (m, 2H, ArH), 7.07 (d, $J = 8.3$ Hz, 1H, ArH), 3.89 (s, 3H,

OCH₃), 3.81 (s, 3H, OCH₃). ¹³C NMR (75 MHz, DMSO-*d*₆): δ 149.33, 148.54, 147.25, 143.28, 135.52, 134.37, 131.91, 131.43, 131.35, 130.10, 129.81, 125.11, 124.93, 120.34, 119.51, 118.33, 112.48, 112.17, 111.17, 94.64, 89.01, 86.05, 55.84, 55.75. HRMS m/z : [M + H]⁺ calcd for C₂₄H₁₇N₃O₂, 380.13934; found, 380.1390.

5-Bromo-1-methyl-1H-pyrrolo[2,3-*b*]pyridine (22). To a solution of 5-bromo-1H-pyrrolo[2,3-*b*]pyridine **4** (200 mg, 1.02 mmol) in THF (5 mL) at 0 °C was added 60% NaH on mineral oil (49 mg, 1.22 mmol). The reaction was stirred at 0 °C for 1.5 h. Methyl iodide (70 μ L, 1.12 mmol) was added, and the mixture was allowed to warm at ambient temperature and then stirred at room temperature for 3 h. After completion, the mixture was quenched with water and extracted three times with ethyl acetate. The combined organic layers were washed with brine, dried over MgSO₄, filtered, and evaporated. The crude residue was purified by silica gel flash column chromatography using a mixture of heptane and ethyl acetate (in a ratio of 8:2) as the mobile phase, yielding the title compound as an oil that subsequently crystallized to an off-white solid (160 mg, 75%). ¹H NMR (300 MHz, DMSO-*d*₆): δ 8.31 (d, $J = 2.07$ Hz, 1H, HetH), 8.20 (d, $J = 2.07$ Hz, 1H, HetH), 7.59 (d, $J = 3.39$ Hz, 1H, HetH), 6.46 (d, $J = 3.42$ Hz, 1H, HetH), 3.81 (s, 3H, CH₃) ppm. HRMS m/z : [M + H]⁺ calcd for C₈H₇N₂Br, 210.98658; found, 210.9866.

5-Bromo-1-methyl-3-nitro-1H-pyrrolo[2,3-*b*]pyridine (23). 5-Bromo-1H-pyrrolo[2,3-*b*]pyridine **22** (130 mg, 0.615 mmol) was added portionwise to a stirring solution of fuming nitric acid (1 mL) at 0 °C over 10 min. The reaction was allowed to stir for 30 min at 0 °C. The mixture was poured out in ice water and the formed precipitate was collected via vacuum filtration. The filter cake was washed generously with water and heptane, yielding the title compound as a pink solid (155 mg, 98%). ¹H NMR (300 MHz, DMSO-*d*₆): δ 8.99 (s, 1H, HetH), 8.61 (s, 1H, HetH), 8.57 (m, 1H, HetH), 3.92 (s, 3H, CH₃) ppm.

5-(3,4-Dimethoxyphenyl)-1-methyl-3-nitro-1H-pyrrolo[2,3-*b*]pyridine (24). To a solution of 5-bromo-1-methyl-3-nitro-1H-pyrrolo[2,3-*b*]pyridine **23** (100 mg, 0.391 mmol) in dioxane (4 mL) were added 3,4-dimethoxyphenylboronic acid (69 mg, 0.469 mmol) and 1 mL of a K₂CO₃ solution (161 mg, 1.17 mmol). The system was purged three times with argon and heated to 105 °C. After stirring for 10 min, Pd(PPh₃)₄ (10 mol %) was added and the reaction was purged once more with argon. The reaction mixture was stirred at 105 °C overnight. After completion, the reaction mixture was cooled to room temperature and filtered through Celite. Extraction was performed with water and ethyl acetate. The combined organic layers were washed with brine, dried over MgSO₄, and evaporated. Purification by silica gel flash chromatography using a mixture of DCM and ethyl acetate (in a ratio of 9:1) as the mobile phase yielded the title compound as a yellow solid (90 mg, 83%). ¹H NMR (300 MHz, DMSO-*d*₆): δ 8.96 (s, 1H, HetH), 8.79 (d, $J = 2.07$ Hz, 1H, HetH), 8.56 (d, $J = 2.01$ Hz, 1H, HetH), 7.30 (m, 2H, PhH), 7.10 (d, $J = 8.22$ Hz, 1H, PhH), 3.96 (s, 3H), 3.88 (s, 3H, OCH₃), 3.82 (s, 3H) ppm.

N-(5-(3,4-Dimethoxyphenyl)-1-methyl-1H-pyrrolo[2,3-*b*]pyridin-3-yl)nicotinamide (26). The title compound was synthesized according to the general procedure described for the synthesis of compounds **8a–h**, starting from 5-(3,4-dimethoxyphenyl)-1-methyl-3-nitro-1H-pyrrolo[2,3-*b*]pyridine **24** (90 mg, 0.287 mmol). Purification by silica gel flash column chromatography using a mixture of DCM and methanol (in a ratio gradually ranging from 98:2 to 95:5) yielded the title compound as a red solid (22 mg, 20%). Purity of 98%. ¹H NMR (300 MHz, DMSO-*d*₆): δ 10.60 (br s, 1H, NH), 9.19 (br s, 1H, NH), 8.77 (d, $J = 2.6$ Hz, 1H, ArH), 8.60 (s, 2H, ArH), 8.36 (d, $J = 8.0$ Hz, 1H, ArH), 8.07 (s, 1H, ArH), 7.59 (m, 1H, ArH), 7.26 (m, 2H, ArH), 7.08 (d, $J = 8.3$ Hz, 1H, ArH), 3.87 (s, 6H, OCH₃/CH₃), 3.80 (s, 3H, OCH₃/CH₃). ¹³C NMR (75 MHz, DMSO-*d*₆): δ 163.33, 152.03, 149.33, 148.87, 148.39, 144.19, 142.14, 135.65, 131.81, 130.43, 127.77, 125.22, 123.63, 121.31, 119.21, 113.40, 113.14, 112.54, 110.93, 55.83, 55.75, 30.91 ppm. HRMS m/z : [M + H]⁺ calcd for C₂₂H₂₀N₄O₃, 389.16080; found, 389.1604.

2-Chloro-5-(3,4-dimethoxyphenyl)nicotinonitrile (28). To a solution of 3,4-dimethoxyphenylboronic acid (460 mg, 2.53 mmol) and 5-bromo-2-chloronicotinonitrile **27** (500 mg, 2.3 mmol) in isopropanol (12 mL) was added a solution of K_2CO_3 (953 mg, 6.9 mmol) in water (4 mL). The reaction mixture was flushed three times with argon and heated to 90 °C. Then, $Pd(PPh_3)_4$ (10 mol %) was added and the system was flushed once more with argon. After stirring at 90 °C for 2.5 h, the reaction was concentrated under reduced pressure. The crude residue was partitioned between ethyl acetate and water and extracted three times. The combined organic phases were washed with brine and dried over $MgSO_4$. The solvent was removed under reduced pressure and the crude residue was purified by silica gel flash column chromatography using a mixture of heptane and ethylacetate (in a ratio of 7:3) as the mobile phase. This was followed by a second purification by silica gel flash column chromatography using a mixture of DCM, heptane, and ethylacetate (in a ratio of 70:25:5) as the mobile phase, yielding the title compound as a white solid (320 mg, 50%). 1H NMR (300 MHz, $DMSO-d_6$): δ 9.06 (d, $J = 2.5$ Hz, 1H, HetH), 8.85 (d, $J = 2.5$ Hz, 1H, HetH), 7.41 (m, 2H, PhH), 7.10 (m, 1H, PhH), 3.87 (s, 3H, OCH_3), 3.82 (s, 3H, OCH_3).

5-(3,4-Dimethoxyphenyl)-1H-pyrazolo[3,4-*b*]pyridin-3-amine (29). To a solution of 2-chloro-5-(3,4-dimethoxyphenyl)nicotinonitrile **28** (100 mg, 0.364 mmol) in pyridine (3 mL) was added a hydrazine monohydrate solution (65% in water, 103 μ L, 0.728 mmol). The reaction was refluxed overnight, and after completion, the solvent was evaporated. The crude residue was purified by silica gel flash column chromatography using a mixture of DCM and methanol (in a ratio of 95:5), yielding the title compound as a yellow solid (90 mg, 91%). 1H NMR (300 MHz, $DMSO-d_6$): δ 11.97 (br s, 1H, NH), 8.66 (d, $J = 2.1$ Hz, 1H, HetH), 8.36 (d, $J = 2.0$ Hz, 1H, HetH), 7.21 (m, 2H, PhH), 7.07 (d, $J = 8.4$ Hz, 1H, PhH), 3.86 (s, 3H, OCH_3), 3.80 (s, 3H, OCH_3).

***N*-(5-(3,4-Dimethoxyphenyl)-1H-pyrazolo[3,4-*b*]pyridin-3-yl)nicotinamide (30).** To a solution of 5-(3,4-dimethoxyphenyl)-1H-pyrazolo[3,4-*b*]pyridin-3-amine **29** (90 mg, 0.332 mmol) in pyridine (3 mL) at 0 °C was added nicotinoyl chloride hydrochloride (71 mg, 0.400 mmol). The reaction was stirred at 0 °C for 1 h and then stirred at room temperature overnight. After reaction completion, water was added and the mixture was extracted three times with ethyl acetate. The combined organic phases were washed with brine, dried over $MgSO_4$, and evaporated to dryness. The crude residue was purified by silica gel flash column chromatography using a mixture of DCM and methanol (in a ratio gradually ranging from 98:2 to 96:4), yielding the title compound as a beige solid (76 mg, 61%). Purity of 99%. 1H NMR (300 MHz, $DMSO-d_6$): δ 13.47 (s, 1H), 11.33 (s, 1H), 9.24 (s, 1H), 8.85 (d, $J = 2.1$ Hz, 1H), 8.79 (d, $J = 3.4$ Hz, 1H), 8.50 (d, $J = 2.0$ Hz, 1H), 8.42 (d, $J = 8.1$ Hz, 1H), 7.59 (dd, $J = 7.7, 4.8$ Hz, 1H), 7.28 (s, 1H), 7.23 (d, $J = 8.4$ Hz, 1H), 7.07 (d, $J = 8.4$ Hz, 1H), 3.86 (s, 3H), 3.80 (s, 3H). ^{13}C NMR (75 MHz, $DMSO-d_6$): δ 164.30, 152.57, 151.36, 149.35, 149.22, 148.89, 148.67, 139.54, 135.92, 130.86, 129.45, 129.25, 129.13, 123.66, 119.50, 112.54, 111.08, 108.70, 55.84, 55.74. HRMS m/z : $[M + H]^+$ calcd for $C_{20}H_{17}N_5O_3$, 376.14040; found, 376.1400.

2-Amino-3,5-dibromopyrazine (32). To a solution of amino-pyrazine **31** (1 g, 10.52 mmol) in $DMSO$ (10 mL) was added *N*-bromosuccinimide (3.94 g, 22.08 mmol) portionwise over 45 min. The resulting mixture was stirred for 3 h at room temperature. The reaction was poured in ice water and extracted five times with ethyl acetate. The combined organic phases were washed with brine, dried over $MgSO_4$, and evaporated to dryness. The crude residue was purified by silica gel flash column chromatography using a mixture of heptane and ethyl acetate (in a ratio of 7:3) as the mobile phase, yielding the desired compound as a fluffy white solid (1.94 g, 73%). 1H NMR (300 MHz, $DMSO-d_6$): δ 8.13 (s, 1H, ArH), 6.99 (br s, 2H, NH_2) ppm. HRMS m/z : $[M + H]^+$ calcd for $C_4H_3N_3Br_2$, 251.87675; found, 251.8765.

5-Bromo-3-((trimethylsilyl)ethyl)pyrazin-2-amine (33). To a solution of 2-amino-3,5-dibromopyrazine **32** (1 g, 3.95 mmol) in degassed THF (15 mL) was added copper iodide (7.53 mg, 0.040 mmol), $Pd(PPh_3)_2Cl_2$ (45 mg, 0.040 mmol), and triethylamine (1.65

mL, 11.86 mmol). The system was flushed with nitrogen, and trimethylsilylacetylene (534 μ L, 1.91 mmol) was added dropwise over 5 min. The reaction was stirred overnight at room temperature. After reaction completion, the solvent was evaporated and water was added. The resulting suspension was extracted three times with ethyl acetate. The combined organic phases were washed with water and brine, dried over $MgSO_4$, and evaporated to dryness. The crude residue was purified by silica gel flash column chromatography using a mixture of heptane and ethylacetate (in a ratio of 80:20) as the mobile phase, yielding the title compound as a bright yellow solid (769 mg, 72%). 1H NMR (300 MHz, $DMSO-d_6$): δ 8.12 (s, 1H, ArH), 6.82 (s, 2H, NH_2), 0.27 (s, 9H, $Si(CH_3)_3$) ppm.

2-Bromo-5H-pyrrolo[2,3-*b*]pyrazine (34). To a solution of 5-bromo-3-((trimethylsilyl)ethyl)pyridin-2-amine **33** (1 g, 3.7 mmol) in dry NMP (10 mL) was added portionwise $KOtBu$ (498 mg, 4.44 mmol). The reaction mixture was flushed with nitrogen and stirred for 3 h at 80 °C. After reaction completion, the mixture was extracted three times with water and ethyl acetate. The combined organic layers were washed twice with water and once with brine, dried over $MgSO_4$, and evaporated in vacuo. The crude residue was then purified by silica gel flash column chromatography using a mixture of heptane/ethyl acetate (in a ratio of 7:3) as the mobile phase, yielding the title compound as a yellow solid (502 mg, 69%). 1H NMR (300 MHz, $DMSO-d_6$): δ 12.42 (br s, 1H, NH), 8.35 (s, 1H, ArH), 7.97 (d, $J = 3.48$ Hz, 1H, ArH), 6.63 (d, $J = 3.48$ Hz, 1H, ArH) ppm.

5-Bromo-3-iodo-1H-pyrrolo[2,3-*b*]pyrazine (35). To a solution of 5-bromo-1H-pyrrolo[2,3-*b*]pyrazine **34** (500 mg, 2.52 mmol) in a minimal volume of acetone was added portionwise *N*-iodosuccinimide (625 g, 2.78 mmol). The reaction mixture was stirred for 2 h at room temperature. The formed precipitate was collected via filtration, yielding the title product as an off-white solid (408 mg, 50%). 1H NMR (300 MHz, $DMSO-d_6$): δ 12.82 (br s, 1H, NH), 8.40 (d, $J = 1.77$ Hz, 1H, ArH), 8.19 (s, 1H, ArH) ppm.

2-Bromo-7-(pyridin-3-ylethynyl)-5H-pyrrolo[2,3-*b*]pyrazine (36). To a degassed solution of 5-bromo-3-iodo-1H-pyrrolo[2,3-*b*]pyrazine **35** (200 mg, 0.617 mmol) in THF (10 mL) were added triethylamine (238 μ L, 1.85 mmol), $Pd(PPh_3)_2Cl_2$ (4.33 mg, 1 mol %), and CuI (2.35 mg, 2 mol %). The resulting mixture was stirred under inert atmosphere for 10 min at room temperature. Then, a solution of 3-ethynylpyridine (61 mg, 0.586 mmol) in THF (1 mL) was added to the reaction mixture. The reaction was stirred for 4 h at room temperature. After completion, the reaction was filtered through Celite, extracted with water and ethyl acetate, washed with brine, dried over $MgSO_4$, and evaporated in vacuo. The crude residue was purified by silica gel flash column chromatography using a mixture of heptane and ethyl acetate (in a ratio of 6:4) as the mobile phase, yielding the title compound as a white solid (130 mg, 71%). 1H NMR (300 MHz, $DMSO-d_6$): δ 12.94 (br s, 1H, NH), 8.76 (s, 1H), 8.59 (d, $J = 3.2$ Hz, 1H, ArH), 8.51 (s, 1H, ArH), 8.45 (s, 1H, ArH), 7.99 (dt, $J = 7.9, 1.8$ Hz, 1H, ArH), 7.47 (dd, $J = 7.8, 4.8$ Hz, 1H, ArH). HRMS m/z : $[M + H]^+$ calcd for $C_{13}H_7N_4Br$, 298.99273; found, 298.9930.

2-(3,4-Dimethoxyphenyl)-7-(pyridin-3-ylethynyl)-5H-pyrrolo[2,3-*b*]pyrazine (37). To a solution of 2-bromo-7-(pyridin-3-ylethynyl)-5H-pyrrolo[2,3-*b*]pyrazine **36** (110 mg, 0.368 mmol) in dioxane (4 mL) was added 3,4-dimethoxyphenylboronic acid (80 mg, 0.441 mmol) and 1 mL of a K_2CO_3 solution (152 mg, 1.1 mmol). The system was purged three times with argon and heated to 105 °C. After stirring for 10 min, $Pd(PPh_3)_4$ (10 mol %) was added and the reaction was purged once more with argon. The reaction mixture was stirred at 105 °C for 3 h. After completion, the reaction mixture was cooled to room temperature and filtered through Celite. The filtrate was extracted with water and ethyl acetate. The combined organic layers were washed with brine, dried over $MgSO_4$, and evaporated in vacuo. Purification by silica gel flash column chromatography using a mixture of DCM and ethylacetate (in a ratio of 1:1) as the mobile phase yielded the title compound as a white solid (37 mg, 28%). Purity of 98%. 1H NMR (300 MHz, $DMSO-d_6$): δ 12.63 (br s, 1H, NH), 8.96 (s, 1H, ArH), 8.78 (s, 1H, ArH), 8.58 (d, $J = 3.3$ Hz, 1H, ArH), 8.35 (s, 1H, ArH), 8.00 (d, $J = 7.8$ Hz, 1H, ArH), 7.76 (m, 2H, ArH), 7.48 (m, 1H, ArH), 7.11 (d, $J = 9.0$ Hz, 1H, ArH), 3.90 (s, 3H,

OCH₃), 3.83 (s, 3H, OCH₃) ppm. ¹³C NMR (75 MHz, DMSO-*d*₆): δ 151.44, 149.97, 149.32, 148.57, 146.70, 139.95, 138.27, 137.69, 136.06, 135.59, 130.21, 123.77, 120.46, 119.60, 112.33, 110.46, 95.69, 88.10, 85.92, 55.88, 55.81 ppm. HRMS *m/z*: [M + H]⁺ calcd for C₂₁H₁₆N₄O₂, 357.13459; found, 357.1346.

Binding-Displacement Assay for NAK Family Selectivity.

Inhibitor binding to NAK family kinase domain proteins was determined using a binding-displacement assay which tests the ability of the inhibitors to displace a fluorescent tracer compound from the ATP binding site of the kinase domain. Inhibitors were dissolved in DMSO and dispensed as 16-point, 2× serial dilutions in duplicate into black multiwell plates (Greiner) using an Echo dispenser (Labcyte Inc). Each well contained 1 nM biotinylated AAK1, BMP2K, GAK or STK16 kinase domain protein ligated to streptavidin-Tb-cryptate (Cisbio), either 12.5 nM (for AAK1 or BMP2K) or 25 nM (for GAK or STK16) Kinase Tracer 236 (Thermo Fisher Scientific), 10 mM 4-(2-hydroxyethyl)-1-piperazineethanesulfonic acid (HEPES) pH 7.5, 150 mM NaCl, 2 mM dithiothreitol, 0.01% bovine serum albumin, 0.01% Tween-20. Final assay volume for each data point was 5 μL, and final DMSO concentration was 1%. The plate was incubated at room temperature for 1.5 h and then read using a TR-FRET protocol on a PheraStarFS plate reader (BMG Labtech). The data were normalized to 0 and 100% inhibition control values and fitted to a four parameter dose–response binding curve in GraphPad Software. For the purpose of estimating the selectivity between each kinase domain, the determined IC₅₀ values were converted to K_i values using the Cheng–Prusoff equation and the concentration and K_D values for the tracer (previously determined).

AAK1 Expression, Purification, and Crystallization.

AAK1 (UniProtKB: Q2M218) residues T27–A365 were cloned, expressed, and purified as described,³⁷ except that the protein was expressed in a cell line together with lambda phosphatase to produce the unphosphorylated protein. The purified protein was concentrated to 12 mg/mL, and compound **1** dissolved in 100% DMSO was added to a final concentration of 1.5 mM (3% final DMSO concentration). The protein–ligand solution was incubated on ice for 30 min, then centrifuged at 14 000 rpm for 10 min, 4 °C, immediately prior to setting up sitting-drop vapour diffusion crystallization plates. The best-diffracting crystals of the AAK1–compound **1** complex were obtained using a reservoir solution containing 26% PEG 3350, 0.1 M bis-Tris pH 5.5 by spiking drops with 20 nL of seed-stock solution immediately prior to incubation at 18 °C. Seed stock was prepared from poorly formed crystals of AAK1–compound **1** grown during previous rounds of crystal optimization, which were diluted in 50–100 μL reservoir solution and vortexed for 2 min in an Eppendorf containing a seed bead. A 1:1 dilution series of seeds was prepared in order to find the optimal seed concentration. Prior to mounting, crystals were cryo-protected in situ by addition of reservoir solution containing an additional 25% ethylene glycol. Crystals were then flash-frozen in liquid nitrogen.

Data Collection, Structure Solution, and Refinement.

Data were collected at Diamond beamline I02 using monochromatic radiation at wavelength 0.9795 Å. Diffraction data were processed using XDS⁴⁵ as part of the xia2 pipeline⁴⁶ and scaled using AIMLESS,⁴⁷ and molecular replacement was carried out in Phaser⁴⁸ with PDB ID 4WSQ as a search model. Data processing and refinement statistics are given in Table S1 from the Supporting Information. REFMAC5,⁴⁹ PHENIX,⁵⁰ and Coot⁵¹ were used for model building and refinement. Coordinates were submitted to the PDB under accession code 5L4Q.

Virus Construct.

DENV2 (New Guinea C strain)^{52,53} *Renilla* reporter plasmid used for in vitro assays was a gift from Pei-Yong Shi (The University of Texas Medical Branch). DENV 16681 plasmid (pD2IC-30P-NBX) used for ex vivo experiments was a gift from Claire Huang (CDC).⁵⁴

Cells.

Huh7 (Apath LLC) cells were grown in Dulbecco's modified Eagle medium (Mediatech) supplemented with 10% fetal bovine serum (FBS; Omega Scientific), nonessential amino acids, 1% L-glutamine, and 1% penicillin–streptomycin (Thermo Fisher Scientific) and maintained in a humidified incubator with 5% CO₂ at 37

°C. MDDCs were prepared as described with slight modifications.⁵⁵

Buffy coats were obtained from the Stanford Blood Center. CD14+ cells were purified by EasySep Human Monocyte Enrichment Kit without CD16 Depletion (Stemcell Technologies). Cells were seeded in 6-well plates (2 × 10⁶ cells per well), stimulated with 500 U/mL granulocyte-macrophage colony-stimulating and 1000 U/mL interleukin-4 (PeproTech), and incubated at 37 °C for 6 days prior to DENV infection [multiplicity of infection (MOI) 1].

Virus Production. DENV2 RNA was transcribed in vitro using mMMESSAGE/mMACHINE (Ambion) kits. DENV was produced by electroporating RNA into BHK-21 cells, harvesting supernatants on day 10 and titering via standard plaque assays on BHK-21 cells. In parallel, on day 2 post-electroporation, a DENV-containing supernatant was used to inoculate C6/36 cells to amplify the virus. EBOV (Kikwit isolate) was grown in Vero E6 cells, and supernatants were collected and clarified and stored at –80 °C until further use. Virus titers were determined via standard plaque assay on Vero E6 cells.

Infection Assays. Huh7 cells were infected with DENV in replicates (*n* = 5) at a MOI of 0.05. Overall infection was measured at 48 h using a *Renilla* luciferase substrate. MDDCs were infected with DENV2 (16881) at an MOI of 1. Standard plaque assays were conducted following a 72 h incubation. Huh7 cells were infected with EBOV at an MOI of 1 or 0.1 under biosafety level 4 conditions. Forty-eight hours after infection, supernatants were collected and stored at –80 °C until further use. Cells were formalin-fixed for 24 h prior to removal from biosafety level 4. Infected cells were detected using an EBOV glycoprotein-specific monoclonal antibody (KZ52) and quantitated by automated fluorescence microscopy using an Operetta High Content Imaging System and the Harmony software package (PerkinElmer). For select experiments, supernatants were assayed by standard plaque assay, as described previously. Briefly, supernatants were thawed, serially diluted in growth media, added to VeroE6 cells, and incubated for 1 h at 37 °C in a humidified 5% CO₂ incubator, prior to being overlaid with agarose. Infected cells were incubated for 7 days and then stained with neutral red vital dye (Gibco). Plaques were counted, and titers were calculated.

Viability Assays. Viability was assessed using alamarBlue reagent (Invitrogen) or CellTiter-Glo reagent (Promega) assay according to manufacturer's protocol. Fluorescence was detected at 560 nm on an InfiniteM1000 plate reader and luminescence on an InfiniteM1000 plate reader (Tecan) or a SpectraMax 340PC.

Effect of Compounds **1**, **8g**, and **21b** on AP-2 Phosphorylation.

Huh7 cells were kept in serum-free medium for 1 h and then treated with the compounds or DMSO in complete medium for 4 h at 37 °C. To allow capturing of phosphorylated AP2M1, 100 nM of the PP2A inhibitor calyculin A (Cell Signalling) was added 30 min prior to lysis in M-PER lysis buffer (Thermo Fisher Scientific) with 1× Halt Protease & phosphatase inhibitor cocktail (Thermo Fisher Scientific). Samples were then subjected to sodium dodecyl sulfate-polyacrylamide gel electrophoresis and blotting with antibodies targeting phospho-AP2M1 (Cell Signaling), total AP2M1 (Santa Cruz Biotechnology), and actin (Sigma-Aldrich). Band intensity was measured with NIH ImageJ.

AAK1 LanthaScreen Eu Binding Assay.

The compounds were subjected to a LanthaScreen binding assay in which 10 titrations of dissolved test compound in DMSO are transferred to a 384-well plate. Sequential addition of the kinase buffer (50 mM HEPES pH 7.5, 0.01% BRIJ-35, 10 mM MgCl and 1 mM EGTA), the 2× kinase antibody (Eu Anti GST) mixture, and the 4× Tracer 222 solution was performed. After shaking for 30 s and a 1 h incubation period at room temperature, the plate was read on a fluorescence plate reader. When the bound tracer in the active site was displaced by the test compound, fluorescence was not observed. The collected data were then compared to a 0% displacement control with pure DMSO and a 100% displacement control with sunitinib, a known inhibitor of AAK1, and plotted against the logarithmic concentration parameter. The IC₅₀ was subsequently extracted.

AAK1 K_D Assay. K_D values for AAK1 were determined as previously described.³⁸ Briefly, the DNA-tagged AAK1, an immobilized ligand on streptavidin-coated magnetic beads, and the test

compound were combined. When binding occurred between AAK1 and a test compound, no binding can occur between AAK1 and the immobilized ligand. Upon washing, the compound-bound, DNA-tagged AAK1 was washed away. The beads carrying the ligands were then resuspended in elution buffer and the remaining kinase concentration was measured by qPCR on the eluate. K_D values were determined using dose–response curves.

Kinase Selectivity Assay. Compound **21b** was screened against a diverse panel of 468 kinases (DiscoverX, KINOMEscan) using an in vitro ATP-site competition binding assay at a concentration of 10 μ M. The results are reported as the percentage of kinase/phage remaining bound to the ligands/beads, relative to a control. High affinity compounds have % of control values close to zero, while weaker binders have higher % control values.

Statistical Analysis. All data were analyzed with GraphPad Prism software. Fifty percent effective concentration (EC_{50} , EC_{90} and CC_{50}) values were measured by fitting data to a three-parameter logistic curve. *P* values were calculated by two-way ANOVA with Bonferroni's multiple comparisons tests or by 2-tailed unpaired *t*-test.

Molecular Modeling. Docking was initiated from the AAK1 PDB structure 5L4Q, from which first all ligands and water molecules were removed. The remaining structure was prepared by AutodockTools⁵⁶ as a receptor: polar hydrogens were added, Gasteiger charges were defined, the AD4 atom type was assigned, and finally everything was saved in a pdbqt file. The original inhibitor lkb (identical to compound **1**) from the PDB file 5L4Q was extracted, processed by AutodockTools, and saved in the pdbqt format. Compounds **8g** and **21b** were drawn in ChemDraw and a 3D structure was generated by Chem3D.⁵⁷ The amide conformation in compound **8g** was initially chosen having an anti-orientation. Autodocktools was used again to prepare the corresponding pdbqt files. Autodock Vina was used for the docking experiments.⁴¹ A cubic box was defined 60 \times 60 \times 60 units (0.375 \AA /unit) and the box was centred at the ALA72:CB atom in the first kinase domain (chain A). The docking process used variable dihedral angles in the ligand while the receptor was defined as rigid. Amide bonds in the ligands were not allowed to rotate.

A control docking was executed using the original inhibitor lkb present in the 5L4Q PDB file. Vina reproduced the original X-ray position very well. For the three docked systems with the best Vina docking score, a MD simulation using the Amber 18 software was performed.⁴² Enzyme parameters and charges were taken from the default amber ff14sb force field. Parameters and atomic charges were calculated by antechamber (gaff2). The barrier of the dihedral torsion parameters for the amide bond was increased from 2.6 (from antechamber) to 10.0 (in line with a peptide bond amide in the standard amber force field).

Three molecular systems (AAK1/compound **1**, AAK1/compound **8g**, and AAK1/compound **21b**) were solvated with TIP3P and neutralized in charge. Standard NPT simulations of 40 ns were started (300 K, periodic conditions with PME, cutoff 10.0 \AA , shake for H bonds constraints, 2 fs time step).

■ ASSOCIATED CONTENT

📄 Supporting Information

The Supporting Information is available free of charge on the ACS Publications website at DOI: 10.1021/acs.jmedchem.9b00136.

Copies of ^1H and ^{13}C NMR spectra of intermediates and final compounds; details of the kinase selectivity profiling of compound **21b**; and data collection and refinement statistics for cocrystallography of compound **1** with AAK1 (PDF)

Molecular formula strings (CSV)

Accession Codes

The coordinates have been deposited in the PDB with accession code 5L4Q.

■ AUTHOR INFORMATION

Corresponding Authors

*E-mail: seinav@stanford.edu. Phone: 650 723 8656 (S.E.).

*E-mail: steven.dejonghe@kuleuven.be. Phone: +32 16 32 26 62 (S.D.J.).

ORCID

Mathy Froeyen: 0000-0002-8675-6540

Stefan Knapp: 0000-0001-5995-6494

Piet Herdewijn: 0000-0003-3589-8503

Shirit Einav: 0000-0001-6441-4171

Steven De Jonghe: 0000-0002-3872-6558

Author Contributions

S.V. and S-Y.P. contributed equally to this work. S.E. and S.D.J. also contributed equally to this work.

Notes

The authors declare no competing financial interest.

Authors will release the atomic coordinates and experimental data upon article publication.

■ ACKNOWLEDGMENTS

This work was supported by award number W81XWH-16-1-0691 from the Department of Defense (DoD), Congressionally Directed Medical Research Programs (CDMRP) to S.E., P.H.; Grant 12393481 from the Defense Threat Reduction Agency (DTRA), Fundamental Research to Counter Weapons of Mass Destruction to S.E., P.H.; and seed grant from the Stanford SPARK program. S.V. is the recipient of a doctoral fellowship from the Research Foundation—Flanders (1S00116N). S.P. was supported by the Child Health Research Institute, Lucile Packard Foundation for Children's Health and the Stanford CSTA (grant number UL1 TR000093). The SGC is a registered charity (number 1097737) that receives funds from AbbVie, Bayer Pharma AG, Boehringer Ingelheim, Canada Foundation for Innovation, Eshelman Institute for Innovation, Genome Canada, Innovative Medicines Initiative (EU/EFPIA) [ULTRA-DD grant no. 115766], Janssen, Merck KGaA Darmstadt Germany, MSD, Novartis Pharma AG, Ontario Ministry of Economic Development and Innovation, Pfizer, São Paulo Research Foundation-FAPESP, Takeda, and Wellcome [106169/ZZ14/Z].

■ ABBREVIATIONS

AAK1, adaptor-associated kinase 1; AP, adaptor protein; BOP, (benzotriazol-1-yloxy)tris(dimethylamino)phosphonium hexafluorophosphate; CC_{50} , half-maximal cytotoxic concentration; CCV, clathrin-coated vesicle; DENV, Dengue virus; EBOV, Ebola virus; EC_{50} , half-maximal effective concentration; EC_{90} , 90% effective concentration; EGFR, epidermal growth factor receptor; GAK, cyclin G-associated kinase; HCV, hepatitis C virus; K_D , dissociation constant; MM/GBSA, molecular mechanics with a generalized Born surface area continuum solvation model; MM/PBSA, molecular mechanics energies combined with the Poisson–Boltzmann surface area continuum solvation model; NAK, numb-associated kinase; PDB, protein data bank; rmsd, root mean square deviation; TGN, trans-Golgi network; WHO, World Health Organization

■ REFERENCES

(1) Murray, N. A. E.; Quam, M. B.; Wilder-Smith, A. Epidemiology of Dengue: Past, Present and Future Prospects. *Clin. Epidemiol.* **2013**, *5*, 299–309.

- (2) WHO. Epidemiology. <http://www.who.int/denguecontrol/epidemiology/en/> (accessed Nov 15, 2018).
- (3) *Weekly Epidemiological Record*; World Health Organization, 2016; Vol. 91 (30), pp 349–364.
- (4) Sanyal, S.; Sinha, S.; Halder, K. K. Pathogenesis of Dengue Haemorrhagic Fever. *J. Indian Med. Assoc.* **2013**, *89*, 152–153.
- (5) WHO. Ebola virus disease <http://www.who.int/news-room/fact-sheets/detail/ebola-virus-disease> (accessed Aug 7, 2018).
- (6) Behnam, M. A. M.; Nitsche, C.; Boldescu, V.; Klein, C. D. The Medicinal Chemistry of Dengue Virus. *J. Med. Chem.* **2016**, *59*, 5622–5649.
- (7) Bekerman, E.; Neveu, G.; Shulla, A.; Brannan, J.; Pu, S.-Y.; Wang, S.; Xiao, F.; Barouch-Bentov, R.; Bakken, R. R.; Mateo, R.; Govero, J.; Nagamine, C. M.; Diamond, M. S.; De Jonghe, S.; Herdewijn, P.; Dye, J. M.; Randall, G.; Einav, S. Anticancer Kinase Inhibitors Impair Intracellular Viral Trafficking and Exert Broad-Spectrum Antiviral Effects. *J. Clin. Invest.* **2017**, *127*, 1338–1352.
- (8) Bekerman, E.; Einav, S. Combating Emerging Viral Threats. *Science* **2015**, *348*, 282–283.
- (9) Grove, J.; Marsh, M. The Cell Biology of Receptor-Mediated Virus Entry. *J. Cell Biol.* **2011**, *195*, 1071–1082.
- (10) Neveu, G.; Ziv-Av, A.; Barouch-Bentov, R.; Berkerman, E.; Mulholland, J.; Einav, S. AP-2-Associated Protein Kinase 1 and Cyclin G-Associated Kinase Regulate Hepatitis C Virus Entry and Are Potential Drug Targets. *J. Virol.* **2015**, *89*, 4387–4404.
- (11) Neveu, G.; Barouch-Bentov, R.; Ziv-Av, A.; Gerber, D.; Jacob, Y.; Einav, S. Identification and Targeting of an Interaction between a Tyrosine Motif within Hepatitis C Virus Core Protein and AP2M1 Essential for Viral Assembly. *PLoS Pathog.* **2012**, *8*, No. e1002845.
- (12) Xiao, F.; Wang, S.; Barouch-Bentov, R.; Neveu, G.; Pu, S.; Beer, M.; Schor, S.; Kumar, S.; Nicolaescu, V.; Lindenbach, B. D.; Randall, G.; Einav, S. Interactions between the Hepatitis C Virus Non-structural 2 Protein and Host Adaptor Proteins 1 and 4 Orchestrate Virus Release. *mBio* **2018**, *9*, 1–21.
- (13) Pu, S.-Y.; Xiao, F.; Schor, S.; Bekerman, E.; Zanini, F.; Barouch-Bentov, R.; Nagamine, C. M.; Einav, S. Feasibility and Biological Rationale of Repurposing Sunitinib and Erlotinib for Dengue Treatment. *Antiviral Res.* **2018**, *155*, 67–75.
- (14) Kostich, W.; Hamman, B. D.; Li, Y.-W.; Naidu, S.; Dandapani, K.; Feng, J.; Easton, A.; Bourin, C.; Baker, K.; Allen, J.; Savelieva, K.; Louis, J. V.; Dokania, M.; Elavazhagan, S.; Vattikundala, P.; Sharma, V.; Das, M. L.; Shankar, G.; Kumar, A.; Holenarsipur, V. K.; Gulianello, M.; Molski, T.; Brown, J. M.; Lewis, M.; Huang, Y.; Lu, Y.; Pieschl, R.; OMalley, K.; Lippy, J.; Nouraldeen, A.; Lanthorn, T. H.; Ye, G.; Wilson, A.; Balakrishnan, A.; Denton, R.; Grace, J. E.; Lentz, K. A.; Santone, K. S.; Bi, Y.; Main, A.; Swaffield, J.; Carson, K.; Mandlekar, S.; Vikramadithyan, R. K.; Nara, S. J.; Dzierba, C.; Bronson, J.; Macor, J. E.; Zaczek, R.; Westphal, R.; Kiss, L.; Bristow, L.; Conway, C. M.; Zambrowicz, B.; Albright, C. F. Inhibition of AAK1 Kinase as a Novel Therapeutic Approach to Treat Neuropathic Pain. *J. Pharmacol. Exp. Ther.* **2016**, *358*, 371–386.
- (15) Bronson, J.; Chen, L.; Ditta, J.; Dzierba, C. D.; Jalagam, P. R.; Luo, G.; Macor, J.; Maishal, T. K.; Nara, S. J.; Rajamani, R.; Sistla, R. K.; Thangavel, S. Biaryl Kinase Inhibitors. WO 2017/059085, 2017.
- (16) Kuai, L.; Ong, S.-E.; Madison, J. M.; Wang, X.; Duvall, J. R.; Lewis, T. A.; Luce, C. J.; Conner, S. D.; Pearlman, D. A.; Wood, J. L.; Schreiber, S. L.; Carr, S. A.; Scolnick, E. M.; Haggarty, S. J. AAK1 Identified as an Inhibitor of Neuregulin-1/ErbB4-Dependent Neurotrophic Factor Signaling Using Integrative Chemical Genomics and Proteomics. *Chem. Biol.* **2011**, *18*, 891–906.
- (17) Bamborough, P.; Drewry, D.; Harper, G.; Smith, G. K.; Schneider, K. Assessment of Chemical Coverage of Kinome Space and Its Implications for Kinase Drug Discovery. *J. Med. Chem.* **2008**, *51*, 7898–7914.
- (18) Barl, N. M.; Sansiaume-Dagousset, E.; Karaghiosoff, K.; Knochel, P. Full Functionalization of the 7-Azaindole Scaffold by Selective Metalation and Sulfoxide/Magnesium Exchange. *Angew. Chem., Int. Ed.* **2013**, *52*, 10093–10096.
- (19) Brumsted, C. J.; Moorlag, H.; Radinov, R. N.; Ren, Y.; Waldmeier, P. Method for Preparation of N-[3-[5-(4-Chlorophenyl)-1H-Pyrrolo[2,3-b]Pyridine-3-Carbonyl]-2,4-Difluorophenyl] Propane-1-Sulfonamide. WO 2012/010538 A2, 2012.
- (20) Han, C.; Green, K.; Pfeifer, E.; Gosselin, F. Highly Regioselective and Practical Synthesis of 5-Bromo-4-Chloro-3-Nitro-7-Azaindole. *Org. Process Res. Dev.* **2017**, *21*, 664–668.
- (21) Stokes, S.; Graham, C. J.; Ray, S. C.; Stefaniak, E. J. 1H-Pyrrolo[2,3-b]Pyridine Derivatives and Their Use as Kinase Inhibitors. WO 2013/114113 A1, 2013.
- (22) Gao, L.-J.; Kovackova, S.; Šála, M.; Ramadori, A. T.; De Jonghe, S.; Herdewijn, P. Discovery of Dual Death-Associated Protein Related Apoptosis Inducing Protein Kinase 1 and 2 Inhibitors by a Scaffold Hopping Approach. *J. Med. Chem.* **2014**, *57*, 7624–7643.
- (23) Le Huerou, Y.; Blake, J.; Gunwardana, I.; Mohr, P.; Wallace, E.; Wang, B.; Chicarella, M.; Lyon, M. Pyrrolopyridines as Kinase Inhibitors. WO 2009/140320, 2009.
- (24) Stavenger, R.; Witherington, J.; Rawlings, D.; Holt, D.; Chan, G. CHK1 Kinase Inhibitors. WO 03/028724, 2003.
- (25) Bahekar, R. H.; Jain, M. R.; Jadav, P. A.; Prajapati, V. M.; Patel, D. N.; Gupta, A. A.; Sharma, A.; Tom, R.; Bandyopadhyaya, D.; Modi, H.; Patel, P. R. Synthesis and antidiabetic activity of 2,5-disubstituted-3-imidazol-2-yl-pyrrolo[2,3-b]pyridines and thieno[2,3-b]pyridines. *Bioorg. Med. Chem.* **2007**, *15*, 6782–6795.
- (26) Chavan, N. L.; Nayak, S. K.; Kusrurkar, R. S. A rapid method toward the synthesis of new substituted tetrahydro α -carboline and α -carboline. *Tetrahedron* **2010**, *66*, 1827–1831.
- (27) Chinta, B. S.; Baire, B. Reactivity of indole-3-alkoxides in the absence of acids: Rapid synthesis of homo- bisindolylmethanes. *Tetrahedron* **2016**, *72*, 8106–8116.
- (28) McCoull, W.; Hennessy, E. J.; Blades, K.; Box, M. R.; Chuaqui, C.; Dowling, J. E.; Davies, C. D.; Ferguson, A. D.; Goldberg, F. W.; Howe, N. J.; Kemmitt, P. D.; Lamont, G. M.; Madden, K.; McWhirter, C.; Varnes, J. G.; Ward, R. A.; Williams, J. D.; Yang, B. Identification and Optimisation of 7-Azaindole PAK1 Inhibitors with Improved Potency and Kinase Selectivity. *MedChemComm* **2014**, *5*, 1533–1539.
- (29) Gourdain, S.; Dairou, J.; Denhez, C.; Bui, L. C.; Rodrigues-Lima, F.; Janel, N.; Delabar, J. M.; Cariou, K.; Dodd, R. H. Development of DANDYs, New 3,5-Diaryl-7-Azaindoles Demonstrating Potent DYRK1A Kinase Inhibitory Activity. *J. Med. Chem.* **2013**, *56*, 9569–9585.
- (30) Gelbard, H.; Dewhurst, S.; Goodfellow, V.; Wiemann, T.; Ravula, S.; Loweth, C. Bicyclic Heteroaryl Kinase Inhibitors and Methods of Use. WO 2011/149950, 2011.
- (31) Knauber, T.; Tucker, J. Palladium Catalyzed Monoselective α -Arylation of Sulfones and Sulfonamides with 2,2,6,6-Tetramethylpiperidine-ZnCl₂-LiCl Base and Aryl Bromides. *J. Org. Chem.* **2016**, *81*, 5636–5648.
- (32) Zhao, B.; Li, Y.; Xu, P.; Dai, Y.; Luo, C.; Sun, Y.; Ai, J.; Geng, M.; Duan, W. Discovery of Substituted 1H-Pyrazolo[3,4-b]pyridine Derivatives as Potent and Selective FGFR Kinase Inhibitors. *ACS Med. Chem. Lett.* **2016**, *7*, 629–634.
- (33) Shi, J.; Xu, G.; Zhu, W.; Ye, H.; Yang, S.; Luo, Y.; Han, J.; Yang, J.; Li, R.; Wei, Y.; Chen, L. Design and Synthesis of 1,4,5,6-Tetrahydropyrrolo[3,4-c]Pyrazoles and Pyrazolo[3,4-b]Pyridines for Aurora-A Kinase Inhibitors. *Bioorg. Med. Chem. Lett.* **2010**, *20*, 4273–4278.
- (34) Van Mileghem, S.; Egle, B.; Gilles, P.; Veryser, C.; Van Meervelt, L.; De Borggraeve, W. M. Carbonylation as a Novel Method for the Assembly of Pyrazine Based Oligoamide Alpha-Helix Mimetics. *Org. Biomol. Chem.* **2017**, *15*, 373–378.
- (35) Maccormick, S.; Storck, P.-H.; Mertimore, M.; Charrier, J.-D.; Knegtel, R.; Young, S.; Pinder, J.; Durrant, S. Compounds Useful as Inhibitors of ATR Kinase. WO 2012/178123, 2012.
- (36) Gelbard, H.; Dewhurst, S.; Goodfellow, V.; Wiemann, T.; Bennet, D. MLK Inhibitors and Methods of Use. WO 2010/068483, 2010.

- (37) Sorrell, F. J.; Szklarz, M.; Abdul Azeez, K. R.; Elkins, J. M.; Knapp, S.; Szklarz, M.; Azeez, K. R. A.; Elkins, J. M.; Knapp, S. Family-wide Structural Analysis of Human Numb-Associated Protein Kinases. *Struct. Des.* **2016**, *24*, 401–411.
- (38) Fabian, M. A.; Biggs, W. H.; Treiber, D. K.; Atteridge, C. E.; Azimioara, M. D.; Benedetti, M. G.; Carter, T. A.; Ciceri, P.; Edeen, P. T.; Floyd, M.; Ford, J. M.; Galvin, M.; Gerlach, J. L.; Grotzfeld, R. M.; Herrgard, S.; Insko, D. E.; Insko, M. A.; Lai, A. G.; Lélías, J.-M.; Mehta, S. A.; Milanov, Z. V.; Velasco, A. M.; Wodicka, L. M.; Patel, H. K.; Zarrinkar, P. P.; Lockhart, D. J. A small molecule-kinase interaction map for clinical kinase inhibitors. *Nat. Biotechnol.* **2005**, *23*, 329–336.
- (39) Rodriguez-Madoz, J. R.; Bernal-Rubio, D.; Kaminski, D.; Boyd, K.; Fernandez-Sesma, A. Dengue Virus Inhibits the Production of Type I Interferon in Primary Human Dendritic Cells. *J. Virol.* **2010**, *84*, 4845–4850.
- (40) Karaman, M. W.; Herrgard, S.; Treiber, D. K.; Gallant, P.; Atteridge, C. E.; Campbell, B. T.; Chan, K. W.; Ciceri, P.; Davis, M. I.; Edeen, P. T.; Faraoni, R.; Floyd, M.; Hunt, J. P.; Lockhart, D. J.; Milanov, Z. V.; Morrison, M. J.; Pallares, G.; Patel, H. K.; Pritchard, S.; Wodicka, L. M.; Zarrinkar, P. P. A Quantitative Analysis of Kinase Inhibitor Selectivity. *Nat. Biotechnol.* **2008**, *26*, 127–132.
- (41) Trott, O.; Olson, A. J. AutoDock Vina: improving the speed and accuracy of docking with a new scoring function, efficient optimization, and multithreading. *J. Comput. Chem.* **2010**, *31*, 455–461.
- (42) Case, D. A.; Ben-Shalom, I.; Brozell, S. R.; Cerutti, D. S.; Cheatham, T.; Cruzeiro, V. W. D.; Darden, T. A.; Duke, R. A.; Ghoreishi, D.; Gilson, M. K.; Gohlke, H.; Goetz, A. W.; Greene, D.; Harris, R.; Homeyer, N.; Huang, Y.; Izadi, S.; Kovalenko, A.; Kurtzman, T.; Lee, T. S.; LeGrand, S.; Li, P.; Lin, C.; Liu, J.; Luchko, T.; Luo, R.; Mermelstein, D. J.; Merz, K. M.; Miao, Y.; Monard, G.; Nguyen, C.; Nguyen, H.; Omelyan, I.; Onufriev, A.; Pan, F.; Qi, R.; Roe, D. R.; Roitberg, A.; Sagui, C.; Schott-Verdugo, S.; Shen, J.; Simmerling, C. L.; Smith, J.; SalomonFerrer, R.; Swails, J.; Walker, R. C.; Wang, J.; Wei, H.; Wolf, R. M.; Wu, X.; Xiao, L.; York, D. M.; Kollman, P. A. *AMBER 2018*; San Francisco, 2018.
- (43) Genheden, S.; Ryde, U. The MM/PBSA and MM/GBSA Methods to Estimate Ligand-Binding Affinities. *Expert Opin. Drug Discovery* **2015**, *10*, 449–461.
- (44) Pettersen, E. F.; Goddard, T. D.; Huang, C. C.; Couch, G. S.; Greenblatt, D. M.; Meng, E. C.; Ferrin, T. E. UCSF Chimera?A Visualization System for Exploratory Research and Analysis. *J. Comput. Chem.* **2004**, *25*, 1605–1612.
- (45) Kabsch, W. XDS. *Acta Crystallogr. Sect. D Biol. Crystallogr.* **2010**, *66*, 125–132.
- (46) Winter, G. xia2: an expert system for macromolecular crystallography data reduction. *J. Appl. Crystallogr.* **2010**, *43*, 186–190.
- (47) Winn, M. D.; Ballard, C. C.; Cowtan, K. D.; Dodson, E. J.; Emsley, P.; Evans, P. R.; Keegan, R. M.; Krissinel, E. B.; Leslie, A. G. W.; McCoy, A.; McNicholas, S. J.; Murshudov, G. N.; Pannu, N. S.; Potterton, E. A.; Powell, H. R.; Read, R. J.; Vagin, A.; Wilson, K. S. Overview of the CCP4 suite and current developments. *Acta Crystallogr., Sect. D: Biol. Crystallogr.* **2011**, *67*, 235–242.
- (48) McCoy, A. J.; Grosse-kunstleve, R. W.; Adams, P. D.; Winn, M. D.; Storoni, L. C.; Read, R. J. Phaser Crystallographic Software Research Papers. *J. Appl. Crystallogr.* **2007**, *40*, 658–674.
- (49) Murshudov, G. N.; Vagin, A. A.; Dodson, E. J. Refinement of Macromolecular Structures by the Maximum-Likelihood Method. *Acta Crystallogr. Sect. D Biol. Crystallogr.* **1997**, *53*, 240–255.
- (50) Adams, P. D.; Afonine, P. V.; Bunkóczi, G.; Chen, V. B.; Davis, I. W.; Echols, N.; Headd, J. J.; Hung, L.-W.; Kapral, G. J.; Grosse-Kunstleve, R. W.; McCoy, A. J.; Moriarty, N. W.; Oeffner, R.; Read, R. J.; Richardson, D. C.; Richardson, J. S.; Terwilliger, T. C.; Zwart, P. H. PHENIX: a comprehensive Python-based system for macromolecular structure solution. *Acta Crystallogr. Sect. D Biol. Crystallogr.* **2010**, *66*, 213–221.
- (51) Emsley, P.; Lohkamp, B.; Scott, W. G.; Cowtan, K. Features and development of Coot. *Acta Crystallogr. Sect. D Biol. Crystallogr.* **2010**, *66*, 486–501.
- (52) Perera, R.; Khaliq, M.; Kuhn, R. J. Closing the Door on Flaviviruses: Entry as a Target for Antiviral Drug Design. *Antiviral Res.* **2008**, *80*, 11–22.
- (53) Xie, X.; Gayen, S.; Kang, C.; Yuan, Z.; Shi, P.-Y. Membrane Topology and Function of Dengue Virus NS2A Protein. *J. Virol.* **2013**, *87*, 4609–4622.
- (54) Huang, C. Y.-H.; Butrapet, S.; Moss, K. J.; Childers, T.; Erb, S. M.; Calvert, A. E.; Silengo, S. J.; Kinney, R. M.; Blair, C. D.; Roehrig, J. T. The Dengue Virus Type 2 Envelope Protein Fusion Peptide Is Essential for Membrane Fusion. *Virology* **2010**, *396*, 305–315.
- (55) Rodriguez-Madoz, J. R.; Bernal-Rubio, D.; Kaminski, D.; Boyd, K.; Fernandez-Sesma, A. Dengue Virus Inhibits the Production of Type I Interferon in Primary Human Dendritic Cells. *J. Virol.* **2010**, *84*, 4845–4850.
- (56) Morris, G. M.; Huey, R.; Lindstrom, W.; Sanner, M. F.; Belew, R. K.; Goodsell, D. S.; Olson, A. J. AutoDock4 and AutoDockTools4: Automated Docking with Selective Receptor Flexibility. *J. Comput. Chem.* **2009**, *30*, 2785–2791.
- (57) Evans, D. A. History of the Harvard ChemDraw Project. *Angew. Chem., Int. Ed.* **2014**, *53*, 11140–11145.



Contents lists available at ScienceDirect

European Journal of Medicinal Chemistry

journal homepage: <http://www.elsevier.com/locate/ejmech>

Research paper

Cyclin G-associated kinase (GAK) affinity and antiviral activity studies of a series of 3-C-substituted isothiazolo[4,3-*b*]pyridinesRandy Wouters^a, Szu-Yuan Pu^b, Mathy Froeyen^a, Eveline Lescrinier^a, Shirit Einav^b, Piet Herdewijn^a, Steven De Jonghe^{a,*},¹^a Medicinal Chemistry, Rega Institute for Medical Research, KU Leuven, Herestraat 49, bus 1041, 3000, Leuven, Belgium^b Department of Medicine, Division of Infectious Diseases and Geographic Medicine, Department of Microbiology and Immunology, Stanford University School of Medicine, Stanford, CA, 94305, USA

ARTICLE INFO

Article history:

Received 10 October 2018

Received in revised form

21 November 2018

Accepted 27 November 2018

Available online 28 November 2018

Keywords:

Cyclin G-associated kinase

isothiazolo[4,3-*b*]pyridine

Dengue virus

Kinase inhibitor

Antiviral drugs

ABSTRACT

Cyclin G-associated kinase (GAK) is a cellular regulator of the clathrin-associated host adaptor proteins AP-1 and AP-2, which regulates intracellular trafficking of dengue virus during early and late stages of the viral lifecycle. Previously, the discovery of isothiazolo[4,3-*b*]pyridines as potent and selective GAK inhibitors with promising antiviral activity was reported. In this manuscript, the synthesis of isothiazolo[4,3-*b*]pyridines with a carbon-linked substituent at position 3 is described by the application of regioselective Suzuki and Sonogashira coupling reactions. A derivative with a 3,4-dimethoxyphenyl residue at position 3 demonstrates low nanomolar binding affinity for GAK and antiviral activity against dengue virus. These findings reveal that appropriate substitution of a phenyl moiety at position 3 of the scaffold can improve GAK binding affinity.

© 2018 Elsevier Masson SAS. All rights reserved.

1. Introduction

Human kinases are a well-established class of drug targets. For more than 30 years, the search for kinase inhibitors has been the focus of significant pharmaceutical research. Today, more than 200 small molecule kinase inhibitors are in clinical trials, and about 30 such drugs have already received marketing approval for use in humans. Because of the central role of kinases in intracellular signal transduction, kinases have mainly been targeted for oncology indications [1]. Deregulation of kinase activity has also been implicated in various other diseases, ranging from inflammatory and autoimmune diseases [2] to neurological disorders [3]. However, indications for kinase-targeted drugs beyond cancer are lagging behind, with a single kinase inhibitor, Tofacitinib, receiving market approval for the treatment of rheumatoid arthritis [4].

Viruses depend on various host cellular kinases for their replication [5]. For example, phosphatidylinositol-4-kinase IIIβ (PI4KIIIβ), is an essential host factor for many viruses, including

enteroviruses, rhinoviruses and hepatitis C virus (HCV) [6]. The specific inhibition of the Raf/MEK/ERK mitogenic kinase cascade by a small molecule was shown to strongly impair the replication of all influenza virus A and B-types [7]. Phosphatidylinositol 3-kinase class II alpha (PI3K-C2A) likely plays a prominent role in the production of infectious human cytomegalovirus (HCMV) virions [8]. Using a combination of small molecule inhibitors and an RNA interference approach, it has been demonstrated that polo-like-kinase 1 activity is crucial for the replication of the hepatitis virus B (HBV) [9]. As these host kinases are required for the viral life cycle, they represent candidate therapeutic targets for antiviral therapy. Although toxicity might be an issue, the restriction of viral replication by targeting host factors is an attractive strategy, since it may confer a higher genetic barrier for the development of resistance than antiviral agents acting on viral factors. In addition, since many viruses rely on overlapping host factors for their life cycle, broad-spectrum antivirals can be developed by targeting cellular kinases [10].

In the past few years, our group has focused on cyclin G-associated kinase (GAK) as an antiviral drug target. GAK is a cellular serine/threonine kinase that plays a major role in clathrin-mediated membrane trafficking, which is dependent on the action of oligomeric clathrin and adaptor protein complexes (APs)

* Corresponding author.

E-mail address: steven.dejonghe@kuleuven.be (S. De Jonghe).¹ Present affiliation: Laboratory of Virology and Chemotherapy, Rega Institute for Medical Research, KU Leuven, Herestraat 49 - bus 1043, 3000 Leuven, Belgium.

[11,12]. These APs coordinate the recruitment and assembly of clathrin-coated vesicles (CCVs) as well as their coupling to cargo proteins [12]. GAK phosphorylates the μ subunits of AP-1 and AP-2, thereby initiating a conformational change and enhancing their binding to sorting signals (in the form of tyrosine- or dileucine-based motifs) within the cargo [13–15]. Moreover, GAK recruits clathrin and AP-2 to the plasma membrane and AP-1 to the *trans*-Golgi network (TGN) [15,16]. GAK also controls the uncoating of CCVs to recycle clathrin back to the cell surface [11–13,15,17]. GAK-dependent phosphorylation of APs has been implicated in the life cycle of multiple viruses including HCV and dengue virus (DENV) (*Flaviviridae* family) and the Ebola virus (EBOV) (*Filoviridae* family) [18–20].

We have previously reported the discovery of 3,6-disubstituted isothiazolo[4,3-*b*]pyridines as potent and selective GAK inhibitors with antiviral activity against HCV, DENV, EBOV and chikungunya virus (CHIKV) (*Togaviridae* family) [21,22]. Structural modifications revealed that an aromatic moiety, and particularly a 3,4-dimethoxyphenyl (compound **1**, Fig. 1), a 3,4,5-trimethoxyphenyl (compound **2**, Fig. 1) and a 3-methoxy-4-aminophenyl (compound **3**, Fig. 1) at position 6 in combination with morpholine at position 3 is optimal for potent GAK affinity [22]. The structure-activity relationship (SAR) at position 3 of the isothiazolo[4,3-*b*]pyridine skeleton was studied more exhaustively [21]. The introduction of different amines revealed that methyl substituted morpholine analogues (Fig. 1) are optimal for GAK binding (low nM Kd values) and for antiviral activity (low μ M EC₅₀ values) [21]. The insertion of other nitrogen containing nucleophiles [21,22] and oxygen nucleophiles (alkoxides) [23] yielded compounds with a greatly diminished GAK affinity. Similarly, introduction of carboxamide side chains reduced activity [23].

In the scheme established for the preparation of a library of 3,6-disubstituted isothiazolo[4,3-*b*]pyridines, 3,6-dibromoisothiazolo[4,3-*b*]pyridine **4** was synthesized as a key intermediate at a large scale [21–23]. Polyhalogenated heteroaromatics are attractive synthons in medicinal chemistry, as they allow for sequential palladium-catalyzed cross-coupling reactions, giving rise to a library of compounds with structural variety. In this manuscript, we describe our efforts to further explore the SAR of the isothiazolo[4,3-*b*]pyridine scaffold with respect to GAK inhibition, by performing hitherto unknown regioselective palladium-catalyzed cross-coupling reactions at the isothiazolo[4,3-*b*]pyridine skeleton.

2. Chemistry

The key intermediate 3,6-dibromoisothiazolo[4,3-*b*]pyridine **4** was resynthesized at a large scale, starting from commercially available 3-nitro-5-bromopyridine-2-carbonitrile in 4 steps, according to a known procedure [21–23].

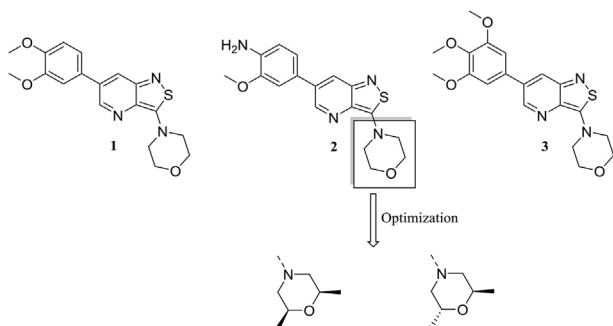


Fig. 1. Optimal substitution pattern of isothiazolo[4,3-*b*]pyridines as GAK inhibitors.

Aryl and heteroaryl groups were regioselectively introduced at position 3 of compound **4** by a Suzuki coupling using classical reaction conditions: Pd(PPh₃)₄ as the catalyst, an appropriate arylboronic acid (R₃B(OH)₂) and K₂CO₃ as the base in a mixture of dioxane and water. This furnished the desired products **5a–e** in yields ranging from 37% to 91% (Scheme 1). Moreover, rather than using the classical arylboronic acids, a Suzuki reaction with (*E*)-styrylboronic acid worked equally well, affording compound **5f**. Before the addition of the palladium catalyst, the mixture was degassed and air was replaced by a nitrogen atmosphere to prevent reaction of the catalyst with oxygen [24]. For the subsequent Suzuki coupling with 3,4-dimethoxyphenylboronic acid, the same reaction conditions were applied but longer reaction times (up to 24 h) were required to yield compounds **6a–f**. To prevent hydrolysis of the ester function of methyl 4-(6-bromoisothiazolo[4,3-*b*]pyridin-3-yl)benzoate **5g**, the second Suzuki coupling at position 6 was carried out in anhydrous conditions using potassium phosphate as a base and dioxane as the solvent, furnishing the desired product **6g** in moderate yield. The synthesis of the di-substituted-3,4-dimethoxyphenyl congener was done by using an excess of boronic acid (3 eq) and a longer reaction time (3 days) resulting in the formation of the desired product **6h**, albeit in a low yield.

The regiochemistry of the first Suzuki reaction was elucidated by a 2D NMR NOESY experiment (Fig. 2), using compound **6b** as a representative example. The clear NOE correlations between Ha – H5/H7 and Hb – H5/H7 confirmed that the 3,4-dimethoxyphenyl moiety is attached to position 6 of the isothiazolo[4,3-*b*]pyridine scaffold.

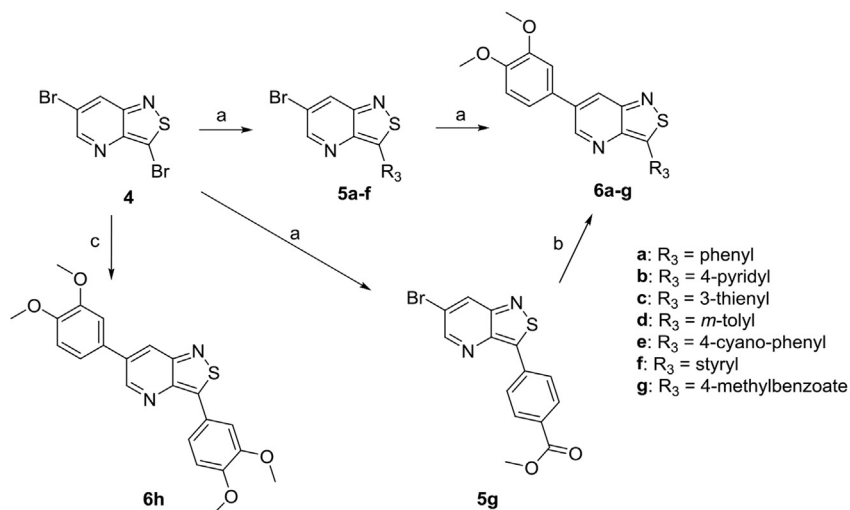
To introduce various aromatic and aliphatic alkene functionalities, a Sonogashira coupling reaction was applied according to a general protocol (Scheme 2). Compounds **7a–c** were isolated in good yields (59–99%) by using an appropriate acetylene derivative, bis(triphenylphosphine)palladium(II) dichloride (Pd(PPh₃)₂Cl₂) and copper iodide as the catalysts, triethylamine (TEA) as the base and THF as the solvent. In contrast to the Suzuki coupling, the reaction mixture was degassed and filled with argon, since using nitrogen gas consistently led to lower yields. In the last step, the Sonogashira coupling products **7a–c** were subjected to a Suzuki coupling with 3,4-dimethoxyphenylboronic acid using the classical reaction conditions (as in Scheme 1) yielding compounds **8a–c**.

To ensure the selectivity of the Sonogashira coupling at position 3, a NOESY spectrum of compound **8b** was recorded (Fig. 3). The observation of NOE contacts between Ha – H5/H7 and Hb – H5/H7 clearly indicated that the 3,4-dimethoxyphenyl ring is present at position 6 of the isothiazolo[4,3-*b*]pyridine scaffold.

The alkyne functionality of compound **8a** was reduced by catalytic hydrogenation using palladium on activated carbon yielding the corresponding alkane **9** in low yield (Scheme 3). Despite carrying out this reaction under 50 psi at room temperature, the reduction never fully achieved completion as a significant amount of alkene **6f** was present (61%). Interestingly, based on the vicinal coupling constant ³J of 16.4 Hz, this alkene turned out to be the thermodynamic *trans*-alkene, rather than the expected kinetic *cis*-alkene. In addition, the spectral data of compound **6f**, obtained either via the Suzuki reaction (Scheme 1) or the catalytic hydrogenation of alkyne **8a** (Scheme 3) were identical. It is possible that upon reduction of the *cis*-alkene to alkane, a rapid isomerisation occurred to the more thermodynamically stable product. Indeed, *cis-trans* isomerizations of alkenes during catalytic hydrogenation have been previously reported in literature [25,26].

3. GAK affinity studies

All compounds were tested for GAK binding affinity using the KINOMEScan™ platform, which quantitatively measures the ability



Scheme 1. Suzuki reactions on the isothiazolo[4,3-*b*]pyridine scaffold. *Reagents and conditions:* a) $R_3B(OH)_2$, K_2CO_3 , $Pd(PPh_3)_4$, dioxane/water, 100 °C; b) 3,4-dimethoxyphenylboronic acid, K_3PO_4 , $Pd(PPh_3)_4$, dioxane, 100 °C; c) 3,4-dimethoxyphenylboronic acid (3 eq), K_2CO_3 , $Pd(PPh_3)_4$, dioxane/water, 100 °C, 3 days.

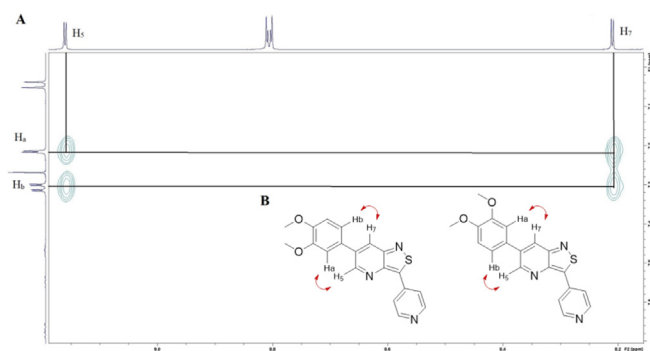


Fig. 2. A) NOESY spectrum of compound **6b**. B) Red arrows showing the spatial interaction between protons of the rotational isomers. (For interpretation of the references to colour in this figure legend, the reader is referred to the Web version of this article.)

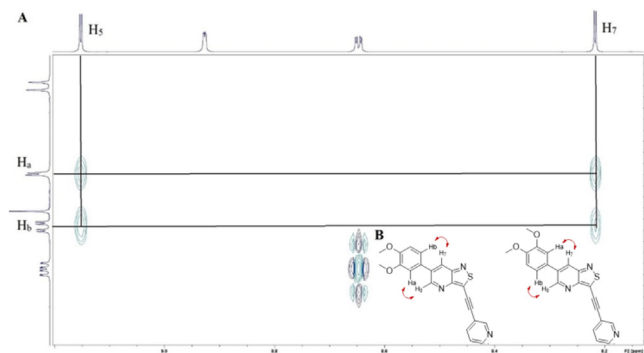
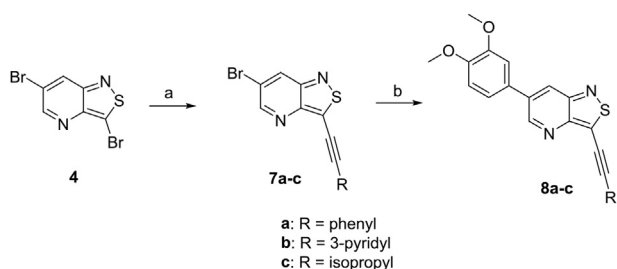
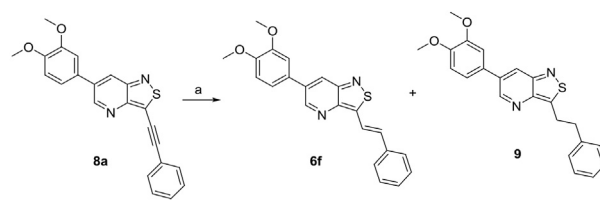


Fig. 3. A) NOESY spectrum of compound **8b**. B) Red arrows represent the spatial interaction between protons of the rotational isomers. (For interpretation of the references to colour in this figure legend, the reader is referred to the Web version of this article.)



Scheme 2. Sonogashira reactions on the isothiazolo[4,3-*b*]pyridine scaffold. *Reagents and conditions:* a) $RCCH$, CuI , $Pd(PPh_3)_2Cl_2$, TEA, THF, rt; b) $ArB(OH)_2$, K_2CO_3 , $Pd(PPh_3)_4$, H_2O , dioxane, 100 °C.

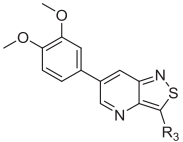
of a compound to compete with an immobilized active-site-directed ligand [27]. Previous research demonstrated that the presence of electron donating groups (e.g. methoxy, amino) at the phenyl moiety at position 6 of the isothiazolo[4,3-*b*]pyridine scaffold is essential for potent GAK affinity [21–23]. Because of the low cost of commercially available 3,4-dimethoxyphenylboronic acid and its high GAK potency (K_d of 52 nM), we selected the 6-(3,4-dimethoxyphenyl) congener **1** with a morpholino residue at position 3 as reference compound (Table 1). Substituting the

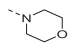
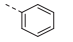
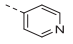
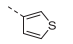
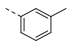
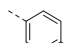
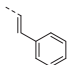
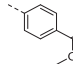
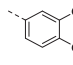
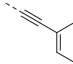
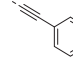
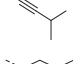
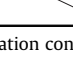


Scheme 3. Catalytic reduction of the alkyne moiety. *Reagents and conditions:* a) H_2 , Pd/C (10%), 50 psi, rt.

morpholine of compound **1** for different aromatic moieties, such as a phenyl (compound **6a**), pyridyl (compound **6b**) or thienyl ring (compound **6c**) resulted in a 10-fold drop in GAK binding affinity. In an effort to restore the potent GAK affinity, various phenyl substituted analogues were synthesized. The introduction of a methyl ester or a cyano functionality at position 4 of the phenyl ring, afforded compounds **6g** and **6e**, respectively, both of which completely lacked GAK affinity ($K_d > 30 \mu M$). In contrast, introducing an *m*-toluyl (compound **6d**) instead of the parent phenyl led to a marginally more active compound ($K_d = 0.4 \mu M$). The presence of a 3,4-dimethoxyphenyl residue at position 3 of the isothiazolo [4,3-*b*]pyridine scaffold (compound **6h**) resulted in a potent GAK

Table 1
SAR at position 3 of isothiazolo[4,3-*b*]pyridine.



Cmpd #	R ₃	K _d (μM) ^a
1		0.052
6a		0.77
6b		0.52
6c		0.86
6d		0.4
6e		>30
6f		2
6g		>30
6h		0.041
8a		>30
8b		7.6
8c		3.2
9		3.2

^a K_d = GAK dissociation constant. Values represent the average of two independent experiments.

ligand, displaying a K_d value of 41 nM.

Different spacers between the phenyl and the central isothiazolo[4,3-*b*]pyridine scaffold were also evaluated. The 3-styryl-isothiazolo[4,3-*b*]pyridine derivative (compound **6f**), having an ethenyl linker, was three fold less active as GAK binder than the corresponding 3-phenyl derivative. The presence of an alkyn linker afforded compound **8a**, which was completely devoid of GAK affinity (K_d > 30 μM). Substituting the phenyl moiety of compound **8a** for either a 3-pyridyl moiety (compound **8b**) or isopropyl group (compound **8c**) restored GAK affinity to a limited extent (K_d values of 7.6 μM and 3.2 μM, respectively). In order to increase the conformational flexibility, an analogue with a saturated ethyl linker (compound **9**) was also prepared, displaying a K_d value of 3.2 μM.

4. Molecular modeling

Among the 3-aryl substituted isothiazolo[4,3-*b*]pyridines, compound **6h** is the only congener endowed with potent GAK

affinity. To explain the improved GAK affinity of compound **6h** compared to the 3-phenyl analogue **6a**, a docking study was performed using Autodock Vina. Docking started from the known co-crystal structure of GAK and compound **2**, displaying a K_d value of 9 nM [22]. The binding mode of both compounds **6a** and **6h** was compared, while compound **2** was used as control. The three compounds (**2**, **6a** and **6h**) are structurally very similar, and hence, they bind in a similar way into the ATP binding site of GAK, with mainly hydrophobic interactions between GAK and the inhibitor. However, compound **6h** prefers an orientation facilitating a hydrogen bond between one of the methoxy groups of the 3,4-dimethoxyphenyl residue at position 3 with the Lys69 side chain. In addition, this orientation creates hydrogen bond opportunities between the two methoxy groups of the 3,4-dimethoxyphenyl moiety at position 6 with the Arg44 side chain thereby anchoring the inhibitor and thus explaining its improved GAK affinity compared to compound **6a**. The resulting top orientation of **6h** superimposed on compound **2** is shown in Fig. 4.

5. Antiviral evaluation

GAK dependent phosphorylation of APs is required for the life cycle of DENV and GAK inhibitors show activity against DENV [19,21,28]. All compounds arising from the current SAR study were therefore evaluated for their antiviral activity. Huh7 cells infected with DENV2 (New Guinea C strain) harboring a luciferase reporter [29,30] were treated with each compound for 48 h. Fifty percent effective concentration (EC₅₀) values were measured via luciferase assays and half-maximal cytotoxic concentration (CC₅₀) values were measured in the same cell culture wells via AlamarBlue assays. In line with the poor GAK affinity of most of the congeners, no antiviral activity was detected up to a concentration of 10 μM. Nevertheless, the most potent isothiazolo[4,3-*b*]pyridine (compound **6h**) displayed modest antiviral activity with an EC₅₀ of 3.35 μM, with a minimal effect on cellular viability at the concentrations tested (Fig. 5).

6. Conclusion

In this manuscript, the synthesis of hitherto unknown 3-*C*-linked isothiazolo[4,3-*b*]pyridines by the application of regioselective Suzuki and Sonogashira cross-coupling reactions is described. Evaluation of the compounds as potential GAK ligands clearly demonstrated that appropriate substitution of the phenyl moiety at position 3 improved GAK affinity. The most potent congener in this series was the 3-(3,4-dimethoxyphenyl) derivative (compound **6h**), which had a strong affinity for GAK (K_d = 42 nM). Compound **6h** is also endowed with moderate anti-DENV activity

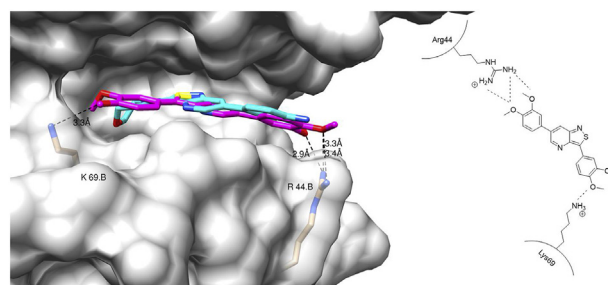


Fig. 4. Autodock Vina docking of inhibitor **6h** (purple carbons) superimposed on the X-ray of compound **2** (cyan carbons). Schematic drawing of interactions of **6h**. (For interpretation of the references to colour in this figure legend, the reader is referred to the Web version of this article.)

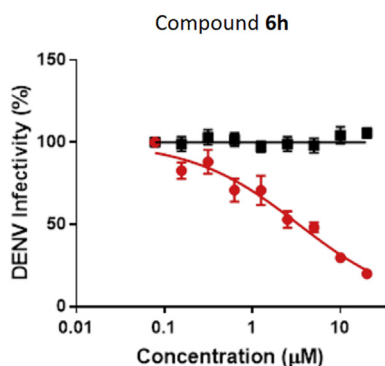


Fig. 5. Inhibition of DENV infection by compound **6h**. Cell viability (black) and dose response of DENV infection (red) to compound **6h** measured by luciferase and alamarBlue assays, respectively, 48 h after infection. Data are plotted relative to vehicle control. Shown is a representative experiment from at least 2 conducted, each with 6 biological replicates; shown are means \pm SD. (For interpretation of the references to colour in this figure legend, the reader is referred to the Web version of this article.)

with an EC_{50} value of 3.35 μ M. Moreover, a docking study showed that the 3,4-dimethoxyphenyl substituent at position 3 of compound **6h** forms a hydrogen bond with Lys44, thereby optimizing its orientation in the ATP-binding site. It allows the formation of additional hydrogen bonds between the 3,4-dimethoxyphenyl moiety at position 6 of the scaffold and GAK, explaining the potent binding affinity of compound **6h**. Since a large number of arylboronic acids are available, this finding paves the way for the synthesis of a library of 3-(hetero)aryl isothiazolo[4,3-*b*]pyridines to further increase GAK affinity and antiviral activity.

7. Experimental section

7.1. Chemistry

For all reactions, analytical grade solvents were used. All moisture-sensitive reactions were carried out in oven-dried glassware (125 °C). ^1H and ^{13}C NMR spectra were recorded on a Bruker Avance 300 MHz instrument (^1H NMR, 300 MHz; ^{13}C NMR, 75 MHz), 500 MHz instrument (^1H NMR, 500 MHz; ^{13}C NMR, 125 MHz) or a 600 MHz instrument (^1H NMR, 600 MHz; ^{13}C NMR, 150 MHz), using tetramethylsilane as internal standard for ^1H NMR spectra and DMSO- d_6 (39.5 ppm) or CDCl_3 (77.2 ppm) for ^{13}C NMR spectra. Abbreviations used are s = singlet, d = doublet, t = triplet, q = quartet, m = multiplet, b = broad. Coupling constants are expressed in Hz. High resolution mass spectra were acquired on a quadrupole orthogonal acceleration time-of-flight mass spectrometer (Synapt G2 HDMS, Waters, Milford, MA). Samples were infused at 3 $\mu\text{L}/\text{min}$ and spectra were obtained in positive or negative ionization mode with a resolution of 15000 (FWHM) using leucine enkephalin as lock mass. Precoated aluminum sheets (Fluka silica gel/TLC-cards, 254 nm) were used for TLC. Column chromatography was performed on silica gel 0.060–0.200 mm, 60 Å (Acros Organics). Purity of final compounds was verified to be >95% by HPLC analysis. HPLC conditions to assess purity were as follows: Shimadzu HPLC equipped with a LC-20AT pump, DGU-20A5 degasser, and a SPD-20A UV-VIS detector; Symmetry C18 column (5 μm , 4.6 mm \times 150 mm); gradient elution of $\text{H}_2\text{O}/\text{CH}_3\text{CN}$ from 95/5 or 70/30 to 5/95 over 25 min; flow rate 1 mL/min; wavelength, UV 254 nm. Preparative HPLC purifications were performed using a Phenomenex Gemini 110A column (C18, 10 μm , 21.2 mm \times 250 mm).

7.1.1. Suzuki coupling at position 3 of the isothiazolo[4,3-*b*]pyridine scaffold

7.1.1.1. General procedure. To a mixture of dioxane/water (in a ratio of 4:1) were added 3,6-dibromoisothiazolo[4,3-*b*]pyridine **4**, an appropriate boronic acid (1.2 equiv) and potassium carbonate (2 equiv). The mixture was degassed and filled with nitrogen. Subsequently, $\text{Pd}(\text{PPh}_3)_4$ (1 mol % - 10 mol%) was added. The mixture was degassed a second time, filled with nitrogen and stirred at 100 °C for the time specified. After completion of the reaction, solvents were evaporated. The following compounds were made according to this procedure.

7.2. 6-Bromo-3-phenylisothiazolo[4,3-*b*]pyridine (**5a**)

This product was prepared from 3,6-dibromoisothiazolo[4,3-*b*]pyridine **4** (200 mg, 0.68 mmol), and phenylboronic acid (100 mg, 0.82 mmol) and stirred for 3 h. The crude residue was purified by silica gel flash column chromatography (using a mixture of heptane/ethyl acetate in a ratio of 90:10 as a mobile phase), yielding the title compound (180 mg, 91%).

^1H NMR (300 MHz, DMSO) δ 8.92 (d, $J = 2.1$ Hz, 1H), 8.66 (d, $J = 2.1$ Hz, 1H), 8.24–8.16 (m, 2H), 7.65–7.52 (m, 3H) ppm.

HRMS m/z $[\text{M}+\text{H}]^+$ calcd for $\text{C}_{12}\text{H}_7\text{BrN}_2\text{S}_1$: 290.95865, found 290.9587.

7.3. 6-Bromo-3-(pyridin-4-yl)isothiazolo[4,3-*b*]pyridine (**5b**)

This product was prepared from 3,6-dibromoisothiazolo[4,3-*b*]pyridine **4** (200 mg, 0.68 mmol), and 4-pyridinylboronic acid (101 mg, 0.82 mmol) and stirred for 4 h. The crude residue was purified by silica gel flash column chromatography (using a mixture of dichloromethane/ethyl acetate in a ratio of 90:10 as a mobile phase), yielding the title compound (107 mg, 54%).

^1H NMR (300 MHz, CDCl_3) δ 8.85 (d, $J = 2.1$ Hz, 1H), 8.81 (dd, $J = 4.6, 1.6$ Hz, 2H), 8.36 (d, $J = 2.1$ Hz, 1H), 8.07 (dd, $J = 4.6, 1.6$ Hz, 2H) ppm.

HRMS m/z $[\text{M}+\text{H}]^+$ calcd for $\text{C}_{11}\text{H}_6\text{BrN}_3\text{S}_1$: 291.9539, found: 291.9539.

7.4. 6-Bromo-3-(thiophen-3-yl)isothiazolo[4,3-*b*]pyridine (**5c**)

This product was prepared from 3,6-dibromoisothiazolo[4,3-*b*]pyridine **4** (200 mg, 0.68 mmol), and 3-thienylboronic acid (105 mg, 0.82 mmol) and stirred for 4 h. The crude residue was purified by silica gel flash column chromatography (using a mixture of dichloromethane/ethyl acetate in a ratio of 90:10 as a mobile phase), yielding the title compound (100 mg, 49%).

^1H NMR (300 MHz, DMSO) δ 8.90 (d, $J = 2.1$ Hz, 1H), 8.68–8.58 (m, 2H), 7.93–7.79 (m, 2H) ppm.

^{13}C NMR (75 MHz, DMSO) δ 153.31, 151.78, 131.29, 131.01, 129.30, 128.38, 126.77, 126.70, 121.12, 120.46 ppm.

HRMS m/z $[\text{M}+\text{H}]^+$ calcd for $\text{C}_{11}\text{H}_6\text{BrN}_3\text{S}_1$: 291.9539, found: 291.9539.

7.5. 6-Bromo-3-(*m*-tolyl)isothiazolo[4,3-*b*]pyridine (**5d**)

This product was prepared from 3,6-dibromoisothiazolo[4,3-*b*]pyridine **4** (75 mg, 0.26 mmol), and *m*-tolylboronic acid (42 mg, 0.31 mmol) and stirred overnight. The crude residue was purified by silica gel flash column chromatography (using a mixture of heptane/ethyl acetate in a ratio of 97:3 as a mobile phase), yielding the title compound (37 mg, 47%).

^1H NMR (300 MHz, CDCl_3) δ 8.77 (d, $J = 2.0$ Hz, 1H), 8.27 (d, $J = 2.1$ Hz, 1H), 7.98–7.80 (m, 2H), 7.47–7.37 (m, 1H), 7.34–7.26 (m, 1H), 2.46 (s, 3H) ppm.

7.6. 4-(6-Bromoisothiazolo[4,3-*b*]pyridin-3-yl)benzotrile (**5e**)

This product was prepared from 3,6-dibromoisothiazolo[4,3-*b*]pyridine **4** (50 mg, 0.17 mmol), and 4-cyanophenylboronic acid (29 mg, 0.20 mmol) and stirred overnight. The crude residue was purified by silica gel flash column chromatography (using a mixture of heptane/ethyl acetate in a ratio of 90:10 as a mobile phase), yielding the title compound (20 mg, 37%).

^1H NMR (300 MHz, CDCl_3) δ 8.83 (d, $J = 2.1$ Hz, 1H), 8.35 (d, $J = 2.1$ Hz, 1H), 8.33–8.30 (m, 2H), 7.86–7.78 (m, 2H) ppm.

7.7. (*E*)-6-Bromo-3-styrylisothiazolo[4,3-*b*]pyridine (**5f**)

This product was prepared from 3,6-dibromoisothiazolo[4,3-*b*]pyridine **4** (100 mg, 0.34 mmol), and (*E*)-styrylboronic acid (105 mg, 0.82 mmol) and stirred overnight. The crude residue was purified by silica gel flash column chromatography (using a mixture of heptane/acetone in a ratio of 90:10 as a mobile phase), yielding the title compound (45 mg, 42%).

^1H NMR (300 MHz, CDCl_3) δ 8.74 (d, $J = 2.1$ Hz, 1H), 8.26 (d, $J = 2.1$ Hz, 1H), 7.82 (d, $J = 16.4$ Hz, 1H), 7.71 (d, $J = 16.7$ Hz, 1H), 7.67–7.64 (m, 2H), 7.48–7.33 (m, 3H) ppm.

^{13}C NMR (151 MHz, CDCl_3) δ 160.79, 156.30, 150.57, 149.77, 149.61, 144.20, 136.15, 136.07, 135.26, 129.83, 129.08, 128.87, 127.22, 125.02, 120.09, 115.78, 111.73, 110.41, 56.03 ppm.

HRMS m/z $[\text{M}+\text{H}]^+$ calcd for $\text{C}_{11}\text{H}_6\text{Br}_1\text{N}_3\text{S}_1$: 316.9743, found: 316.9778.

7.8. Methyl 4-(6-bromoisothiazolo[4,3-*b*]pyridin-3-yl)benzoate (**5g**)

This product was prepared from 3,6-dibromoisothiazolo[4,3-*b*]pyridine **4** (100 mg, 0.34 mmol), and 3-methoxycarbonylphenylboronic acid (74 mg, 0.41 mmol) and stirred overnight. The crude residue was purified by silica gel flash column chromatography (using a mixture of heptane/acetone in a ratio of 95:5 as a mobile phase), yielding the title compound (60 mg, 51%).

^1H NMR (300 MHz, CDCl_3) δ 8.83 (d, $J = 2.1$ Hz, 1H), 8.33 (d, $J = 2.1$ Hz, 1H), 8.27–8.17 (m, 4H), 3.97 (s, 3H) ppm.

HRMS m/z $[\text{M}+\text{H}]^+$ calcd for $\text{C}_{14}\text{H}_9\text{Br}_1\text{N}_2\text{O}_2\text{S}_1$: 348.9641, found: 348.9637.

7.8.1. Sonogashira coupling at position 3 of the isothiazolo[4,3-*b*]pyridine scaffold

7.8.1.1. General procedure. To a solution of 3,6-dibromoisothiazolo[4,3-*b*]pyridine **4** in dry THF were added an appropriate acetylene derivative (0.95 eq), triethylamine (3 eq), CuI (1 mol%) and Pd(PPh₃)₂Cl₂ (1 mol%). The mixture was degassed and filled with argon three times, and stirred at room temperature overnight. After disappearance of the starting material, the volatiles were evaporated *in vacuo* and the crude residue was purified by silica gel flash chromatography. The following compounds were made according to this procedure.

7.9. 6-Bromo-3-(phenylethynyl)isothiazolo[4,3-*b*]pyridine (**7a**)

This product was prepared from 3,6-dibromoisothiazolo[4,3-*b*]pyridine **4** (100 mg, 0.34 mmol), and phenylacetylene (33 mg, 0.32 mmol) and stirred for 3 h. The crude residue was purified by silica gel flash column chromatography (using a mixture of heptane/ethyl acetate in a ratio of 95:5 as a mobile phase), yielding the title compound (86 mg, 80%).

^1H NMR (300 MHz, DMSO) δ 8.94 (d, $J = 2.0$ Hz, 1H), 8.73 (d, $J = 2.0$ Hz, 1H), 7.73–7.44 (m, 5H) ppm.

^{13}C NMR (75 MHz, CDCl_3) δ 155.20, 153.54, 152.76, 147.00, 146.22, 132.25, 131.57, 130.18, 128.83, 121.97, 121.11, 109.30 ppm.

HRMS m/z $[\text{M}+\text{H}]^+$ calcd for $\text{C}_{14}\text{H}_7\text{Br}_1\text{N}_2\text{S}_1$: 314.9587, found: 314.9586.

7.10. 6-Bromo-3-(pyridin-3-ylethynyl)isothiazolo[4,3-*b*]pyridine (**7b**)

This product was prepared from 3,6-dibromoisothiazolo[4,3-*b*]pyridine **4** (100 mg, 0.34 mmol), and 3-ethynylpyridine (33 mg, 0.32 mmol) and stirred overnight. The crude residue was purified by silica gel flash column chromatography (using a mixture of heptane/acetone in a ratio of 60:40 as a mobile phase), yielding the title compound (60 mg, 59%).

^1H NMR (300 MHz, CDCl_3) δ 8.92–8.88 (m, 1H), 8.84 (d, $J = 2.1$ Hz, 1H), 8.67–8.62 (m, 1H), 8.35 (d, $J = 2.1$ Hz, 1H), 7.98–7.93 (m, 1H), 7.39–7.33 (m, 1H) ppm.

^{13}C NMR (75 MHz, CDCl_3) δ 155.21, 153.55, 153.18, 152.65, 150.32, 139.03, 131.67, 123.46, 121.26, 119.28, 105.22, 79.79 ppm.

HRMS m/z $[\text{M}+\text{H}]^+$ calcd for $\text{C}_{13}\text{H}_6\text{Br}_1\text{N}_3\text{S}_1$: 315.9539, found: 315.9536.

7.11. 6-Bromo-3-(3-methylbut-1-yn-1-yl)isothiazolo[4,3-*b*]pyridine (**7c**)

This product was prepared from 3,6-dibromoisothiazolo[4,3-*b*]pyridine **4** (100 mg, 0.34 mmol), and 3-methyl-1-butyne (23 mg, 0.32 mmol) and stirred overnight. The crude residue was purified by silica gel flash column chromatography (using a mixture of heptane/ethyl acetate in a ratio of 90:10 as a mobile phase), yielding the title compound (95 mg, 99%).

^1H NMR (300 MHz, CDCl_3) δ 8.77 (d, $J = 2.1$ Hz, 1H), 8.28 (d, $J = 2.1$ Hz, 1H), 3.04 (hept, $J = 6.9$ Hz, 1H), 1.38 (s, 3H), 1.36 (s, 3H) ppm.

HRMS m/z $[\text{M}+\text{H}]^+$ calcd for $\text{C}_{11}\text{H}_9\text{Br}_1\text{N}_2\text{S}_1$: 280.9743, found: 280.9743.

7.11.1. Suzuki coupling at position 6 of the isothiazolo[4,3-*b*]pyridine scaffold

7.11.1.1. General procedure. To a mixture of dioxane/water (in a ratio of 4:1) were added the appropriate 3-substituted-6-bromoisothiazolo[4,3-*b*]pyridine analogue **5a-f**, 3,4-dimethoxyphenylboronic acid (1.2 equiv) and potassium carbonate (2 equiv). The mixture was degassed, filled with nitrogen and Pd(PPh₃)₄ (1 mol% - 10 mol%) was added. The mixture was degassed a second time, filled with nitrogen and stirred at 100 °C. After completion of the reaction, the solvents were evaporated *in vacuo*. The crude residue was purified by silica gel flash chromatography and, when needed, further purified by RP-HPLC yielding the title compounds.

7.12. 6-(3,4-Dimethoxyphenyl)-3-phenylisothiazolo[4,3-*b*]pyridine (**6a**)

The title compound was prepared from 6-bromo-3-phenylisothiazolo[4,3-*b*]pyridine **5a** (100 mg, 0.34 mmol). The crude residue was purified by silica gel flash column chromatography (using a mixture of heptane/ethyl acetate in a ratio of 90:10 as a mobile phase), yielding the title compound (60 mg, 59%).

^1H NMR (300 MHz, DMSO) δ 9.29 (d, $J = 2.2$ Hz, 1H), 8.45 (d, $J = 2.2$ Hz, 1H), 8.35–8.15 (m, 2H), 7.74–7.32 (m, 5H), 7.12 (d, $J = 8.9$ Hz, 1H), 3.91 (s, 3H), 3.84 (s, 3H) ppm.

^{13}C NMR (75 MHz, DMSO) δ 161.23, 156.78, 151.83, 149.80, 149.52, 142.87, 134.99, 130.26, 129.98, 129.47, 128.72, 128.23, 124.51, 120.13, 112.41, 111.12, 55.88, 55.79 ppm.

HRMS m/z $[M+H]^+$ calcd for $C_{20}H_{16}N_2O_2S_1$: 349.1005, found: 349.1006.

7.13. 6-(3,4-Dimethoxyphenyl)-3-(pyridin-4-yl)isothiazolo[4,3-*b*]pyridine (**6b**)

The title compound was prepared from 6-bromo-3-(pyridin-4-yl)isothiazolo[4,3-*b*]pyridine **5b** (107 mg, 0.37 mmol). The crude residue was purified by silica gel flash column chromatography (using a mixture of dichloromethane/acetone in a ratio of 80:20 as a mobile phase), yielding the title compound (67 mg, 52%).

1H NMR (300 MHz, $CDCl_3$) δ 9.16 (d, $J = 2.1$ Hz, 1H), 8.83–8.79 (m, 2H), 8.21 (d, $J = 2.1$ Hz, 1H), 8.14 (dd, $J = 4.6, 1.5$ Hz, 2H), 7.31 (dd, $J = 8.3, 2.1$ Hz, 1H), 7.22 (d, $J = 2.0$ Hz, 1H), 7.05 (d, $J = 8.3$ Hz, 1H), 4.00 (s, 3H), 3.97 (s, 3H) ppm.

^{13}C NMR (151 MHz, $CDCl_3$) δ 158.43, 157.04, 152.36, 150.77, 149.98, 149.70, 144.09, 137.27, 136.00, 129.37, 125.18, 122.00, 120.17, 111.79, 110.36, 56.05.

HRMS m/z $[M+H]^+$ calcd for $C_{19}H_{15}N_3O_2S_1$: 350.0958, found: 350.0955.

7.14. 6-(3,4-Dimethoxyphenyl)-3-(thiophen-3-yl)isothiazolo[4,3-*b*]pyridine (**6c**)

The title compound was prepared from 6-bromo-3-(thiophen-3-yl)isothiazolo[4,3-*b*]pyridine **5c** (70 mg, 0.24 mmol). The crude residue was purified by silica gel flash column chromatography (using a mixture of dichloromethane/ethyl acetate in a ratio of 80:20 as a mobile phase), yielding the title compound (50 mg, 59%).

1H NMR (300 MHz, DMSO) δ 9.26 (d, $J = 2.0$ Hz, 1H), 8.71–8.62 (m, 1H), 8.41 (d, $J = 2.0$ Hz, 1H), 7.99–7.89 (m, 1H), 7.89–7.79 (m, 1H), 7.56–7.44 (m, 2H), 7.12 (d, $J = 8.9$ Hz, 1H), 3.91 (s, 3H), 3.84 (s, 3H) ppm.

^{13}C NMR (75 MHz, DMSO) δ 156.38, 156.29, 151.52, 149.77, 149.51, 142.75, 135.16, 129.90, 128.79, 128.16, 126.78, 126.00, 124.39, 120.14, 112.40, 111.13, 55.87, 55.78 ppm.

HRMS m/z $[M+H]^+$ calcd for $C_{18}H_{14}N_2O_2S_2$: 355.0569, found: 355.0569.

7.15. 6-(3,4-Dimethoxyphenyl)-3-(*m*-tolyl)isothiazolo[4,3-*b*]pyridine (**6d**)

The title compound was prepared from 6-bromo-3-(*m*-tolyl)isothiazolo[4,3-*b*]pyridine **5d** (35 mg, 0.11 mmol). The crude residue was purified by silica gel flash column chromatography (using a mixture of heptane/acetone in a ratio of 90:10 as a mobile phase), yielding the title compound (17 mg, 43%).

1H NMR (300 MHz, $CDCl_3$) δ 9.11 (d, $J = 2.1$ Hz, 1H), 8.16 (d, $J = 2.1$ Hz, 1H), 8.02–7.95 (m, 2H), 7.48–7.41 (m, 1H), 7.30 (dd, $J = 8.3, 2.1$ Hz, 2H), 7.22 (d, $J = 2.1$ Hz, 1H), 7.03 (d, $J = 8.3$ Hz, 1H), 3.99 (s, 3H), 3.96 (s, 3H), 2.49 (s, 3H) ppm.

^{13}C NMR (75 MHz, $CDCl_3$) δ 163.02, 157.10, 151.46, 150.16, 150.02, 143.72, 139.25, 135.73, 131.00, 130.53, 130.18, 129.42, 129.28, 125.92, 125.34, 120.39, 112.20, 110.87, 56.35, 21.78 ppm.

HRMS m/z $[M+H]^+$ calcd for $C_{21}H_{18}N_2O_2S_1$: 363.1162, found: 363.1158.

7.16. 4-(6-(3,4-Dimethoxyphenyl)isothiazolo[4,3-*b*]pyridin-3-yl)benzonitrile (**6e**)

The title compound was prepared from 4-(6-bromoisothiazolo[4,3-*b*]pyridin-3-yl)benzonitrile **5e** (20 mg, 0.063 mmol). The crude residue was purified by silica gel flash column chromatography (using a mixture of heptane/acetone in a ratio of 97:3 as a mobile phase). The residue was further purified by RP-HPLC

(eluting with a mixture of acetonitrile/water using a gradient from 35/65 to 95/5 over 35 min) yielding the title compound (4 mg, 17%).

1H NMR (600 MHz, $CDCl_3$) δ 9.15 (d, $J = 2.1$ Hz, 1H), 8.43–8.34 (m, 2H), 8.21 (d, $J = 2.1$ Hz, 1H), 7.90–7.79 (m, 2H), 7.31 (dd, $J = 8.3, 2.2$ Hz, 1H), 7.22 (d, $J = 2.1$ Hz, 1H), 7.05 (d, $J = 8.3$ Hz, 1H), 4.00 (s, 3H), 3.97 (s, 3H) ppm.

^{13}C NMR (151 MHz, $CDCl_3$) δ 159.19, 157.08, 152.31, 150.02, 149.73, 143.74, 136.02, 134.55, 132.91, 129.39, 128.74, 125.23, 120.19, 118.46, 113.01, 111.82, 110.39, 56.08 ppm.

HRMS m/z $[M+H]^+$ calcd for $C_{21}H_{15}N_3O_2S_1$: 374.0958, found: 374.0950.

7.17. (E)-6-(3,4-Dimethoxyphenyl)-3-styrylisothiazolo[4,3-*b*]pyridine (**6f**)

The title compound was prepared from (E)-6-bromo-3-styrylisothiazolo[4,3-*b*]pyridine **5f** (45 mg, 0.14 mmol). The crude residue was purified by silica gel flash column chromatography (using a mixture of heptane/acetone in a ratio of 90:10 as a mobile phase), yielding the title compound (28 mg, 53%).

1H NMR (600 MHz, $CDCl_3$) δ 9.03 (d, $J = 2.1$ Hz, 1H), 8.12 (d, $J = 2.1$ Hz, 1H), 7.87 (d, $J = 16.4$ Hz, 1H), 7.71 (d, $J = 16.4$ Hz, 1H), 7.67–7.64 (m, 2H), 7.43–7.40 (m, 2H), 7.37–7.33 (m, 1H), 7.28 (dd, $J = 8.3, 2.2$ Hz, 1H), 7.20 (d, $J = 2.1$ Hz, 1H), 7.02 (d, $J = 8.3$ Hz, 1H), 3.99 (s, 3H), 3.96 (s, 3H) ppm.

^{13}C NMR (151 MHz, $CDCl_3$) δ 160.79, 156.30, 150.57, 149.77, 149.61, 144.20, 136.15, 136.07, 135.26, 129.83, 129.08, 128.87, 127.22, 125.02, 120.09, 115.78, 111.73, 110.41, 56.03 ppm.

HRMS m/z $[M+H]^+$ calcd for $C_{22}H_{18}N_2O_2S_1$: 375.1162, found: 375.1159.

7.18. Methyl 4-(6-(3,4-dimethoxyphenyl)isothiazolo[4,3-*b*]pyridin-3-yl)benzoate (**6g**)

To a solution of methyl 4-(6-bromoisothiazolo[4,3-*b*]pyridin-3-yl)benzoate **5g** (60 mg, 0.17 mmol) in dioxane (5 mL) were added 3,4-dimethoxyphenylboronic acid (37 mg, 0.20 mmol) and potassium phosphate tribasic (72 mg, 0.34 mmol). The mixture was degassed, filled with nitrogen and Pd(PPh_3)₄ (20 mg, 0.017 mmol) was added. The mixture was degassed a second time, filled with nitrogen and stirred at 100 °C overnight. After completion, the solvents were evaporated in *vacuo* and crude residue was purified by silica gel flash column chromatography (using a mixture of heptane/acetone in a ratio of 99:1 as a mobile phase), yielding the title compound (22 mg, 32%).

1H NMR (300 MHz, $CDCl_3$) δ 9.15 (d, $J = 2.1$ Hz, 1H), 8.34–8.30 (m, 2H), 8.24–8.18 (m, 3H), 7.31 (dd, $J = 8.3, 2.1$ Hz, 1H), 7.22 (d, $J = 2.0$ Hz, 1H), 7.04 (d, $J = 8.3$ Hz, 1H), 4.00 (s, 3H), 3.98–3.96 (m, $J = 1.4$ Hz, 6H) ppm.

^{13}C NMR (75 MHz, $CDCl_3$) δ 166.79, 160.95, 157.30, 152.19, 150.31, 150.09, 144.02, 136.10, 134.78, 131.27, 130.70, 129.96, 128.51, 125.47, 120.48, 112.25, 110.88, 56.38, 52.58 ppm.

HRMS m/z $[M+H]^+$ calcd for $C_{22}H_{18}N_2O_4S_1$: 407.1060, found: 407.1052.

7.19. 6-(3,4-Dimethoxyphenyl)-3-(phenylethynyl)isothiazolo[4,3-*b*]pyridine (**8a**)

The title compound was prepared from 6-bromo-3-(phenylethynyl)isothiazolo[4,3-*b*]pyridine **7a** (80 mg, 0.27 mmol). The crude residue was purified by silica gel flash column chromatography (using a mixture of heptane/acetone in a ratio of 90:10 as a mobile phase). The residue was further purified by RP-HPLC (eluting with a mixture of acetonitrile/water using a gradient

from 55/45 to 95/5 over 15 min) yielding the title compound (60 mg, 60%).

^1H NMR (300 MHz, CDCl_3) δ 9.11 (d, $J = 2.0$ Hz, 1H), 8.18 (d, $J = 2.0$ Hz, 1H), 7.74–7.58 (m, 2H), 7.47–7.31 (m, 3H), 7.27 (dd, $J = 8.3$, 2.1 Hz, 1H), 7.18 (d, $J = 2.0$ Hz, 1H), 7.01 (d, $J = 8.3$ Hz, 1H), 3.97 (s, 3H), 3.95 (s, 4H) ppm.

^{13}C NMR (75 MHz, CDCl_3) δ 155.59, 152.36, 150.38, 150.12, 147.88, 144.78, 136.48, 132.21, 129.91, 128.77, 127.53, 125.65, 122.34, 120.57, 112.28, 111.00, 108.35, 56.41, 56.38 ppm.

HRMS m/z $[\text{M}+\text{H}]^+$ calcd for $\text{C}_{22}\text{H}_{16}\text{N}_2\text{O}_2\text{S}_1$: 373.1005, found: 373.1007.

7.20. 6-(3,4-Dimethoxyphenyl)-3-(pyridin-3-ylethynyl)isothiazolo[4,3-*b*]pyridine (**8b**)

The title compound was prepared from 6-bromo-3-(pyridin-3-ylethynyl)isothiazolo[4,3-*b*]pyridine **7b** (60 mg, 0.18 mmol). The crude residue was purified by silica gel flash column chromatography (using a mixture of heptane/acetone in a ratio of 60:40 as a mobile phase), yielding the title compound (40 mg, 60%).

^1H NMR (300 MHz, CDCl_3) δ 9.16 (d, $J = 2.1$ Hz, 1H), 8.95–8.91 (m, 1H), 8.65 (dd, $J = 4.9$, 1.6 Hz, 1H), 8.22 (d, $J = 2.1$ Hz, 1H), 8.01–7.95 (m, 1H), 7.37 (ddd, $J = 7.9$, 4.9, 0.8 Hz, 1H), 7.30 (dd, $J = 8.3$, 2.1 Hz, 1H), 7.20 (d, $J = 2.0$ Hz, 1H), 7.04 (d, $J = 8.4$ Hz, 1H), 4.00 (s, 3H), 3.97 (s, 3H) ppm.

^{13}C NMR (151 MHz, CDCl_3) δ 155.27, 152.48, 152.34, 150.02, 149.81, 149.72, 147.72, 143.30, 138.69, 136.33, 129.36, 125.40, 123.14, 120.26, 119.26, 111.80, 110.45, 104.05, 56.07 ppm.

HRMS m/z $[\text{M}+\text{H}]^+$ calcd for $\text{C}_{21}\text{H}_{15}\text{N}_3\text{O}_2\text{S}_1$: 374.0958, found: 374.0952.

7.21. 6-(3,4-Dimethoxyphenyl)-3-(3-methylbut-1-yn-1-yl)isothiazolo[4,3-*b*]pyridine (**8c**)

The title compound was prepared from 6-bromo-3-(pyridin-3-ylethynyl)isothiazolo[4,3-*b*]pyridine **7c** (95 mg, 0.34 mmol). The crude residue was purified by silica gel flash column chromatography (using a mixture of heptane/acetone in a ratio of 90:10 as a mobile phase), yielding the title compound (64 mg, 56%).

^1H NMR (300 MHz, CDCl_3) δ 9.08 (d, $J = 2.1$ Hz, 1H), 8.15 (d, $J = 2.1$ Hz, 1H), 7.26 (dd, $J = 8.3$, 2.1 Hz, 1H), 7.17 (d, $J = 2.1$ Hz, 1H), 7.02 (d, $J = 8.4$ Hz, 1H), 3.98 (s, 3H), 3.95 (s, 3H), 3.05 (hept, $J = 6.9$ Hz, 1H), 1.40 (s, 3H), 1.37 (s, 3H) ppm.

^{13}C NMR (75 MHz, CDCl_3) δ 155.46, 151.97, 150.28, 150.06, 147.69, 145.86, 136.20, 129.96, 125.59, 120.48, 116.13, 112.24, 110.96, 68.28, 56.34, 22.74, 22.53 ppm.

HRMS m/z $[\text{M}+\text{H}]^+$ calcd for $\text{C}_{19}\text{H}_{18}\text{N}_2\text{O}_2\text{S}_1$: 339.1162, found: 339.1164.

7.22. 6-(3,4-Dimethoxyphenyl)-3-phenethylisothiazolo[4,3-*b*]pyridine (**9**)

To a solution of 6-(3,4-dimethoxyphenyl)-3-(phenylethynyl)isothiazolo[4,3-*b*]pyridine **8a** (50 mg, 0.13 mmol) in dioxane (10 mL) was added palladium on activated carbon (10% Pd, 50% wet with water, 50 mg). The mixture was degassed, filled with hydrogen gas and stirred at 60 psi at room temperature for 7 h. After disappearance of the starting material, the palladium on carbon residue was filtered off and the filtrate was evaporated *in vacuo*. The crude residue was purified by RP-HPLC (using a gradient mixture of acetonitrile/water in a ratio of 40:60 to 95:5 over 40 min) to yield title compound (10 mg, 20%) and (*E*)-6-(3,4-dimethoxyphenyl)-3-styrylisothiazolo[4,3-*b*]pyridine **6f** (25 mg, 51%).

^1H NMR (300 MHz, CDCl_3) δ 9.02 (d, $J = 2.0$ Hz, 1H), 8.13 (d,

$J = 2.1$ Hz, 1H), 7.35–7.27 (m, 3H), 7.26–7.21 (m, 3H), 7.19 (d, $J = 2.1$ Hz, 1H), 7.03 (d, $J = 8.3$ Hz, 1H), 3.99 (s, 3H), 3.96 (s, 3H), 3.79 (t, $J = 7.6$ Hz, 2H), 3.23 (t, $J = 7.6$ Hz, 2H) ppm.

^{13}C NMR (75 MHz, CDCl_3) δ 165.15, 155.87, 150.55, 150.16, 150.06, 147.17, 145.48, 140.44, 135.99, 130.46, 128.87, 126.86, 125.32, 120.44, 112.28, 111.05, 99.66, 56.37, 36.82, 28.27 ppm.

HRMS m/z $[\text{M}+\text{H}]^+$ calcd for $\text{C}_{22}\text{H}_{20}\text{N}_2\text{O}_2\text{S}_1$: 377.1318, found: 377.1317.

7.23. 3,6-Bis(3,4-dimethoxyphenyl)isothiazolo[4,3-*b*]pyridine (**6h**)

To a mixture of dioxane/water (in a ratio of 4:1) were added 3,6-dibromoisothiazolo[4,3-*b*]pyridine **4** (50 mg, 0.17 mmol), 3,4-dimethoxyphenylboronic acid (62 mg, 0.51 mmol, 3 eq) and potassium carbonate (2 equiv). The mixture was degassed, filled with nitrogen and Pd(PPh₃)₄ (10 mol%) was added. The mixture was degassed a second time, filled with nitrogen and stirred at 100 °C for 3 days. After completion of the reaction, solvents were evaporated *in vacuo*. The crude residue was purified by silica gel flash chromatography (using a mixture of heptane/acetone in a ratio of 95:5 as a mobile phase), yielding the title compound (12 mg, 17%).

^1H NMR (300 MHz, CDCl_3) δ 9.07 (d, $J = 2.0$ Hz, 1H), 8.13 (d, $J = 2.0$ Hz, 1H), 7.87 (d, $J = 1.8$ Hz, 1H), 7.76 (dd, $J = 8.4$, 1.9 Hz, 1H), 7.29 (dd, $J = 8.3$, 2.0 Hz, 1H), 7.20 (d, $J = 1.8$ Hz, 1H), 7.02 (d, $J = 8.4$ Hz, 2H), 4.02 (s, 3H), 3.98 (s, 3H), 3.96 (s, 3H), 3.95 (s, 3H) ppm.

^{13}C NMR (75 MHz, CDCl_3) δ 162.79, 157.17, 151.16, 151.08, 150.22, 150.07, 149.87, 143.56, 135.80, 130.30, 125.40, 123.71, 121.84, 120.43, 112.28, 112.06, 111.92, 110.99, 56.45, 56.37 ppm.

HRMS m/z $[\text{M}+\text{H}]^+$ calcd for $\text{C}_{22}\text{H}_{20}\text{N}_2\text{O}_4\text{S}_1$: 409.1216, found: 409.1210.

7.24. Molecular modeling

Docking started from the GAK structure available in PDB entry 4y8d, from which all ligands and water molecules were removed. The remaining structure was prepared by AutodockTools as a receptor: polar hydrogens were added, Gasteiger charges were added, the AD4 atom type was assigned and finally everything was saved in a PDBQT file. The original inhibitor 12i (compound **2**) from PDB4y8d was extracted and processed by AutodockTool [31]. Polar hydrogens were added, Gasteiger charges were calculated, autodock4 atom types were assigned and everything was saved in a PDBQT file. Compounds **6a** and **6h** were drawn in Chemdraw and a 3D structure was generated by Chem3D. Then, Autodocktools was used again to prepare the PDBQT files. Autodock vina was used for the docking experiments [32]. A cubic box was defined 50 × 50 × 50 units (0.375 Å/unit) and the box was centred at the B.ALA67.CB atom in the second kinase domain (chain B). During docking, the enzyme was rigid and the ligand flexible around the torsion angles. A control docking was executed using the original inhibitor 12i present in the 4y8d PDB file. The root mean square deviation (RMSD) between docked and crystallized ligand is 0.9 Å, showing that the docking program Vina can reproduce the crystallized conformation quite well. Compounds **6a** and **6h** were then docked using the same protocol.

7.25. GAK binding assay

K_d values for GAK were determined as previously described [27]. Briefly, the DNA-tagged GAK, an immobilized ligand on streptavidin-coated magnetic beads, and the test compound are combined. When binding occurs between GAK and a test compound, no binding can occur between GAK and the immobilized ligand. Upon washing, the compound-bound, DNA-tagged GAK is

washed away. The beads carrying the ligands are then resuspended in elution buffer and the remaining kinase concentration measured by qPCR on the eluate. Kd values are determined using dose-response curves.

7.26. Antiviral assays

Virus construct. DENV2 (New Guinea C strain) [29,30] *Renilla* reporter plasmid used for *in vitro* assays was a gift from Pei-Yong Shi (The University of Texas Medical Branch).

Cells. Huh7 (Apath LLC) cells were grown in DMEM (Mediatech) supplemented with 10% FBS (Omega Scientific), nonessential amino acids, 1% L-glutamine, and 1% penicillin-streptomycin (Thermo-Fisher Scientific) and maintained in a humidified incubator with 5% CO₂ at 37 °C.

Virus Production. DENV2 RNA was transcribed *in vitro* using mMessage/mMachine (Ambion) kits. DENV was produced by electroporating RNA into BHK-21 cells, harvesting supernatants on day 10 and titering via standard plaque assays on BHK-21 cells. Virus titers were determined via standard plaque assay on Vero 76 cells.

Infection assays. Huh7 cells were infected with DENV in replicates ($n = 3-10$) for 4 h at MOI of 0.05. Overall infection was measured at 48 h using a *Renilla* luciferase substrate.

Viability assays. Viability was assessed using AlamarBlue[®] reagent (Invitrogen) or Cell-Titer-Glo[®] reagent (Promega) assay according to manufacturer's protocol. Fluorescence was detected at 560 nm on InfiniteM1000 plate reader and luminescence on InfiniteM1000 plate reader (Tecan) or a Spectramax 340 PC.

Acknowledgements

R.W. is the recipient of a doctoral fellowship from the Agency for Innovation by Science and Technology, Flanders (IWT.141103). This work was supported by award number W81XWH-16-1-0691 from the Department of Defense, Congressionally Directed Medical Research Programs to S.E. and P.-H.; and seed grant from the Stanford SPARK program.

Abbreviations

AP	adaptor protein complex
CCV	clathrin-coated vesicle
CHIKV	chikungunya virus
DENV	dengue virus
EBOV	ebola virus
GAK	cyclin G-associated kinase
HBV	hepatitis B virus
HCMV	human cytomegalovirus
HCV	hepatitis C virus
PI3K-C2A	phosphatidylinositol 3-kinase class II alpha
PI4KIIIβ	phosphatidylinositol-4-kinase IIIβ
SAR	structure activity relationship
TEA	triethylamine
TGN	trans-golgi network

Appendix A. Supplementary data

Supplementary data to this article can be found online at <https://doi.org/10.1016/j.ejmech.2018.11.065>.

References

[1] D. Fabbro, S.W. Cowan-Jacob, H. Möbitz, G. Martiny-Baron, Targeting cancer with small-molecular-weight kinase inhibitors, *Methods Mol. Biol.* 795 (2012)

- 1–34, https://doi.org/10.1007/978-1-62703-239-1_1.
- [2] M.C. Bryan, N.S. Rajapaksa, Kinase inhibitors for the treatment of immunological disorders: recent advances, *J. Med. Chem.* (2018), <https://doi.org/10.1021/acs.jmedchem.8b00667> acs.jmedchem.8b00667.
- [3] Y. Shi, M. Mader, Brain penetrant kinase inhibitors: learning from kinase neuroscience discovery, *Bioorg. Med. Chem. Lett.* 28 (2018) 1981–1991, <https://doi.org/10.1016/j.bmcl.2018.05.007>.
- [4] Y. Tanaka, Recent progress and perspective in JAK inhibitors for rheumatoid arthritis: from bench to bedside, *J. Biochem.* 158 (2015) 173–179, <https://doi.org/10.1093/jb/mvv069>.
- [5] S. Schor, S. Einav, Repurposing of kinase inhibitors as broad-spectrum antiviral drugs, *DNA Cell Biol.* 37 (2018) 63–69, <https://doi.org/10.1089/dna.2017.4033>.
- [6] H.M. van der Schaar, P. Leyssen, H.J. Thibaut, A. de Palma, L. van der Linden, K.H.W. Lanke, C. Lacroix, E. Verbeken, K. Conrath, A.M. Macleod, D.R. Mitchell, N.J. Palmer, H. van de Poël, M. Andrews, J. Neyts, F.J.M. van Kuppeveld, A novel, broad-spectrum inhibitor of enterovirus replication that targets host cell factor phosphatidylinositol 4-kinase IIIβ, *Antimicrob. Agents Chemother.* 57 (2013) 4971–4981, <https://doi.org/10.1128/AAC.01175-13>.
- [7] E. Haasbach, C. Müller, C. Ehrhardt, A. Schreiber, S. Pleschka, S. Ludwig, O. Planz, The MEK-inhibitor CI-1040 displays a broad anti-influenza virus activity *in vitro* and provides a prolonged treatment window compared to standard of care *in vivo*, *Antivir. Res.* 142 (2017) 178–184, <https://doi.org/10.1016/j.antiviral.2017.03.024>.
- [8] W.S. Polachek, H.F. Moshirif, M. Franti, D.M. Coen, V.B. Sreenu, B.L. Strang, High-Throughput small interfering RNA screening identifies phosphatidylinositol 3-kinase class II alpha as important for production of human cytomegalovirus virions, *J. Virol.* 90 (2016) 8360–8371, <https://doi.org/10.1128/JVI.01134-16>.
- [9] A. Diab, A. Foca, F. Fusil, T. Lahlali, P. Jalaguier, F. Amirache, L. N'Guyen, N. Isorce, F.-L. Cosset, F. Zoulim, O. Andrisani, D. Durantel, Polo-like-kinase 1 is a proviral host factor for hepatitis B virus replication, *Hepatology* 66 (2017) 1750–1765, <https://doi.org/10.1002/hep.29236>.
- [10] M. Robinson, S. Schor, R. Barouch-Bentov, S. Einav, Viral journeys on the intracellular highways, *Cell. Mol. Life Sci.* 75 (2018) 3693–3714, <https://doi.org/10.1007/s00018-018-2882-0>.
- [11] H.T. McMahon, E. Boucrot, Molecular mechanism and physiological functions of clathrin-mediated endocytosis, *Nat. Rev. Mol. Cell Biol.* 12 (2011) 517–533, <https://doi.org/10.1038/nrm3151>.
- [12] M.A. Edeling, C. Smith, D. Owen, Life of a clathrin coat: insights from clathrin and AP structures, *Nat. Rev. Mol. Cell Biol.* 7 (2006) 32–44, <https://doi.org/10.1038/nrm1786>.
- [13] D. Ricotta, S.D. Conner, S.L. Schmid, K. Von Figura, S. Höning, Phosphorylation of the AP2 μ subunit by AAK1 mediates high affinity binding to membrane protein sorting signals, *J. Cell Biol.* 156 (2002) 21–9525, <https://doi.org/10.1083/jcb.200111068>.
- [14] L. Zhang, O. Gjoerup, T.M. Roberts, The serine/threonine kinase cyclin G-associated kinase regulates epidermal growth factor receptor signaling, *Proc. Natl. Acad. Sci. Unit. States Am.* 101 (2004) 10296–10301, <https://doi.org/10.1073/pnas.0403175101>.
- [15] P. Ghosh, S. Kornfeld, AP-1 binding to sorting signals and release from clathrin-coated vesicles is regulated by phosphorylation, *J. Cell Biol.* 160 (2003) 699–708, <https://doi.org/10.1083/jcb.200211080>.
- [16] D.-W. Lee, X. Zhao, F. Zhang, E. Eisenberg, L.E. Greene, Depletion of GAK/auxilin 2 inhibits receptor-mediated endocytosis and recruitment of both clathrin and clathrin adaptors, *J. Cell Sci.* 118 (2005) 4311–4321, <https://doi.org/10.1242/jcs.02548>.
- [17] S.K. Lemmon, Clathrin uncoating: auxilin comes to life, *Curr. Biol.* 11 (2001) R49–R52, [https://doi.org/10.1016/S0960-9822\(01\)00010-0](https://doi.org/10.1016/S0960-9822(01)00010-0).
- [18] G. Neveu, A. Ziv-Av, R. Barouch-Bentov, E. Berkerman, J. Mulholland, S. Einav, AP-2-Associated protein kinase 1 and cyclin G-associated kinase regulate hepatitis C virus entry and are potential drug targets, *J. Virol.* 89 (2015) 4387–4404, <https://doi.org/10.1128/JVI.02705-14>.
- [19] E. Berkerman, G. Neveu, A. Shulla, J. Brannan, S.Y. Pu, S. Wang, F. Xiao, R. Barouch-Bentov, R.R. Bakken, R. Mateo, J. Govero, C.M. Nagamine, M.S. Diamond, S. De Jonghe, P. Herdewijn, J.M. Dye, G. Randall, S. Einav, Anticancer kinase inhibitors impair intracellular viral trafficking and exert broad-spectrum antiviral effects, *J. Clin. Invest.* 127 (2017) 1338–1352, <https://doi.org/10.1172/JCI89857>.
- [20] F. Xiao, S. Wang, R. Barouch-Bentov, G. Neveu, S. Pu, M. Beer, S. Schor, S. Kumar, V. Nicolaescu, B.D. Lindenbach, G. Randall, S. Einav, Interactions between the hepatitis C virus nonstructural 2 protein and host adaptor proteins 1 and 4 orchestrate virus release, *mBio* 9 (2018), <https://doi.org/10.1128/mBio.02233-17> e02233-17.
- [21] S.-Y. Pu, R. Wouters, S. Schor, J. Rozenski, R. Barouch-Bentov, L.I. Prugar, C.M. O'Brien, J.M. Brannan, J.M. Dye, P. Herdewijn, S. De Jonghe, S. Einav, Optimization of isothiazolo[4,3-b]pyridine-based inhibitors of cyclin G associated kinase (GAK) with broad-spectrum antiviral activity, *J. Med. Chem.* 61 (2018) 6178–6192, <https://doi.org/10.1021/acs.jmedchem.8b00613>.
- [22] S. Kovackova, L. Chang, E. Berkerman, G. Neveu, R. Barouch-Bentov, A. Chaikuad, C. Heroven, M. Sála, S. De Jonghe, S. Knapp, S. Einav, P. Herdewijn, Selective inhibitors of cyclin G associated kinase (GAK) as anti-hepatitis C agents, *J. Med. Chem.* 58 (2015) 3393–3410.
- [23] J. Li, S. Kovackova, S. Pu, J. Rozenski, S. De Jonghe, S. Einav, P. Herdewijn, Isothiazolo[4,3-b]pyridines as inhibitors of cyclin G associated kinase:

- synthesis, structure–activity relationship studies and antiviral activity, *Medchemcomm* 6 (2015) 1666–1672, <https://doi.org/10.1039/C5MD00229J>.
- [24] C.J. Nyman, C.E. Wymore, G. Wilkinson, Reactions of tris(triphenylphosphine)platinum(0) and tetrakis(triphenylphosphine)palladium(0) with oxygen and carbon dioxide, *J. Chem. Soc. A Inorganic, Phys. Theor.* 0 (1968) 561, <https://doi.org/10.1039/j19680000561>.
- [25] B. Brandt, J.-H. Fischer, W. Ludwig, J. Libuda, F. Zaera, S. Schauermaier, H.-J. Freund, Isomerization and hydrogenation of *cis*-2-Butene on Pd model catalyst, *J. Phys. Chem. C* 112 (2008) 11408–11420, <https://doi.org/10.1021/jp800205j>.
- [26] I. Heertje, G.K. Koch, W.J. Wösten, Mechanism of heterogeneous catalytic *cis*-trans isomerization and double-bond migration of octadecenoates, *J. Catal.* 32 (1974) 337–342, [https://doi.org/10.1016/0021-9517\(74\)90085-2](https://doi.org/10.1016/0021-9517(74)90085-2).
- [27] M.A. Fabian, W.H. Biggs, D.K. Treiber, C.E. Atteridge, M.D. Azimioara, M.G. Benedetti, T.A. Carter, P. Ciceri, P.T. Edeen, M. Floyd, J.M. Ford, M. Galvin, J.L. Gerlach, R.M. Grotzfeld, S. Herrgard, D.E. Insko, M.A. Insko, A.G. Lai, J.-M. Lélías, S.A. Mehta, Z. V. Milanov, A.M. Velasco, L.M. Wodicka, H.K. Patel, P.P. Zarrinkar, D.J. Lockhart, A small molecule–kinase interaction map for clinical kinase inhibitors, *Nat. Biotechnol.* 23 (2005) 329–336, <https://doi.org/10.1038/nbt1068>.
- [28] S.-Y. Pu, F. Xiao, S. Schor, E. Bekerman, F. Zanini, R. Barouch-Bentov, C.M. Nagamine, S. Einav, Feasibility and biological rationale of repurposing sunitinib and erlotinib for dengue treatment, *Antivir. Res.* 155 (2018) 67–75, <https://doi.org/10.1016/j.antiviral.2018.05.001>.
- [29] X. Xie, S. Gayen, C. Kang, Z. Yuan, P.-Y. Shi, Membrane topology and function of dengue virus NS2A protein, *J. Virol.* 87 (2013) 4609–4622, <https://doi.org/10.1128/JVI.02424-12>.
- [30] G. Zou, H.Y. Xu, M. Qing, Q.Y. Wang, P.Y. Shi, Development and characterization of a stable luciferase dengue virus for high-throughput screening, *Antivir. Res.* 91 (2011) 11–19, <https://doi.org/10.1016/j.antiviral.2011.05.001>.
- [31] G.M. Morris, R. Huey, W. Lindstrom, M.F. Sanner, R.K. Belew, D.S. Goodsell, A.J. Olson, AutoDock4 and AutoDockTools4: automated docking with selective receptor flexibility, *J. Comput. Chem.* 30 (2009) 2785–2791, <https://doi.org/10.1002/jcc.21256>.
- [32] O. Trott, A.J. Olson, AutoDock Vina, Improving the speed and accuracy of docking with a new scoring function, efficient optimization, and multi-threading, *J. Comput. Chem.* 31 (2010) 455–461, <https://doi.org/10.1002/jcc.21334>.



Contents lists available at ScienceDirect

Bioorganic & Medicinal Chemistry

journal homepage: www.elsevier.com/locate/bmc

Structure-activity relationship study of the pyridine moiety of isothiazolo[4,3-*b*]pyridines as antiviral agents targeting cyclin G-associated kinase

Belén Martínez-Gualda^a, Szu-Yuan Pu^b, Mathy Froeyen^a, Piet Herdewijn^a, Shirir Einav^b, Steven De Jonghe^{c,*}

^a KU Leuven, Rega Institute for Medical Research, Laboratory of Medicinal Chemistry, Herestraat 49, 3000 Leuven, Belgium

^b Department of Medicine, Division of Infectious Diseases and Geographic Medicine, and Department of Microbiology and Immunology, Stanford University School of Medicine, Stanford, CA 94305, USA

^c KU Leuven, Department of Microbiology, Immunology and Transplantation, Rega Institute for Medical Research, Laboratory of Virology and Chemotherapy, Herestraat 49, 3000 Leuven, Belgium

ARTICLE INFO

Keywords:

Cyclin G-associated kinase
 Isothiazolo[4,3-*b*]pyridine
 Dengue virus
 Kinase inhibitor
 Antiviral drugs

ABSTRACT

Previously, we reported the discovery of 3,6-disubstituted isothiazolo[4,3-*b*]pyridines as potent and selective cyclin G-associated kinase (GAK) inhibitors with promising antiviral activity. In this manuscript, the structure-activity relationship study was expanded to synthesis of isothiazolo[4,3-*b*]pyridines with modifications of the pyridine moiety. This effort led to the discovery of an isothiazolo[4,3-*b*]pyridine derivative with a 3,4-dimethoxyphenyl residue at position 5 that displayed low nanomolar GAK binding affinity and antiviral activity against dengue virus.

1. Introduction

Cyclin G-associated kinase (GAK), also known as auxilin 2, is a cellular serine/threonine kinase that belongs to the numb-associated kinases (NAK). This family also includes adaptor-associated kinase 1 (AAK1), BMP-2 inducible kinase (BIKE/BMP2K) and myristoylated and palmitoylated serine/threonine kinase 1 (MPSK1, also known as serine/threonine kinase 16 or STK16).¹ GAK, ubiquitously expressed within the cell in the Golgi apparatus, cytoplasm and nucleus, regulates the clathrin-mediated intracellular trafficking of cellular cargo proteins.² Interactions between clathrin-associated adaptor protein (AP) complexes and transmembrane cargo play an important role in membrane trafficking, as these AP complexes orchestrate the formation of vesicles destined for transport in distinct intracellular pathways.^{3,4} Phosphorylation of the μ subunits of AP1 and AP2 by GAK leads to a conformational change that enhances their binding to sorting motifs within cargo proteins.^{5,6} GAK regulates the recruitment of clathrin and AP-2 to the plasma membrane and of AP-1 to the *trans*-Golgi network (TGN).^{3,7,8} GAK also controls the uncoating of clathrin coated vesicles (CCVs) for recycling clathrin back to the cell surface.^{3,5}

Viruses hijack these intracellular membrane trafficking machineries, as indicated by the important roles played by various AP complexes in the life cycle of multiple unrelated viruses.^{7,9,10} It has been demonstrated that GAK regulates early and late stages of the viral lifecycle and

hence, functions as a master regulator of viral infection. GAK is therefore a promising target for the discovery of novel antiviral agents. Such a host-targeted approach offers advantages, including a high barrier to resistance and an opportunity to develop broad-spectrum antiviral agents when focusing on host factors, such as GAK, that are essential for the life cycle of multiple viruses¹¹.

Erlotinib (Fig. 1), an approved anticancer drug with potent GAK affinity (dissociation constant value or $K_D = 3.1$ nM), has shown antiviral activity against an array of unrelated viruses including hepatitis C virus (HCV), dengue virus (DENV), and Zika virus (ZIKV) from the Flaviviridae family, the filovirus Ebola (EBOV) and the alpha virus Chikungunya (CHIKV).⁹ However, since erlotinib targets EGFR with a comparable affinity to GAK and several other kinases at a lower affinity, it is not an ideal chemical tool to study the role of GAK in viral infection. Several medicinal chemists were thus inspired to develop potent, drug-like and selective GAK inhibitors. Exploring the chemistry of 4-anilino-quinazolines and -quinolines¹² led to the discovery of SGC-GAK-1 (Fig. 1) that was endowed with very strong GAK affinity ($K_D = 1.9$ nM) and displayed an excellent kinase selectivity profile. This compound was not investigated for its antiviral activity, yet it showed cytotoxic activity against selected prostate cancer cell lines.¹³

Our group reported the discovery of 3,6-disubstituted isothiazolo [4,3-*b*]pyridines as potent and selective GAK inhibitors. The original series of compounds, as represented by compound 2 (Fig. 1), carried a

* Corresponding author.

E-mail address: steven.dejonghe@kuleuven.be (S. De Jonghe).

<https://doi.org/10.1016/j.bmc.2019.115188>

Received 28 August 2019; Received in revised form 21 October 2019; Accepted 25 October 2019

0968-0896/© 2019 Elsevier Ltd. All rights reserved.

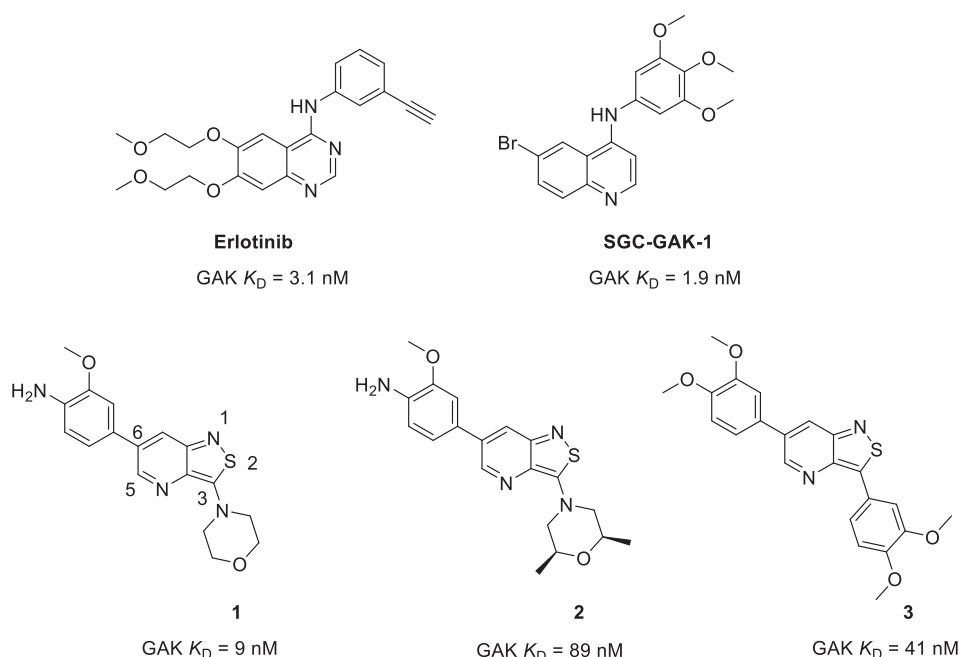


Fig. 1. Previously studied GAK inhibitors.

morpholino residue at position 3 and was endowed with high affinity for GAK (K_D = 9 nM), but displayed only low μ M antiviral activity against HCV and DENV.¹⁴ Subsequent optimization revealed that a *cis*-2,6-dimethylmorpholino residue at this position (compound **2**, Fig. 1) had a detrimental effect on the GAK affinity (K_D = 89 nM), but a favourable effect on the activity against DENV, EBOV and CHIKV.¹⁵ The incorporation of other amines, alcohols, and carboxamides at position 3 yielded compounds that were much less active as GAK ligands and/or showed weaker antiviral activity.¹⁶ To increase the structural variety at this position, palladium-catalyzed cross couplings (such as Suzuki and Sonogashira reactions) have been performed, leading to the discovery of a congener (compound **3**, Fig. 1) with high GAK affinity (K_D = 41 nM) and a moderate antiviral activity against DENV.¹⁷ More recently, the importance of the isothiazolo[4,3-*b*]pyridine core has been evaluated by a scaffold hopping approach, yielding a series of novel scaffolds that displayed a reduced GAK affinity relative to the original scaffold.¹⁸

Although a broad structural variety has been introduced at position 3 of the isothiazolo[4,3-*b*]pyridine scaffold, and a wide range of heterocyclic core structures have been prepared, the substitution pattern on the pyridine moiety of the isothiazolo[4,3-*b*]pyridine scaffold has not been previously studied in detail. In our prior medicinal chemistry optimization campaigns,^{14–18} an aryl group was always present at position 6 of the isothiazolo[4,3-*b*]pyridine scaffold, with a 3,4-dimethoxyphenyl, 3,4,6-trimethoxyphenyl and 3-methoxy-4-amino-phenyl being optimal for GAK affinity (Fig. 2). In the present work, we describe our efforts to introduce structural modifications on the

pyridine ring of the isothiazolo[4,3-*b*]pyridine core, keeping the *cis*-2,6-dimethylmorpholino substituent fixed. Several variations were introduced. Besides additional Suzuki couplings, several linkers (amino, alkenyl and alkynyl) were inserted between the phenyl ring at position 6 and the isothiazolo[4,3-*b*]pyridine scaffold. In addition, a number of previously unknown 5-aryl-isothiazolo[4,3-*b*]pyridines were prepared. All compounds were evaluated for their GAK affinity and the most potent GAK ligands were also assessed for anti-DENV activity.

2. Chemistry

For the synthesis of the 6-substituted isothiazolo[4,3-*b*]pyridines, the known 6-bromo-3-(*cis*-2,6-dimethylmorpholino)isothiazolo[4,3-*b*]pyridine **4** was selected as the key intermediate (Scheme 1).¹⁵ Aryl groups were conveniently introduced by Suzuki cross-couplings using classical reaction circumstances: an appropriate arylboronic acid, Pd(PPh₃)₄ as catalyst and potassium carbonate as base in a mixture of dioxane/water. This procedure allowed to assemble a focused library of 6-aryl-isothiazolo[4,3-*b*]pyridines **5a-f** in yields ranging from 78% to 91%. The insertion of an ethenyl linker between the central core structure and the phenyl ring was performed by a palladium-catalyzed cross-coupling between styrene and isothiazolo[4,3-*b*]pyridine **4** applying Heck reaction conditions, using Pd(OAc)₂ as catalyst, *N*-phenylurea as ligand and potassium carbonate as base (step b, Scheme 1).¹⁹ This allowed the isolation of the desired compound **5g** in high yield (88%). Coupling of different anilines at position 6 of the isothiazolo[4,3-*b*]pyridine scaffold was achieved via a Buchwald reaction using Pd

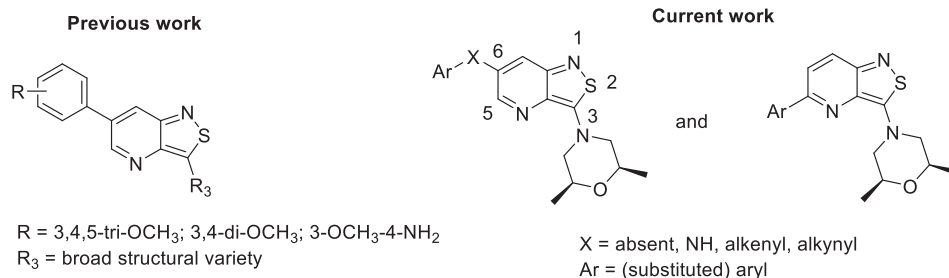
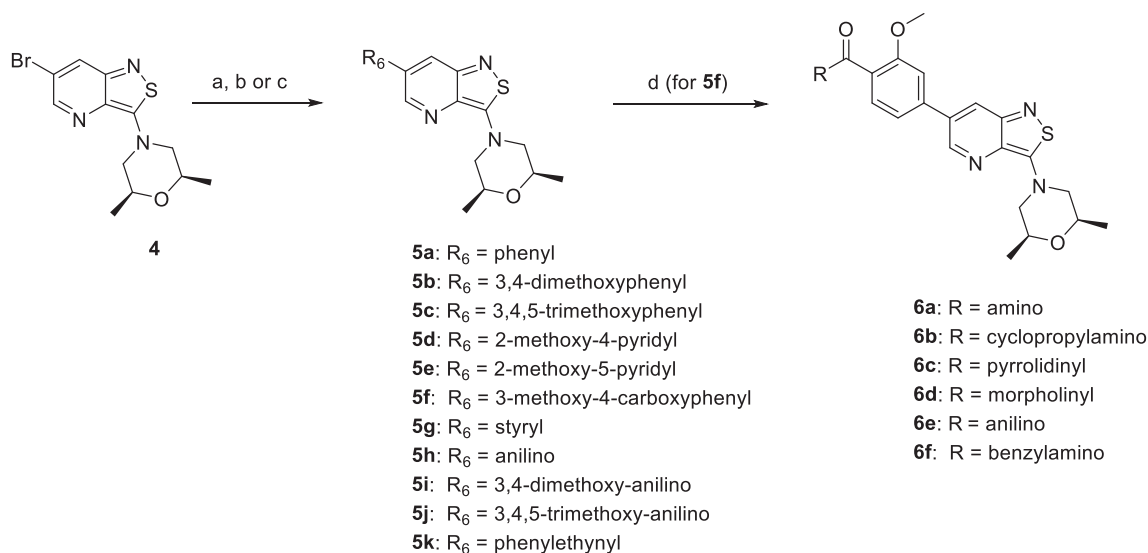


Fig. 2. Medicinal chemistry strategy.



Scheme 1. Reagents and conditions. (a) R₆B(OH)₂, Pd(PPh₃)₄, K₂CO₃, dioxane/water, 90 °C; (b) styrene, *N*-phenylurea, Pd(OAc)₂, K₂CO₃, DMF, 120 °C, overnight; (c) aniline or phenylacetylene, Pd(dba)₂, SPhos, *t*BuOK, toluene, 90 °C; (d) (i) SOCl₂, DCM, 40 °C, 3 h; (ii) amine, Et₃N, rt, 3 h.

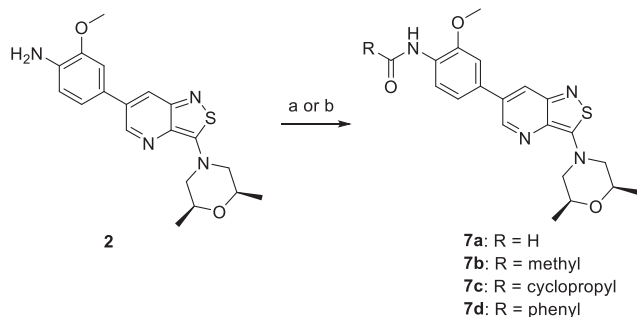
(dba)₂ as catalyst, SPhos as ligand, potassium *tert*-butoxide as base and toluene as solvent, yielding compounds **5h–j** in good yields ranging from 73% to 85%.²⁰ For the insertion of a phenylethynyl residue at position 6 of isothiazolo[4,3-*b*]pyridine scaffold, classical Sonogashira reaction conditions (using ethynylbenzene, Pd(PPh₃)₂Cl₂ and copper(I) iodide) were initially applied, but failed. However, when the same Buchwald conditions, previously employed for the coupling of anilines, were used for the coupling of phenylacetylene (step c, **Scheme 1**), compound **5k** was obtained in good yield (87%). Prior to the addition of the catalyst, it was necessary to pass a continuous flow of argon for 5–10 min through the reaction mixture, as this led to increased reaction yields in all these palladium-catalyzed cross-couplings.

The carboxylic acid moiety of compound **5f** was converted to several amides.²¹ The acid chloride was generated *in situ* by reaction with thionyl chloride, followed by reaction with a number of amines generating target compounds **6a–f** in yields varying from 68% to 85%. Similarly, the amino group of compound **2** was also used to prepare a number of amides (**Scheme 2**). The formylamino congener **7a** was prepared using MnO₂ as catalyst and formamide as solvent.²² The reaction of compound **2** with acetic anhydride, cyclopropanecarbonyl chloride and benzoyl chloride provided compounds **7b**, **7c** and **7d**, respectively.

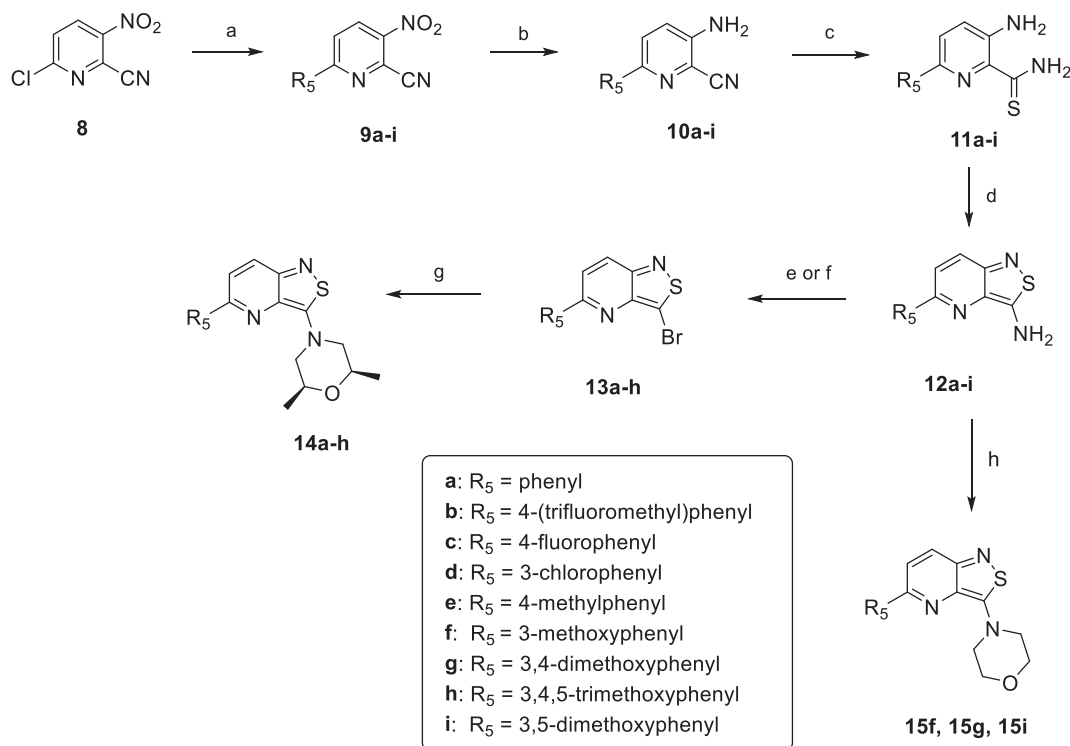
For the synthesis of 5-substituted isothiazolo[4,3-*b*]pyridines, an alternative synthetic pathway was followed. Initial attempts were focused on the synthesis of an intermediate (i.e. 3-bromo-5-chloro-isothiazolo[4,3-*b*]pyridine) that could serve as key synthon from which structural variety at two different positions of the scaffold could be

easily introduced. Commercially available 6-chloro-2-cyano-3-nitropyridine **8** was selected as starting material. Reduction of the nitro group to the corresponding amino group led to a concomitant complete hydrolysis of the cyano moiety affording 3-amino-6-chloropicolinic acid as the sole product. As an alternative, we introduced the corresponding aryl group via a Suzuki cross-coupling reaction in the first step of the synthesis (**Scheme 3**). These reactions were carried out in toluene as solvent (except for compound **9h** bearing a 3,4,5-trimethoxyphenyl group) instead of the dioxane/water mixture that was commonly applied for the preparation of 6-substituted derivatives. Thus, several aryl groups were introduced at position 6 of compound **8** generating derivatives **9a–i** in yields ranging from 76% to 96%. The nitro group of compounds **9a–i** was reduced by treatment with iron under acidic conditions (acetic acid at 60 °C) affording 3-amino-6-aryl-picolinonitriles **10a–i**. Inevitably, small amounts of the corresponding 3-amino-6-phenylpicolinamides were formed, resulting from hydrolysis of the cyano group. These mixtures were used as such for the next step. Thionation of the nitrile functionality using phosphorus pentasulfide yielded thioamides **11a–i**. The isothiazole moiety was then constructed by an oxidative ring closure using hydrogen peroxide in methanol. As this reaction proceeded smoothly and cleanly, purification of the crude residue was not necessary, and the corresponding 5-aryl-3-amino-isothiazolo[4,3-*b*]pyridines **12a–i** were isolated in excellent yields. The conversion of the amino group to a bromine was achieved via a Sandmeyer reaction. Applying the classical reaction conditions (NaNO₂, HBr, CuBr, water) was successful for compounds **13a–d** and **13h**. However, for the analogues (compounds **12e–g**), in which the 5-phenyl moiety carried one or two electron-donating substituents (methyl or methoxy groups), none to very low yields the most were obtained. This result was attributed to multiple brominations at different positions of the 5-phenyl ring. To minimise these aromatic bromination side reactions, milder conditions (*t*BuONO, CuBr₂ and dry acetonitrile) were used.²³ This slightly improved the yields of compounds **13e–g** (34–51%), but not of compound **13i**. Finally, *cis*-2,6-dimethylmorpholine was introduced at position 3 of the isothiazolo[4,3-*b*]pyridine scaffold, affording the desired compounds **14a–h** in yields ranging from 55% to 91%.

To circumvent the Sandmeyer reaction, a 3-*N*-morpholinyl moiety was directly synthesized from the corresponding 3-amino congeners. Reaction of compounds **12f**, **12g** and **12i** with 2-bromoethyl ether and potassium carbonate as a base generated the desired compounds **15f**, **15g** and **15i** in decent yields (71–77%).



Scheme 2. Reagents and conditions. (a) formamide, MnO₂, 150 °C, 5 h; (b) acetic anhydride or RCOCl, Et₃N, DCM, rt, overnight.



Scheme 3. Reagents and conditions. (a) $R_3B(OH)_2$, Pd(PPh₃)₄, K₂CO₃, toluene or dioxane/H₂O, 95 °C; (b) Fe, CH₃COOH, 60 °C; (c) P₂S₅, EtOH, 75 °C; (d) 35% aq-H₂O₂, MeOH, rt; (e) NaNO₂, HBr, CuBr, H₂O, 0 °C to rt; (f) *t*BuONO, CuBr₂, dry CH₃CN, -10 °C to rt; (g) 2,6-dimethylmorpholine, EtOH, reflux, overnight; (h) 2-bromoethyl ether, K₂CO₃, DMF, 100 °C, 4–5 h.

3. GAK binding affinity

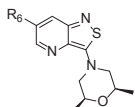
The binding affinity of compounds **5a-k**, **6a-f**, **7a-d**, **14a-h**, **15f**, **15g** and **15i** for GAK was evaluated via a commercially available LanthaScreen® Europium kinase binding assay.²⁴ In this assay format, an Alexa Fluor 647-labeled conjugate or tracer competes with the GAK ligand for the ATP binding site. Signal detection is dependent on the time-resolved fluorescence resonance energy transfer (TR-FRET) signal resulting from the antibody and tracer binding. When the ATP site is occupied by the tracer, there is a high TR-FRET signal. When the tracer is displaced by the GAK inhibitor, a reduction in TR-FRET signal is observed. The GAK binding affinity of reference compound **2** was measured via a LanthaScreen assay with an IC₅₀ value of 0.0394 μM, which is in agreement with the K_i of 0.089 μM previously measured via the DiscoverX screening assay.¹⁵ To drive the subsequent structure-activity relationship (SAR) study, the GAK binding affinity of all compounds was evaluated in the Lanthascreen assay (Tables 1 and 2).

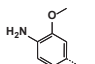
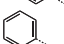
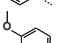
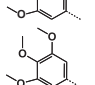
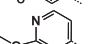
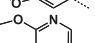
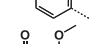
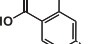
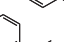
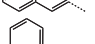
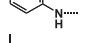
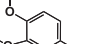
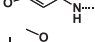
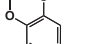
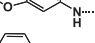
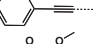
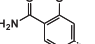
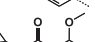
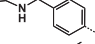
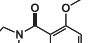
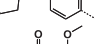
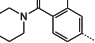
Prior SAR studies of 3-*N*-morpholino-isothiazolo[4,3-*b*]pyridines demonstrated that electron-donating substituents (e.g. methoxy, amino) at the 6-phenyl moiety are optimal for GAK binding. Yet, combination of a *cis*-2,6-dimethylmorpholinyl substituent at position 3, which is known to confer potent antiviral activity,¹⁵ with structural variation of the 6-phenyl moiety has not been previously explored. Based on the beneficial effect of methoxy groups on GAK binding,¹⁴ the 6-(3,4-dimethoxy)- and 6-(3,4,5-trimethoxyphenyl) derivatives were synthesized (Table 1). The presence of a 3,4-dimethoxyphenyl residue (compound **5b**) caused a 3-fold drop in GAK affinity (IC₅₀ = 0.136 μM) relative to compound **2**. Conversely, the 3,4,5-trimethoxyphenyl congener (compound **5c**) showed a slightly improved GAK affinity (IC₅₀ = 0.071 μM). Removal of the methoxy groups furnished compound **5a** which shows an IC₅₀ of 0.661 μM, which is about 10-fold less potent than the trimethoxyphenyl congener **5c**. Replacement of one of the methoxy groups by an endocyclic pyridine nitrogen gave rise to compounds **5d** and **5e** that display IC₅₀ values of 0.545 μM and >

3.33 μM, respectively. This indicated that the methoxy group at position 3 is more important for GAK binding than the one at position 4. Therefore, keeping the 3-methoxy group fixed, a number of derivatives were prepared with alternative functional groups at position 4 of the aromatic ring. The presence of a 4-carboxylic acid resulted in compound **5f** that showed very potent GAK inhibition (IC₅₀ = 0.042 μM). The carboxylic acid was used as a chemical handle to make a small set of amides, including a simple carboxamide analogue (compound **6a**), cycloaliphatic amides (compounds **6b-d**) and aromatic amides (**6e-f**). Based on the X-ray crystallographic data that we previously reported,¹⁴ this region (i.e. the 6-phenyl moiety) is oriented towards the solvent and therefore tolerates structural variety. This is in agreement with the experimentally determined IC₅₀ values, as several of these compounds, and particularly the carboxamide congener **6a** (IC₅₀ = 0.022 μM), show good GAK affinity. Because of the good affinity of these amides, a number of reverse amides (compounds **7a-d**) with aliphatic and aromatic side chains were prepared, displaying GAK IC₅₀ values in the range of 0.1 to 0.4 μM. To further explore the SAR, the effect of various linkers between the isothiazolo[4,3-*b*]pyridine scaffold and the 6-phenyl moiety on GAK affinity were investigated. An alkenyl (compound **5g**) or alkynyl (compound **5k**) spacer gave compounds that were completely devoid of GAK affinity. Albeit weak, an anilino substituent at position 6 (compound **5h**) gave rise to GAK affinity with an IC₅₀ of 1.63 μM. In an effort to restore GAK affinity of the 6-anilino congener, the 3,4-dimethoxy- (compound **5i**) and 3,4,5-trimethoxy-anilino (compound **5j**) congeners were prepared. Consistent with the 6-phenyl series, the 3,4,5-trimethoxyanilino derivative **5j** showed the most potent GAK affinity, with an IC₅₀ of 0.458 μM.

To expand the SAR, a series of regioisomeric 5-aryl-isothiazolo[4,3-*b*]pyridines (compounds **14a-i**) was synthesized (Table 2). Because of synthetic difficulties (*vide supra*), a number of derivatives (compounds **15f**, **15g** and **15i**) carrying a morpholine instead of a *cis*-2,6-dimethylmorpholino residue were synthesized. An unsubstituted phenyl (compound **14a**), halogen substituted phenyls (compounds **14c-d**) and

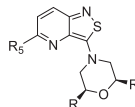
Table 1
GAK binding affinity of 6-substituted isothiazolo[4,3-*b*]pyridines.

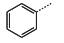
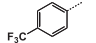
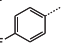
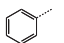
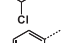
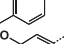
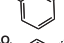
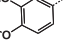
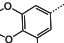
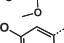
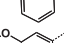


Cmpd	R ₆	GAK IC ₅₀ (μM)
2		0.0394
5a		0.661
5b		0.136
5c		0.071
5d		0.545
5e		> 3.33
5f		0.042
5g		> 3.33
5h		1.63
5i		1.29
5j		0.458
5k		> 10
6a		0.022
6b		0.118
6c		0.083
6d		0.101
6e		> 0.37
6f		0.073
7a		0.113
7b		0.132
7c		0.173
7d		0.37

p-tolyl (compound **14e**) at position 5 of the isothiazolo[4,3-*b*]pyridine scaffold yielded compounds that displayed GAK IC₅₀ values in the 0.1–0.3 μM range. Only the 4-trifluoromethylphenyl analogue (compound **14b**) was less active as GAK ligand. As methoxy substitution of

Table 2
GAK binding affinity of 5-aryl-isothiazolo[4,3-*b*]pyridines.



Cmpd	R	R ₅	GAK IC ₅₀ (μM)
14a	CH ₃		0.364
14b	CH ₃		> 0.37
14c	CH ₃		0.11
14d	CH ₃		0.262
14e	CH ₃		0.214
14f	CH ₃		0.099
14g	CH ₃		0.024
14h	CH ₃		0.422
15f	H		0.136
15g	H		0.124
15i	H		0.126

the 6-phenyl ring is known to be advantageous for GAK affinity,¹⁴ the phenyl at position 5 was also substituted with one, two or three methoxy groups affording compounds **14f-h**, **15f-g** and **15i**. This series displayed GAK IC₅₀ values in the 0.1–0.5 μM range, with compound **14g** (carrying a 3,4-dimethoxyphenyl at position 5 and a *cis*-2,6-dimethylmorpholinyl group at position 3) having the most potent GAK affinity (IC₅₀ = 0.024 μM). In contrast, the corresponding 3-*N*-morpholinyl derivative (compound **15g**) is 5-fold less active as a GAK ligand (IC₅₀ = 0.124 μM).

4. Antiviral activity against DENV

The compounds with the strongest GAK binding affinity (IC₅₀ < 0.1 μM) were assessed for antiviral activity in human hepatoma (Huh7) cells infected with DENV2 expressing a luciferase reporter (Table 3). Their effect on DENV2 infection was measured at 48 h post-infection via luciferase assays, and the half-maximal effective concentration (EC₅₀ value) was calculated. In parallel, the cytotoxicity of the compounds in the infected cells (expressed as the half-maximal cytotoxic concentration or CC₅₀ value) was measured via an Alamar-Blue assay. Compound **2** was included as a reference compound, as it was previously shown to have a promising anti-DENV2 activity, with an EC₅₀ of 0.82 μM and no apparent cytotoxicity.⁹ The 6-(3,4,5-trimethoxyphenyl) derivative **5c** reduces the anti-DENV activity by 3 folds relative to compound **2**. This is in line with its slightly reduced GAK affinity. Although compound **5f** is a very potent GAK ligand (IC₅₀ = 0.042 μM), it lacks antiviral activity. This might be due to impaired cellular permeability resulting from the presence of a polar carboxylic acid group. The corresponding amides (compounds **6a** and **6c**) and particularly compound **6f** (EC₅₀ = 5.83 μM) show an improved antiviral activity when compared to the carboxylic acid derivative **5f**. These findings suggest that this site of the molecule tolerates some structural variation with respect to GAK affinity, and that this position can therefore be used to tune physicochemical properties, such as

Table 3
Antiviral activity against DENV2.

Cmpd	R	R ₅	R ₆	DENV	
				EC ₅₀ (μ M) ^a	CC ₅₀ (μ M) ^b
2	CH ₃	H		0.82	> 25
5c	CH ₃	H		2.79	> 10
5f	CH ₃	H		> 10	> 10
6a	CH ₃	H		10.05	> 10
6c	CH ₃	H		8.85	> 10
6f	CH ₃	H		5.83	> 10
14f	CH ₃		H	> 10	> 10
14g	CH ₃		H	1.049	> 10
Erlotinib	-	-	-	1.22	> 10

^a EC₅₀ = half-maximal effective concentration.

^b CC₅₀ = half-maximal cytotoxic concentration.

aqueous solubility and cellular permeability. Within the 5-aryl-isothiazolo[4,3-*b*]pyridines, two compounds were investigated for antiviral activity. Whereas compound **14f** did not show antiviral activity, the 5-(3,4-dimethoxyphenyl) derivative **14g** was a potent GAK inhibitor (IC₅₀ = 0.024 μ M) demonstrating potent antiviral activity (EC₅₀ and CC₅₀ values of 1.049 μ M and > 10 μ M, respectively). Despite the fact that compound **14g** is less active as GAK ligand when compared to erlotinib (K_d = 3.1 nM), both compounds are equally active as anti-DENV agents. As erlotinib is known to affect multiple other kinases besides GAK, compound **14g** might be a better lead for the discovery of GAK inhibitors as antiviral drugs.

5. Molecular docking of compound **14g** into GAK

To rationalize the potent GAK affinity of compound **14g**, molecular docking was initiated starting from the co-crystal X-ray structure of GAK and compound **1** (PDB 4Y8D),¹⁴ with a docking protocol as described before,¹⁷ using the software packages Autodocktools and Autodock vina.^{25,26} Compound **14g** has a slightly different substituent at position 3 of the isothiazolo[4,3-*b*]pyridine scaffold from the original crystallized GAK inhibitor **1**. More specifically, compound **14g** bears a *cis*-2,6-dimethylmorpholino ring of which the intrinsic torsion angles are not flexible during docking. However, since the choice of the ring conformation might be important for the final docking orientation and since morpholine can exist in different conformations in crystallized structures,²⁷ we used different conformations of the morpholino ring of compound **14g** for docking. This analysis revealed that a chair conformation with both methyl groups in an equatorial orientation was optimal. The nitrogen has more a sp² character and lays in the same plane as the aromatic ring system. Compound **14g** docked in a favourable way in the ATP binding site. Primarily hydrophobic interactions were observed between GAK and compound **14g**, similarly to compound **1** (Fig. 3). One hydrogen bond with Thr123.B was observed.

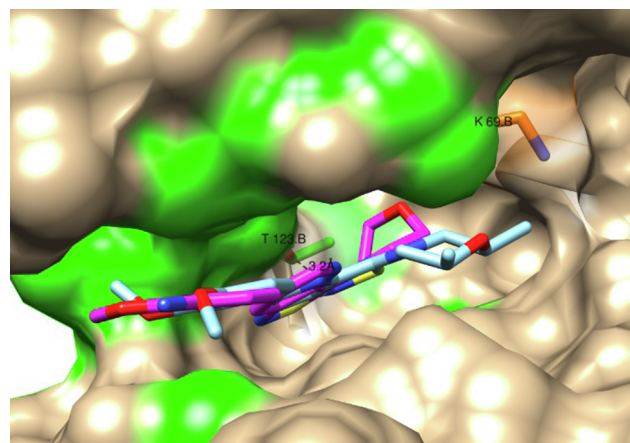


Fig. 3. Autodock Vina docking of compound **14g** (cyan carbons) superimposed on compound **1** (magenta carbons). Amino acids having van der Waals interactions are coloured as green surface.

During this docking process, a rigid enzyme conformation and a flexible ligand by variable torsion angles was applied. Taking into account induced fit effects, the observed interactions may in fact be more favourable. For instance, the Lys69.B side chain is within interaction distance with the oxygen atom of the morpholino ring, possibly forming a hydrogen bond, that is currently not detected.

6. Conclusion

Isothiazolo[4,3-*b*]pyridines are well known as potent and selective GAK inhibitors with antiviral activity. Prior research has focused on structural modifications of the scaffold and the substituent at position 3. In this manuscript, the SAR of the pyridine moiety of the isothiazolo [4,3-*b*]pyridine core structure was studied in detail. The insertion of various linkers between the 6-phenyl ring and the central scaffold generated compounds with decreased GAK affinity. However, position 4 of the 6-phenyl moiety tolerates some structural variety with respect to GAK affinity, and structural variation at this site can be used to modulate the antiviral activity. Furthermore, a novel class of 5-substituted isothiazolo[4,3-*b*]pyridines was synthesized, yielding selected congeners with potent GAK affinity and anti-DENV activity.

7. Experimental section

7.1. Chemistry

For all reactions, analytical grade solvents were used. Argon was used to carry out reactions under an inert atmosphere. Melting points were recorded with a Stuart SMP20 melting point apparatus. ¹H and ¹³C NMR spectra were recorded on a Bruker Avance 300 MHz instrument (¹H NMR, 300 MHz; ¹³C NMR, 75 MHz), 500 MHz instrument (¹H NMR, 500 MHz; ¹³C NMR, 125 MHz) or a 600 MHz instrument (¹H NMR, 600 MHz; ¹³C NMR, 150 MHz, ¹⁹F NMR, 471 MHz), using tetramethylsilane as internal standard for ¹H NMR spectra and DMSO-*d*₆ (39.5 ppm) or CDCl₃ (77.2 ppm) for ¹³C NMR spectra. Abbreviations used are s = singlet, d = doublet, t = triplet, q = quartet, m = multiplet, b = broad. Coupling constants are expressed in Hz. High resolution mass spectra were acquired on a quadrupole orthogonal acceleration time-of-flight mass spectrometer (Synapt G2 HDMS, Waters, Milford, MA). Samples were infused at 3 mL/min and spectra were obtained in positive or negative ionization mode with a resolution of 15,000 (FWHM) using leucine enkephalin as lock mass. Precoated aluminum sheets (Fluka silica gel/TLC-cards, 254 nm) were used for TLC. Column chromatography was performed on silica gel 0.060–0.200 mm, 60 (Acros Organics). Purity of final compounds was

verified to be > 95% by HPLC analysis. HPLC conditions to assess purity were as follows: Shimadzu HPLC equipped with a LC-20AT pump, DGU-20A5 degasser, and a SPD-20A UV-VIS detector; Symmetry C18 column (5 μ m, 4.6 mm \times 150 mm); gradient elution of H₂O/CH₃CN from 95/5 or 70/30 to 5/95 over 25 min; flow rate 1 mL/min; wavelength, UV 254 nm. Preparative HPLC purifications were performed using a Phenomenex Gemini 110A column (C18, 10 μ m, 21.2 mm \times 250 mm).

7.1.1. Synthesis of 6-aryl-3-(cis-2,6-dimethylmorpholino)isothiazolo[4,3-b]pyridines

General procedure. A solution of 6-bromo-3-(cis-2,6-dimethylmorpholino) isothiazolo[4,3-b]pyridine (1 equiv) in a mixture of dioxane/water (ratio 4:1) was degassed with argon and subsequently, were added the corresponding boronic acid (1.2 equiv), Pd(PPh₃)₄ (0.02 equiv) and K₂CO₃ (2 equiv). The mixture was degassed a second time, filled with argon and stirred at 90 °C overnight. After completion of the reaction as monitored by TLC, the volatiles were evaporated to dryness and the crude residue was diluted with EtOAc (20 mL) and washed with water (2 \times 20 mL). The organic layer was dried over anhydrous Na₂SO₄ and concentrated *in vacuo*. The resulting residue was purified by silica gel flash chromatography, yielding the corresponding 6-substituted-3-(cis-2,6-dimethylmorpholino)isothiazolo[4,3-b]pyridines. The following compounds were made according to this general procedure.

7.1.1.1. 3-(cis-2,6-Dimethylmorpholino)-6-(phenyl)isothiazolo[4,3-b]pyridine (5a). This compound was obtained using phenylboronic acid. The crude residue was purified by silica gel flash chromatography using a mixture of hexane and ethyl acetate (in a ratio of 4:1) as mobile phase, affording the title compound as an amorphous yellow solid in 89% yield (88.3 mg, 0.27 mmol). Mp 141.5–142.3 °C. ¹H NMR (500 MHz, CDCl₃) δ : 1.31 (d, *J* = 6.2, Hz, 6H, 2 \times CH₃), 2.91 (dd, *J* = 12.6, 10.7 Hz, 2H, 2 \times NCH), 3.91–3.99 (m, 2H, 2 \times OCH), 4.50–4.54 (m, 2H, 2 \times NCH), 7.41–7.45 (m, 1H, arom H), 7.48–7.52 (m, 2H, arom H), 7.62–7.68 (m, 2H, arom H), 7.90 (d, *J* = 2.1 Hz, 1H, arom H), 8.63 (d, *J* = 2.1 Hz, 1H, arom H) ppm. ¹³C NMR (126 MHz, CDCl₃) δ : 18.8 (CH₃), 55.4 (CH₂), 71.2 (CH), 125.6 (CH), 127.4 (CH), 128.4 (CH), 129.1 (CH), 134.2 (C), 135.8 (C), 137.6 (C), 144.3 (CH), 156.3 (C), 172.9 (C) ppm. HR-MS *m/z* [M + H]⁺ calcd for C₁₈H₁₉N₃O₂S: 326.1322, found 326.1319.

7.1.1.2. 6-(3,4-Dimethoxyphenyl)-3-(cis-2,6-dimethylmorpholino)isothiazolo[4,3-b]pyridine (5b). This compound was obtained using 3,4-dimethoxyphenylboronic acid. The crude residue was purified by silica gel flash chromatography using a mixture of hexane and ethyl acetate (in a ratio of 7:3) as mobile phase, affording the title compound as an amorphous yellow solid in 90% yield (52.7 mg, 0.13 mmol). Mp 156.2–157.9 °C. ¹H NMR (600 MHz, CDCl₃) δ : 1.32 (d, *J* = 6.3 Hz, 6H, 2 \times CH₃), 2.91 (dd, *J* = 12.5, 10.7 Hz, 2H, 2 \times NCH), 3.92–3.96 (m, 5H, OCH₃, 2 \times OCH), 3.96 (s, 3H, OCH₃), 4.51 (dd, *J* = 12.7, 1.9 Hz, 2H, 2 \times NCH), 7.00 (d, *J* = 8.3 Hz, 1H, arom H), 7.16 (d, *J* = 2.1 Hz, 1H, arom H), 7.24 (dd, *J* = 8.3, 2.1 Hz, 1H, arom H), 7.85 (d, *J* = 2.1 Hz, 1H, arom H), 8.63 (d, *J* = 2.1 Hz, 1H, arom H) ppm. ¹³C NMR (151 MHz, CDCl₃) δ : 18.8 (CH₃), 55.4 (CH₂), 56.0 (OCH₃), 56.0 (OCH₃), 71.2 (CH), 110.3 (CH), 111.6 (CH), 119.8 (CH), 124.8 (CH), 130.3 (C), 133.9 (C), 135.5 (C), 144.3 (CH), 149.5 (C), 149.5 (C), 156.4 (C), 172.9 (C) ppm. HR-MS *m/z* [M + H]⁺ calcd for C₂₀H₂₃N₃O₃S: 386.1532, found 386.1527.

7.1.1.3. 6-(3,4,5-Trimethoxyphenyl)-3-(cis-2,6-dimethylmorpholino)isothiazolo[4,3-b]pyridine (5c). This compound was obtained using 3,4,5-trimethoxyphenylboronic acid. The crude residue was purified by silica gel flash chromatography using a mixture of hexane and ethyl acetate (in a ratio of 7:3) as mobile phase, affording the title compound as an amorphous yellow solid in 91% yield (57.7 mg, 0.14 mmol). Mp 154.1–155.5 °C. ¹H NMR (500 MHz, CDCl₃) δ : 1.32 (d, *J* = 6.3 Hz, 6H,

2 \times CH₃), 2.92 (dd, *J* = 12.5, 10.7 Hz, 2H, 2 \times NCH), 3.91 (s, 3H, OCH₃), 3.93–3.97 (m, 8H, 2 \times OCH, 2 \times OCH₃), 4.52 (dd, *J* = 12.7, 1.9 Hz, 2H, 2 \times NCH), 6.85 (s, 2H, arom H), 7.87 (d, *J* = 2.1 Hz, 1H, arom H), 8.62 (d, *J* = 2.1 Hz, 1H, arom H) ppm. ¹³C NMR (126 MHz, CDCl₃) δ : 18.8 (CH₃), 55.4 (CH₂), 56.2 (OCH₃), 61.0 (OCH₃), 71.2 (CH), 104.6 (CH), 125.3 (CH), 133.3 (C), 134.1 (C), 135.8 (C), 138.5 (C), 144.1 (CH), 153.7 (C), 156.2 (C), 172.9 (C) ppm. HR-MS *m/z* [M + H]⁺ calcd for C₂₁H₂₅N₃O₄S: 416.1638, found 416.1629.

7.1.1.4. 6-(2-Methoxy-4-pyridyl)-3-(cis-2,6-dimethylmorpholino)isothiazolo[4,3-b]pyridine (5d). This compound was obtained using 2-methoxy-4-pyridine-4-boronic acid. The crude residue was purified by silica gel flash chromatography using a mixture of hexane and ethyl acetate (in a ratio of 7:3) as mobile phase, affording the title compound as an amorphous yellow solid in 87% yield (47.2 mg, 0.13 mmol). Mp 160.5–162.1 °C. ¹H NMR (600 MHz, CDCl₃) δ : 1.32 (d, *J* = 6.3 Hz, 6H, 2 \times CH₃), 2.93 (dd, *J* = 12.6, 10.7 Hz, 2H, 2 \times NCH), 3.91–3.97 (m, 2H, 2 \times OCH), 4.01 (s, 3H, OCH₃), 4.52 (dd, *J* = 12.7, 1.9 Hz, 2H, 2 \times NCH), 7.01–7.02 (m, 1H, arom H), 7.15 (dd, *J* = 5.3, 1.5 Hz, 1H, arom H), 7.94 (d, *J* = 2.1 Hz, 1H, arom H), 8.27–8.29 (m, 1H, arom H), 8.59 (d, *J* = 2.1 Hz, 1H, arom H) ppm. ¹³C NMR (151 MHz, CDCl₃) δ : 18.8 (CH₃), 53.6 (CH), 55.4 (CH₂), 71.2 (OCH₃), 108.9 (CH), 115.2 (CH), 126.4 (CH), 133.0 (C), 135.0 (C), 142.9 (CH), 147.7 (CH), 147.8 (C), 155.7 (C), 164.9 (C), 173.2 (C) ppm. HR-MS *m/z* [M + H]⁺ calcd for C₁₈H₂₀N₄O₂S: 357.1380, found 357.1374.

7.1.1.5. 6-(2-Methoxy-5-pyridyl)-3-(cis-2,6-dimethylmorpholino)isothiazolo[4,3-b]pyridine (5e). This compound was obtained using 2-methoxy-5-pyridineboronic acid. The crude residue was purified by silica gel flash chromatography using a mixture of hexane and ethyl acetate (in a ratio of 7:3) as mobile phase, affording the title compound as an amorphous yellow solid in 88% yield (47.7 mg, 0.13 mmol). Mp 160.2–162.1 °C. ¹H NMR (600 MHz, CDCl₃) δ : 1.32 (d, *J* = 6.3 Hz, 6H, 2 \times CH₃), 2.92 (dd, *J* = 12.5, 10.7 Hz, 2H, 2 \times NCH), 3.91–3.97 (m, 2H, 2 \times OCH), 4.00 (s, 3H, OCH₃), 4.51 (dd, *J* = 12.7, 1.9 Hz, 2H, 2 \times NCH), 6.88 (dd, *J* = 8.6, 0.6 Hz, 1H, arom H), 7.82–7.87 (m, 2H, arom H), 8.47 (dd, *J* = 2.5, 0.6 Hz, 1H, arom H), 8.57 (d, *J* = 2.1 Hz, 1H, arom H) ppm. ¹³C NMR (151 MHz, CDCl₃) δ : 18.8 (CH₃), 53.7 (OCH₃), 55.4 (CH₂), 71.2 (CH), 111.4 (CH), 125.0 (CH), 126.5 (C), 132.6 (C), 134.1 (C), 137.4 (CH), 143.4 (CH), 145.4 (CH), 156.0 (C), 164.2 (C), 173.0 (C) ppm. HR-MS *m/z* [M + H]⁺ calcd for C₁₈H₂₀N₄O₂S: 357.1380, found 357.1374.

7.1.1.6. 6-(3-Methoxy-4-carboxyphenyl)-3-(cis-2,6-dimethylmorpholino)isothiazolo[4,3-b]pyridine (5f). This compound was obtained using 3-methoxy-4-carboxyphenylboronic acid. After completion of the reaction, a solution of HCl (1 M) was added until reach pH acid. The crude residue was purified by silica gel flash chromatography using a mixture of dichloromethane and methanol (in a ratio of 20:1) as mobile phase, affording the title compound as an amorphous yellow solid in 78% yield (47.4 mg, 0.12 mmol). Mp 251.3–253.1 °C. ¹H NMR (600 MHz, DMSO) δ : 1.20 (d, *J* = 6.2 Hz, 6H, 2 \times CH₃), 2.91 (dd, *J* = 12.1, 11.0 Hz, 2H, 2 \times NCH), 3.83–3.89 (m, 2H, 2 \times OCH), 3.94 (s, 3H, OCH₃), 4.52 (d, *J* = 12.0 Hz, 2H, 2 \times NCH), 7.45 (dd, *J* = 8.0, 1.4 Hz, 1H, arom H), 7.52 (d, *J* = 1.2 Hz, 1H, arom H), 7.75 (d, *J* = 7.9 Hz, 1H, arom H), 8.15 (d, *J* = 2.0 Hz, 1H, arom H), 8.81 (d, *J* = 2.0 Hz, 1H, arom H) ppm. ¹³C NMR (151 MHz, DMSO) δ : 18.6 (CH₃), 54.8 (CH₂), 56.1 (OCH₃), 70.6 (CH), 111.5 (CH), 118.9 (CH), 121.1 (C), 125.7 (CH), 131.5 (CH), 133.8 (C), 134.0 (C), 141.4 (C), 143.8 (CH), 155.4 (C), 158.7 (C), 167.1 (C), 172.5 (C) ppm. HR-MS *m/z* [M + H]⁺ calcd for C₂₀H₂₁N₃O₄S: 400.1325, found 400.1324.

7.1.1.7. 6-(trans-Styryl)-3-(cis-2,6-dimethylmorpholino)isothiazolo[4,3-b]pyridine (5g). A solution of 6-bromo-3-(cis-2,6-dimethylmorpholino)isothiazolo[4,3-b]pyridine (1 equiv) in DMF was degassed with argon. Styrene (1.5 equiv), *N*-phenylurea (0.02 equiv), Pd(OAc)₂ (0.01 equiv)

and K_2CO_3 (2 equiv) were added. The resulting mixture was degassed a second time, filled with argon and stirred at 120 °C overnight. After completion of the reaction as monitored by TLC, the volatiles were evaporated to dryness and the crude residue was diluted with EtOAc (20 mL) and washed with a 0.5 M HCl solution (2 × 10 mL) and water (20 mL). The organic layer was dried over anhydrous Na_2SO_4 and concentrated *in vacuo*. The resulting residue was purified by silica gel flash chromatography using a mixture of hexane and ethyl acetate (in a ratio of 4:1) as mobile phase, affording the title compound as an amorphous yellow solid in 88% yield (47 mg, 0.13 mmol). Mp 177.4–178.5 °C. 1H NMR (600 MHz, $CDCl_3$) δ : 1.31 (d, $J = 6.3$ Hz, 6H, 2 × CH_3), 2.89 (dd, $J = 12.2, 10.9$ Hz, 2H, 2 × NCH), 3.90–3.97 (m, 2H, 2 × OCH), 4.48 (dd, $J = 12.7, 1.6$ Hz, 2H, NCH), 7.12 (d, $J = 16.4$ Hz, 1H, double bond CH), 7.28 (d, $J = 16.4$ Hz, 1H, double bond CH), 7.32 (t, $J = 7.3$ Hz, 1H, arom H), 7.40 (t, $J = 7.7$ Hz, 2H, arom H), 7.56 (d, $J = 7.5$ Hz, 2H, arom H), 7.74 (d, $J = 1.8$ Hz, 1H, arom H), 8.61 (d, $J = 1.9$ Hz, 1H, arom H) ppm. ^{13}C NMR (151 MHz, $CDCl_3$) δ : 18.8 (CH_3), 55.4 (CH_2), 71.2 (CH), 124.9 (CH), 125.3 (CH), 126.8 (CH), 128.4 (CH), 128.8 (CH), 131.7 (CH), 132.2 (C), 134.0 (C), 136.5 (C), 143.4 (CH), 156.4 (C), 172.7 (C) ppm. HR-MS m/z [$M+H$] $^+$ calcd for $C_{20}H_{21}N_3OS$: 352.1478, found 352.1473.

7.1.2. Synthesis of 6-anilino-3-(*cis*-2,6-dimethylmorpholino)isothiazolo[4,3-*b*]pyridines

General procedure. Pd(dba) $_2$ (0.03 equiv) and SPhos (0.06 equiv) were added to a degassed solution of toluene (15 mL). The resulting mixture was stirred under argon for 5–10 min. Subsequently, 6-bromo-3-(*cis*-2,6-dimethylmorpholino)isothiazolo[4,3-*b*]pyridine (1 equiv), the appropriate aniline or ethynylbenzene (1.5 equiv) and *t*-BuOK (1.5 equiv) were added and the mixture was degassed a second time. The reaction was filled with argon and stirred at 90 °C for 4–5 h. After completion of the reaction as monitored by TLC, the volatiles were evaporated to dryness. The crude residue was diluted with EtOAc (20 mL) and washed twice with a 0.5 M HCl solution (2 × 10 mL) and brine (20 mL). The organic layer was dried over anhydrous Na_2SO_4 and concentrated *in vacuo*. The resulting residue was purified by silica gel flash chromatography, yielding the corresponding 6-substituted-3-(*cis*-2,6-dimethylmorpholino)isothiazolo[4,3-*b*]pyridines. The following compounds were made according to this procedure.

7.1.2.1. 3-(*cis*-2,6-Dimethylmorpholino)-6-(phenylamino)isothiazolo[4,3-*b*]pyridine (5h). This compound was obtained using aniline. The crude residue was purified by silica gel flash chromatography using a mixture of hexane and ethyl acetate (in a ratio of 7:3) as mobile phase, affording the title compound as an amorphous yellow solid in 85% yield (44 mg, 0.13 mmol). Mp 186.1–187.5 °C. 1H NMR (600 MHz, $CDCl_3$) δ : 1.29 (d, $J = 6.3$ Hz, 6H, 2 × CH_3), 2.83–2.89 (m, 2H, 2 × NCH), 3.87–3.95 (m, 2H, 2 × OCH), 4.41 (d, $J = 12.3$ Hz, 2H, 2 × NCH), 6.04 (bs, 1H, NH), 7.04 (t, $J = 7.3$ Hz, 1H, arom H), 7.17 (d, $J = 7.7$ Hz, 2H, arom H), 7.26 (s, 1H, arom H), 7.32 (t, $J = 7.8$ Hz, 2H, arom H), 8.10 (d, $J = 2.4$ Hz, 1H, arom H) ppm. ^{13}C NMR (151 MHz, $CDCl_3$) δ : 18.8 (CH_3), 55.3 (CH_2), 71.2 (CH), 106.7 (CH), 119.6 (CH), 122.9 (CH), 129.5 (CH), 129.9 (C), 139.2 (C), 140.1 (CH), 140.8 (C), 157.2 (C), 172.0 (C) ppm. HR-MS m/z [$M+H$] $^+$ calcd for $C_{18}H_{20}N_4OS$: 341.1431, found 341.1431.

7.1.2.2. 6-(3,4-Dimethoxyphenylamino)-3-(*cis*-2,6-dimethylmorpholino)isothiazolo[4,3-*b*]pyridine (5i). This compound was obtained using 3,4-dimethoxyaniline. The crude residue was purified by silica gel flash chromatography using a mixture of hexane and ethyl acetate (in a ratio of 3:2) as mobile phase, affording the title compound as an amorphous yellow solid in 79% yield (48 mg, 0.12 mmol). Mp 207.1–208.9 °C. 1H NMR (600 MHz, $CDCl_3$) δ : 1.29 (d, $J = 6.3$ Hz, 6H, 2 × CH_3), 2.86 (dd, $J = 12.5, 10.7$ Hz, 2H, 2 × NCH), 3.86 (s, 3H, OCH_3), 3.89 (s, 3H, OCH_3), 3.90–3.94 (m, 2H, 2 × OCH), 4.40 (dd, $J = 12.6, 1.6$ Hz, 2H, 2 × NCH), 5.78 (bs, 1H, NH), 6.75–6.79 (m, 2H, arom H), 6.85 (d,

$J = 8.2$ Hz, 1H, arom H), 7.06 (d, $J = 2.4$ Hz, 1H, arom H), 8.05 (d, $J = 2.5$ Hz, 1H, arom H) ppm. ^{13}C NMR (151 MHz, $CDCl_3$) δ : 18.9 (CH_3), 55.5 (CH_2), 56.1 (OCH_3), 56.4 (OCH_3), 71.4 (CH), 105.1 (CH), 106.5 (CH), 112.2 (CH), 113.9 (CH), 129.7 (C), 133.9 (C), 139.8 (CH), 140.9 (C), 146.1 (C), 149.9 (C), 157.5 (C), 172.1 (C) ppm. HR-MS m/z [$M+H$] $^+$ calcd for $C_{20}H_{24}N_4O_3S$: 401.1642, found 401.1638.

7.1.2.3. 6-(3,4,5-Trimethoxyanilino)-3-(*cis*-2,6-dimethylmorpholino)isothiazolo[4,3-*b*]pyridine (5j). This compound was obtained using 3,4,5-trimethoxyaniline. The crude residue was purified by silica gel flash chromatography using a mixture of hexane and ethyl acetate (in a ratio of 3:2) as mobile phase, affording the title compound as an amorphous yellow solid in 73% yield (47.8 mg, 0.11 mmol). Mp 252.2–253.5 °C. 1H NMR (300 MHz, $CDCl_3$) δ : 1.29 (d, $J = 6.3$ Hz, 6H, 2 × CH_3), 2.86 (dd, $J = 12.5, 10.7$ Hz, 2H, 2 × NCH), 3.83 (s, 6H, 2 × OCH_3), 3.83 (s, 3H, OCH_3), 3.86–3.98 (m, 2H, 2 × OCH), 4.41 (dd, $J = 12.8, 2.0$ Hz, 2H, 2 × NCH), 5.88 (bs, 1H, NH), 6.42 (s, 2H, arom H), 7.18 (d, $J = 2.5$ Hz, 1H, arom H), 8.08 (d, $J = 2.5$ Hz, 1H, arom H) ppm. ^{13}C NMR (151 MHz, $CDCl_3$) δ : 18.8 (CH_3), 55.3 (CH_2), 56.2 (OCH_3), 61.0 (OCH_3), 71.2 (CH), 98.2 (CH), 106.4 (CH), 129.8 (C), 134.3 (C), 136.8 (C), 139.7 (C), 139.8 (CH), 154.0 (C), 157.2 (C), 172.1 (C) ppm. HR-MS m/z [$M+H$] $^+$ calcd for $C_{21}H_{26}N_4O_4S$: 431.1747, found 431.1745.

7.1.2.4. 3-(*cis*-2,6-Dimethylmorpholino)-6-(phenylethynyl)isothiazolo[4,3-*b*]pyridine (5k). This compound was obtained using ethynylbenzene. The crude residue was purified by silica gel flash chromatography using a mixture of hexane and ethyl acetate (in a ratio of 4:1) as mobile phase, affording the title compound as an amorphous yellow solid in 87% yield (46.3 mg, 0.13 mmol). Mp 162.4–163.8 °C. 1H NMR (500 MHz, $CDCl_3$) δ : 1.31 (d, $J = 6.1$ Hz, 6H, 2 × CH_3), 2.90 (t, $J = 11.5$ Hz, 2H, 2 × NCH), 3.90–3.98 (m, 2H, 2 × OCH), 4.47 (d, $J = 12.5$ Hz, 2H, 2 × NCH), 7.35–7.41 (m, 3H, arom H), 7.56–7.61 (m, 2H, arom H), 7.89 (s, 1H, arom H), 8.39 (s, 1H, arom H) ppm. ^{13}C NMR (126 MHz, $CDCl_3$) δ : 18.8 (CH_3), 55.4 (CH_2), 71.2 (CH), 86.6 (C), 93.4 (C), 119.4 (C), 122.5 (C), 128.5 (CH), 128.9 (CH), 130.9 (CH), 131.8 (CH), 133.6 (C), 145.5 (CH), 155.0 (C), 173.0 (C) ppm. HR-MS m/z [$M+H$] $^+$ calcd for $C_{20}H_{19}N_3OS$: 350.1322, found 350.1315.

7.1.3. Synthesis of 6-(benzamide-4-yl)-3-(*cis*-2,6-dimethylmorpholino)isothiazolo[4,3-*b*]pyridines

General procedure. To a solution of compound 5f (6-(3-methoxy-4-carboxyphenyl)-3-(*cis*-2,6-dimethylmorpholino)isothiazolo[4,3-*b*]pyridine) (1 equiv) in dry dichloromethane (15 mL) was added thionyl chloride ($SOCl_2$) (2 equiv). The mixture was stirred at 40 °C for 3 h. Then, triethylamine (2 equiv) and the appropriate amine (2 equiv) were added and the resulting mixture was stirred at room temperature overnight. After completion of the reaction as monitored by TLC, the residue was diluted with dichloromethane (20 mL) and washed with 0.5 M HCl solution (2 × 10 mL) and water (20 mL). The organic layer was dried over anhydrous Na_2SO_4 and concentrated *in vacuo*. The resulting residue was purified by silica gel flash chromatography, yielding the title compound. The following compounds were made according to this procedure.

7.1.3.1. 6-(2-Methoxybenzamide-4-yl)-3-(*cis*-2,6-dimethylmorpholino)isothiazolo[4,3-*b*]pyridine (6a). This compound was obtained using aqueous ammonia (25%) (2 mL). After completion of the reaction as monitored by TLC, water (15 mL) was added, followed by extraction with dichloromethane (2 × 20 mL). The organic layer was dried over anhydrous Na_2SO_4 and concentrated *in vacuo*. The resulting residue was purified by silica gel flash chromatography, using a mixture of dichloromethane and methanol (20:0.5) as mobile phase, yielding the title compound as an amorphous yellow solid in 67% yield (33.4 mg, 0.08 mmol). Mp 270.6–272.2 °C. 1H NMR (300 MHz, DMSO) δ : 1.20 (d, $J = 6.2$ Hz, 6H, 2 × CH_3), 2.90 (dd, $J = 12.2, 11.0$ Hz, 2H, 2 × NCH),

3.87 (dd, $J = 12.3, 4.3$ Hz, 2H, $2 \times$ OCH), 4.03 (s, 3H, OCH₃), 4.51 (d, $J = 12.3$ Hz, 2H, $2 \times$ NCH), 7.48 (dd, $J = 8.1, 1.5$ Hz, 1H, arom H), 7.53 (s, 1H, arom H), 7.62 (bs, 1H, NH), 7.70 (bs, 1H, NH), 7.91 (d, $J = 8.0$ Hz, 1H, arom H), 8.15 (d, $J = 2.1$ Hz, 1H, arom H), 8.81 (d, $J = 2.1$ Hz, 1H, arom H) ppm. ¹³C NMR (75 MHz, DMSO) δ : 18.7 (CH₃), 55.0 (CH₂), 56.3 (OCH₃), 70.7 (CH), 111.1 (CH), 119.4 (CH), 122.7 (C), 125.6 (CH), 131.6 (CH), 133.8 (C), 134.1 (C), 140.9 (C), 143.9 (CH), 155.5 (C), 157.9 (C), 166.0 (C), 172.5 (C) ppm. HR-MS m/z [M+H]⁺ calcd for C₂₀H₂₂N₄O₃S: 399.1485, found 399.1483.

7.1.3.2. 6-(N-Cyclopropyl-2-methoxybenzamide-4-yl)-3-(cis-2,6-dimethylmorpholino) isothiazolo[4,3-b]pyridine (6b). This compound was obtained using cyclopropylamine. The crude residue was purified by silica gel flash chromatography using a mixture of hexane and ethyl acetate (in a ratio of 3:7) as mobile phase, affording the title compound as an amorphous yellow solid in 70% yield (38 mg, 0.09 mmol). Mp 195.1–196.8 °C. ¹H NMR (600 MHz, CDCl₃) δ : 0.61–0.64 (m, 2H, CH₂), 0.86–0.91 (m, 2H, CH₂), 1.33 (d, $J = 6.3$ Hz, 6H, $2 \times$ CH₃), 2.91–2.99 (m, 3H, CH, $2 \times$ NCH), 3.92–3.99 (m, 2H, $2 \times$ OCH), 4.03 (s, 3H, OCH₃), 4.53 (dd, $J = 12.7, 1.8$ Hz, 2H, $2 \times$ NCH), 7.20 (d, $J = 1.6$ Hz, 1H, arom H), 7.38 (dd, $J = 8.1, 1.6$ Hz, 1H, arom H), 7.91 (d, $J = 2.8$ Hz, 1H, NH), 7.93 (d, $J = 2.1$ Hz, 1H, arom H), 8.35 (d, $J = 8.1$ Hz, 1H, arom H), 8.63 (d, $J = 2.1$ Hz, 1H, arom H) ppm. ¹³C NMR (151 MHz, CDCl₃) δ : 6.9 (CH₂), 18.8 (CH₃), 22.9 (CH), 55.4 (CH₂), 56.1 (OCH₃), 71.2 (CH), 110.3 (CH), 120.3 (CH), 121.3 (C), 126.1 (CH), 133.1 (CH), 134.5 (C), 134.8 (C), 142.1 (C), 143.6 (CH), 155.9 (C), 157.8 (C), 166.1 (C), 173.1 (C) ppm. HR-MS m/z [M+H]⁺ calcd for C₂₃H₂₆N₄O₃S: 439.1798, found 439.1798.

7.1.3.3. (4-(3-(cis-2,6-Dimethylmorpholino)isothiazolo[4,3-b]pyridin-6-yl)-2-methoxyphenyl)(pyrrolidin-1-yl)methanone (6c). This compound was obtained using pyrrolidine. The crude residue was purified by silica gel flash chromatography using a mixture of dichloromethane and methanol (in a ratio of 10:0.1) as mobile phase, affording the title compound as an amorphous yellow solid in 65% yield (36.6 mg, 0.08 mmol). Mp 173.1–174.9 °C. ¹H NMR (600 MHz, CDCl₃) δ : 1.32 (d, $J = 6.3$ Hz, 6H, $2 \times$ CH₃), 1.86–1.92 (m, 2H, CH₂), 1.94–2.01 (m, 2H, CH₂), 2.93 (dd, $J = 12.5, 10.7$ Hz, 2H, $2 \times$ NCH), 3.30 (t, $J = 6.7$ Hz, 2H, CH₂), 3.68 (t, $J = 7.0$ Hz, 2H, CH₂), 3.92 (s, 3H, OCH₃), 3.93–3.98 (m, 2H, $2 \times$ OCH), 4.53 (dd, $J = 12.7, 1.8$ Hz, 2H, $2 \times$ NCH), 7.16 (d, $J = 1.4$ Hz, 1H, arom H), 7.27 (dd, $J = 7.7, 1.5$ Hz, 1H, arom H), 7.40 (d, $J = 7.7$ Hz, 1H, arom H), 7.90 (d, $J = 2.1$ Hz, 1H, arom H), 8.61 (d, $J = 2.1$ Hz, 1H, arom H) ppm. ¹³C NMR (151 MHz, CDCl₃) δ : 18.8 (CH₃), 24.6 (CH₂), 25.8 (CH₂), 45.6 (CH₂), 47.7 (CH₂), 55.4 (CH₂), 55.7 (OCH₃), 71.2 (CH), 110.2 (CH), 119.9 (CH), 125.8 (CH), 127.5 (C), 128.6 (CH), 134.3 (C), 135.3 (C), 139.9 (C), 143.9 (CH), 155.8 (C), 156.0 (C), 167.2 (C), 173.0 (C) ppm. HR-MS m/z [M+H]⁺ calcd for C₂₄H₂₈N₄O₃S: 453.1955, found 453.1945.

7.1.3.4. (4-(3-(cis-2,6-Dimethylmorpholino)isothiazolo[4,3-b]pyridin-6-yl)-2-methoxyphenyl)(morpholino)methanone (6d). This compound was obtained using morpholine. The crude residue was purified by silica gel flash chromatography using a mixture of hexane and ethyl acetate (in a ratio of 3:7) as mobile phase, affording the title compound as an amorphous yellow solid in 68% yield (39 mg, 0.08 mmol). Mp 134.2–135.9 °C. ¹H NMR (600 MHz, CDCl₃) δ : 1.32 (d, $J = 6.3$ Hz, 6H, $2 \times$ CH₃), 2.90–2.97 (m, 2H, $2 \times$ NCH), 3.27–3.40 (m, 2H, CH₂), 3.58–3.71 (m, 2H, CH₂), 3.76–3.89 (m, 4H, $2 \times$ CH₂), 3.93 (s, 3H, OCH₃), 3.93–3.98 (m, 2H, $2 \times$ OCH), 4.53 (d, $J = 11.3$ Hz, 2H, $2 \times$ NCH), 7.15 (d, $J = 1.2$ Hz, 1H, arom H), 7.29 (dd, $J = 7.7, 1.4$ Hz, 1H, arom H), 7.39 (d, $J = 7.7$ Hz, 1H, arom H), 7.90 (d, $J = 1.7$ Hz, 1H, arom H), 8.60 (d, $J = 1.9$ Hz, 1H, arom H) ppm. ¹³C NMR (151 MHz, CDCl₃) δ : 18.8 (CH₃), 42.2 (CH₂), 47.4 (CH₂), 55.4 (CH₂), 55.7 (OCH₃), 66.8 (CH₂), 67.0 (CH₂), 71.2 (CH), 110.0 (CH), 120.2 (CH), 125.3 (C), 125.9 (CH), 128.9 (CH), 135.1 (C), 140.3 (C), 143.7 (CH), 155.8 (C), 167.3 (C), 173.1 (C) ppm. HR-MS m/z [M+H]⁺

calcd for C₂₄H₂₈N₄O₃S: 469.1904, found 469.1898.

7.1.3.5. 3-(cis-2,6-Dimethylmorpholino)-6-(N-phenyl-2-methoxybenzamide-4-yl)isothiazolo[4,3-b]pyridine (6e). This compound was obtained using aniline. The crude residue was purified by silica gel flash chromatography using a mixture of hexane and ethyl acetate (in a ratio of 3:2) as mobile phase, affording the title compound as an amorphous yellow solid in 76% yield (45 mg, 0.09 mmol). Mp 251.1–252.5 °C. ¹H NMR (600 MHz, CDCl₃) δ : 1.33 (d, $J = 6.3, 6$ Hz, $2 \times$ CH₃), 2.94 (dd, $J = 12.6, 10.7$ Hz, 2H, $2 \times$ NCH), 3.92–3.98 (m, 2H, $2 \times$ OCH), 4.14 (s, 3H, OCH₃), 4.53 (dd, $J = 12.6, 1.7$ Hz, 2H, $2 \times$ NCH), 7.13–7.16 (m, 1H, arom H), 7.27 (d, $J = 1.5$ Hz, 1H, arom H), 7.36–7.40 (m, 2H, arom H), 7.42 (dd, $J = 8.1, 1.6$ Hz, 1H, arom H), 7.69–7.71 (dd, $J = 8.5, 1.0$ Hz, 2H, arom H), 7.95 (d, $J = 2.1$ Hz, 1H, arom H), 8.40 (d, $J = 8.1$ Hz, 1H, arom H), 8.64 (d, $J = 2.1$ Hz, 1H, arom H), 9.79 (s, 1H, NH) ppm. ¹³C NMR (151 MHz, CDCl₃) δ : 18.8 (CH₃), 55.4 (CH₂), 56.4 (OCH₃), 71.2 (CH), 110.5 (CH), 120.4 (CH), 120.6 (CH), 121.6 (C), 124.3 (CH), 126.1 (CH), 129.0 (CH), 133.4 (CH), 134.5 (C), 138.3 (C), 142.6 (C), 143.5 (CH), 155.8 (C), 157.6 (C), 162.7 (C), 173.1 (C) ppm. HR-MS m/z [M+H]⁺ calcd for C₂₆H₂₆N₄O₃S 475.1798, found 475.1799.

7.1.3.6. 6-(N-Benzyl-2-methoxybenzamide-4-yl)-3-(cis-2,6-dimethylmorpholino) isothiazolo[4,3-b]pyridine (6f). This compound was obtained using benzylamine. The crude residue was purified by silica gel flash chromatography using a mixture of hexane and ethyl acetate (in a ratio of 1:1) as mobile phase, affording the title compound as an amorphous yellow solid in 85% yield (51.2 mg, 0.11 mmol). Mp 172.2–173.4 °C. ¹H NMR (600 MHz, CDCl₃) δ : 1.32 (d, $J = 6.2$ Hz, 6H, $2 \times$ CH₃), 2.93 (dd, $J = 12.2, 11.0$ Hz, 2H, $2 \times$ NCH), 3.91–3.98 (m, 2H, $2 \times$ OCH), 4.00 (s, 3H, OCH₃), 4.53 (d, $J = 11.6$ Hz, 2H, $2 \times$ NCH), 4.72 (d, $J = 5.6$ Hz, 2H, CH₂), 7.21 (d, $J = 0.8$ Hz, 1H, arom H), 7.27–7.31 (m, 1H, arom H), 7.33–7.42 (m, 5H, arom H), 7.93 (d, $J = 1.9$ Hz, 1H, arom H), 8.20 (m, 1H, NH), 8.38 (d, $J = 8.1$ Hz, 1H, arom H), 8.63 (d, $J = 1.9$ Hz, 1H, arom H) ppm. ¹³C NMR (151 MHz, CDCl₃) δ : 18.8 (CH₃), 43.8 (CH₂), 55.4 (CH₂), 56.1 (OCH₃), 71.2 (CH), 110.3 (CH), 120.3 (CH), 121.3 (C), 126.1 (CH), 127.3 (CH), 127.5 (CH), 128.7 (CH), 133.3 (CH), 134.5 (C), 134.7 (C), 138.7 (C), 142.2 (C), 143.6 (CH), 155.9 (C), 157.9 (C), 164.8 (C), 173.1 (C) ppm. HR-MS m/z [M+H]⁺ calcd for C₂₇H₂₈N₄O₃S: 489.1955, found 489.1946.

7.1.3.7. 6-(3-Methoxy-4-formamidophenyl)-3-(cis-2,6-dimethylmorpholino)isothiazolo[4,3-b]pyridine (7a). To a solution of 6-(4-amino-3-methoxyphenyl)-3-(cis-2,6-dimethylmorpholino)isothiazolo[4,3-b]pyridine (1 equiv) in formamide (10 mL) was added MnO₂ (5% mol) in one portion. The reaction mixture was stirred at 150 °C for 5 h. After completion of the reaction as monitored by TLC, the volatiles were evaporated to dryness and the residue was purified by silica gel flash chromatography, using a mixture of hexane and acetyl acetate, yielding the title compound as an amorphous yellow solid in 73% yield (39.2 mg, 0.10 mmol). Mp 234.3–235.7 °C. Doubling of signals for the protons of the amine and the formyl group in the ¹H NMR spectrum at 25 °C was observed, due to restricted rotation around the C–N amide bond. Based on the integration of the signals in ¹H NMR spectrum, the ratio of the isomers was determined to be 95:5 (*cis:trans*).²⁸ When running the ¹H NMR spectrum at 50 °C, coalescence of both signals is observed (see Supporting Information). ¹H NMR (600 MHz, DMSO) δ : 1.19 (d, $J = 6.2$ Hz, 6H, $2 \times$ CH₃), 2.89 (t, $J = 11.5$ Hz, 2H, $2 \times$ NCH), 3.83–3.89 (m, 2H, $2 \times$ OCH), 3.98 (s, 3H, OCH₃), 4.51 (d, $J = 12.0$ Hz, 1H, $2 \times$ NCH), 7.42 (dd, $J = 8.3, 1.3$ Hz, 1H, arom H), 7.50 (d, $J = 1.4$ Hz, 1H, arom H), 8.06 (d, $J = 1.8$ Hz, 1H, arom H), 8.31 (d, $J = 8.3$ Hz, 1H, arom H), 8.35 (d, $J = 1.3$ Hz, 1H, HCO), 8.80 (d, $J = 1.8$ Hz, 1H, arom H), 9.80 (s, 1H, NH) ppm. ¹³C NMR (151 MHz, DMSO) δ : 18.6 (CH₃), 54.8 (CH₂), 56.2 (OCH₃), 70.6 (CH), 110.0 (CH), 119.5 (CH), 120.5 (CH), 124.3 (CH), 127.5 (C), 132.3 (C), 133.3 (C), 134.5 (C), 144.0 (CH), 149.0 (C), 155.7 (C), 160.3 (HCO), 172.3 (C)

ppm. HR-MS m/z $[M+H]^+$ calcd for $C_{20}H_{22}N_4O_3S$: 399.1485, found 399.1485.

7.1.4. Synthesis of 6-(4-aminyl-3-methoxyphenyl)-3-(cis-2,6-dimethylmorpholino) isothiazolo[4,3-b]pyridine

General procedure. To a solution of the precursor (6-(4-amino-3-methoxyphenyl)-3-(cis-2,6-dimethylmorpholino)isothiazolo[4,3-b]pyridine) (1 equiv) in dry dichloromethane (15 mL), was added trimethylamine (2 equiv). The reaction mixture was stirred under argon for 10 min and cooled to 0 °C. Then, the appropriate acid chloride (1.5 equiv) or acetic anhydride (2 equiv) was added and the resulting mixture was stirred at room temperature overnight. After completion of the reaction as monitored by TLC, dichloromethane was added (10 mL) and the reaction mixture was washed with 0.5 M HCl solution (2 × 10 mL) and water (20 mL). The organic layer was dried over anhydrous Na_2SO_4 and concentrated *in vacuo*. The resulting residue was purified by silica gel flash chromatography, yielding the title compound. The following compounds were made according to this procedure.

7.1.4.1. 6-(3-Methoxy-4-acetamidophenyl)-3-(cis-2,6-dimethylmorpholino) isothiazolo[4,3-b]pyridine (7b). This compound was obtained using acetic anhydride. The crude residue was purified by silica gel flash chromatography using a mixture of dichloromethane and acetone (in a ratio of 95:5) as mobile phase, affording the title compound as an amorphous yellow solid in 73% yield (32.5 mg, 0.08 mmol). Mp 255.1–256–4 °C. 1H NMR (600 MHz, $CDCl_3$) δ : 1.32 (d, $J = 6.3$ Hz, 6H, 2 × CH_3), 2.24 (s, 3H, CH_3), 2.92 (dd, $J = 12.6, 10.7$ Hz, 2H, 2 × NCH), 3.92–3.98 (m, 5H, 2 × OCH, OCH_3), 4.52 (dd, $J = 12.8, 1.9$ Hz, 2H, 2 × NCH), 7.14 (d, $J = 1.9$ Hz, 1H, arom H), 7.28 (dd, $J = 8.3, 1.9$ Hz, 1H, arom H), 7.82 (s, 1H, NH), 7.86 (d, $J = 2.1$ Hz, 1H, arom H), 8.49 (d, $J = 8.4$ Hz, 1H, arom H), 8.63 (d, $J = 2.1$ Hz, 1H, arom H) ppm. ^{13}C NMR (151 MHz, $CDCl_3$) δ : 18.8 (CH_3), 25.0 (CH_3), 55.4 (CH_2), 55.8 (OCH_3), 71.2 (CH), 108.7 (CH), 120.1 (CH), 120.2 (CH), 125.0 (CH), 128.1 (C), 132.9 (C), 134.0 (C), 135.4 (C), 144.1 (CH), 148.1 (C), 156.3 (C), 168.2 (C), 172.9 (C) ppm. HR-MS m/z $[M+H]^+$ calcd for $C_{21}H_{24}N_4O_3S$: 413.1642, found 413.1638.

7.1.4.2. 6-(3-Methoxy-4-cyclopropylamidophenyl)-3-(cis-2,6-dimethylmorpholino) isothiazolo[4,3-b]pyridine (7c). This compound was obtained using cyclopropanecarbonyl chloride. The crude residue was purified by silica gel flash chromatography using a mixture of hexane and ethyl acetate (in a ratio of 6:4) as mobile phase, affording the title compound as an amorphous yellow solid in 79% yield (37 mg, 0.08 mmol). Mp 256.4–257.8 °C. 1H NMR (500 MHz, $CDCl_3$) δ : 0.85–0.91 (m, 2H, CH_2), 1.10–1.14 (m, 2H, CH_2), 1.32 (d, $J = 6.3$ Hz, 6H, 2 × CH_3), 1.57–1.64 (m, 1H, CH), 2.92 (dd, $J = 12.5, 10.7$ Hz, 2H, 2 × NCH), 3.94 (m, 2H, 2 × OCH), 3.98 (s, 3H, OCH_3), 4.51 (dd, $J = 12.6, 1.7$ Hz, 2H, 2 × NCH), 7.15 (d, $J = 1.9$ Hz, 1H, arom H), 7.26–7.28 (m, 1H, arom H), 7.86 (d, $J = 2.1$ Hz, 1H, arom H), 8.05 (bs, 1H, NH), 8.48 (d, $J = 8.2$ Hz, 1H, arom H), 8.64 (d, $J = 2.1$ Hz, 1H, arom H) ppm. ^{13}C NMR (126 MHz, $CDCl_3$) δ : 8.1 (CH_2), 18.8 (CH_3), 55.4 (CH_2), 55.8 (CH_3), 71.2 (CH), 108.8 (CH), 120.0 (CH), 120.2 (CH), 124.9 (CH), 128.4 (C), 132.6 (C), 134.0 (C), 135.5 (C), 144.2 (CH), 148.0 (C), 156.3 (C), 171.8 (C), 172.9 (C) ppm. HR-MS m/z $[M+H]^+$ calcd for $C_{23}H_{26}N_4O_3S$: 439.1798, found 439.1794.

7.1.4.3. 6-(3-Methoxy-4-phenylamidophenyl)-3-(cis-2,6-dimethylmorpholino) isothiazolo[4,3-b]pyridine (7d). This compound was obtained using benzoyl chloride. The crude residue was purified by silica gel flash chromatography using a mixture of dichloromethane and acetone (in a ratio of 95:5) as mobile phase, affording the title compound as an amorphous yellow solid in 81% yield (41.1 mg, 0.09 mmol). Mp 195.4–196.3 °C. 1H NMR (600 MHz, $CDCl_3$) δ : 1.32 (d, $J = 6.3$ Hz, 6H, 2 × CH_3), 2.93 (dd, $J = 12.5, 10.7$ Hz, 2H, 2 × NCH), 3.93–3.98 (m, 2H, 2 × OCH), 4.02 (s, 3H, OCH_3), 4.53 (dd, $J = 12.7, 1.8$ Hz, 2H, 2 × NCH),

7.20 (d, $J = 1.9$ Hz, 1H, arom H), 7.35 (dd, $J = 8.3, 1.9$ Hz, 1H, arom H), 7.50–7.55 (m, 2H, arom H), 7.56–7.60 (m, 1H, arom H), 7.90 (d, $J = 2.1$ Hz, 1H, arom H), 7.91–7.95 (m, 2H, arom H), 8.62 (bs, $J = 8.2$ Hz, 1H, NH), 8.66–8.69 (m, 2H, arom H) ppm. ^{13}C NMR (151 MHz, $CDCl_3$) δ : 18.8 (CH_3), 55.4 (CH_2), 56.0 (OCH_3), 71.2 (CH), 108.8 (CH), 120.2 (CH), 120.3 (CH), 125.0 (CH), 127.1 (CH), 128.2 (C), 128.8 (CH), 131.9 (CH), 133.2 (C), 134.1 (C), 135.1 (C), 135.4 (C), 144.2 (CH), 148.6 (C), 156.3 (C), 165.3 (C), 172.9 (C) ppm. HR-MS m/z $[M+H]^+$ calcd for $C_{26}H_{26}N_4O_3S$: 475.1798, found 475.1794.

7.1.4.4. Synthesis of 6-aryl-3-nitropyridine-2-carbonitriles (9a-i). **General procedure.** A solution of 6-chloro-2-cyano-3-nitropyridine (1 equiv) in toluene or dioxane/water (see compound description) was degassed with argon and subsequently, the corresponding aryl boronic acid (1.2 equiv), $Pd(PPh_3)_4$ (0.02 equiv) and K_2CO_3 (2 equiv) were added. The mixture was degassed a second time, filled with argon and stirred at 95 °C overnight. After completion of the reaction as monitored by TLC, the volatiles were evaporated to dryness and the crude residue was diluted with EtOAc (20 mL) and washed with water (2 × 20 mL). The organic layer was dried over anhydrous Na_2SO_4 and concentrated *in vacuo*. The resulting residue was purified by silica gel flash chromatography, yielding the corresponding 6-aryl-3-nitropyridine-2-carbonitrile. The following compounds were made according to this procedure.

7.1.4.5. 3-Nitro-6-phenylpyridine-2-carbonitrile (9a). This compound was obtained using phenyl boronic acid and toluene as solvent. The crude residue was purified by silica gel flash chromatography using a mixture of hexane and ethyl acetate (in a ratio of 8:2) as mobile phase, affording the title compound as an amorphous light yellow solid in 81% yield (397.6 mg, 1.8 mmol). 1H NMR (300 MHz, $CDCl_3$) δ : 8.65 (d, $J = 8.9$ Hz, 1H, arom H), 8.11–8.19 (m, 3H, arom H), 7.53–7.62 (m, 3H, arom H) ppm. HR-MS m/z $[M+H]^+$ calcd for $C_{12}H_7N_3O_2$: 226.0611, found 226.0611.

7.1.4.6. 6-(4-(Trifluoromethyl)phenyl)-3-nitropyridine-2-carbonitrile (9b). This compound was obtained using 4-(trifluoromethyl)phenyl boronic acid and toluene as solvent. The crude residue was purified by silica gel flash chromatography using a mixture of hexane and dichloromethane (in a ratio of 4:6) as mobile phase, affording the title compound as an amorphous light yellow solid in 85% yield (543.3 mg, 1.85 mmol). 1H NMR (600 MHz, $CDCl_3$) δ : 7.84 (dd, $J = 8.7, 0.5$ Hz, 2H, arom H), 8.22 (d, $J = 8.8$ Hz, 1H, arom H), 8.27 (dd, $J = 8.8, 0.7$ Hz, 2H, arom H), 8.72 (d, $J = 8.8$ Hz, 1H, arom H) ppm. HR-MS m/z $[M+Na]^+$ calcd for $C_{13}H_6F_3N_3O_2$: 316.0305, found 316.0312.

7.1.4.7. 6-(4-Fluorophenyl)-3-nitropyridine-2-carbonitrile (9c). This compound was obtained using 4-fluorophenylboronic acid and toluene as solvent. The crude residue was purified by silica gel flash chromatography using a mixture of hexane and dichloromethane (in a ratio of 4:6) as mobile phase, affording the title compound as an amorphous light yellow solid in 94% yield (498.3 mg, 2.05 mmol). 1H NMR (300 MHz, $CDCl_3$) δ : 7.21–7.29 (m, 2H, arom H), 8.11 (d, $J = 8.9$ Hz, 1H, arom H), 8.14–8.20 (m, 2H, arom H), 8.65 (d, $J = 8.9$ Hz, 1H, arom H) ppm. HR-MS m/z $[M+H]^+$ calcd for $C_{12}H_6FN_3O_2$: 244.0517, found 244.0521.

7.1.4.8. 6-(3-Chlorophenyl)-3-nitropyridine-2-carbonitrile (9d). This compound was obtained using 3-chlorophenylboronic acid and toluene as solvent. The crude residue was purified by silica gel flash chromatography using a mixture of hexane and dichloromethane (in a ratio of 4:6) as mobile phase, affording the title compound as an amorphous white solid in 98% yield (545.2 mg, 2.1 mmol). 1H NMR (300 MHz, $CDCl_3$) δ : 7.47–7.60 (m, 2H, arom H), 8.01 (dt, $J = 7.3, 1.6$ Hz, 1H, arom H), 8.12–8.17 (m, 2H, arom H), 8.67 (d, $J = 8.8$ Hz,

1H, arom H) ppm. HR-MS m/z $[M+Na]^+$ calcd for $C_{12}H_6ClN_3O_2$: 282.0041 found 282.0044.

7.1.4.9. 6-(4-Methylphenyl)-3-nitropyridine-2-carbonitrile (9e). This compound was obtained using 4-methylphenylboronic acid and toluene as solvent. The crude residue was purified by silica gel flash chromatography using a mixture of hexane and ethyl acetate (in a ratio of 7:3) as mobile phase, affording the title compound as an amorphous light yellow solid in 93% yield (485 mg, 2.03 mmol). 1H NMR (300 MHz, $CDCl_3$) δ : 2.46 (s, 3H, CH_3), 7.36 (d, $J = 8.1$ Hz, 2H, arom H), 8.04 (d, $J = 8.3$ Hz, 2H, arom H), 8.10 (d, $J = 8.9$ Hz, 1H, arom H), 8.60 (d, $J = 8.9$ Hz, 1H, arom H) ppm. HR-MS m/z $[M+H]^+$ calcd for $C_{13}H_9N_3O_2$: 240.0767, found 240.0775.

7.1.4.10. 6-(3-Methoxyphenyl)-3-nitropyridine-2-carbonitrile (9f). This compound was obtained using 3-methoxyphenylboronic acid and toluene as solvent. The crude residue was purified by silica gel flash chromatography using a mixture of hexane and ethyl acetate (in a ratio of 7:3) as mobile phase, affording the title compound as an amorphous yellow solid in 94% yield (523 mg, 2.05 mmol). 1H NMR (300 MHz, $CDCl_3$) δ : 3.92 (s, 3H, OCH_3), 7.09–7.15 (m, 1H, arom H), 7.47 (t, $J = 8.0$ Hz, 1H, arom H), 7.63–7.68 (m, 1H, arom H), 7.68–7.72 (m, 1H, arom H), 8.13 (d, $J = 8.9$ Hz, 1H, arom H), 8.63 (d, $J = 8.9$ Hz, 1H, arom H) ppm. HR-MS m/z $[M+H]^+$ calcd for $C_{13}H_9N_3O_3$: 256.0717, found 256.0715.

7.1.4.11. 6-(3,4-Dimethoxyphenyl)-3-nitropyridine-2-carbonitrile (9g). This compound was obtained using 3,4-dimethoxyphenylboronic acid and toluene as solvent. The crude residue was purified by silica gel flash chromatography using a mixture of hexane and acetone (in a ratio of 7:3) as mobile phase, affording the title compound as an amorphous orange solid in 78% yield (485.1 mg, 1.7 mmol). 1H NMR (300 MHz, DMSO) δ : 3.87 (s, 3H, OCH_3), 3.90 (s, 3H, OCH_3), 7.17 (d, $J = 8.6$ Hz, 1H, arom H), 7.77 (d, $J = 2.0$ Hz, 1H, arom H), 7.87 (dd, $J = 8.5$, 2.1 Hz, 1H, arom H), 8.54 (d, $J = 9.0$ Hz, 1H, arom H), 8.75 (d, $J = 9.0$ Hz, 1H, arom H) ppm. HR-MS m/z $[M+H]^+$ calcd for $C_{14}H_{11}N_3O_4$: 286.0822, found 286.0822.

7.1.4.12. 6-(3,4,5-Trimethoxyphenyl)-3-nitropyridine-2-carbonitrile (9h). This compound was obtained using 3,4,5-trimethoxyphenylboronic acid and dioxane/water (in ratio 4:1) as solvent. The crude residue was purified by silica gel flash chromatography using a mixture of hexane and acetone (in a ratio of 7:3) as mobile phase, affording the title compound as an amorphous orange solid in 96% yield (659.8 mg, 2.1 mmol). 1H NMR (300 MHz, $CDCl_3$) δ : 3.94 (s, 3H, OCH_3), 4.00 (s, 6H, $2 \times OCH_3$), 7.37 (s, 2H, arom H), 8.09 (d, $J = 8.9$ Hz, 1H, arom H), 8.61 (d, $J = 8.9$ Hz, 1H, arom H) ppm. HR-MS m/z $[M+H]^+$ calcd for $C_{15}H_{13}N_3O_5$: 316.0928, found 316.0931.

7.1.4.13. 6-(3,5-Dimethoxyphenyl)-3-nitropyridine-2-carbonitrile (9i). This compound was obtained using 3,5-dimethoxyphenylboronic acid and toluene as solvent. The crude residue was purified by silica gel flash chromatography using a mixture of hexane and acetone (in a ratio of 7:3) as mobile phase, affording the title compound as an amorphous orange solid in 81% yield (503.5 mg, 2.1 mmol). 1H NMR (300 MHz, $CDCl_3$) δ : 3.91 (s, 6H, $2 \times OCH_3$), 6.66 (t, $J = 2.2$ Hz, 1H, arom H), 7.25 (d, $J = 2.2$ Hz, 2H, arom H), 8.10 (d, $J = 8.9$ Hz, 1H, arom H), 8.62 (d, $J = 8.9$ Hz, 1H, arom H) ppm. HR-MS m/z $[M+H]^+$ calcd for $C_{14}H_{11}N_3O_4$: 286.0822, found 286.0818.

7.1.4.14. Synthesis of 3-amino-6-aryl-pyridine-2-carbonitriles (10a-i). *General procedure.* To a stirred suspension of iron powder (3 equiv) in acetic acid (40 mL) at 60 °C, the corresponding 6-aryl-3-nitropyridine-2-carbonitrile (1 equiv) was added. The reaction mixture was stirred at 60 °C until disappearance of the starting material as monitored by TLC (3–6 h). After cooling, the volatiles were evaporated

to dryness and the crude was diluted with EtOAc (50 mL) and filtered through a paper filter. The filter cake was washed repeated times with ethyl acetate. The organic phase was washed with aqueous solution 1 N NaOH (3 \times 30 mL), dried over anhydrous Na_2SO_4 and evaporated to dryness. This mixture of two compounds (3-amino-6-aryl-pyridine-2-carbonitrile as the major and 3-amino-6-aryl-pyridine-2-carboxamide as the minor compound) was used as such in the next reaction.

7.1.4.15. Synthesis of 3-amino-6-aryl-pyridine-2-carbothioamides (11a-i). *General procedure.* To a solution of the crude mixture of 3-amino-6-aryl-pyridine-2-carbonitrile and 3-amino-6-aryl-pyridine-2-carboxamide in absolute ethanol (40 mL), was added phosphorus pentasulfide (1.2 equiv). The corresponding solution was then heated overnight at 75 °C overnight. After the completion of the reaction as monitored by TLC, the solvent was evaporated to dryness and the residue was washed with an aqueous 1 N NaOH (2 \times 30 mL) solution, dried over anhydrous Na_2SO_4 and evaporated to dryness. The residue was purified by silica gel flash chromatography yielding the 3-amino-6-aryl-pyridine-2-carbothioamide. The following compounds were made according to this procedure.

7.1.4.15.1. 3-Amino-6-phenylpyridine-2-carbothioamide (11a). This compound was obtained from a crude mixture of 3-amino-6-phenylpyridine-2-carbonitrile and 3-amino-6-phenylpyridine-2-carboxamide. The residue was purified by silica gel flash chromatography using a mixture of hexane and ethyl acetate (in a ratio of 8:2) as mobile phase, affording the title compound as an amorphous yellow solid in 71% yield (166.8 mg, 0.73 mmol). 1H NMR (300 MHz, DMSO) δ : 7.35 (m, 2H, arom H), 7.43 (m, 2H, arom H), 7.84 (bs, 2H, NH_2), 7.90 (d, $J = 8.7$ Hz, 1H, arom H), 8.08 (d, $J = 7.4$ Hz, 2H, arom H), 9.66 (bs, 1H, NH), 9.74 (bs, 1H, NH) ppm. HR-MS m/z $[M+H]^+$ calcd for $C_{12}H_{11}N_3S$: 230.0746, found 230.0743.

7.1.4.15.2. 3-Amino-6-(4-trifluoromethylphenyl)pyridine-2-carbothioamide (11b). This compound was obtained from a crude mixture of 3-amino-6-(4-trifluoromethylphenyl)pyridine-2-carbonitrile and 3-amino-6-(4-trifluoromethylphenyl)pyridine-2-carboxamide. The residue was purified by silica gel flash chromatography using a mixture of hexane and ethyl acetate (in a ratio of 7:3) as mobile phase, affording the title compound as an amorphous yellow solid in 81% yield (183 mg, 0.62 mmol). 1H NMR (300 MHz, DMSO) δ : 7.37 (d, $J = 8.8$ Hz, 1H, arom H), 7.75 (d, $J = 8.4$ Hz, 2H, arom H), 7.99 (d, $J = 8.8$ Hz, 1H, arom H), 7.93 (bs, 2H, NH_2), 8.32 (d, $J = 8.2$ Hz, 2H, arom H), 9.74 (s, 1H, NH), 9.78 (s, 1H, NH) ppm. HR-MS m/z $[M+H]^+$ calcd for $C_{13}H_{10}F_3N_3S$: 298.0620, found 298.0614.

7.1.4.15.3. 3-Amino-6-(4-fluorophenyl)pyridine-2-carbothioamide (11c). This compound was obtained from a crude mixture of 3-amino-6-(4-fluorophenyl)pyridine-2-carbonitrile and 3-amino-6-(4-fluorophenyl)pyridine-2-carboxamide. The residue was purified by flash chromatography using a mixture of hexane and ethyl acetate (in a ratio of 8:2) as mobile phase, affording the title compound as an amorphous yellow solid in 79% yield (160.4 mg, 0.65 mmol). 1H NMR (300 MHz, DMSO) δ : 7.23 (t, $J = 8.8$ Hz, 2H, arom H), 7.34 (d, $J = 8.8$ Hz, 1H, arom H), 7.83 (s, 2H, NH_2), 7.88 (d, $J = 8.8$ Hz, 1H, arom H), 8.15 (dd, $J = 8.7$, 5.6 Hz, 2H, arom H), 9.75 (bs, 1H, NH), 9.66 (bs, 1H, NH) ppm. HR-MS m/z $[M+H]^+$ calcd for $C_{12}H_{10}FN_3S$: 248.0652, found 248.0651.

7.1.4.15.4. 3-Amino-6-(3-chlorophenyl)pyridine-2-carbothioamide (11d). This compound was obtained from a crude mixture of 3-amino-6-(3-chlorophenyl)pyridine-2-carbonitrile and 3-amino-6-(3-chlorophenyl)pyridine-2-carboxamide. The residue was purified by silica gel flash chromatography using a mixture of hexane and ethyl acetate (in a ratio of 8:2) as mobile phase, affording the title compound as an amorphous yellow solid in 71% yield (173 mg, 0.62 mmol). 1H NMR (300 MHz, DMSO) δ : 7.31–7.48 (m, 3H, arom H), 7.86 (bs, 2H, NH_2), 7.94 (d, $J = 8.8$ Hz, 1H, arom H), 8.04 (d, $J = 7.6$ Hz, 1H, arom H), 8.19 (t, $J = 1.6$ Hz, 1H, arom H), 9.68 (bs, 1H, NH), 9.79 (bs, 1H, NH) ppm. HR-MS m/z $[M+H]^+$ calcd for $C_{12}H_{10}ClN_3S$: 264.0357, found 264.0353.

7.1.4.15.5. 3-Amino-6-(4-methylphenyl)pyridine-2-carbothioamide

(11e). This compound was obtained from a crude mixture of 3-amino-6-(4-methylphenyl)pyridine-2-carbonitrile and 3-amino-6-(4-methylphenyl)pyridine-2-carboxamide. The residue was purified by silica gel flash chromatography using a mixture of hexane and ethyl acetate (in a ratio of 8:2) as mobile phase, affording the title compound as an amorphous yellow solid in 83% yield (242.3 mg, 1.0 mmol). ^1H NMR (300 MHz, DMSO) δ : 2.34 (s, 3H, CH_3), 7.23 (d, $J = 8.0$ Hz, 2H, arom H), 7.32 (d, $J = 8.8$ Hz, 1H, arom H), 7.80 (bs, 2H, NH_2), 7.86 (d, $J = 8.8$ Hz, 1H, arom H), 7.97 (d, $J = 8.2$ Hz, 2H, arom H), 9.63 (bs, 1H, NH), 9.72 (bs, 1H, NH) ppm. HR-MS m/z $[\text{M} + \text{H}]^+$ calcd for $\text{C}_{13}\text{H}_{13}\text{N}_3\text{S}$: 244.0903, found 244.0916.

7.1.4.15.6. 3-Amino-6-(3-methoxyphenyl)pyridine-2-carbothioamide (11f). This compound was obtained from a crude mixture of 3-amino-6-(3-methoxyphenyl)pyridine-2-carbonitrile and 3-amino-6-(4-methoxyphenyl)pyridine-2-carboxamide. The residue was purified by silica gel flash chromatography using a mixture of hexane and ethyl acetate (in a ratio of 8:2) as mobile phase, affording the title compound as an amorphous yellow solid in 72% yield (261.4 mg, 1.0 mmol). ^1H NMR (300 MHz, DMSO) δ : 3.83 (s, 3H, OCH_3), 6.91 (dd, $J = 8.1, 2.5$ Hz, 1H, arom H), 7.30–7.38 (m, 2H, arom H), 7.57–7.66 (m, 2H, arom H), 7.89 (d, $J = 8.8$ Hz, 1H, arom H), 9.66 (bs, 1H, NH), 9.72 (bs, 1H, NH) ppm. HR-MS m/z $[\text{M} + \text{H}]^+$ calcd for $\text{C}_{13}\text{H}_{13}\text{N}_3\text{OS}$: 260.0852, found 260.0848.

7.1.4.15.7. 3-Amino-6-(3,4-dimethylphenyl)pyridine-2-carbothioamide (11g). This compound was obtained from a crude mixture of 3-amino-6-(3,4-dimethylphenyl)pyridine-2-carbonitrile and 3-amino-6-(3,4-dimethylphenyl)pyridine-2-carboxamide. The residue was purified by silica gel flash chromatography using a mixture of hexane and ethyl acetate (in a ratio of 7:3) as mobile phase, affording the title compound as an amorphous yellow solid in 73% yield (165.4 mg, 0.57 mmol). ^1H NMR (300 MHz, DMSO) δ : 3.79 (s, 3H, OCH_3), 3.86 (s, 3H, OCH_3), 6.99 (d, $J = 8.4$ Hz, 1H, arom H), 7.32 (d, $J = 8.8$ Hz, 1H, arom H), 7.55–7.60 (m, 1H, arom H), 7.62 (d, $J = 1.9$ Hz, 1H, arom H), 7.76 (bs, 2H, NH_2), 7.86 (d, $J = 8.8$ Hz, 1H, arom H), 9.62 (bs, 1H, NH), 9.71 (bs, 1H, NH) ppm. HR-MS m/z $[\text{M} + \text{H}]^+$ calcd for $\text{C}_{14}\text{H}_{15}\text{N}_3\text{O}_2\text{S}$: 290.0958, found 290.0941.

7.1.4.15.8. 3-Amino-6-(3,4,5-trimethoxyphenyl)pyridine-2-carbothioamide (11h). This compound was obtained from a crude mixture of 3-amino-6-(3,4,5-trimethoxyphenyl)pyridine-2-carbonitrile and 3-amino-6-(3,4,5-trimethoxyphenyl)pyridine-2-carboxamide. The residue was purified by silica gel flash chromatography using a mixture of hexane and ethyl acetate (in a ratio of 6:4) as mobile phase, affording the title compound as an amorphous yellow solid in 76% yield (170.1 mg, 0.53 mmol). ^1H NMR (600 MHz, CDCl_3) δ : 3.90 (s, 3H, OCH_3), 3.95 (s, 6H, $2 \times \text{OCH}_3$), 6.94 (bs, 2H, NH_2), 7.05 (s, 2H, arom H), 7.15–7.18 (m, 1H, arom H), 7.30 (bs, 1H, NH), 7.62–7.64 (m, 1H, arom H), 9.64 (bs, 1H, NH) ppm. HR-MS m/z $[\text{M} + \text{H}]^+$ calcd for $\text{C}_{15}\text{H}_{17}\text{N}_3\text{O}_3\text{S}$: 320.1063, found 320.1072.

7.1.4.15.9. 3-Amino-6-(3,5-dimethylphenyl)pyridine-2-carbothioamide (11i). This compound was obtained from a crude mixture of 3-amino-6-(3,5-dimethylphenyl)pyridine-2-carbonitrile and 3-amino-6-(3,5-dimethylphenyl)pyridine-2-carboxamide. The residue was purified by silica gel flash chromatography using a mixture of hexane and ethyl acetate (in a ratio of 7:3) as mobile phase, affording the title compound as an amorphous yellow solid in 76% yield (258.3 mg, 1.17 mmol). ^1H NMR (300 MHz, DMSO) δ : 3.81 (s, 6H, $2 \times \text{OCH}_3$), 6.48 (t, $J = 2.1$ Hz, 1H, arom H), 7.18 (d, $J = 2.2$ Hz, 2H, arom H), 7.32 (d, $J = 8.8$ Hz, 1H, arom H), 7.81 (bs, 2H, NH_2), 7.88 (d, $J = 8.8$ Hz, 1H, arom H), 9.65 (bs, 1H, NH), 9.70 (bs, 1H, NH) ppm. HR-MS m/z $[\text{M} + \text{H}]^+$ calcd for $\text{C}_{14}\text{H}_{15}\text{N}_3\text{O}_2\text{S}$: 290.0958, found 290.0963.

7.1.5. Synthesis of 3-amino-5-(aryl)isothiazolo[4,3-b]pyridines (12a-i)

General procedure. To a solution of a 3-amino-6-(aryl)pyridine-2-carbothioamides (1 equiv) in methanol (50 mL) was added dropwise a 35% H_2O_2 (2.5 equiv) solution in water at 0 °C. The reaction mixture was stirred overnight at room temperature. After disappearance of the

starting material as monitored by TLC, the solvent was evaporated to dryness affording the desired 3-amino-5-aryl-isothiazolo[4,3-b]pyridine, that was used as such in the next reaction without any further purification. The following compounds were made according to this procedure.

7.1.5.1. 3-Amino-5-(phenyl)isothiazolo[4,3-b]pyridine (12a). This compound was prepared from 3-amino-6-phenylpyridine-2-carbothioamide affording the title compound as an amorphous yellow solid in 95% yield (89.4 mg, 0.39 mmol). ^1H NMR (600 MHz, DMSO) δ : 7.41–7.46 (m, 1H, arom H), 7.48–7.53 (m, 2H, arom H), 7.81 (d, $J = 9.2$, 1H, arom H), 7.96 (d, $J = 9.3$ Hz, 1H, arom H), 8.20–8.24 (m, 2H, arom H) ppm. HR-MS m/z $[\text{M} + \text{H}]^+$ calcd for $\text{C}_{12}\text{H}_9\text{N}_3\text{S}$: 228.0590, found 228.0583.

7.1.5.2. 3-Amino-5-(4-trifluoromethylphenyl)isothiazolo[4,3-b]pyridine (12b). This compound was prepared from 3-amino-6-(4-fluorophenyl)pyridine-2-carbothioamide affording the title compound as an amorphous yellow solid in 97% yield (120.3 mg, 0.41 mmol). ^1H NMR (300 MHz, DMSO) δ : 7.79–7.89 (m, 3H, arom H), 8.01 (d, $J = 9.4$ Hz, 1H, arom H), 8.10 (bs, 2H, NH_2), 8.44 (d, $J = 8.1$ Hz, 2H, arom H) ppm. HR-MS m/z $[\text{M} + \text{H}]^+$ calcd for $\text{C}_{13}\text{H}_8\text{F}_3\text{N}_3\text{S}$: 296.0464, found 296.0471.

7.1.5.3. 3-Amino-5-(4-fluorophenyl)isothiazolo[4,3-b]pyridine (12c). This compound was prepared from 3-amino-6-(4-fluorophenyl)pyridine-2-carbothioamide affording the title compound as an amorphous yellow solid in 98% yield (106.9 mg, 0.44 mmol). ^1H NMR (600 MHz, DMSO) δ : 7.30–7.36 (m, 2H, arom H), 7.79 (d, $J = 9.3$ Hz, 1H, arom H), 7.90 (bs, 2H, NH_2), 7.91 (d, $J = 9.4$ Hz, 1H, arom H), 8.25–8.30 (m, 2H, arom H) ppm. HR-MS m/z $[\text{M} + \text{H}]^+$ calcd for $\text{C}_{12}\text{H}_8\text{FN}_3\text{S}$: 246.0496, found 246.0506.

7.1.5.4. 3-Amino-5-(3-chlorophenyl)isothiazolo[4,3-b]pyridine (12d). This compound was prepared from 3-amino-6-(3-chlorophenyl)pyridine-2-carbothioamide affording the title compound as an amorphous yellow solid in 97% yield (192.9 mg, 0.74 mmol). ^1H NMR (300 MHz, DMSO) δ : 7.45–7.57 (m, 2H, arom H), 7.79 (d, $J = 9.4$ Hz, 1H, arom H), 7.97 (d, $J = 9.4$ Hz, 1H, arom H), 8.07 (bs, 2H, NH_2), 8.15 (d, $J = 7.4$ Hz, 1H, arom H), 8.36 (s, 1H, arom H) ppm. HR-MS m/z $[\text{M} + \text{H}]^+$ calcd for $\text{C}_{12}\text{H}_8\text{ClN}_3\text{S}$: 262.0200, found 262.0196.

7.1.5.5. 3-Amino-5-(4-methylphenyl)isothiazolo[4,3-b]pyridine (12e). This compound was prepared from 3-amino-6-(4-methylphenyl)pyridine-2-carbothioamide affording the title compound as an amorphous yellow solid in 98% yield (194.0 mg, 0.8 mmol). ^1H NMR (300 MHz, DMSO) δ : 2.37 (s, 3H, CH_3), 7.31 (d, $J = 8.1$ Hz, 2H, arom H), 7.78 (d, $J = 9.4$ Hz, 1H, arom H), 7.93 (d, $J = 9.3$ Hz, 1H, arom H), 7.96 (bs, 2H, NH_2), 8.13 (d, $J = 8.1$ Hz, 2H, arom H) ppm. HR-MS m/z $[\text{M} + \text{H}]^+$ calcd for $\text{C}_{13}\text{H}_{11}\text{N}_3\text{S}$: 242.0746, found 242.0750.

7.1.5.6. 3-Amino-5-(3-methoxyphenyl)isothiazolo[4,3-b]pyridine (12f). This compound was prepared from 3-amino-6-(3-methoxyphenyl)pyridine-2-carbothioamide affording the title compound as an amorphous yellow solid in 91% yield (117.4 mg, 0.46 mmol). ^1H NMR (600 MHz, DMSO) δ : 3.86 (s, OCH_3), 7.02 (dd, $J = 8.1, 2.2$ Hz, 1H, arom H), 7.41 (t, $J = 7.9$ Hz, 1H, arom H), 7.78 (d, $J = 7.7$ Hz, 1H, arom H), 7.81–7.85 (m, 2H, arom H), 8.01 (d, $J = 9.0$ Hz, 2H, arom H) ppm. HR-MS m/z $[\text{M} + \text{H}]^+$ calcd for $\text{C}_{13}\text{H}_{11}\text{N}_3\text{OS}$: 258.0696, found 258.0688.

7.1.5.7. 3-Amino-5-(3,4-dimethoxyphenyl)isothiazolo[4,3-b]pyridine (12g). This compound was prepared from 3-amino-6-(3,4-dimethylphenyl)pyridine-2-carbothioamide affording the title compound as an amorphous yellow solid in 92% yield (79.3 mg, 0.28 mmol). ^1H NMR (600 MHz, DMSO) δ : 3.83 (s, 3H, OCH_3), 3.90 (s, 3H, OCH_3), 7.05

(d, $J = 8.5$ Hz, 1H, arom H), 7.72 (dd, $J = 8.4, 2.1$ Hz, 1H, arom H), 7.76 (d, $J = 9.4$ Hz, 1H, arom H), 7.91 (d, $J = 2.0$ Hz, 1H, arom H), 7.94 (d, $J = 9.4$ Hz, 1H, arom H) ppm. HR-MS m/z $[M+H]^+$ calcd for $C_{14}H_{13}N_3O_2S$: 288.0801, found 288.0798.

7.1.5.8. 3-Amino-5-(3,4,5-trimethoxyphenyl)isothiazolo[4,3-*b*]pyridine (12h). This compound was prepared from 3-amino-6-(3,4,5-trimethylphenyl)pyridine-2-carbothioamide affording the title compound as an amorphous orange solid in 94% yield (112.1 mg, 0.35 mmol). 1H NMR (300 MHz, DMSO) δ : 3.73 (s, 3H, OCH₃), 3.92 (s, 6H, 2 \times OCH₃), 7.54 (s, 2H, arom H), 7.78 (d, $J = 9.4$ Hz, 1H, arom H), 8.02 (d, $J = 9.4$ Hz, 1H, arom H) ppm. HR-MS m/z $[M+H]^+$ calcd for $C_{15}H_{15}N_3O_3S$: 318.0907, found 318.0904.

7.1.5.9. 3-Amino-5-(3,5-dimethoxyphenyl)isothiazolo[4,3-*b*]pyridine (12i). This compound was prepared from 3-amino-6-(3,5-dimethylphenyl)pyridine-2-carbothioamide affording the title compound as an amorphous yellow solid in 93% yield (92.2 mg, 0.35 mmol). 1H NMR (300 MHz, DMSO) δ : 3.85 (s, 6H, 2 \times OCH₃), 6.57 (bs, 1H, arom H), 7.40 (s, 2H, arom H), 7.77 (d, $J = 9.4$ Hz, 1H, arom H), 7.95 (d, $J = 9.4$ Hz, 1H, arom H), 8.05 (bs, 2H, NH₂) ppm. HR-MS m/z $[M+H]^+$ calcd for $C_{14}H_{13}N_3O_2S$: 288.0801, found 288.0803.

7.1.6. Synthesis of 5-aryl-3-bromoisothiazolo[4,3-*b*]pyridines (13a-h)

General procedure A. A solution of 5-aryl-3-aminoisothiazolo[4,3-*b*]pyridine (1 equiv) in HBr (30 mL) was stirred for 10 min at room temperature, and then CuBr was added (2 equiv). The resulting mixture was cooled at 0 °C. A solution of sodium nitrite (3 equiv) in H₂O (15 mL) was added dropwise over a period of 30 min. The reaction mixture was stirred for 2 h at 0 °C and overnight at room temperature. The mixture was cooled at 0 °C and carefully neutralized with a 2 N NaOH solution. The mixture was extracted with ethyl acetate (3 \times 30 mL) and the combined organic layers were dried over anhydrous Na₂SO₄ and evaporated to dryness. The crude residue was purified by silica gel flash chromatography (using a mixture of hexane/ethyl acetate as mobile phase), yielding the corresponding 5-aryl-3-bromoisothiazolo[4,3-*b*]pyridine.

General procedure B. To a stirred solution of CuBr₂ (1.2 equiv) and 5-aryl-3-aminoisothiazolo[4,3-*b*]pyridine (1 equiv) in dry acetonitrile (15 mL) under argon atmosphere at -10 °C, was slowly added *tert*-butylnitrite (1.3 equiv). The resulting mixture was stirred at 0 °C for 2 h and additional 3 h at room temperature. After disappearance of the starting material as monitored by TLC, the volatiles were evaporated and the crude residue was purified by silica gel flash column chromatography (using a mixture of hexane/ethyl acetate as eluent) yielding the corresponding 5-aryl-3-bromoisothiazolo[4,3-*b*]pyridine.

The following compounds were made according to the general procedure A:

7.1.6.1. 3-Bromo-5-(phenyl)isothiazolo[4,3-*b*]pyridine (13a). This compound was prepared from 3-amino-5-phenylisothiazolo[4,3-*b*]pyridine and the residue was purified by flash chromatography using a mixture of hexane and ethyl acetate (in a ratio of 9:1) as mobile phase, affording the title compound as an amorphous white solid in 61% yield (39 mg, 0.13 mmol). 1H NMR (300 MHz, CDCl₃) δ : 7.48–7.58 (m, 3H, arom H), 7.90 (d, $J = 9.3$ Hz, 1H, arom H), 8.11–8.22 (m, 3H, arom H) ppm. HR-MS m/z $[M+H]^+$ calcd for $C_{12}H_7BrN_2S$: 290.9587, found 290.9590.

7.1.6.2. 3-Bromo-5-(4-trifluoromethylphenyl)isothiazolo[4,3-*b*]pyridine (13b). This compound was prepared from 3-amino-5-(4-trifluoromethylphenyl)isothiazolo[4,3-*b*]pyridine and the residue was purified by flash chromatography using a mixture of hexane and ethyl acetate (in a ratio of 9:1) as mobile phase, affording the title compound as an amorphous white solid in 57% yield (48.3 mg, 0.13 mmol). 1H NMR (300 MHz, CDCl₃) δ : 7.79 (d, $J = 8.4$ Hz, 2H, arom H), 7.91 (d, $J = 9.3$ Hz,

1H, arom H), 8.20 (d, $J = 9.3$ Hz, 1H, arom H), 8.30 (d, $J = 8.4$ Hz, 2H, arom H) ppm. HR-MS m/z $[M+H]^+$ calcd for $C_{13}H_6BrF_3N_2S$: 358,9460, found 358,9464.

7.1.6.3. 3-Bromo-5-(4-fluorophenyl)isothiazolo[4,3-*b*]pyridine (13c). This compound was prepared from 3-amino-5-(4-fluorophenyl)isothiazolo[4,3-*b*]pyridine and the residue was purified by flash chromatography using a mixture of hexane and ethyl acetate (in a ratio of 9:1) as mobile phase, affording the title compound as an amorphous white solid in 60% yield (105 mg, 0.34 mmol). 1H NMR (300 MHz, CDCl₃) δ : 7.21 (m, 2H, arom H), 7.86 (d, $J = 9.4$ Hz, 1H, arom H), 8.14 (d, $J = 9.4$ Hz, 1H, arom H), 8.17–8.23 (m, 2H, arom H) ppm. HR-MS m/z $[M+H]^+$ calcd for $C_{12}H_6BrFN_2S$: 308,9492, found 308,9503.

7.1.6.4. 3-Bromo-5-(3-chlorophenyl)isothiazolo[4,3-*b*]pyridine (13d). This compound was prepared from 3-amino-5-(3-chlorophenyl)isothiazolo[4,3-*b*]pyridine and the residue was purified by flash chromatography using a mixture of hexane and ethyl acetate (in a ratio of 8:2) as mobile phase, affording the title compound as an amorphous white solid in 51% yield (25.4 mg, 0.08 mmol). 1H NMR (300 MHz, CDCl₃) δ : 7.41–7.45 (m, 2H, arom H), 7.87 (d, $J = 9.4$ Hz, 1H, arom H), 8.02–8.09 (m, 1H, arom H), 8.17 (d, $J = 9.4$ Hz, 1H, arom H), 8.21 (s, 1H, arom H) ppm. HR-MS m/z $[M+H]^+$ calcd for $C_{12}H_6BrClN_2S$: 324.9197, found 324.9191.

The following compounds were made according to the general procedure B:

7.1.6.5. 3-Bromo-5-(4-methylphenyl)isothiazolo[4,3-*b*]pyridine (13e). This compound was prepared from 3-amino-5-(4-methylphenyl)isothiazolo[4,3-*b*]pyridine and the residue was purified by silica gel flash chromatography using a mixture of hexane and ethyl acetate (in a ratio of 9:1) as mobile phase, affording the title compound as an amorphous white solid in 51% yield (25.5 mg, 0.08 mmol). 1H NMR (300 MHz, CDCl₃) δ : 2.44 (s, 3H, CH₃), 7.34 (d, $J = 8.1$ Hz, 2H, arom H), 7.89 (d, $J = 9.4$ Hz, 1H, arom H), 8.07–8.15 (m, 3H, arom H) ppm. HR-MS m/z $[M+H]^+$ calcd for $C_{13}H_9BrN_2S$: 304.9743, found 304.9748.

7.1.6.6. 3-Bromo-5-(3-methoxyphenyl)isothiazolo[4,3-*b*]pyridine (13f). This compound was prepared from 3-amino-5-(3-methoxyphenyl)isothiazolo[4,3-*b*]pyridine and the residue was purified by silica gel flash chromatography using a mixture of hexane and ethyl acetate (in a ratio of 9:1) as mobile phase, affording the title compound as an amorphous light yellow solid in 34% yield (62 mg, 0.19 mmol). 1H NMR (300 MHz, CDCl₃) δ : 3.93 (s, 3H, OCH₃), 7.06 (dd, $J = 8.0, 2.3$ Hz, 1H, arom H), 7.44 (t, $J = 8.0$ Hz, 1H, arom H), 7.72 (d, $J = 7.8$ Hz, 1H, arom H), 7.77–7.81 (m, 1H, arom H), 7.89 (d, $J = 9.4$ Hz, 1H, arom H), 8.14 (d, $J = 9.4$ Hz, 1H, arom H) ppm. HR-MS m/z $[M+H]^+$ calcd for $C_{13}H_9BrN_2S$: 320.9692, found 320.9693.

7.1.6.7. 3-Bromo-5-(3,4-dimethoxyphenyl)isothiazolo[4,3-*b*]pyridine (13g). This compound was prepared from 3-amino-5-(3,4-dimethoxyphenyl)isothiazolo[4,3-*b*]pyridine and the residue was purified by silica gel flash chromatography using a mixture of hexane and ethyl acetate (in a ratio of 8:2) as mobile phase, affording the title compound as an amorphous light yellow solid in 56% yield (58.2 mg, 0.17 mmol). 1H NMR (300 MHz, CDCl₃) δ : 3.97 (s, 3H, OCH₃), 4.04 (s, 3H, OCH₃), 6.98 (d, $J = 8.4$ Hz, 1H, arom H), 7.68 (dd, $J = 8.4, 2.1$ Hz, 1H, arom H), 7.89 (dd, $J = 6.6, 6.0$ Hz, 2H, arom H), 8.09 (d, $J = 9.4$ Hz, 1H, arom H) ppm. HR-MS m/z $[M+H]^+$ calcd for $C_{14}H_{11}BrN_2O_2S$: 350.9798, found 350.9796.

7.1.6.8. 3-Bromo-5-(3,4,5-trimethoxyphenyl)isothiazolo[4,3-*b*]pyridine (13h). This compound was prepared from 3-amino-5-(3,4,5-trimethoxyphenyl)isothiazolo[4,3-*b*]pyridine and the residue was

purified by silica gel flash chromatography using a mixture of hexane and ethyl acetate (in a ratio of 7:3) as mobile phase, affording the title compound as an amorphous light yellow solid in 35% yield (19.7 mg, 0.05 mmol). ^1H NMR (300 MHz, CDCl_3) δ : 3.93 (s, 3H, OCH_3), 4.01 (s, 6H, $2 \times \text{OCH}_3$), 7.42 (s, 2H, arom H), 7.87 (d, $J = 9.4$ Hz, 1H, arom H), 8.14 (d, $J = 9.3$ Hz, 1H, arom H) ppm. HR-MS m/z $[\text{M} + \text{H}]^+$ calcd for $\text{C}_{15}\text{H}_{13}\text{BrN}_2\text{O}_3\text{S}$: 380.9903, found 380.9888.

7.1.7. Synthesis of 5-aryl-3-(*cis*-2,6-dimethylmorpholino)isothiazolo[4,3-*b*]pyridines (**14a-h**)

General procedure. To a solution of a 5-substituted-3-bromoisothiazolo[4,3-*b*]pyridine (1 equiv) in absolute ethanol (20 mL) was added *cis*-2,6-dimethylmorpholine (3 equiv) and the mixture was stirred at reflux overnight. After disappearance of the starting material as monitored by TLC, the volatiles were evaporated to dryness and the residue was purified by silica gel flash column chromatography yielding the 5-substituted-3-(*cis*-2,6-dimethylmorpholino)isothiazolo[4,3-*b*]pyridine. The following compounds were made according to this procedure:

7.1.7.1. 3-(*cis*-2,6-Dimethylmorpholino)-5-phenylisothiazolo[4,3-*b*]pyridine (14a**).** This compound was prepared from 3-bromo-5-phenylisothiazolo[4,3-*b*]pyridine. The residue was purified by silica gel flash chromatography using a mixture of hexane and ethyl acetate (in a ratio of 4:1) as mobile phase, affording the title compound as an amorphous yellow solid in 91% yield (40.5 mg, 0.12 mmol). Mp 154.1–155.8 °C. ^1H NMR (600 MHz, CDCl_3) δ : 1.32 (d, $J = 6.3$ Hz, 6H, $2 \times \text{CH}_3$), 2.96 (dd, $J = 12.5, 10.8$ Hz, 2H, $2 \times \text{NCH}$), 3.92–4.00 (m, 2H, $2 \times \text{OCH}$), 4.66 (d, $J = 11.6$ Hz, 2H, $2 \times \text{NCH}$), 7.40–7.44 (m, 1H, arom H), 7.47–7.50 (m, 2H, arom H), 7.72 (d, $J = 9.4$ Hz, 1H, arom H), 7.83 (d, $J = 9.4$ Hz, 1H, arom H), 7.97–8.01 (m, 2H, arom H) ppm. ^{13}C NMR (151 MHz, CDCl_3) δ : 18.8 (CH_3), 55.6 (CH_2), 71.2 (CH), 121.2 (CH), 126.7 (CH), 128.8 (CH), 128.9 (CH), 129.5 (CH), 134.8 (C), 139.1 (C), 150.6 (C), 155.5 (C), 172.5 (C) ppm. HR-MS m/z $[\text{M} + \text{H}]^+$ calcd for $\text{C}_{18}\text{H}_{19}\text{N}_3\text{OS}$: 326.1322, found 326.1321.

7.1.7.2. 5-(4-Trifluoromethylphenyl)-3-(*cis*-2,6-dimethylmorpholino)isothiazolo[4,3-*b*]pyridine (14b**).** This compound was prepared from 3-bromo-5-(4-trifluoromethylphenyl)isothiazolo[4,3-*b*]pyridine. The residue was purified by silica gel flash chromatography using a mixture of hexane and ethyl acetate (in a ratio of 7:3) as mobile phase, affording the title compound as an amorphous yellow solid in 85% yield (37 mg, 0.09 mmol). Mp 238.2–239.7 °C. ^1H NMR (600 MHz, CDCl_3) δ : 1.33 (d, $J = 6.3$ Hz, 6H, $2 \times \text{CH}_3$), 2.99 (dd, $J = 12.6, 10.7$ Hz, 2H, $2 \times \text{NCH}$), 3.93–3.99 (m, 2H, $2 \times \text{OCH}$), 4.64 (d, $J = 11.8$ Hz, 2H, $2 \times \text{NCH}$), 7.72 (d, $J = 9.4$ Hz, 1H, arom H), 7.74 (d, $J = 8.2$ Hz, 2H, arom H), 7.87 (d, $J = 9.4$ Hz, 1H, arom H), 8.09 (d, $J = 8.1$ Hz, 2H, arom H) ppm. ^{13}C NMR (151 MHz, CDCl_3) δ : 18.9 (CH_3), 55.6 (CH_2), 71.2 (CH), 121.0 (CH), 124.2 (q, $J = 272.0$ Hz, C), 125.7 (bq, $J = 3.2$ Hz, CH), 126.9 (CH), 129.8 (CH), 130.6 (q, $J = 32.4$ Hz, C), 135.0 (C), 142.5 (C), 148.9 (C), 155.3 (C), 173.0 (C) ppm. ^{19}F NMR (471 MHz, CDCl_3) δ : –62.23 ppm. HR-MS m/z $[\text{M} + \text{H}]^+$ calcd for $\text{C}_{19}\text{H}_{18}\text{F}_3\text{N}_3\text{OS}$: 394.1195, found 394.1200.

7.1.7.3. 5-(4-Fluorophenyl)-3-(*cis*-2,6-dimethylmorpholino)isothiazolo[4,3-*b*]pyridine (14c**).** This compound was prepared from 3-bromo-5-(4-fluorophenyl)isothiazolo[4,3-*b*]pyridine. The residue was purified by silica gel flash chromatography using a mixture of hexane and ethyl acetate (in a ratio of 7:3) as mobile phase, affording the title compound as an amorphous yellow solid in 91% yield (40 mg, 0.12 mmol). Mp 165.5–166.9 °C. ^1H NMR (600 MHz, CDCl_3) δ : 1.32 (d, $J = 6.3$ Hz, 6H, $2 \times \text{CH}_3$), 2.95 (dd, $J = 12.5, 10.7$ Hz, 2H, $2 \times \text{NCH}$), 3.92–3.99 (m, 2H, $2 \times \text{OCH}$), 4.62 (dd, $J = 12.5, 1.3$ Hz, 1H, $2 \times \text{NCH}$), 7.13–7.20 (m, 2H, arom H), 7.66 (d, $J = 9.4$ Hz, 1H, arom H), 7.83 (d, $J = 9.4$ Hz, 1H, arom H), 7.94–7.98 (m, 2H, arom H) ppm. ^{13}C NMR (151 MHz, CDCl_3) δ : 18.8 (CH_3), 55.6 (CH_2), 71.2 (C), 115.70 (d, $J = 21.6$ Hz, CH), 120.9 (CH), 128.43 (d, $J = 8.2$ Hz, CH), 129.7 (C), 134.7 (C), 135.3 (C),

149.6 (C), 155.3 (C), 163.4 (d, $J = 248.9$ Hz, C), 172.50 (C) ppm. ^{19}F NMR (471 MHz, CDCl_3) δ : –111.93 ppm. HR-MS m/z $[\text{M} + \text{H}]^+$ calcd for $\text{C}_{18}\text{H}_{18}\text{FN}_3\text{OS}$: 344.1227, found 344.1235.

7.1.7.4. 5-(3-Chlorophenyl)-3-(*cis*-2,6-dimethylmorpholino)isothiazolo[4,3-*b*]pyridine (14d**).** This compound was prepared from 3-bromo-5-(3-chlorophenyl)isothiazolo[4,3-*b*]pyridine and the residue was purified by silica gel flash chromatography using a mixture of hexane and ethyl acetate (in a ratio of 4:1) as mobile phase, affording the title compound as an amorphous yellow solid in 78% yield (34.5 mg, 0.09 mmol). Mp 160.3–161.9 °C. ^1H NMR (600 MHz, CDCl_3) δ : 1.33 (d, $J = 6.3$ Hz, 6H, $2 \times \text{CH}_3$), 2.95–3.01 (m, 2H, $2 \times \text{NCH}$), 3.93–4.00 (m, 2H, $2 \times \text{OCH}$), 4.65 (d, $J = 12.5$ Hz, 2H, $2 \times \text{NCH}$), 7.36–7.43 (m, 2H, arom H), 7.67 (d, $J = 9.4$ Hz, 1H, arom H), 7.82–7.85 (m, 2H, arom H), 8.00–8.02 (m, 1H, arom H) ppm. ^{13}C NMR (151 MHz, CDCl_3) δ : 18.8 (CH_3), 55.6 (CH_2), 71.3 (CH), 120.7 (CH), 124.6 (CH), 126.9 (CH), 128.8 (CH), 129.7 (CH), 130.0 (CH), 134.8 (C), 134.9 (C), 140.8 (C), 148.8 (C), 155.4 (C), 172.7 (C) ppm. HR-MS m/z $[\text{M} + \text{H}]^+$ calcd for $\text{C}_{18}\text{H}_{18}\text{ClN}_3\text{OS}$: 360.0932, found 360.0932.

7.1.7.5. 3-(*cis*-2,6-Dimethylmorpholino)-5-(4-methylphenyl)isothiazolo[4,3-*b*]pyridine (14e**).** This compound was prepared from 3-bromo-5-(4-methylphenyl)isothiazolo[4,3-*b*]pyridine. The residue was purified by silica gel flash chromatography using a mixture of hexane and ethyl acetate (in a ratio of 4:1) as mobile phase, affording the title compound as an amorphous orange solid in 88% yield (39.1 mg, 0.12 mmol). Mp 198.1–199.8 °C. ^1H NMR (600 MHz, CDCl_3) δ : 1.32 (d, $J = 6.3$ Hz, 6H, $2 \times \text{CH}_3$), 2.42 (s, 3H, CH_3), 2.95 (dd, $J = 12.6, 10.7$ Hz, 2H, $2 \times \text{NCH}$), 3.93–4.00 (m, 2H, $2 \times \text{OCH}$), 4.66 (d, $J = 11.2$ Hz, 2H, $2 \times \text{NCH}$), 7.30 (d, $J = 7.9$ Hz, 2H, arom H), 7.70 (d, $J = 9.4$ Hz, 1H, arom H), 7.82 (d, $J = 9.4$ Hz, 1H, arom H), 7.89 (d, $J = 8.2$ Hz, 2H, arom H) ppm. ^{13}C NMR (151 MHz, CDCl_3) δ : 18.8 (CH_3), 21.3 (CH_3), 55.6 (CH_2), 71.2 (CH), 121.1 (CH), 126.6 (CH), 129.4 (CH), 129.5 (CH), 134.7 (C), 136.4 (C), 139.0 (C), 150.7 (C), 155.5 (C), 172.3 (C) ppm. HR-MS m/z $[\text{M} + \text{H}]^+$ calcd for $\text{C}_{19}\text{H}_{21}\text{N}_3\text{OS}$: 340.1478, found 340.1473.

7.1.7.6. 3-(*cis*-2,6-Dimethylmorpholino)-5-(3-methoxyphenyl)isothiazolo[4,3-*b*]pyridine (14f**).** This compound was prepared from 3-bromo-5-(3-methoxyphenyl)isothiazolo[4,3-*b*]pyridine and the residue was purified by silica gel flash chromatography using a mixture of hexane and ethyl acetate (in a ratio of 7:3) as mobile phase, affording the title compound as an amorphous yellow solid in 91% yield (40 mg, 0.11 mmol). Mp 146.2–147.9 °C. ^1H NMR (600 MHz, CDCl_3) δ : 1.32 (d, $J = 6.3$ Hz, 6H, $2 \times \text{CH}_3$), 2.97 (dd, $J = 12.5, 10.8$ Hz, 2H, $2 \times \text{NCH}$), 3.89 (s, 3H, OCH_3), 3.93–4.00 (m, 2H, $2 \times \text{OCH}$), 4.67 (d, $J = 11.6$ Hz, 2H, $2 \times \text{NCH}$), 6.98 (ddd, $J = 8.2, 2.6, 0.7$ Hz, 1H, arom H), 7.40 (t, $J = 7.9$ Hz, 1H, arom H), 7.55–7.57 (m, 1H, arom H), 7.58–7.61 (m, 1H, arom H), 7.71 (d, $J = 9.4$ Hz, 1H, arom H), 7.83 (d, $J = 9.4$ Hz, 1H, arom H) ppm. ^{13}C NMR (151 MHz, CDCl_3) δ : 18.8 (CH_3), 55.2 (OCH_3), 55.5 (CH_2), 71.2 (CH), 111.9 (CH), 114.8 (CH), 119.2 (CH), 121.2 (CH), 129.5 (CH), 129.8 (CH), 134.7 (C), 140.5 (C), 150.3 (C), 155.5 (C), 160.0 (C), 172.5 (C) ppm. HR-MS m/z $[\text{M} + \text{H}]^+$ calcd for $\text{C}_{19}\text{H}_{21}\text{N}_3\text{O}_2\text{S}$: 356.1427, found 356.1427.

7.1.7.7. 3-(*cis*-2,6-Dimethylmorpholino)-5-(3,4-dimethoxyphenyl)isothiazolo[4,3-*b*]pyridine (14g**).** This compound was prepared from 3-bromo-5-(3,4-dimethoxyphenyl)isothiazolo[4,3-*b*]pyridine. The residue was purified by silica gel flash chromatography using a mixture of hexane and ethyl acetate (in a ratio of 7:3) as mobile phase, affording the title compound as an amorphous yellow solid in 55% yield (24 mg, 0.06 mmol). Mp 200.4–201.7 °C. ^1H NMR (600 MHz, CDCl_3) δ : 1.31 (d, $J = 6.3$ Hz, 6H, $2 \times \text{CH}_3$), 2.95 (dd, $J = 12.3, 10.8$ Hz, 2H, $2 \times \text{NCH}$), 3.93–4.00 (m, 8H, $2 \times \text{OCH}_3, 2 \times \text{OCH}$), 4.64 (d, $J = 11.4$ Hz, 2H, $2 \times \text{NCH}$), 6.96 (d, $J = 8.3, 1\text{H}$, arom H), 7.52 (dd, $J = 8.4, 2.0$ Hz, 1H, arom H), 7.68 (d, $J = 2.0$ Hz, 1H, arom H), 7.69–7.72 (m, 1H, arom H),

7.81 (d, $J = 9.4$ Hz, 1H, arom H) ppm. ^{13}C NMR (151 MHz, CDCl_3) δ : 18.8 (CH_3), 55.5 (CH_2), 55.6 (OCH_3), 56.0 (OCH_3), 71.2 (CH), 109.4 (CH), 111.0 (CH), 119.4 (CH), 120.8 (CH), 129.5 (CH), 131.9 (CH), 149.2 (C), 150.1 (C), 150.2 (C), 155.5 (C), 172.1 (C) ppm. HR-MS m/z [$\text{M} + \text{H}$] $^+$ calcd for $\text{C}_{20}\text{H}_{23}\text{N}_3\text{O}_3\text{S}$: 386.1533, found 386.1526.

7.1.7.8. 3-(cis-2,6-Dimethylmorpholino)-5-(3,4,5-trimethoxyphenyl)isothiazolo[4,3-b]pyridine (14h). This compound was prepared from 3-bromo-5-(3,4,5-trimethoxyphenyl)isothiazolo[4,3-b]pyridine. The residue was purified by silica gel flash chromatography using a mixture of hexane and ethyl acetate (in a ratio of 3:2) as mobile phase, affording the title compound as an amorphous yellow solid in 80% yield (34.8 mg, 0.08 mmol). Mp 196.3–198.1 °C. ^1H NMR (600 MHz, CDCl_3) δ : 1.31 (d, $J = 6.3$ Hz, 6H, $2 \times \text{CH}_3$), 2.94–3.00 (m, 2H, $2 \times \text{NCH}$), 3.92 (s, $J = 2.5$ Hz, 3H, OCH_3), 3.95–3.99 (m, 9H, $2 \times \text{OCH}$, $2 \times \text{OCH}_3$), 4.64–4.68 (m, 2H, $2 \times \text{NCH}$), 7.27 (s, 2H, arom H), 7.69 (d, $J = 9.4$ Hz, 1H, arom H), 7.84 (d, $J = 9.4$ Hz, 1H, arom H) ppm. ^{13}C NMR (151 MHz, CDCl_3) δ : 18.8 (CH_3), 55.5 (CH_2), 56.1 (OCH_3), 61.0 (OCH_3), 71.2 (CH), 104.0 (CH), 121.0 (CH), 129.6 (CH), 134.7 (C), 139.2 (C), 150.2 (C), 153.5 (C), 155.4 (C), 172.3 (C) ppm. HR-MS m/z [$\text{M} + \text{H}$] $^+$ calcd for $\text{C}_{21}\text{H}_{25}\text{N}_3\text{O}_4\text{S}$: 416.16384, found 416.1636.

7.1.8. Synthesis of 5-aryl-3-(N-morpholino)isothiazolo[4,3-b]pyridines

General procedure. To a solution of 3-amino-5-arylisothiazolo[4,3-b]pyridine (1 equiv) in DMF (15 mL), was added K_2CO_3 (2 equiv) and 2-bromoethyl ether (0.7 equiv). The reaction mixture was stirred at 100 °C for 4–5 h. After disappearance of the starting material as monitored by TLC, the volatiles were evaporated to dryness and the residue was purified by silica gel flash chromatography, yielding the corresponding 5-aryl-3-(N-morpholino)isothiazolo[4,3-b]pyridines. The following compounds were made according to this procedure:

7.1.8.1. 5-(3-Methoxyphenyl)-3-(N-morpholino)isothiazolo[4,3-b]pyridine (15f). This compound was prepared from 3-amino-5-(3-methoxyphenyl)isothiazolo[4,3-b]pyridine. The residue was purified by silica gel flash chromatography using a mixture of hexane and ethyl acetate (in a ratio of 7:3) as mobile phase, affording the title compound as an amorphous yellow solid in 77% yield (24.5 mg, 0.08 mmol). Mp 169.1–170.6 °C. ^1H NMR (600 MHz, CDCl_3) δ : 3.89 (s, 3H, OCH_3), 3.97–4.00 (m, 4H, $2 \times \text{OCH}_2$), 4.02–4.04 (m, 4H, $2 \times \text{NCH}_2$), 6.98 (ddd, $J = 8.2, 2.5, 0.9$ Hz, 1H, arom H), 7.40 (t, $J = 7.9$ Hz, 1H, arom H), 7.55–7.58 (m, 2H, arom H), 7.71 (d, $J = 9.4$ Hz, 1H, arom H), 7.85 (d, $J = 9.4$ Hz, 1H, arom H) ppm. ^{13}C NMR (151 MHz, CDCl_3) δ : 50.5 (CH_2), 55.3 (OCH_3), 66.2 (CH_2), 112.6 (CH), 114.3 (CH), 119.4 (CH), 121.4 (CH), 129.6 (CH), 129.8 (CH), 135.0 (C), 140.6 (C), 150.8 (C), 155.5 (C), 160.0 (C), 173.0 (C) ppm. HR-MS m/z [$\text{M} + \text{H}$] $^+$ calcd for $\text{C}_{17}\text{H}_{17}\text{N}_3\text{O}_2\text{S}$: 328.1114, found 328.1111.

7.1.8.2. 5-(3,4-Dimethoxyphenyl)-3-(N-morpholino)isothiazolo[4,3-b]pyridine (15g). This compound was prepared from 3-amino-5-(3,4-dimethoxyphenyl)isothiazolo[4,3-b]pyridine. The residue was purified by silica gel flash chromatography using a mixture of hexane and ethyl acetate (in a ratio of 3:2) as mobile phase, affording the title compound as an amorphous yellow solid in 73% yield (18.1 mg, 0.05 mmol). Mp 151.2–152.9 °C. ^1H NMR (600 MHz, CDCl_3) δ : 3.95 (s, 3H, OCH_3), 3.97–4.00 (m, 7H, OCH_3 , $2 \times \text{OCH}_2$), 4.01–4.04 (m, 4H, $2 \times \text{NCH}_2$), 6.98 (d, $J = 8.3$ Hz, 1H, arom H), 7.55 (dd, $J = 8.3, 2.1$ Hz, 1H, arom H), 7.62 (d, $J = 2.1$ Hz, 1H, arom H), 7.70 (d, $J = 9.4$ Hz, 1H, arom H), 7.84 (d, $J = 9.4$ Hz, 1H, arom H) ppm. ^{13}C NMR (151 MHz, CDCl_3) δ : 50.6 (CH_2), 55.8 (OCH_3), 56.0 (OCH_3), 66.2 (CH_2), 109.8 (CH), 111.1 (CH), 119.7 (CH), 121.1 (CH), 129.6 (CH), 132.1 (C), 135.0 (C), 149.2 (C), 150.2 (C), 150.8 (C), 155.4 (C), 172.6 (C) ppm. HR-MS m/z [$\text{M} + \text{H}$] $^+$ calcd for $\text{C}_{18}\text{H}_{19}\text{N}_3\text{O}_3\text{S}$: 358.1220, found 358.1220.

7.1.8.3. 5-(3,5-Dimethoxyphenyl)-3-(N-morpholino)isothiazolo[4,3-b]pyridine (15i). This compound was prepared from 3-amino-5-(3,5-dimethoxyphenyl)isothiazolo[4,3-b]pyridine. The residue was purified by silica gel flash chromatography using a mixture of hexane and ethyl acetate (in a ratio of 3:2) as mobile phase, affording the title compound as an amorphous yellow solid in 71% yield (17.5 mg, 0.05 mmol). Mp 149.2–150.8 °C. ^1H NMR (600 MHz, CDCl_3) δ : 3.87 (s, 6H, $2 \times \text{OCH}_3$), 3.96–3.99 (m, 4H, $2 \times \text{OCH}_2$), 4.01–4.04 (m, 4H, $2 \times \text{NCH}_2$), 6.54 (t, $J = 2.3$ Hz, 1H, arom H), 7.14 (d, $J = 2.3$ Hz, 2H, arom H), 7.67 (d, $J = 9.4$ Hz, 1H, arom H), 7.84 (d, $J = 9.4$ Hz, 1H, arom H) ppm. ^{13}C NMR (151 MHz, CDCl_3) δ : 50.5 (CH_2), 55.4 (OCH_3), 66.2 (CH_2), 100.7 (CH), 105.2 (CH), 121.5 (CH), 129.5 (CH), 134.9 (C), 141.3 (C), 150.7 (C), 155.5 (C), 161.1 (C), 173.0 (C) ppm. HR-MS m/z [$\text{M} + \text{H}$] $^+$ calcd for $\text{C}_{18}\text{H}_{19}\text{N}_3\text{O}_3\text{S}$: 358.1220, found 358.1221.

7.2. GAK LanthaScreen™ Eu binding assay

The compounds were subjected to a LanthaScreen™ binding assay in which 10 titrations of dissolved test compound in DMSO are transferred to a 384-well plate. Sequential addition of the kinase buffer (50 mM HEPES pH 7.5, 0.01% BRIJ-35, 10 mM MgCl and 1 mM EGTA), the 2X kinase antibody (Eu Anti GST) mixture and the 4X Tracer 222 solution was performed. After shaking for 30 s and a one hour incubation period at room temperature, the plate was read on a fluorescence plate reader. When the bound tracer in the active site was displaced by the test compound, fluorescence was not observed. The collected data were then compared to a 0% displacement control with pure DMSO and a 100% displacement control with staurosporine, a known inhibitor of GAK and plotted against the logarithmic concentration parameter. The IC_{50} was subsequently extracted.

7.3. Antiviral assays

Virus construct. DENV2 (New Guinea C strain)^{29,30} Renilla reporter plasmid used for the antiviral assays was a gift from Pei-Yong Shi (The University of Texas Medical Branch).

Cells. Huh7 (Apath LLC) cells were grown in DMEM (Mediatech) supplemented with 10% FBS (Omega Scientific), nonessential aminoacids, 1% L-glutamine, and 1% penicillin-streptomycin (Thermo-Fisher Scientific) and maintained in a humidified incubator with 5% CO_2 at 37 °C.

Virus Production. DENV2 RNA was transcribed *in vitro* using mMessage/mMachine (Ambion) kits. DENV was produced by electroporating RNA into BHK-21 cells, harvesting supernatants on day 10 and titering via standard plaque assays on BHK-21 cells. Virus titers were determined via standard plaque assay on Vero76 cells.

Infection assays. Huh7 cells were infected with DENV in replicates ($n = 3$ –10) for 4 h at MOI of 0.05. Overall infection was measured at 48 h by standard luciferase assays.

Viability assays. Viability was assessed using AlamarBlue® reagent (Invitrogen) according to manufacturer's protocol. Fluorescence was detected at 560 nm on InfiniteM1000 plate reader.

Declaration of Competing Interest

None.

Acknowledgments

This work was supported by award number W81XWH-16-1-0691 from the Department of Defense (DoD), Congressionally Directed Medical Research Programs (CDMRP) to S.E, P.H; Grant 12393481 from the Defense Threat Reduction Agency (DTRA), Fundamental Research to Counter Weapons of Mass Destruction to S.E. and P.H.

Appendix A. Supplementary material

Supplementary data to this article can be found online at <https://doi.org/10.1016/j.bmc.2019.115188>.

References

- Sorrell FJ, Szklarz M, Abdul Azeed KR, Elkins JM, Knapp S. Family-wide structural analysis of human Numb-associated protein kinases. *Structure*. 2016;24:401–411.
- Edeling MA, Smith C, Owen D. Life of a clathrin coat: insights from clathrin and AP structures. *Nat Rev Mol Cell Biol*. 2006;7:32–44.
- Zhang CX, Engqvist-Goldstein AEY, Carreno S, Owen DJ, Smythe E, Drubin DG. Multiple roles for cyclin G-associated kinase in clathrin-mediated sorting events. *Traffic*. 2005;6:1103–1113.
- Korolchuk VI, Banting G. CK2 and GAK/auxilin2 are major protein kinases in clathrin-coated vesicles. *Traffic*. 2002;3:428–439.
- Ghosh P, Kornfeld S. AP-1 binding to sorting signals and release from clathrin-coated vesicles is regulated by phosphorylation. *J Cell Biol*. 2003;160:699–708.
- Umeda A, Meyerholz A, Ungewickell E. Identification of the universal cofactor (auxilin 2) in clathrin coat dissociation. *Eur J Cell Biol*. 2000;79:336–342.
- Neveu G, Barouch-Bentov R, Ziv-Av A, Gerber D, Jacob Y, Einav S. Identification and targeting of an interaction between a tyrosine motif within hepatitis C virus core protein and AP2M1 essential for viral assembly. *PLoS Pathog*. 2012;8:e1002845.
- McMahon HT, Boucrot E. Molecular mechanism and physiological functions of clathrin-mediated endocytosis. *Nat Rev Mol Cell Biol*. 2011;12:517–533.
- Bekerman E, Neveu G, Shulla A, et al. Anticancer kinase inhibitors impair intracellular viral trafficking and exert broad-spectrum antiviral effects. *J Clin Invest*. 2017;127:1338–1352.
- Neveu G, Ziv-Av A, Barouch-Bentov R, Berkerman E, Mulholland J, Einav S. AP-2-associated protein kinase 1 and cyclin G-associated kinase regulate hepatitis C virus entry and are potential drug targets. *J Virol*. 2015;89:4387–4404.
- Bekerman E, Einav S. Infectious disease. Combating emerging viral threats. *Science*. 2015;348:282–283.
- Asquith CRM, Laitinen T, Bennett JM, et al. Identification and optimization of 4-anilinoquinolines as inhibitors of cyclin G associated kinase. *ChemMedChem*. 2018;13:48–66.
- Asquith CRM, Berger BT, Wan J, et al. SGC-GAK-1: a chemical probe for cyclin G associated kinase (GAK). *J Med Chem*. 2019;62:2830–2836.
- Kovackova S, Chang L, Bekerman E, et al. Selective inhibitors of cyclin G associated kinase (GAK) as anti-hepatitis C agents. *J Med Chem*. 2015;58:3393–3410.
- Pu SY, Wouters R, Schor S, Rozenski J, Barouch-Bentov R, Prugar LI, O'Brien CM, Brannan JM, et al. *J Med Chem*. 2018;61:6178–6192.
- Li J, Kovackova S, Pu SY, et al. Isothiazolo[4,3-b]pyridines as inhibitors of cyclin G associated kinase: synthesis, structure–activity relationship studies and antiviral activity. *Med Chem Comm*. 2015;6:1666–1672.
- Wouters R, Pu SY, Froeyen M, et al. Cyclin G-associated kinase (GAK) affinity and antiviral activity studies of a series of 3-C-substituted isothiazolo[4,3-b]pyridines. *Eur J Med Chem*. 2019;163:256–265.
- Wouters R, Tian J, Herdewijn P, De Jonghe S. A scaffold-hopping strategy toward the identification of inhibitors of cyclin G associated kinase. *ChemMedChem*. 2018;13:1–19.
- Cui X, Zhou Y, Wang N, Liu L, Guo QX. N-Phenylurea as an inexpensive and efficient ligand for Pd-catalyzed Heck and room-temperature Suzuki reactions. *Tetrahedron Lett*. 2007;48:163–167.
- Hanthorn JJ, Valgimigli L, Pratt DA. Preparation of highly reactive pyridine- and pyrimidine-containing diarylamine antioxidants. *J Org Chem*. 2012;77:6908–6916.
- Zhongzhong Y, Aiping L, Mingzhi H, et al. Design, synthesis, DFT study and antifungal activity of the derivatives of pyrazolecarboxamide containing thiazole or oxazole ring. *Eur J Med Chem*. 2018;149:170–181.
- Subhash LY, Denvert SD, Bhalchandra MB. MnO₂ catalyzed formylation of amines and transamidation of amides under solvent-free conditions. *RSC Adv*. 2015;5:80441–80449.
- Striela R, Urbelis G, Sudzius J, Stoncius S, Sadzeviciene R, Labanauskas L. Synthesis of bromocyclopropylpyridines via the Sandmeyer reaction. *Tetrahedron Lett*. 2017;58:1681–1683.
- Lebakken CS, Riddle SM, Singh U, Frazee WJ, Eliason HC, et al. Development and applications of a broad-coverage, TR-FRET-based kinase binding assay platform. *J Biomol Screening*. 2009;14:924–935.
- Morris GM, Huey R, Lindstrom W, et al. Autodock4 and AutoDockTools4: automated docking with selective receptor flexibility. *J Comput Chem*. 2009;16:2785–2791.
- Trott O, Olson AJ. AutoDock Vina: improving the speed and accuracy of docking with a new scoring function, efficient optimization and multithreading. *J Comput Chem*. 2010;31:455–461.
- Bandaru SSM, Kapdi AR, Schulzke C. Crystal structure of 4-(pyrazin-2-yl)morpholine. *Acta Crystallogr E Crystallogr Commun*. 2018;74:137–140.
- Quintanilla-Licea R, Colunga-Valladares JF, Caballero-Quintero A, et al. NMR Detection of isomers arising from restricted rotation of the C-N amide bond of N-formyl-o-tolidine and N,N'-bis-formyl-o-tolidine. *Molecules*. 2002;7:662–673.
- Xie X, Gayen S, Kang C, Yuan Z, Shi P-Y. Membrane topology and function of dengue virus NS2A protein. *J Virol*. 2013;87:4609–4622.
- Zou G, Xu HY, Qing M, Wang QY, Shi PY. Development and characterization of a stable luciferase dengue virus for high-throughput screening. *Antivir Res*. 2011;91:11–19.